The Economical Production of Bryostatin & Et-743 with Biological Activity

Giso Abadi

A thesis submitted in fulfillment of the requirements of the University of Sunderland for the degree of Doctor of Philosophy

This research program was carried out in collaboration with Valdosta State University, Valdosta, Georgia, USA and the University of Sunderland, Sunderland, UK

July 2009

ACKNOWLEDGEMENTS

I would like to thank the University of Sunderland and Valdosta State University for making this collaboration possible. My sincere gratitude to my supervisors Prof. Paul Groundwater, Dr. Lyn Noble, Prof. Roz Anderson, and Dr. Thomas Manning, as well as Dr. James Baxter for their unconditional support during my course of work.

I am also indebted to the National Cancer Institute for providing us with pure samples of bryostatin 1 and Et-743 to compare our raw extracts to. This helped us hugely in interpreting our data and providing me with my work's direction.

I would like to thank Jack Rudloe for providing us with marine specimen throughout this research. Jack is a genuine and smart man who introduced and the idea of developing "drugs from the sea" to the world.

My gratitude also to the University of Georgia for providing us with MALDI-MS data and the United States Department of Agriculture for LC-MS data throughout my research project.

My sincere appreciation to Dr. Nicolas Haroune from chemiSpec at the University of Sunderland for his assistance with LC-MS data.

My thanks to Dr. John Lough at the University of Sunderland for providing me with a HPLC system to conduct my work.

The Medical College of Georgia is also thanked for conducting cell line testing which tremendously helped us in further patenting our compound.

To my beloved mother, Shohrat Daneshjou, and two brothers, Geev and Hamed for their unconditional support and love. I could not have done this without you.

Always fall in with what you're asked to accept.
Take what is given, and make it over your way.
My aim in life has always been to hold my own with whatever's going.
Not against: with.

Robert Frost

ABSTRACT

Within the past fifty years, drugs from the sea have become an increasing industry for the identification and isolation of new medicinal agents. Bryozoa, sea squirts and corals are examples of many organisms that have been collected and tested for medicinal activity. Clinical testing's of drugs such as bryostatin 1 and Et-743 have shown much success against various cancers such as kidney, prostate, and leukemia, *etc*.. However, there are many problems affecting the economical availability of such drugs such as: 1. the potential endangerment of marine organisms due to massive quantities required for clinical use; 2. seasonal availability of the organisms and 3. numerous synthetic steps resulting in low percent yields to name a few.

Detailed analyses conducted of the environment of these marine organisms resulted in the composition of chemicals that were used as an artificial property to mimic the host organisms and their environments, resulting in the cultivation of the bacteria suggestively responsible for the production of these active compounds. Other experiments conducted, involved the esterification of bryostatin 1 under various conditions, in order to show that such compounds produced, are more environmentally obtainable as opposed to being specie dependent. Computational studies binding Fe^{3+} to different marine natural products was also conducted in order to determine any siderophore properties that each may have. From this study cell line tests were conducted in order to determine the efficacy of a bryostatin-Fe^{3+} complex in comparison to bryostatin 1.

Preliminary results from all the artificial media used to isolate and produce the bryostatins and Et-743 showed prominence; however, results were inconclusive due low detection values and marginal errors.

SYMBOLS AND ABBREVIATIONS

α	alpha
Å	angstrom
AcOH	acetyl hydroxide
AD	Alzheimer's disease
AEO	aboral, equatorial and oral
AIDS-KS	Acquired Immune Deficiency Syndrome-Kaposi's sarcoma
Al_2O_3	aluminum oxide
AS	artificial surfaces
BAC	bacterial amplification chamber
BER	base excision repair
BH_3	borane
Boc	di-tert-butyl dicarbonate
BSA	bovine serum albumin
cdk2	cyclin d kinase 2
CH_2Cl_2	methylene chloride
$Cl(CH_2)_2Cl$	1,2-dichloro ethane
δ	delta
DAG	diacylglycerol
DCC	Dicyclohexylcarbodiimide
DEX	dexamethasone
DMAP	4-Dimethylaminopyridine
DMF	dimethylformamide
DMSO	dimethyl sulphoxide
DNA	deoxyribonucleic acid

DTPA	diethylene triaminepentaacetic acid
D/V	dipole moment/surface volume ratio
ED_{50}	effective dose
EDTA	ethylenediaminetetraacetic acid
Et-743	Ecteinascidin 743
Et_3N	triethylamine
FGI	functional group interconversion
γ	gamma
g	gram
GF	growth factor
GFP	green fluorescent protein
$Hg(OAc)_2$	mercury(II) acetate
HNO_3	nitric acid
HRFABMS	High resolution fast atom bombardment mass spectrometry
HRMS	high resolution mass spectrometry*
IC_{50}	inhibitory concentration
IM	imatinib mesylate
INF-γ	interferon-γ
KHMDS	potassium hexamethyldisilazane
LC-MS	liquid chromatography mass spectrometer
LG	leaving group
M	molar
m-CPBA	*meta*-Chloroperoxybenzoic acid

* The molecular weights for the compounds stated in this thesis are all based on the calculated HRMS mass of each compound.

MALDI-TOF-MS	Matrix assisted laser desorption ionization-time of flight mass spectrometry
MeCN	acetonitrile
MNP	marine natural product
MRCL	myxoid/round cell liposarcoma
MTT	3(4, 5-dimethylthiazolyl-2)2, 5-diphenyltetrazolum bromide
$NaBH_4$	sodium borohydride
NAHMDS	sodium hexamethyldisilazide
Na_2HPO_4	Disodium hydrogen phosphate
NaOH	sodium hydroxide
NCI	National Cancer Institute
NER	nucleotide excision repair
NF-y	nuclear transcription factor –y
NP	natural product
NSCLC	non-small cell lung cancer
OA	octanoic acid
OTMS	O-tetramethylsilyl
PAI-1	plasminogen activator inhibitor-1
PBS	phosphate buffered saline
PCR	polymerase chain reaction
PKC	protein kinase c
PKS	protein kinase synthase
PMB	*p*-methoxybenzyl
PnBz	*p*-nitrobenzoyl
ppm	parts per million

PPTS	pyridinium *p*-toluenesulfonate
PSA	prostate specific antigen
PVC	polyvinyl chloride
RT	room temperature
SEM	scanning electron microscope
TBS	t-butyldimethylsilyl
TES	triethylsilyl
TFA	trifluoroacetic acid
THF	tetrahydrofuran
TPA	12-O-tetradecanoylphorbol-13-acetate
USD	United States Dollars
UV	ultra-violet
UV-VIS	ultra-violet visible spectrometry

CONTENTS

CHAPTER 1. History of Bryostatin 1, Et-743 and Taxol

CHAPTER 2. A composition of chemicals used as an artificial source for the production of the bryostatins

Chapter 3. Artificial surfaces treated with a composition of chemicals for the production of the bryostatins

CHAPTER 7. Computational studies of the bryostatins and MNPs as potential siderophores

CHAPTER 8. Cell line testing of a bryostatin-Fe^{3+} complex versus bryostatin 1

CHAPTER 9. Future work

CHAPTER 1

History of Bryostatin 1, Et-743 and Taxol

1.1 Introduction

In the 1960's, Jack Rudloe, a marine specimen collector appeared on the television promoting his new book, The Sea Brings Forth.[1] Following his appearance on the show, he was contacted by David Newman from the National Cancer Institute (NCI), requesting over three hundred marine organisms ranging from sponges to sharks. From all the marine organisms that were tested against the PS-100 leukaemia virus strain in mice, *Bugula neritina*, a bryozoa showed the most prominent activity.

Since then, the ocean has become a treasure chest for compounds with potential medicinal activity, with approximately a third of all drugs marketed today extracted from natural resources.[2] Extracting, collecting and identifying drugs from marine organisms has opened a new door for the pharmaceutical industry and gives possible hope to patients suffering from various cancers as well as Alzheimer's and other diseases.[3,4]

Marine organisms such as bryozoa, tunicates, and sponges *etc*., all around the world, have been isolated for the extraction of medicinal agents, many of which have shown efficacy against various cell lines.[5] Considering that the ocean contains a huge pool of microbial populations, it has been suggested that many of these natural products (NPs), which have been isolated from different invertebrates, are secondary metabolites produced by the marine bacteria found in these marine organisms.[6,7] Secondary metabolites are compounds produced by organisms that have no effect on the growth, development or reproduction of the organisms. The functions of these secondary metabolites are still being determined but many marine organisms are believed to produce these biologically active compounds as a chemical defence mechanism (prey, predator or compete for territory due to the overgrowth of species), and/or as a secondary method for survival.[8] These secondary metabolites fall into different chemical

classes, such as terpenoids, alkaloids, polyketides, peptides, sugars, and steroids *etc*..[9]

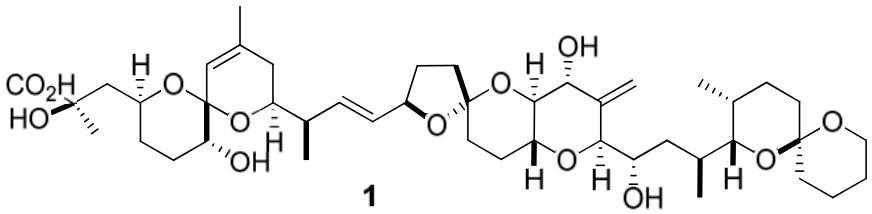

1

Fig. 1. Okadaic acid ($C_{44}H_{68}O_{13}$, 804.4654 g/mol) is a toxin produced by *Dinophysis* and *Prorocentrum dinoflagelates*m which causes diarrhetic shellfish poisoning in humans.

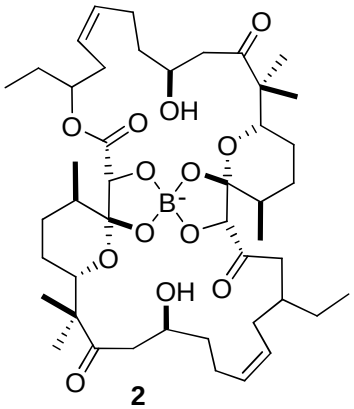

2

Fig. 2. Borophycin ($C_{45}H_{70}BO_{13}$, 829.4904 g/mol) is a natural product isolated from *Nostoc linkia* and *N. spongaeforme*.

There are two types of marine secondary metabolites: 1) toxins produced by phytoplanktons, which have severe effects in humans and 2) bioactive natural products produced by cyanobacteria found in marine invertebrates with potency as medicinal agents. For example, phytoplanktons produce phytotoxins, such as okadaic acid **1** (Fig. 1), that are ingested by filter feeders (*e.g.* shellfish), which can be toxic to humans when consumed.[10] On the other hand, borophycin **2** (Fig. 2) originally isolated from *Nostoc linkia* and *N. spongaeforme* has shown efficacy as an anti-cancer agent against human colorectal adenocarcinoma cell line.[10]

Marine invertebrates are filter feeders and can therefore ingest bacteria from the ocean, which can later settle in the marine organism. It is suggested that marine bacteria can account for up to 40% of the volume of sponges.[11] Many

groups are now studying the ocean to further understand the source of production of these NPs. In a study conducted by Toledo *et al.*, 42% of bacteria isolated from encapsulated sponge symbionts and sediment extracts were novel, compared with 7% obtained from plating samples placed directly into marine agar.[12]

Based on studies showing the true source of NPs from marine bacteria, new attempts are being made to develop methods for the isolation and identification of the marine bacteria responsible for the production of bioactive agents. Despite the identification of several marine bacteria as the true source of bioactive compounds, the identification and isolation of such compounds still remains a problem.

Table 1, below, shows examples of marine natural products (MNPs), that have been isolated from various marine invertebrates, each showing potency as medicinal agents.

Table 1. A summary of MNPs that have shown efficacy as medicinal agents.

Drug name	Medicinal activity	Source
Dolastatins **3** (Fig. 3)[13]	A potent anti-proliferative agent with an ED_{50} = $4.6X10^{-5}$ µg/mL against murine PS leukaemia cells.[14] Dolastatin acts as a potent non-competitive inhibitor of tubulin.[15]	Isolated from the sea hare, *Dolabella auricularia* in the 1970s. It was later shown that the natural product was actually produced by the cyanobacterium *Symploca*, found in the sea hare.[16]
Peloruside A **4** (Fig. 4)[17,18]	Is a 16-membered polyketide macrocyclic lactone with potent anti-mitotic activity. Peloruside A binds to tubulin with microtubule-stabilizing properties that arrest cells in the G2/M phase of the cell cycle.	Isolated from the sponge, *M. hentscheli* in New Zealand in 2000. Aquaculture systems of sponge is conducted by Marlborough Mussels Ltd., to produce the drug more efficiently.[19]
Trunkamide **5** (Fig. 5) [20,21]	A cyclic heptapeptide with cytotoxic activity.	Isolated from the tropical Indo-Pacific aplousobranch ascidian *Lissoclinum patella* in 1996.
Aplidine **6** (Fig. 6) [10,22]	Aplidine interferes with cell-cycle progression at the G1 phase. It entered Phase I clinical trials for the treatment of solid tumours and lymphoma and Phase II for relapsing or refractory multiple myeloma.[5]	Isolated from the Mediterranean tunicate, *Aplidium albicans*.
Onnamide A **7** (Fig. 7)[23,24,25]	Induces plasminogen activator inhibitor-1 (PAI-1), gene expression in Mv1Lu cells, at concentrations of 50 nM.	Originally isolated from the sponge, *Theonella swinhoei*. Recent study has shown that the bioactive compound is produced by the polyketide synthase genes from the uncultured bacteria symbiont, *Pseudomonas spp.* in the sponge.

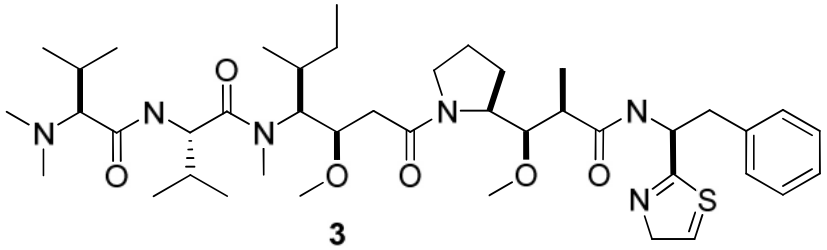

3

Fig. 3. Dolastatin 10 ($C_{42}H_{70}N_6O_6S$, 786.5072 g/mol), isolated from the sea hare, *Dolabella auricularia*.

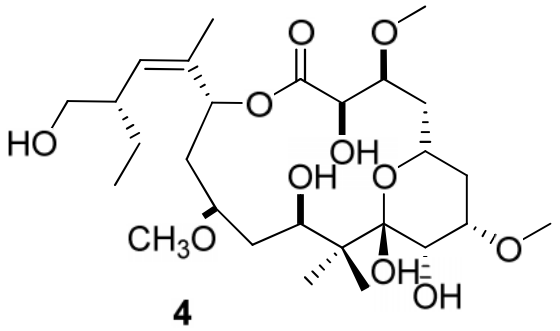

4

Fig. 4. Peloruside A ($C_{27}H_{48}O_{11}$, 548.3191 g/mol), isolated from the sponge, *M. hentscheli*.

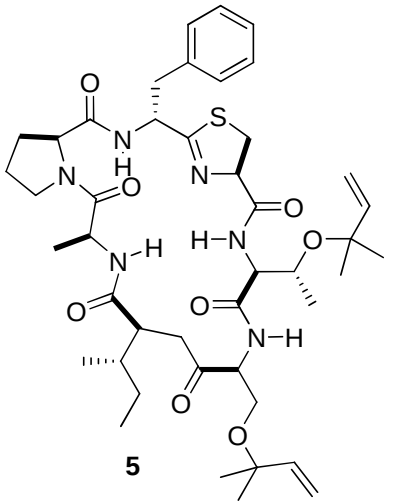

5

Fig. 5. Trunkamide ($C_{44}H_{64}N_6O_8S$, 836.4501 g/mol), tropical Indo-Pacific aplouobranch ascidian *Lissoclinum*

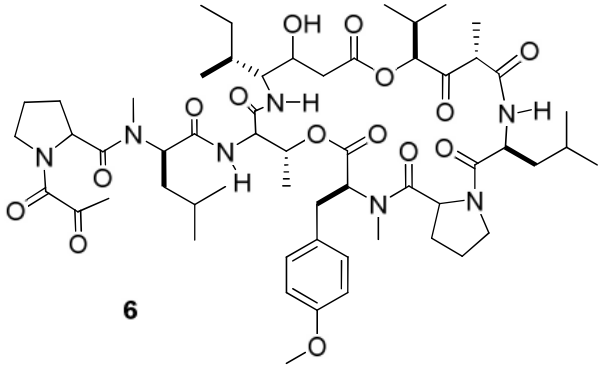

6

Fig. 6. Aplidine ($C_{57}H_{87}N_7O_{15}$, 1109.6255 g/mol), isolated from the Caribbean tunicate, *Tridedemnum solidum*.

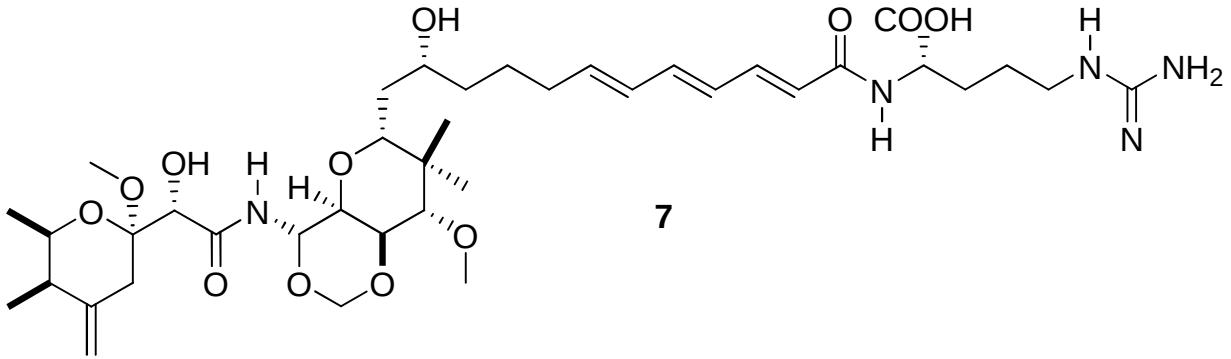

7

Fig. 7. Onnamide A ($C_{39}H_{63}N_5O_{12}$, 793.4468 g/mol) isolated from *Pseudomonas spp.*, bacteria symbiont of the sponge, *Theonella swinhoei*.

1.2 Bryozoa

Bryozoa are classified as sessile invertebrates and colonial feeders found in both fresh and salt water environments. *Bugula neritina* (Fig. 8 (a, b), 9) a salt water species, is very temperature dependent (18 to 22°C), contains $CaCO_3$ on its outer most layer and is a seasonal organism commonly found from October to April along the coast of California, the Gulf of México and other coastal areas. However, it is also found during the summer season along the Gulf of México.[26,27]

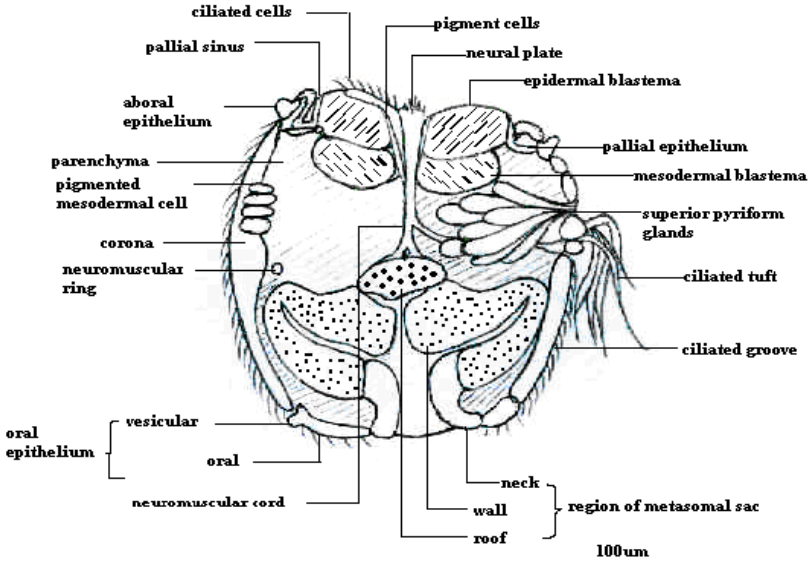

Fig. 8a. Right-lateral view of the midsagittal section of the larvae, *B. neritina*. The structure is classified as an (AEO) Aboral, Equatorial and Oral larval type because its surface is formed by the orally-aborally elongate coronal cells, and as its equatorial neuromuscular rings contract, the larva appears to have a dumbbell appearance.[28]

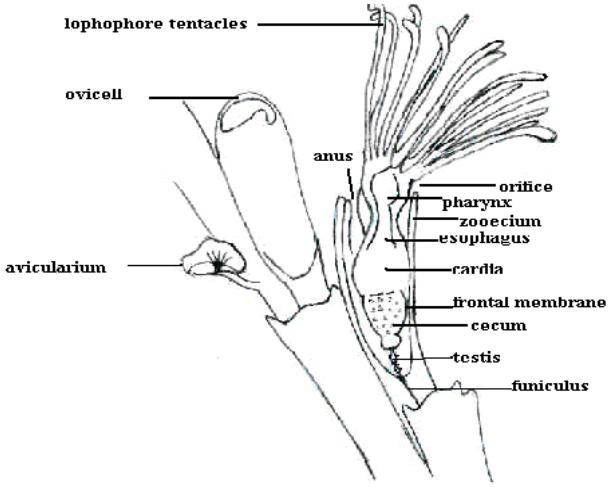

Fig. 8b. Detailed structure of *B. neritina*.[28]

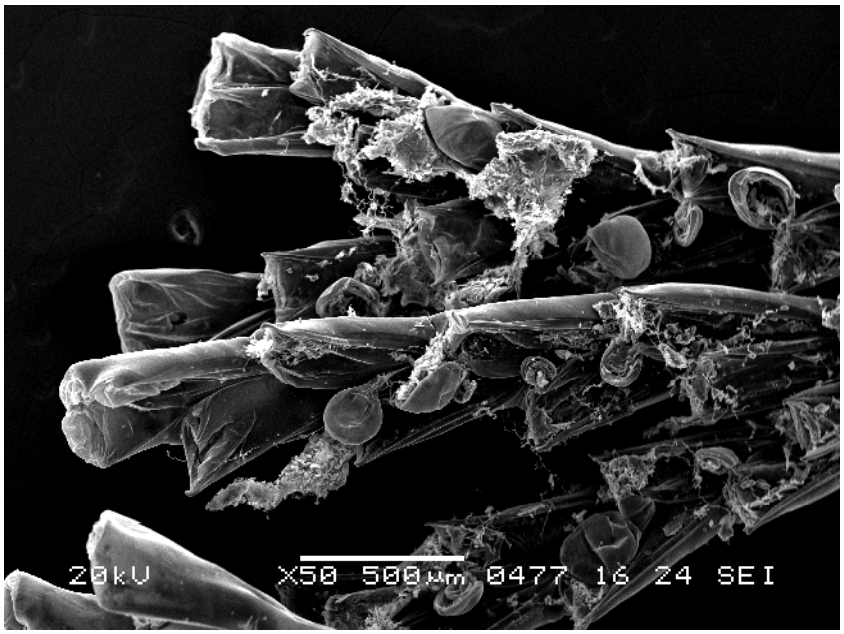

Fig. 9. An SEM image of a branch of the colonial filter feeder *Bugula neritina*.

In May and June *Bugula* may be impossible to find attached to different substrates such as rocks, docks and/or boat bottoms as it usually is in winter. *Bugula* can, however, be found washed up on beaches suggesting that deep water *Bugula* have a longer season due to the cooler temperatures found at these depths. As mentioned previously, the outer layer of *Bugula* has a calcified layer ($CaCO_3$), which must be dissolved before any extraction can take place. The role of the bryostatins found in *Bugula* is not known as yet but it has been suggested by other groups, that it is produced by symbiotic bacteria that reside within the organism. The bryostatins may play a role in the defense mechanism of the animal, similar to other secondary metabolites or it may act as a siderophore. Siderophores are iron chelating compounds, produced by marine bacteria in marine organisms and secreted by marine organisms to bind iron; as many cannot bind iron alone.[29,30] Twenty bryostatin compounds have been isolated from the marine organism, since the discovery of its efficacy as a medicinal agent. Aside from the bryostatins, neristatin **8** (Fig. 10) has also been isolated from *Bugula neritina*. [31]

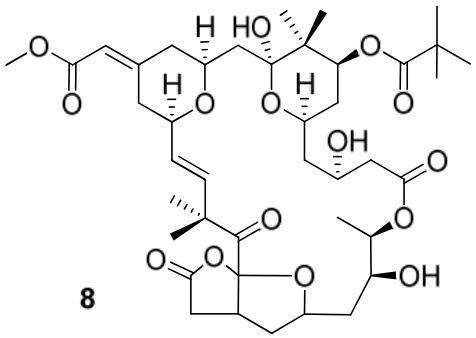

8

Fig. 10. Neristatin ($C_{41}H_{60}O_{15}$, 792.3927 g/mol), is a marine natural product isolated from *Bugula neritina*, in the Gulf of México.

Yields from the extraction of bryostatin 1 from *Bugula* are consistently very low (10^{-5} to 10^{-7}%). The harvesting, extraction and purification processes are time consuming, expensive and pose many environmental concerns. For this reason, the cost for high purity bryostatin 1 is several million USD per gram. Due to such circumstances, several methods have been conducted to improve the isolation and production of bryostatin 1 from the marine organism; as one of many alternatives towards the production of bryostatin 1.

A recent study was conducted in order to try to modify the growth of the larvae of *Bugula neritina* by first analyzing its behaviour under various conditions, in the hope of developing an efficient method of maximizing the production of the organism in an artificial setting. Results showed that conditions such as light, water flow and aeration strongly affect the overall production of these larvae; however, the change in the schedule of feeding broths did not impact the overall percent yield of the larvae produced; resulting in the harvesting of the marine organism for several weeks.[32] Another similar study looked at the effects of different chemicals (potassium, calcium, serotonin, *etc.*) on larvae attachment, in an attempt to prolong the life and production of the organism when using aquaculture methods. Results showed that potassium induced the attachment of larvae to containers, as did chemicals such as serotonin, l-dopa and γ-aminobutyric acid, while chemicals such as Mg^{2+} inhibited the production of

larvae, and others, such as Ca^{2+}, had no impact on the larvae within the system.[33]

1.2.1 Bryostatin 1

Bryostatin 1 **9a** (Fig. 11) is a marine natural product extracted from the bryozoa, *Bugula neritina*. It was first discovered in the 1960s when the NCI conducted an extensive study testing hundreds of marine organisms for any potential medicinal applications. From all the marine organisms tested, *Bugula neritina,* showed the most prominent activity. In 1982 the active compound isolated from the marine organism was identified as bryostatin 1, a cyclic macrolide structure (Fig. 11), by Pettit *et al.*.[34] X-Ray crystallography and spectroscopy were used to determine the macrolide's unusual structure.[34]

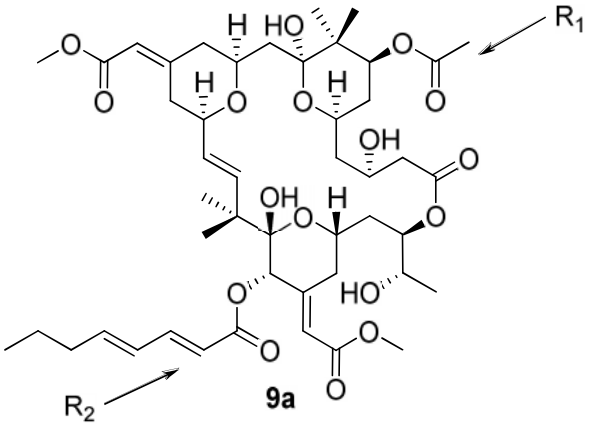

Fig. 11. Bryostatin 1 ($C_{47}H_{68}O_{17}$, 904.4451 g/mol). The groups on bryostatin 1 are an acetate group at R_1 and a C8 group at R_2.

In the extraction procedure for the isolation of bryostatin 1, 500 kg of wet *Bugula* was used. This extract was fractionated by solvent partition sequencing, purified by column chromatography, and recrystallized to produce crystal formations of bryostatin 1.[34] Since then, nineteen other bryostatin compounds have been identified from the marine bryozoa, each differing in the R_1 and R_2 groups on the bryophan ring (Fig. 11). As shown above, bryostatin 1 has many ester groups which maintain the basic frame of the bryostatin compound.

1.2.2 Synthesis of bryostatin 7

Studies have been conducted on the complete synthesis of the C_1-C_{16} portion of bryostatin 1, in order to prepare the compound more efficiently in higher percentage yield.[35,36] The synthesis of bryostatin 7 by Masamune *et al*., is shown in Fig. 12 and 13.[37,38]

In the figure below, fragments (ring synthons) were connected in the sequence **A′** (C3-C10), **B**, **C** and, finally, the introduction of the C1-C2 unit. All of the fragments required were available from the previous work of this group. The synthesis shown below focuses solely on the key steps for the coupling of these fragments or those which lead to diastereoisomeric discrimination. The **A′B** fragment was prepared *via* an initial aldol reaction of aldehyde **10** with ketone **11**, catalysed by (*R,R*)-2,5-dimethylborolanyl triflate, to give the β-hydroxyketone **12** in 86 % yield, with an 11*S*:11*R* ratio of 8:1 (Fig. 12). Construction of the two pyran rings involved initial deacetonization to pyran **13**, followed by a mercuric acetate-mediated cyclization onto the alkene, to give a diastereoisomeric ratio of alkylmercurials **14** of 1:1, from which the isomer **15** with the equatorial aldehyde group was obtained *via* equilibration of the isomers on alumina.

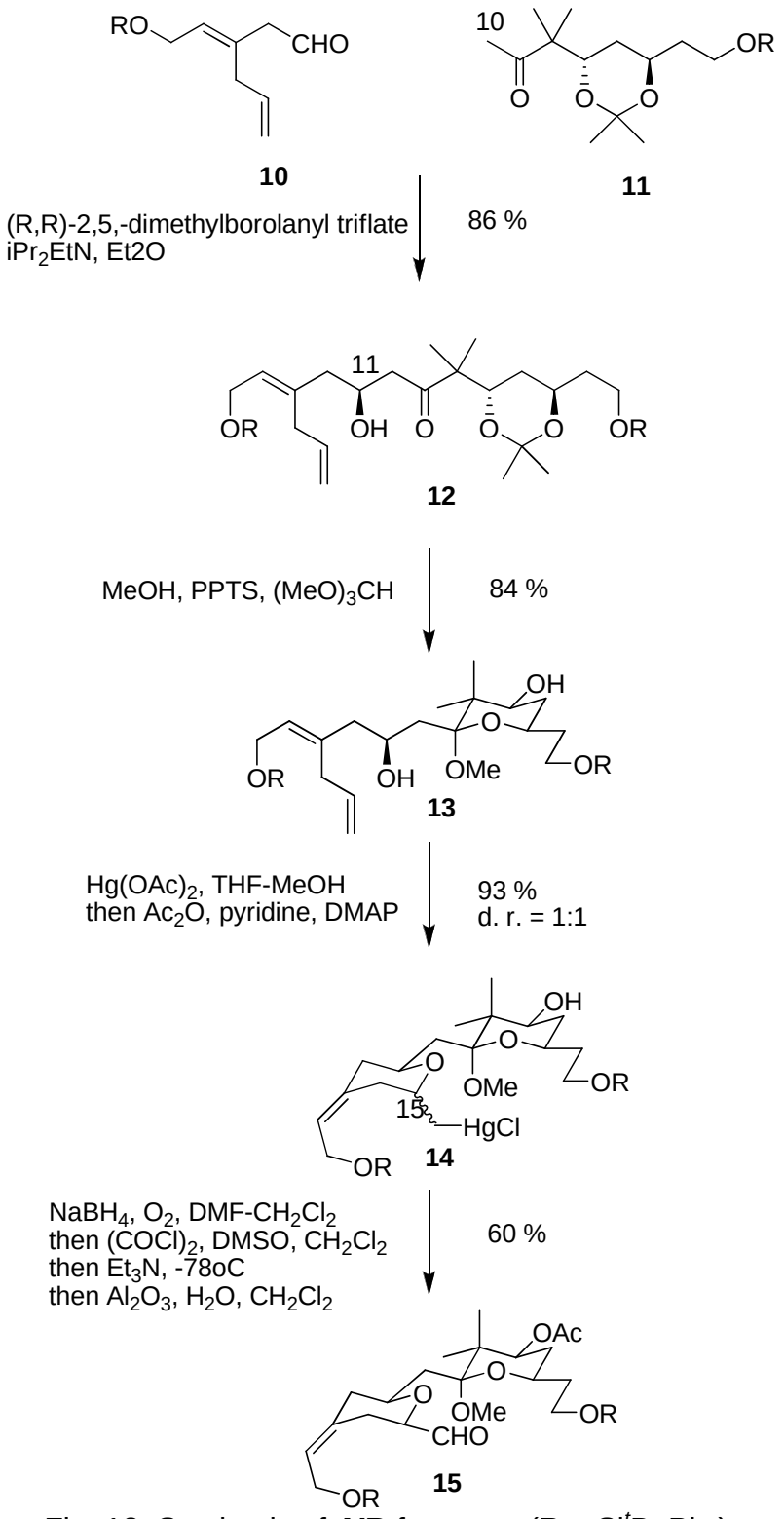

Fig. 12. Synthesis of **A′B** fragment (R = Si^{t}BuPh$_2$).

Coupling of this aldehyde **15** (ring **A′B** synthon) with ring **C** synthon **16** under Julia-Lythgoe conditions gave the tripyran **17**. Functional group interconversions (FGI) (Fig. 13) then gave the hydroxyacid **18,** which was converted to the macrocyclic lactone **19** using dicyclohexy

lcarbodiimide and pyridine (in 51 % yield). Finally, a series of FGI gave bryostatin 7 (Fig. 13).

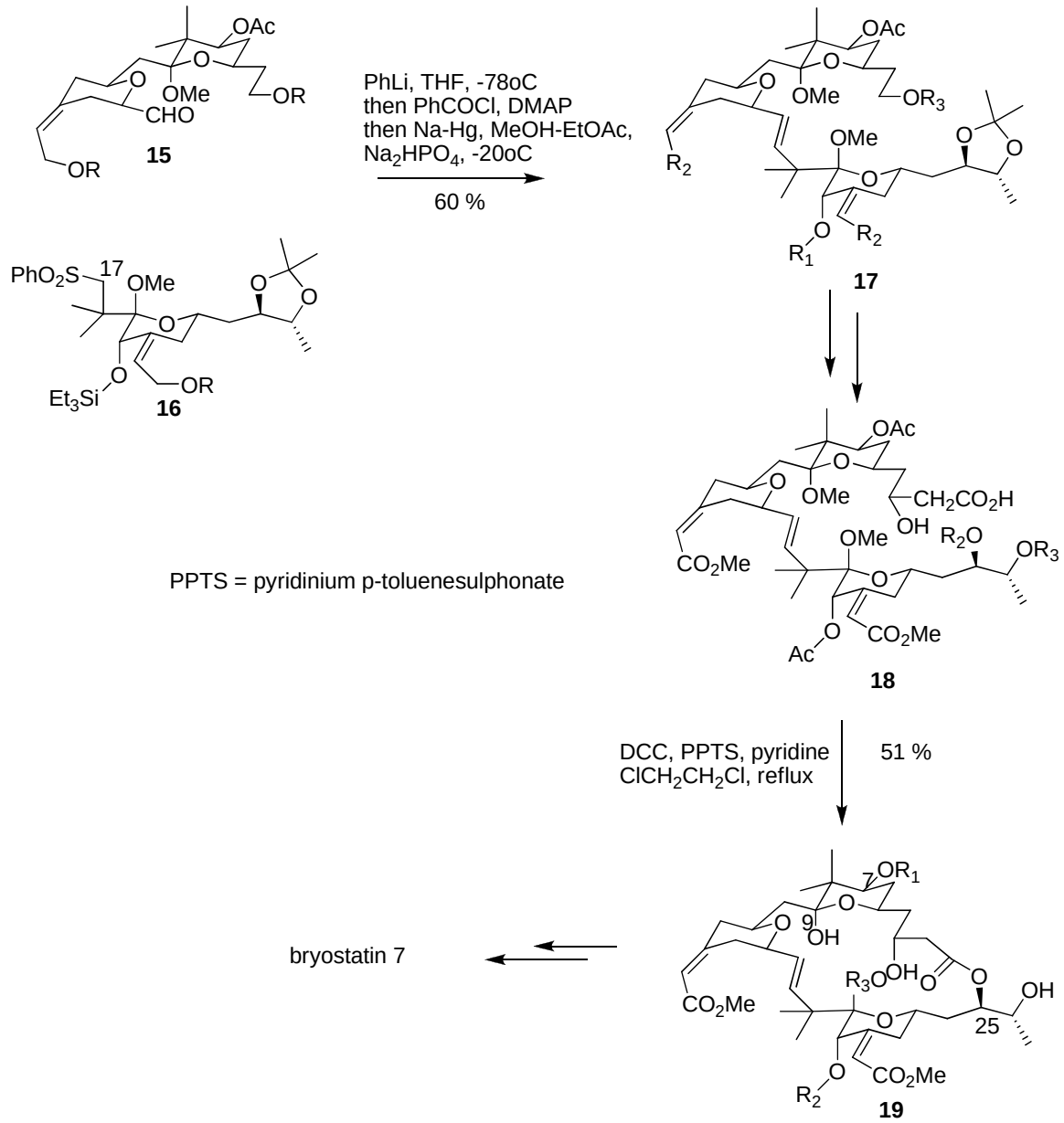

Fig. 13. Synthesis of bryostatin 7.

1.2.3 Synthesis of bryostatin 2

The synthesis of bryostatin 1[39,40] was followed by the total synthesis of bryostatin 2 by Evans *et al.*, which was then utilized by Pettit *et al.*, to prepare bryostatin 1 by a process involving the selective protection and de-protection of the C-26 hydroxyl group.[41,42] In the figure below, the retrosynthetic analysis of

the core bryostatin structure **20** led to three possible ring synthons **21-23**, all of which could be derived from *anti*-1,3-diol subunits **24-26**. Since this stereo-chemical motif is readily accessed *via* aldol reactions followed by stereo-selective reduction, this methodology forms a key part of this synthetic route to bryostatin 2.

This total synthesis will now be discussed in three main sections; synthesis of ring **A-C** synthons **21-23**, macrocyclization, and functional group transformations (including the introduction of the enoate functions onto rings **B** and **C**) on the substituted macrocycle. In discussing each of these sections, we will concentrate upon the key reactions for the introduction of essential functionality or for stereoisomer discrimination.

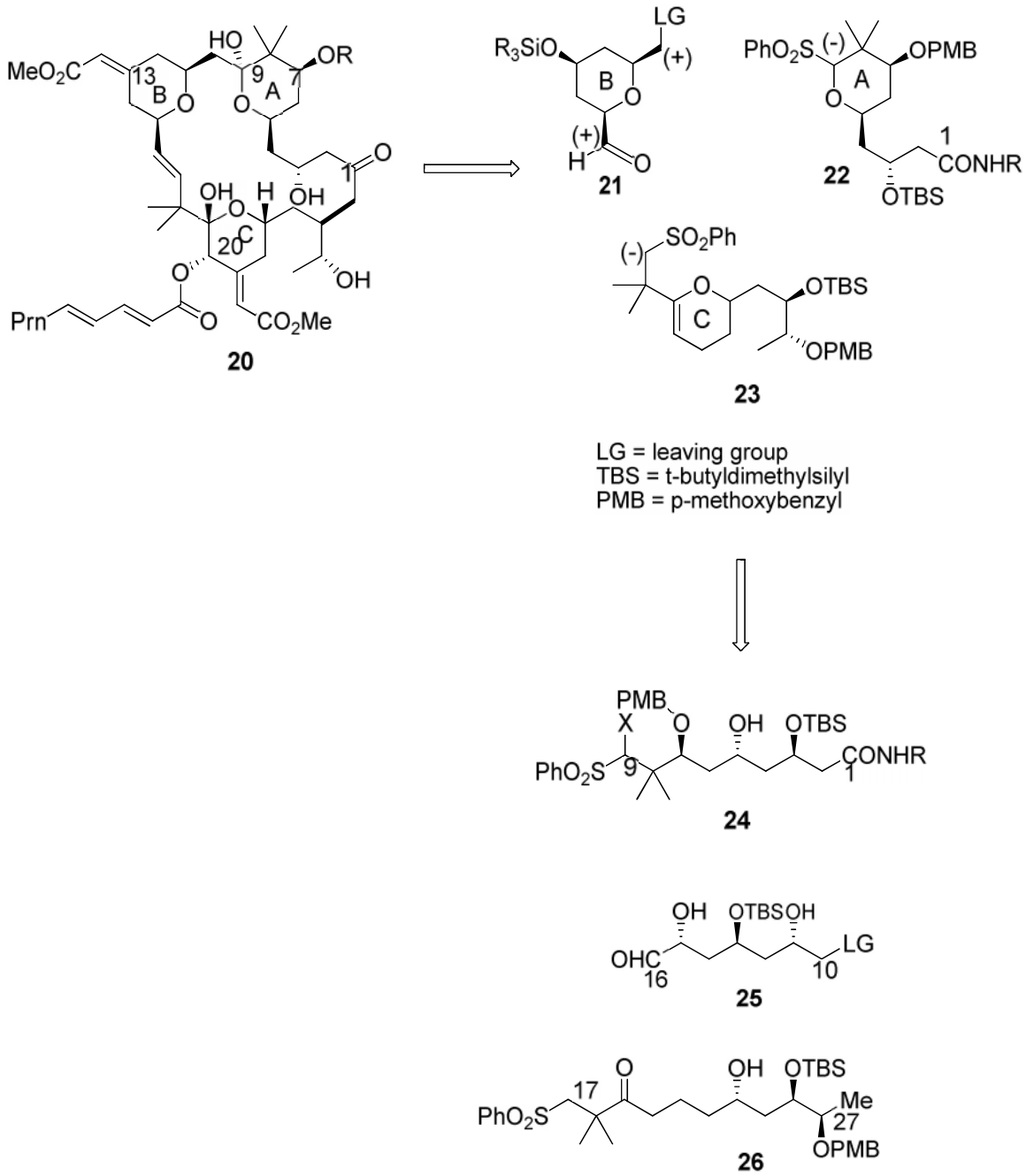

Fig. 14. Retrosynthetic analysis of bryostatin core structure.

Synthesis of the ring **A** synthon **22** began with a dibutylboron triflate-mediated aldol reaction of aldehyde **27** with the chloroacetyloxazolidinone **28** to give imide **29** (in a diastereoisomeric ratio of 90:10), followed by subsequent elaboration to give the β-alkoxyaldehyde **30 (**Fig. 15). Aldol condensation of this aldehyde **30** with the diene **31**, catalysed only by $TiCl_2(O^iPr)_2$ gave the β-hydroxyketone **32** in 83 % yield with high diastereoselectivity (94:6). Subsequent hydroxyl-directed reduction with $Me_2NBH(Oac)_3$ at -35ºC gave the diol **33**. Subsequent transformations, including cyclization, protection, oxidative cleavage,

introduction of an α-sulphone (*via* nucleophilic substitution by a thiol followed by oxidation with *m*-CPBA), and amidation (thereby allowing the metallation at C-9 required for the later coupling of rings **A** and **B**) gave the ring **A** synthon **22**.

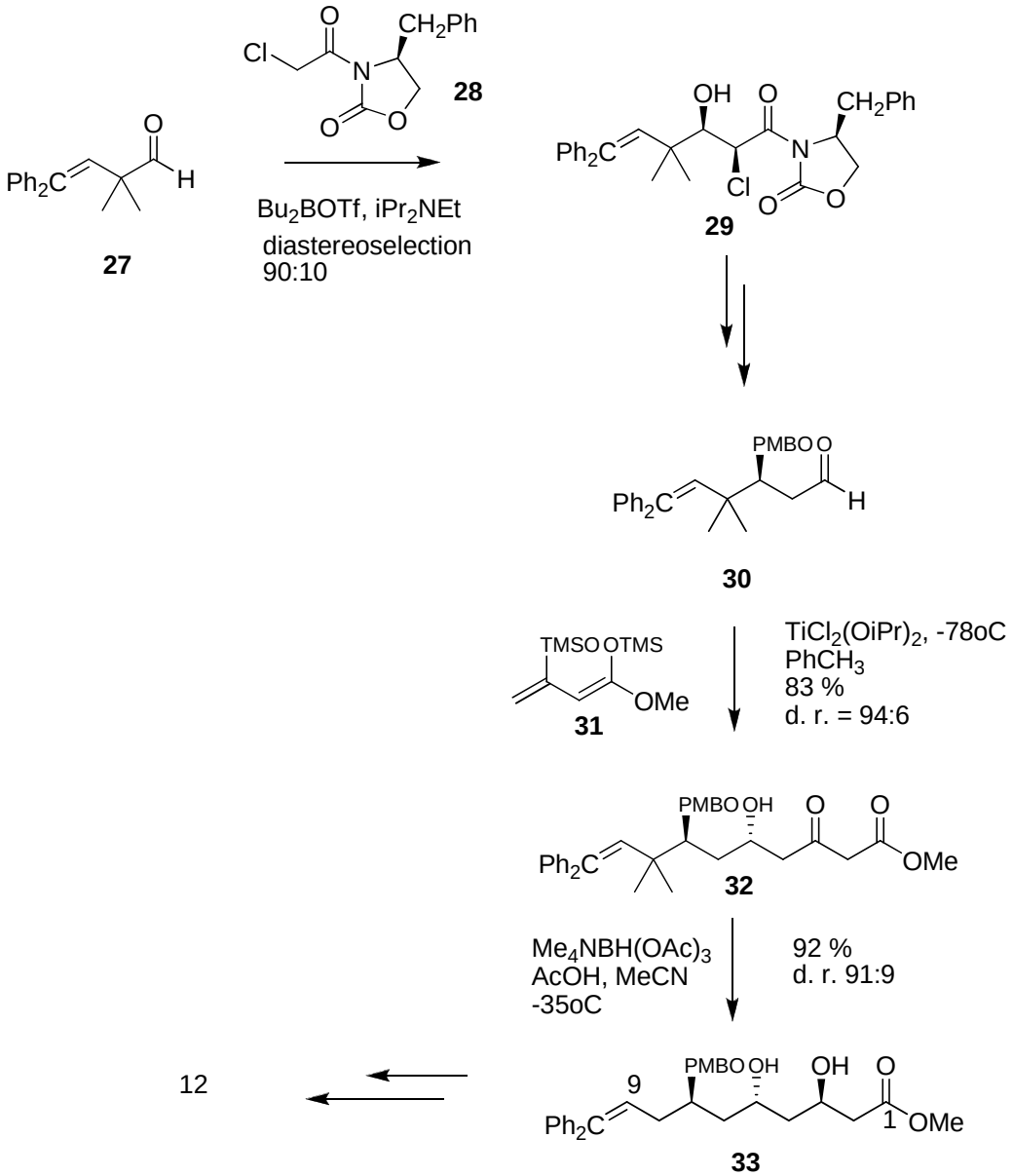

Fig. 15. Synthesis of ring **A** synthon **12**.

Synthesis of the ring **B** synthon (C_{10}-C_{16}) also began with an enantioselective aldol reaction, of diene **34** with α-benzyloxyacetophenone **35** (Fig. 16), catalysed by 5 mol% of the copper complex **36**. Once again, hydroxyl-directed 1,3-anti reduction of the β-ketoester **37** gave a diol **38** (in 91:9 diasteroisomeric ratio), which, in this case, was further elaborated to the ring **B**

synthon **21**. This elaboration included homologation (with *p*-methoxybenzyloxymethyllithium) and, finally, debenzylation and Swern oxidation.

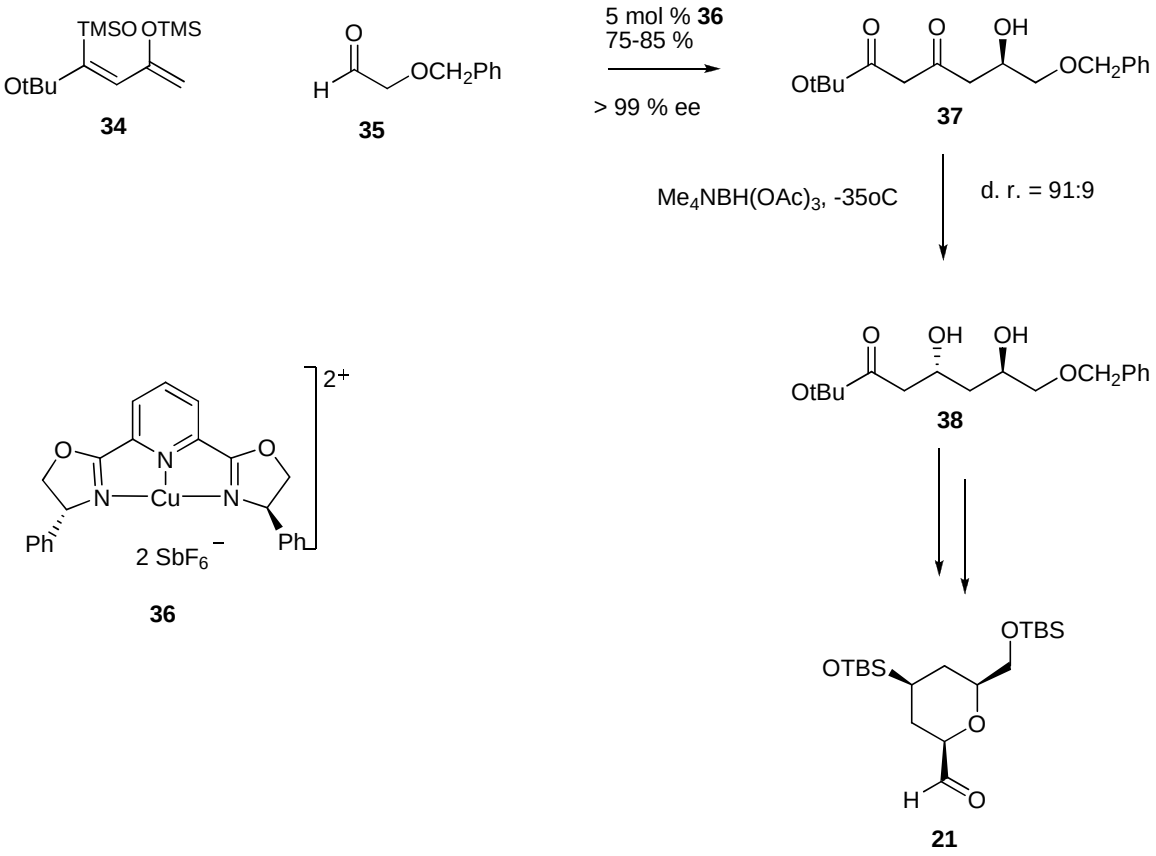

Fig. 16. Synthesis of ring **B** synthon **13**.

Synthesis of the ring **C** synthon (Fig. 17) involved an initial aldehyde **39** homologation to give aldehyde **40** (*via* a reaction sequence including a Grignard reaction with a pentenylmagnesium bromide, Swern oxidation and periodate cleavage) then an aldol addition with ketone **41**, using a chiral boryl enolate (chlorodiisopinocampheylborane) (in a diastereoisomeric ratio of 93:7) to give β-hydroxyketone **42**, followed by a samarium-promoted Tishchenko reduction to diol **43** (in a diastereoisomeric ratio of > 95:5). Further elaboration and cyclization gave the pyran (ring **C** synthon).

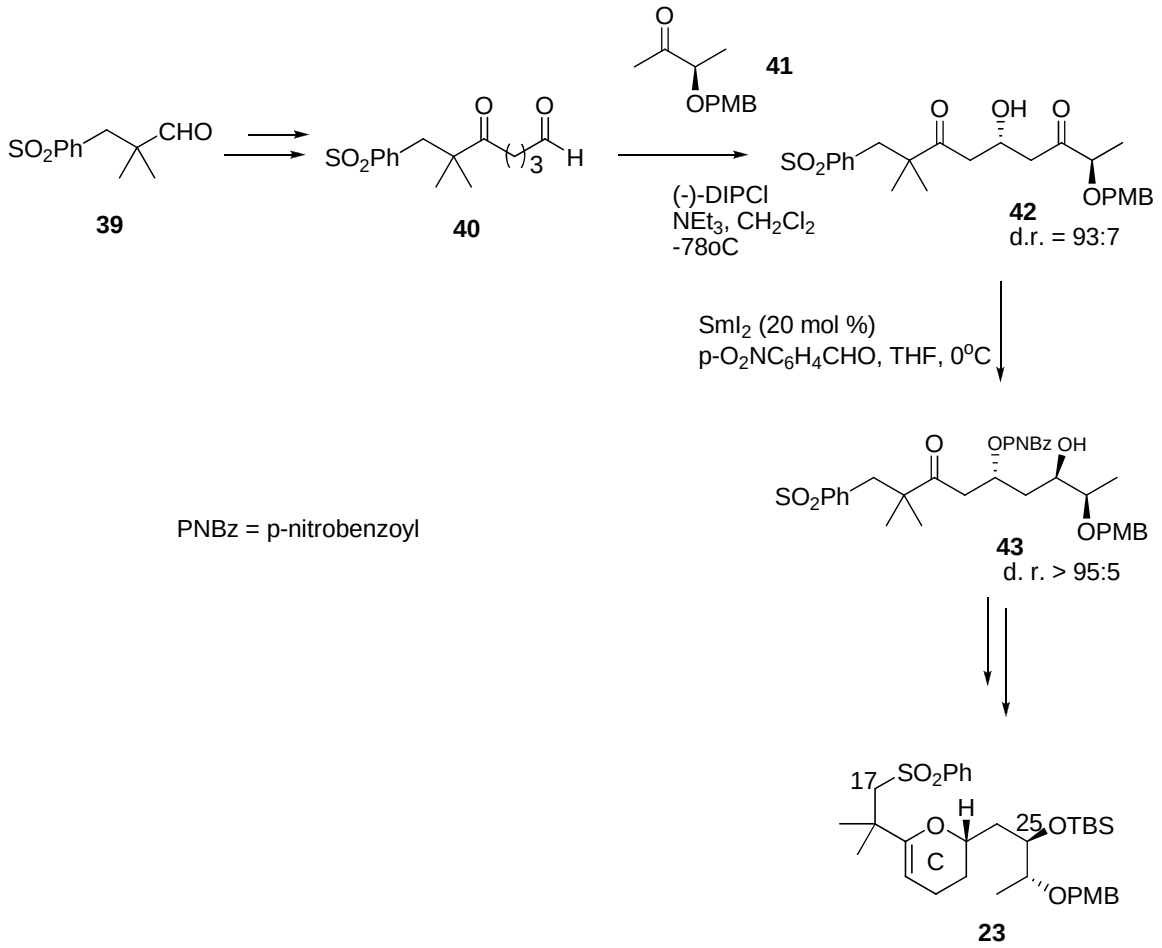

Fig. 17. Synthesis of ring **C** synthon **14**.

The preferred order of coupling of the ring synthons was established as **C** → **CB** → **CBA**. Coupling of the lithiated ring **C** synthon **23** with aldehyde **21** (ring **B** synthon) gave a hydroxysulphone which was transformed into the *trans*-olefin **44** *via* a modified Julia procedure. After selective deprotection of the 10-hydroxyl group and trifluoromethylsulphonation, the ring **CB** fragment **45** was coupled with the lithiated ring **A** synthon **22** (Fig. 18).

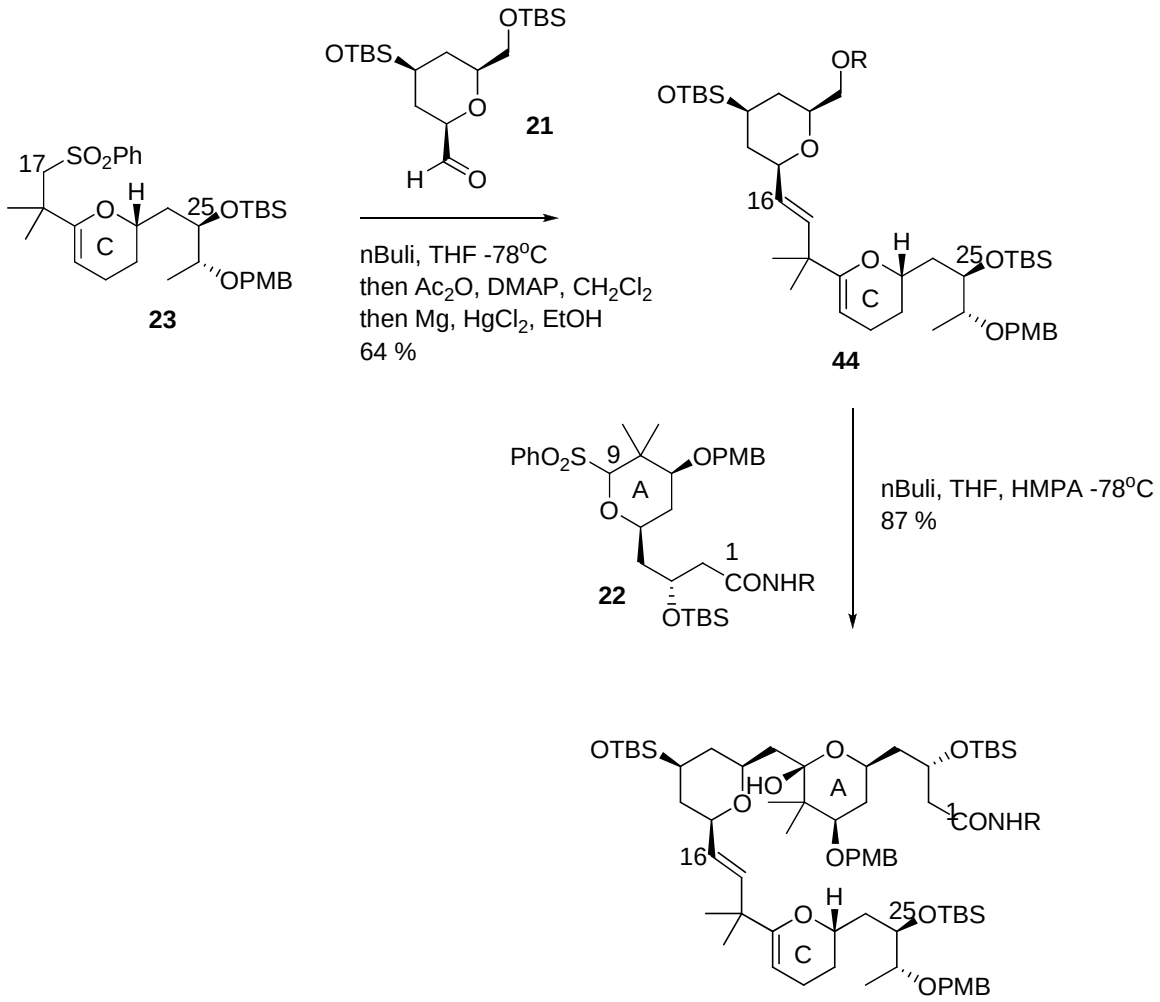

Fig. 18. Coupling of the ring **A-C** synthons.

Refunctionalization to the optimal macrocycle precursor, to give acid **46**, and lactonization *via* a modified Yamaguchi procedure (using 2,4,6-trichlorobenzoyl chloride) on the monohydroxyacid **46** gave the macrocycle **47** (Fig. 19).

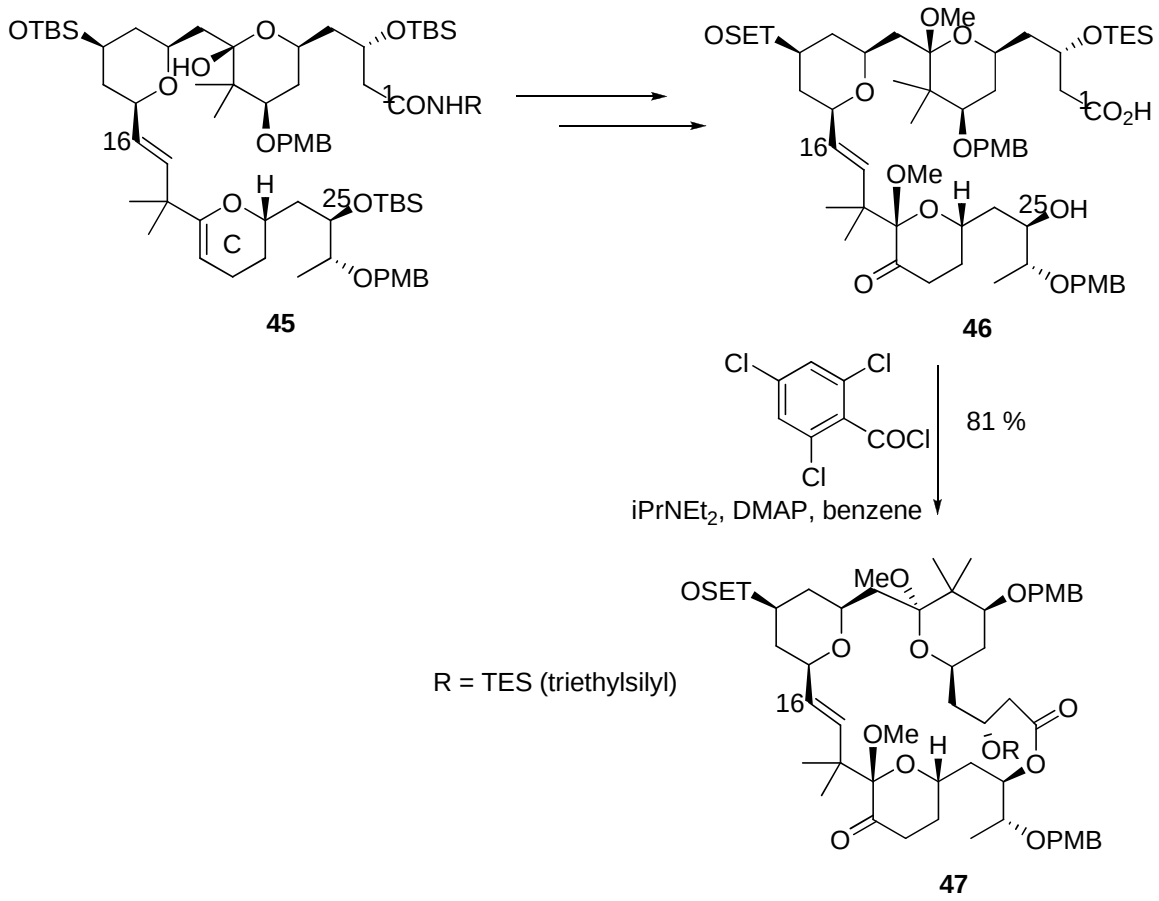

Fig. 19. Macrocyclization.

Finally, introduction of the ring **B** and **C** enoate functionalities included Dess-Martin oxidation, reaction of ring **B** pyranone **48** with the sodiated Fuji's chiral phosphonate **49** gave the enoate **50** (diastereoisomeric ratio 86:14) (Fig. 20), base-catalysed enoate **51** formation on ring **C** with $OHCCO_2Me$ (Fig. 21), reduction with a chiral boron reagent **52** (in a diastereoisomeric ratio of > 91:9) to give the ester **53** after esterification, and acylation (with diisopropylcarbodiimide, DMAP) / deprotection to give bryostatin 2.

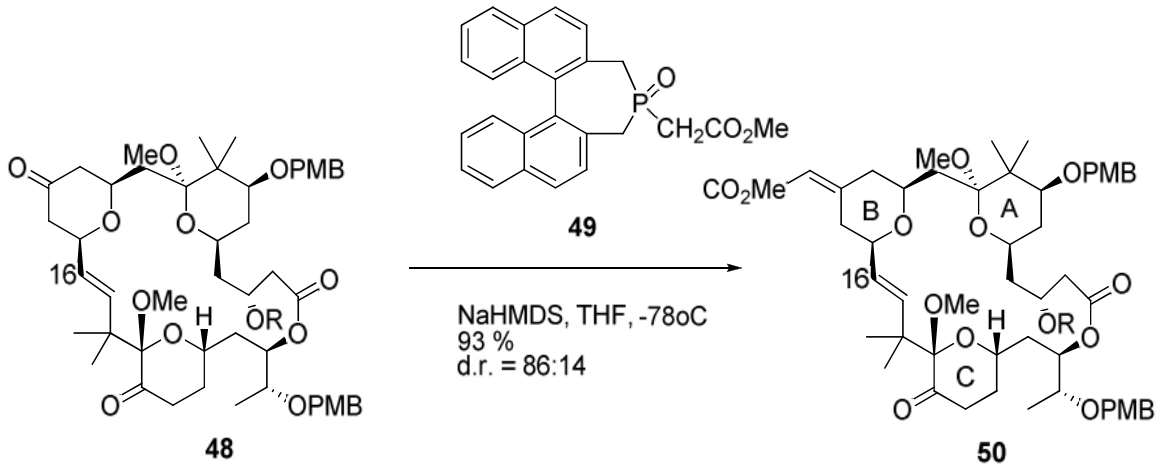

Fig. 20. Enoate formation on ring **B**.

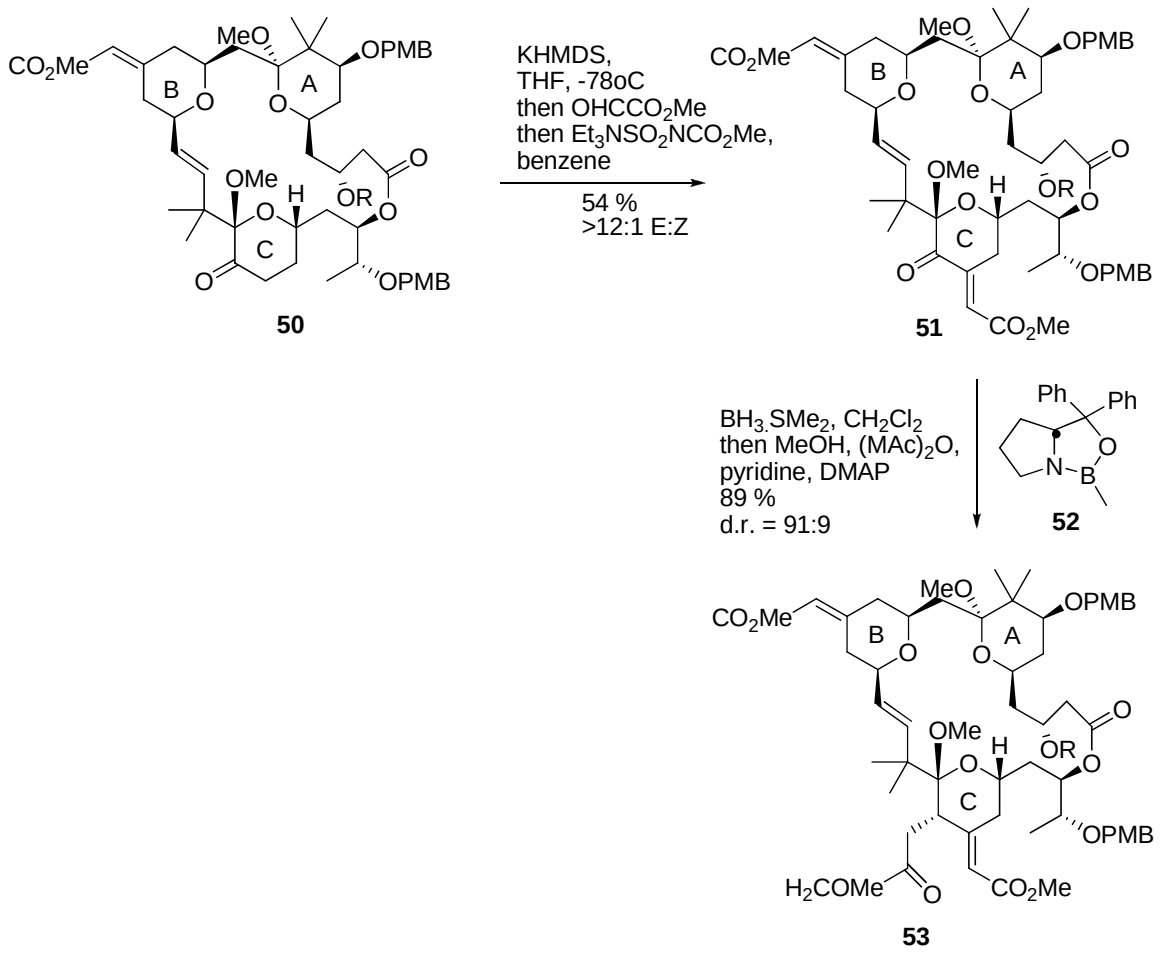

Fig. 21. Enoate formation on ring **C** and reduction.

The synthesis of bryostatin 2 by Evans and co-workers also constitutes a formal total synthesis of bryostatin 1 as an earlier report from by Pettit *et al.*, described the synthesis of bryostatin 1 from bryostatin 2 by selective protection and de-protection involving the C-26 hydroxyl group.[38]

1.2.4 Bryostatin analogues

Numerous studies have been conducted regarding the preparation of bryostatin 1 in an attempt to economically produce the drug for pharmaceutical and clinical use. Synthetic bryostatin analogues (Fig. 22) have been developed, with some having potency as effective as bryostatin 1.[43,44,45] From the analogues that have been prepared, 7b,c **54** and 8 **55** all bind strongly to PKC isozymes, with 7c showing the greatest potency of (1.8-170 ng/ml) against several human cancer cell lines. Analogue 9 **56** showed no binding affinity for PKC.[43]

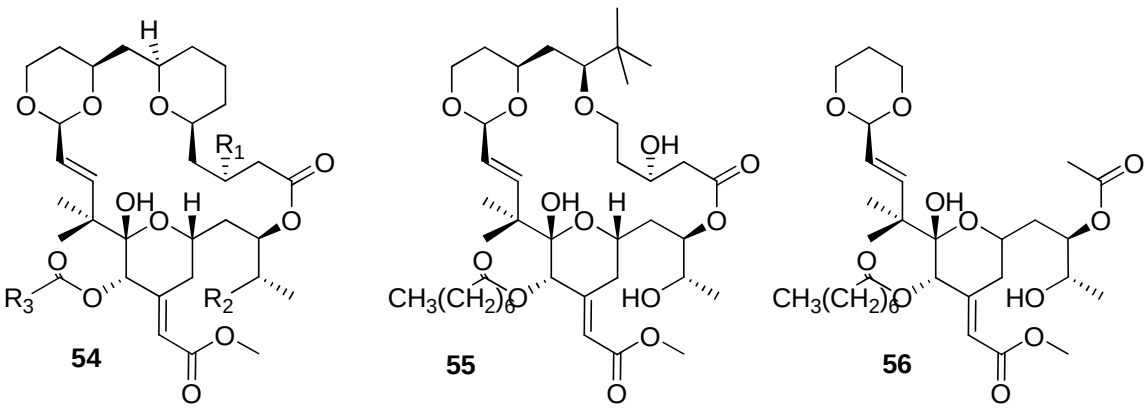

7(a-d) 8 9

7a: R1 = OH, R2 = OH, R3 = CH_3
7b: R1 = H, R2 = OH, R3 = $(CH_2)_6CH_3$
7c: R1 = OH, R2 = OH, R3 = $(CH_2)_6CH_3$
7d: R1 = OH, R2 = OAc R3 = $(CH_2)_6CH_3$

Fig. 22. Bryostatin analogues.[43]

1.2.5 Aquaculture of *B. neritina*

Aside from developing synthetic applications for the production of bryostatin 1, studies have also been conducted in order to further examine its host organism. These findings have facilitated the development of an efficient aquaculture system for the isolation of larger quantities of bryostatin 1.

Between 1990 and 1994, larva settlement experiments and laboratory facilities for grow-outs were maintained along the shore of Aqua Hedionda lagoon, San Diego, CA. The tank cultured system included seawater filters (sand, UV, carbon, 16 µm filters, and 0.2 µm filters, *etc*.), wastewater settling tank filters,

algal and zooplankton production units, and a large raceway used as a culturing tank. The process started with wild stock of *Bugula neritina* being collected from the coastal regions of Southern California and then the larvae were placed in a hatchery on artificial substrates (PVC). The larvae and substrate were then tested in greenhouse grow-outs, as well as on underwater platforms that were secured in the ocean. The *Bugula* was harvested and extracted and the bryostatin purified. This was a fairly complex approach to producing *Bugula* that included a greenhouse culture system with a capital intensive water treatment and feeding system and this paper provides many of the technical details for these grow-outs.[46]

Several important results were discussed in this paper. Firstly, the production of bryostatin 1 was not consistent. For example, in tank grow-outs the yields were disappointing and ranged from 0 to 14.2 micrograms of bryostatin 1 per gram of *Bugula*. The limiting factor in this approach is the cost of the system, the authors estimated that construction costs for a 50,000 kg/year unit would be approximately $7.5 million and a 25,000 kg/year unit would cost $4.2 million to construct. The start up cost for the first two years for the larger unit would be approximately $3.8 million and it would not produce any bryostatin in the first two years, costing approximately $2.4 million per year to maintain.[46]

In addition to the high capital and overhead cost, shifts in climate can dramatically impact the *Bugula* growth and the water temperature typically needs to drop below 22°C for an extended period of time for *Bugula* to grow. Climate effects, such as El Niño in the Pacific, can decimate a crop. In summary, this article described a sophisticated approach to growing *Bugula* but the bryostatin yields (approximately 10^{-6} %), coupled with the capital cost, have precluded it from being a viable production method.[46]

1.2.6 Symbiont bacteria in *B. neritina*

Based on the supposition that marine invertebrates ingest marine bacteria which produce the bioactive compounds found in marine organisms such as *Bugula neritina*, studies have been conducted at the Scripps Oceanography Institute to investigate this theory for the production of the bryostatins in *Bugul*a. This group has proposed that a marine bacterium is responsible for production of the bryostatins found in the bryozoa. This suggestion was based on several studies that have been conducted to determine a commonality of marine bacteria in *Bugula neritina* found along the coast of California and *Bugula* found in the Atlantic ocean (near North Carolina). Several attempts have been made to cultivate the marine bacteria, *Candidatus endobugula* sertula, which has been proposed as the key bacterium responsible for the production of bryostatin 1.[47]

Other work by this group has been conducted to show that the marine bacteria use polyketide synthase (pks) gene fragments to produce the bryophan ring, which is the basic structure of all the bryostatin compounds. To further support this work, *Bugula* was treated with antibiotics which resulted in a decreased concentration of bryostatin 1 as well as a decrease in the function of the pks genes.[48,49,50]

The different bryostatin compounds that have been isolated from the marine organism were identified in *Bugula* found in different areas of the World. For example, bryostatin 4 is extracted from *Bugula* found in the Gulf of México, the Gulf of California and the Gulf of Sagami.[51] Bryostatins 12 and 13 can be extracted from *Bugula* collected off the Eastern Pacific Ocean.[52] For this reason, this same group has also suggested that the variation in the production of all twenty known structures of the bryostatins is based on the chemotypes (M and O) in the subspecies of the bryozoa, *Bugula neritina*.[53] No conclusive evidence, however, has yet been reported for the production of the bryostatins and the

bacterium responsible for the production of the drug is yet to be isolated. In addition, all of the approaches mentioned have been unsuccessful in their attempts to produce bryostatin 1 in a cost efficient process.

1.2.7 Clinical trials

In 1984, the first European patent on the separation and purification of bryostatin 1 was published.[54] Following the isolation and identification of bryostatin 1, the drug has been used in over thirty phase I and phase II clinical trials for various cancers such as breast, kidney, prostate, and ovarian as well as Alzheimer's disease.[5] Bryostatin 1 has hydrophobic properties which restricts it from being administered easily and for this reason, it is used in an ethanol or a polyethylene glycol formulation for delivery in patients.[55] Bryostatin 1 has been successful against various cancers in clinical trials, both as a sole agent and as part of combination therapy but a few studies have been less successful. Modifications to these trials are ongoing in order to determine if any possible improvement in efficacy is possible. For example, the administering of paclitaxel (Taxol) followed by bryostatin 1 for the treatment of renal cell carcinoma gave promising results. When the drug order was reversed, however, the results showed reduced inhibition of tumour growth in comparison to Taxol alone, as bryostatin's effect on the mitosis of cancer cells resulted in decreased activity of Taxol**.**[56,57] Another study, investigating the use of bryostatin 1 against leukaemia (HL-60) cells showed that bryostatin 1 alone enhanced ULBP1 (a binding protein ligand of the NKG2D receptor, which is expressed in natural killer cells and T cells) three fold and, in combination with myeloid GFs (growth factors) and interferon-γ enhanced ULBP1 by ten fold.[58]

Studies have shown bryostatin 1 to be successful for the treatment of cervical cancer when administered synergistically with cisplatin. Based on this

finding, 50 μg/m^2 of bryostatin 1 and 50 mg/m^2 of cisplatin was administered for 1 hr every 3 wk with the results showing that 71% of patients completed both cycle treatments. The overall success of the treatment, however, was not as good in comparison to data on the use of cisplatin alone. Further studies are being conducted with both these drugs and others to determine a feasible combination for the treatment of patients with advanced carcinoma of the cervix.[59]

Table 2 summarizes the clinical trials not yet recruiting patients,[5] while Table 3 summarizes some of the many clinical trials that have been completed.[5] Table 4 summarizes the clinical trials that are no longer recruiting patients for treatment using bryostatin 1.[5] Some of the clinical trials have been less promising than others, but most suggest that bryostatin 1 is effective both, as a sole agent and in synergy with other chemotherapeutic agents.

Table 2. Clinical trials of bryostatin not yet recruiting patients. [5]

Title, Location, date	Purpose	Goals set
Safety, efficacy, pharmacokinetics, and pharmacodynamics study of bryostatin 1 in patients with Alzheimer's disease Chestnut Ridge Center, West Virginia University, Dep. Behavioural Med. and Psychiatry, Morgantown, WV Started: April 2008 NCT00606164	Phase II randomized study to determine the safety, efficacy, pharmacokinetics and pharmacodynamics of administering bryostatin 1 to patients with mild to moderate Alzheimer's disease.	To determine: 1. The safety and efficacy of a single dose of bryostatin 1 in patients. 2. How bryostatin 1 works in the body and its interaction with PKC enzymes. 3. Levels of bryostatin 1 in blood.

Bryostatin 1 has only recently been proposed as a possible treatment for Alzheimer's disease (AD) and for the reduction of brain damage due to stroke.[60] Patients with AD have an abnormality in their PKC (protein kinase c) isozymes and a deficiency of PKC function. Since bryostatin 1 is known to activate PKC isozymes, and with results from preclinical data showing the efficacy of bryostatin 1 on learning and memory, the drug has been proposed as a possible treatment

for patients with AD. This area has potential as: the highest concentration of PKC is found in the brain, PKC is involved in intracellular signalling of information passaging, and PKC inhibition impairs learning and memory. Bryostatin 1 restores dysfunction of PKC enzymes, activates classic PKC in active neurons, and stabilizes growth associated proteins necessary for long term memory.[60,61,62,63,64,65] Patients with AD also showed abnormalities in the PKC activated phosphorylation of mitogen activated protein kinase ERK1/2, a sign of early stage AD in patients.[66,67] The correlation of PKC to AD has been beneficial in the search for a suitable drug to prevent or treat the disease, and knowing that bryostatin 1 activates PKC, has made this drug a substantial marker for the treatment of AD.

Initial pre-clinical studies have been conducted by administering bryostatin 1 to Hermissenda sea slugs, in order to determine whether there was any improvement in their memory in comparison to untreated sea slugs, and the results showed that bryostatin 1 bio-chemically enhanced the memory of sea slugs. Under normal conditions, the sea slugs lost the skill of reacting in the presence of light after seven minutes, but those that were administered with bryostatin 1 retained the stimulus for at least 5 days.[68,69]

Studies have also been conducted testing the memory capacity of rats and rabbits, by teaching them to perform certain functions after administering bryostatin 1. This data was compared to rats and rabbits not treated with bryostatin 1 in order to determine the overall efficacy of bryostatin 1 in learning and memory function.[70,71,72,73] This study showed that, when given the appropriate dosage levels, the rats were able to retain the ability to perform certain tasks by memory. Treatment with bryostatin 1 also reduced any moods of depression in these animals.[72] Results from the study using rabbits showed that

the administration of bryostatin 1 has the ability to enhance classical conditioning of the nictitating membrane response in rabbit [73]

As a result of these encouraging results, more studies are currently being conducted in order to determine the potential for bryostatin 1 as a treatment for patients with AD. With approximately 5.1 million people reported to have Alzheimer's in the United States alone, the need for a prevention is imperative.[74]

Table 3. A few examples of clinical trials that have been completed. [5]

Title, Location, Date	Purpose	Goals set
Bryostatin 1, paclitaxel and cisplatin to treat patients with advanced solid tumours Memorial Sloan-Kettering Cancer Center, NY Started: February 1998 NCT00003242	Phase I trial to determine the effectiveness of administering paclitaxel, bryostatin 1 and cisplatin to patients with advanced solid tumours.	To determine: 1. The maximum tolerated dosage of bryostatin 1 when given with paclitaxel and cisplatin. 2. The pharmacokinetics of paclitaxel when combined with bryostatin 1. 3. The therapeutic activity of these drugs in patients.
Interleukin-2 plus bryostatin 1 to treat patients with melanoma or kidney cancer Massey Cancer Center, Richmond, VA Started: September 2000 NCT00006022	Phase I trial studying the modulation of the biological responses having administered bryostatin 1 for the treatment of interleukin-2.	To determine: 1. The tumour response rate and survival time after treatment. 2. The immune response of the drug in patients. 3. The tolerated dosage for treatment.
Bryostatin 1 to treat patients with relapsed non-Hodgkin's lymphoma or chronic lymphocytic leukaemia Barbara Ann Karmanos Cancer Institute Detroit, MI Started: December 1996 NCT00002908	Phase I /II trial to determine the effectiveness of bryostatin 1 in patients with relapsed non-Hodgkin's lymphoma or chronic lymphocytic leukaemia.	To determine: 1. The duration of response and survival rate after treatment. 2. The qualitative and quantitative toxicity effect of the drug in patients. 3. The efficacy of bryostatin 1 as a 72 hr infusion drug.
Bryostatin 1 and high dose cytarabine in treating patients with refractory or relapsed leukaemia or lymphoma New York Presbyterian Hospital, Cornell Campus, NY Started: September 1997 NCT00003079	Phase I trial to study the efficacy of bryostatin 1 and high doses of cytarabine in patients with refractory or relapsed acute myelocytic, acute lymphocytic leukaemia, chronic myelogenous leukaemia, and refractory or relapsed lymphoblastic lymphoma.	To determine: 1. The maximum tolerated dosage of bryostatin 1. 2. The toxicity level of bryostatin 1 and high dose level of cytarabine in patients. 3. The time course of bryostatin 1 in patients. 4. The pharmacokinetics of bryostatin 1.

Bryostatin 1 in treating patients with myelodysplastic syndrome Barbara Ann Karmanos Cancer Institute Detroit, MI Started: May 1998 NCT00003171	Phase II trial to determine the efficacy of administering bryostatin 1 in patients with myelodysplastic syndrome.	To determine: 1. The response rate in patients. 2. The qualitative and quantitative toxicity levels of bryostatin 1. 3. The duration of response and survival rate in patients.
A study of all-*trans* retinoic acid (ATRA) and bryostatin 1 in patients with acute myeloid leukaemia (AML) and myelodysplastic syndrome (MDS) Dana-Farber Cancer Institute, Boston, MA Started: May 1997 Completed: August 2000 NCT00136461	Phase II trial to study the effects of ATRA and one of two schedules of bryostatin 1 in patients with AML or MDS.	To determine: 1. The therapeutic effects of bryostatin 1. 2. The maximum tolerated dosage of retinoic acid. 3. The effectiveness of bryostatin 1 when combined with retinoic acid.
Bryostatin 1 plus gemcitabine in treating patients with advanced cancer Barbara Ann Karmanos Cancer Institute Detroit, MI Started: May 2000 NCT00004144	Phase I trial to study the effectiveness of giving bryostatin 1 with gemcitabine to patients with advanced cancer not having responded to previous chemotherapy treatments.	To determine: 1. The maximum tolerated dosage of both drugs respectively. 2. The response rate, duration of response, and overall survival rate in patients. 3. The influence of bryostatin 1 on the pharmacokinetics of gemcitabine. 4. The pattern of toxicity of the drug in patients.
Bryostatin 1 plus cladribine in treating patients with relapsed chronic lymphocytic leukaemia Barbara Ann Karmanos Cancer Institute Detroit, MI Started: May 1998 NCT00003174	Phase I trial studying the side effects and best dosage level of cladribine with bryostatin 1 to patients with relapsed chronic lymphocytic leukaemia.	To determine: 1. The maximum tolerated dosage of cladribine when combined with bryostatin 1. 2. The qualitative and quantitative toxicity level of both drugs in patients.

Bryostatin 1 in treating patients with metastatic or recurrent head and neck cancer Memorial Sloan-Kettering Cancer Center, NY Started: July 1998 NCT00003443	Phase II trial studying the efficacy of bryostatin 1 in patients with metastatic or recurrent head and neck cancer.	To determine: 1. The safety and toxicity levels of the drug in patients. 2. The anti-tumour activity of the drug in patients. 3. The cyclin dependent kinase 2 and PKC activity and apoptosis levels of cells in patients.
Bryostatin 1 plus paclitaxel in treating patients with locally advanced or metastatic oesophageal cancer or stomach cancer Albert Einstein Clinical Cancer Center, Bronx, NY Started: February 2000 NCT00005599	Phase II trial to determine the effectiveness of giving bryostatin 1 and paclitaxel to patients with advanced or metastatic oesophageal cancer or stomach cancer.	To determine: 1. The toxicity level of both drugs in patients. 2. The survival rate in patients after treatment. 3. The quality of life for patients treated. 4. The complete and partial response rate in patients. 5. The pre and post-treatment tissue biopsy markers in patients.
Bryostatin 1 plus fludarabine in treating patients with chronic lymphocytic leukaemia or relapsed indolent non-Hodgkin's lymphoma New York Presbyterian Hospital, Cornell Campus, NY Started: September 1998 NCT00005580	Phase I trial studying the success rate of bryostatin 1 and fludarabine in patients with chronic lymphocytic leukaemia or relapsed, indolent non-Hodgkin's lymphoma.	To determine: 1. The toxicity effect and maximum tolerated dosage of both drugs in patients. 2. The anti-tumour activity of both drugs. 3. The apoptosis, differentiation and PKC activity when both drugs are administered.
Bryostatin 1 plus vincristine in treating patients with recurrent or refractory HIV-related lymphoma Herbert Irving Comprehensive Cancer Centre, NY Started: August 2001 NCT00022555	Phase I trial to study the effectiveness of administering bryostatin 1 and vincristine in patients with recurrent or refractory lymphoma.	To determine: 1. The toxicity level of both drugs in patients. 2. The maximum tolerated dose of both drugs. 3. The objective response and survival rate of patients. 4. The immuno-modulatory effects on interleukin-2 (IL-2), IL-2 receptor and IL-6 cytokine levels.

		5. The effects on CD4+ lymphocyte count and HIV load. 6. The effect on human herpes virus-8 load.
Bryostatin 1 in treating patients with stage IV breast cancer University of Colorado Cancer Center, Denver, CO Started: April 1998 NCT00003205	Phase II trial to determine the efficacy of bryostatin 1 in patients with stage IV breast cancer.	To determine: 1. The clinical response of bryostatin 1 in patients. 2. The efficacy of the drug in patients. 3. The pharmacokinetics of bryostatin 1 as a 24 hr infusion drug. 4. The ability of the drug to regulate lymphocyte function. 5. The effects of the drug on platelet functions and PKC activity.
Bryostatin 1 and rituximab in treating patients with b-cell non-Hodgkin's lymphoma or chronic lymphocytic leukaemia NIH - Warren Grant Magnuson Clinical Center, Bethesda, MD Started: July 2004 NCT00087425	Phase II trial studying the efficacy of bryostatin 1 and rituximab in treating patients with B-cell non-Hodgkin's lymphoma or chronic lymphocytic leukaemia not having responded to previous treatment with rituximab alone.	To determine: 1. The safety and efficacy of both drugs in patients. 2. The effects of cells before and after treatment.
Paclitaxel and bryostatin 1 in treating patients with metastatic prostate cancer Greater Baltimore Medical Centre and Cancer Center, Baltimore, MD Started: May 2000 NCT00005028	Phase II trial to determine the efficacy of paclitaxel and bryostatin 1 in patients with metastatic prostate cancer not having responded to hormone therapy.	To determine: 1. The toxicity level of both drugs in patients. 2. The overall survival rate of patients treated. 3. The onset, duration and degree of response in patients.

Table 4. Clinical trials of bryostatin that are no longer recruiting patients. [5]

Title, Location, Date	Purpose	Goals set
Bryostatin 1 plus cisplatin in treating patients with recurrent or advanced cancer of the cervix Albert Einstein Comprehensive Cancer Center, Bronx, NY Started: August 2000 NCT00005965	Phase II trial to study the effectiveness of cisplatin and bryostatin 1 in patients with recurrent or advanced cancer of the cervix.	To determine: 1. The efficacy and safety of both drugs in patients. 2. The response rate, progression free interval and duration of survival in patients.
Bryostatin 1 and cytarabine in treating patients with relapsed acute myelogenous leukaemia Herbert Irving Comprehensive Cancer Center, Columbia University, NY Started: July 2001 NCT00017342	Phase II trial to determine the efficacy of giving bryostatin 1 and cytarabine to patients with relapsed primary acute myelogenous leukaemia.	To determine: 1. The toxic effect of both drugs in patients. 2. The relapse-free survival and overall survival in patients. 3. The response rate in patients.
Bryostatin 1 plus paclitaxel in treating patients with stage IIIB, stage IV, or recurrent NSCLC Central Illinois Haematology Oncology Center, Springfield, IL Started: April 2000 NCT00005849	Phase II trial to determine the efficacy of both drugs in patients with stage IIIB, stage IV or recurrent non-small cell lung cancer.	To determine: 1. The overall survival and progression rate. 2. The T-cell subset analysis and serum levels of interleukin-6 and tumour necrosis factor alpha after receiving bryostatin 1. 3. The overall, partial and complete response rate after treatment.
Bryostatin 1 and cisplatin in treating patients with metastatic or unresectable stomach cancer City of Hope Comprehensive Cancer Center, Duarte, CA Started: November 2000 NCT00006389	Phase II trial to determine the efficacy of bryostatin 1 and cisplatin in patients with metastatic or unresectable stomach cancer.	To determine: 1. The toxicity levels of both drugs in patients. 2. The molecular determinant response of the drugs in patients. 3. The response and survival rate in patients.

Paclitaxel and bryostatin 1 in treating patients with locally advanced, unresectable or metastatic pancreatic cancer Albert Einstein Clinical Cancer Center, Bronx, NY Started: January 2002 NCT00031694	Phase II trial to determine the effectiveness of paclitaxel and bryostatin 1 for the treatment of locally advanced unresectable or metastatic pancreatic cancer.	To determine: 1. The response and survival rate of both drugs in patients. 2. Any toxicity and pharmacokinetic effects of the drugs in patients.
Bryostatin 1 and cisplatin in treating advanced recurrent or residual ovarian epithelial, fallopian tube, or primary peritoneal cancer Cedars-Sinai Comprehensive Cancer Centre, Cedars-Sinai Medical Center, LA, CA Started: January 2001 NCT00006942	Phase II trial to study the efficacy of administering bryostatin 1 and cisplatin to patients with advanced recurrent or residual ovarian epithelial, fallopian tube, or primary peritoneal cancer.	To determine: 1. The duration of response in patients. 2. The toxicity level of both drugs in patients. 3. The overall response rate and the complete response rate of both drugs in patients.
Combination chemotherapy in treating patients with chronic lymphocytic leukaemia, non-Hodgkin's lymphoma, or multiple myeloma Ireland Cancer Center, Cleveland, OH Started: May 1998 NCT00003166	Phase I trial to determine the efficacy of bryostatin 1 and vincristine in patients with chronic lymphocytic leukaemia, non-Hodgkin's lymphoma, or multiple myeloma.	To determine: 1. The maximum tolerated dosage of bryostatin 1 when combined with vincristine. 2. The clinical response of both drugs in patients.
Combination chemotherapy in treating patients with unresectable locally advanced or metastatic stomach cancer University of Texas, MD Anderson Cancer Center, Houston, TX Started: June 2000 NCT00006081	Phase II trial to study the effectiveness of both bryostatin 1 and paclitaxel to treat patients with unresectable locally advanced or metastatic stomach cancer.	To determine: 1. The qualitative and quantitative toxicity levels of both drugs in patients. 2. The response rate of the drugs in patients.

1.2.8 Cell line tests

The first cell line testing on bryostatin 1 was conducted in the 1960s when bryostatin 1 was injected into laboratory mice carrying a PS-100 leukaemia virus strain and showed potency as a promising medicinal agent. Since then, *in vitro* trials have shown bryostatin 1 to act synergistically with other anti-cancer drugs, modulating PKC activity and having effective anti-leukaemia activity and efficacy against lung, prostate and non-Hodgkin's lymphoma tumour cells. *In vivo* trials have also shown that bryostatin 1, along with the calcium ionophore ionomycin, activates T-cells from murine tumour lymph nodes, and represents a possible anti-tumour agent.[75] Bryostatin 1 and IM (imatinib mesylate, a tyrosine kinase inhibitor) were recently tested for activity (of both compounds alone and synergistically) against chronic myeloid leukaemia of stem cell origin. Results from this study showed that bryostatin 1 alone did not suppress the cell cycle progression of K562 cells, but IM alone resulted in the inhibition of these cells (at initial concentrations of 5 μM). The effects of both drugs in combination were no different to results of IM alone, but the administration of bryostatin 1 prior to IM led to a significant reduction in the K562 cell numbers.[76] Tables 5 and 6 outline the numerous cell line tests that have been conducted with bryostatin 1, both synergistically and as a sole agent.

Table 5. Some of the earliest recorded cell line tests using bryostatin 1 both as a sole agent and in combination with other anti-cancer agents.

Title	Purpose	Results
Three activators of PKC, bryostatin, dioleins and phorbol esters, show differing specificities of action on GH4 pituitary cells.[77]	To examine the actions on GH4C5 cells of TPA (12-O-tetradecanoylphorbol-13-acetate) and two other classes of protein kinase C activators, synthetic cell permanent dioleins and bryostatin 1.	Data showed that bryostatin 1, diolein and phorbol esters all bind to the same site on PKC. Each drug altered the biological responses in GH4C5 cells, with selectivity and efficacies that differ in each.
Bryostatin 1 antagonizes the terminal differentiating action of 12-O-etradecanoylphorbol-13-acetate in human colon cancer cells.[78]	Identification of the cellular processes involved in the induced terminal differentiation of human colon cancer cells.	Bryostatin 1 completely counteracted the effects of TPA and promoted continued replication of the cells.
Bryostatin 1, an activator of protein kinase C, mimics as well as inhibits biological effects of the phorbol ester TPA *in vivo* and *in vitro*.[79]	To understand the TPA effects that can be induced by bryostatin 1.	Results showed that bryostatin 1 inhibited the specific Ca^{2+} ion component of TPA action.
Bryostatin 1 activates protein kinase C and induces monocytic differentiation of HL-60 cells.[80]	To determine if the induction of differentiation may involve the activation of phorbol ester in PKC (phospholipid and calcium dependent).	Bryostatin 1 trans-located the activity of PKC from the cytosol to the membrane in HL-60 cells. Bryostatin 1 also induced the growth of HL-60 cells.

Table 6. Some of the most recent cell line tests on bryostatin, both as a sole agent and in combination with other drugs.

Title	Purpose	Results
Simplified analogues of bryostatin with anti-cancer activity display great potency for translocation of PKC delta GFP.[81]	To highlight the importance of using binding affinity in conjunction with standard measurements of protein localization for the pharmacological profiling of biologically active agents.	The potency of the compounds to induce the translocation responses, which appeared to be only qualitatively related to binding affinity of PKC.
Bryostatin 1 and UCN-01 potentiate 1β-D-arabino furanosylcytosine induced apoptosis in human myeloid leukaemia cells through disparate mechanisms.[82]	To study the effects of bryostatin 1 and 7-hydroxystaurosporine (UCN-01) for the treatment of human myelomonocytic leukaemia cells.	The potentiation of ara-C lethality in human leukaemia cells by bryostatin 1 involves the activation of PKC.
Bryostatin 1 a novel PKC inhibitor in clinical development.[83]	A review on the modulation of PKC, which represents a novel approach to cancer therapy.	Short-term exposure to bryostatin 1 showed to promote activation of PKC, and prolonged exposure to bryostatin 1 significantly promotes the down-regulation of PKC.
The anti-neoplastic agent bryostatin 1 differentially regulates interferon γ receptor subunits in monocytic cells: transcriptional and post transcriptional control of interferon γ R_2.[84]	To investigate the effects of bryostatin on the expression and regulation of INF (interferon) γ chains in monocytic cells.	Bryostatin up-regulates INF-γ R_2 expression in monocytic cells. Bryostatin 1 also showed the ability to overcome some of the immunological defects observed in cancer patients.

1.2.9 Bryostatin and Protein Kinase C

Protein kinases C (PKC) are enzymes that regulate the activity of intracellular signalling pathways for hormones, growth factors, neurotransmitters and cytokines. These enzymes catalyse the modification of amino acids such as serine, tyrosine and theonine by phosphorylation. Protein kinases play a significant role in cellular responses arbitrated by diacylglycerol **57** (DAG, Fig. 23) and phorbol ester **58** (Fig. 24), two tumour promoters.(85)

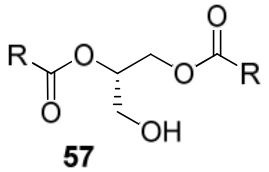

57

Fig. 23. Structure of 1,2 diacyl-sn-glycerol (DAG). The R groups represent alkyl groups.

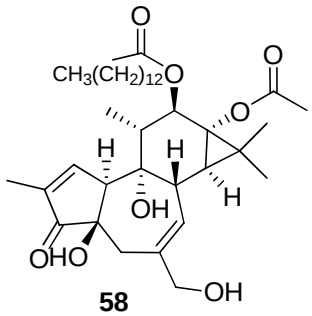

58

Fig. 24. The most common phorbol ester, 12-O-tetradecanoylphorbol-13-acetate (TPA), a tumour promoter that mimics the action of DAG on PKC.

The structure of PKC is unknown, but it is said to consist of a regulatory and a catalytic domain (Fig. 25). The regulatory domain consists of two sub regions, C_1 and C_2. The C_1 domain contains the binding site for both DAG and phorbol ester, and the C_2 domain functions as a Ca^{2+} sensor, which consists of three regions (aPKC, nPKC, and cPKC) comprising 40% of the amino acid sequence.(82) Uncontrolled proliferation resulting in cancerous cells is believed to be related to the dysregulation of PKC signalling, however in other aspects it only affects mitogenic signalling. This shift can be correlated to the different isozymes of PKC, resulting in the formation of different uncontrolled proliferations.(86)

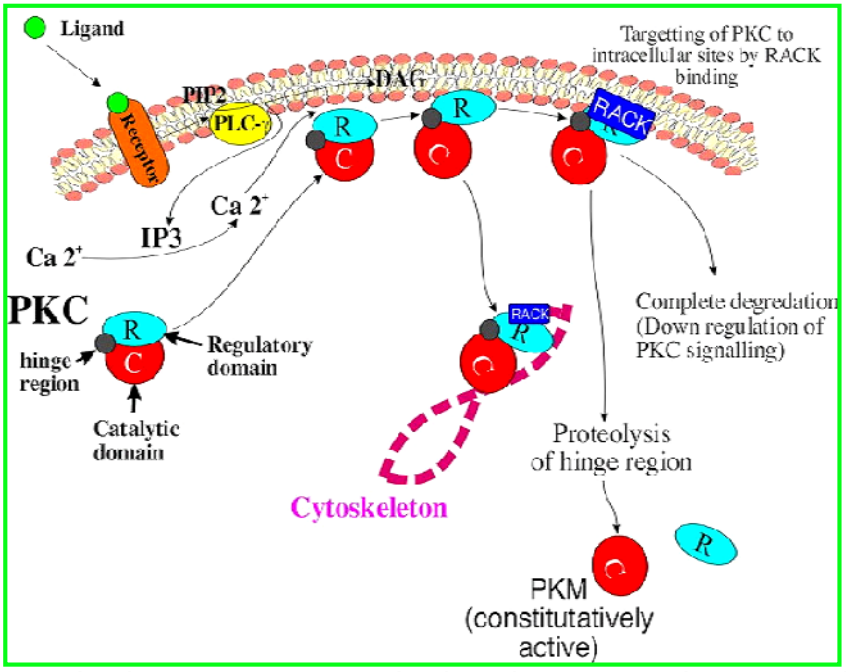

Fig 25. The activation of PKC towards the plasma membrane resulting in the down-regulation of the enzyme by separating the enzyme into two regions (catalytic and regulatory).[87]

Bryostatin 1 transforms the activity of PKC in competing with DAG and phorbol ester for the binding site on the enzyme, inducing the initial activation and translocation of PKC by binding to the C_1 regulatory domain on the kinase; resulting in the down-regulation of the PKC enzyme at the plasma membrane and the sensitization of cancer cells in the body.[88,89] For example, bryostatin 1 activates PKC from leukaemia cells *in vitro* and decreases the cytoplasmic activity *in vivo*.[90] When the PKC enzymes are activated, they move towards the plasma membrane and bind to it, releasing the regulatory domain, where the process is repeated again.

In addition to bryostatin 1 activating PKC, it also affects cell cycle regulatory protein p21. Inhibition of p21, as well as cdk2 (cyclin d kinase 2), has been correlated with the inhibition of tumour growth in cells treated with bryostatin 1.[91] A recent study supported the claim that bryostatin 1, a PKC agonist, limits the growth of K-Ras12V dependent tumours. This showed that bryostatin 1 has specific activity against these cells as there was no effect on K-Ras12V181A cells. This specificity is proposed to be due to the presence of S181 in K-Ras12V

cells (S181 are phosphate acceptors at the C-terminal region of K-Ras, which mediates the localization of K-Ras as a direct substrate for PKC) resulting in the degradation of those cells.[92]

1.2.10 Problems with production

As mentioned earlier, despite bryostatin's activity as a prominent anti-cancer agent, there are several factors that limit its production, availability and universal application. The collections of approximately 14 tons of *Bugula neritina* from its marine environment is needed to extract 18 g of the drug, with yields of 10^{-6} %. Retrieving the drug by this method is time consuming, expensive and poses numerous ecological concerns. For this reason, the accessibility and high cost for quality pure bryostatin 1 is prohibitive, costing millions of USD per gram of the drug. Several other techniques such as aqua culture (section 1.2.5), the genetic determination of the bacteria in the marine organism (section 1.2.6), and microbial broths have been attempted in the hope of making drug production more economically feasible. The seasonal availability and large quantity of *Bugula* needed for the extraction and purification results in the recovery of only minute quantities of bryostatin 1.

1.3 Sea squirt

Tunicates (Fig. 26) are sessile filter feeders that grow to about 5 cm tall and 4 cm inches wide. They have a flexible, tough outer surface, usually greyish green in colour and can often be found attached to rocks and mangrove roots in the Caribbean Sea and in the West Indies. These organisms have two cavities in their body, an incurrent siphon for taking in food and an excurrent siphon for excreting waste material from the body. Ecteinascidin 743 **60b** (Et-743, Fig. 27) also known as Yolendis or Trabectedin, is a marine natural product extracted

from the sea squirt, *Ecteinascidia turbinata*.[3,93] This tetrahydroisoquinoline marine alkaloid was first studied for medicinal activity in the 1970s and was isolated in 1990 from sea squirt found in the West Indies by Rinehart *et al*..[93,94] Later, the drug was licensed by PharmaMar, Spain.[95]

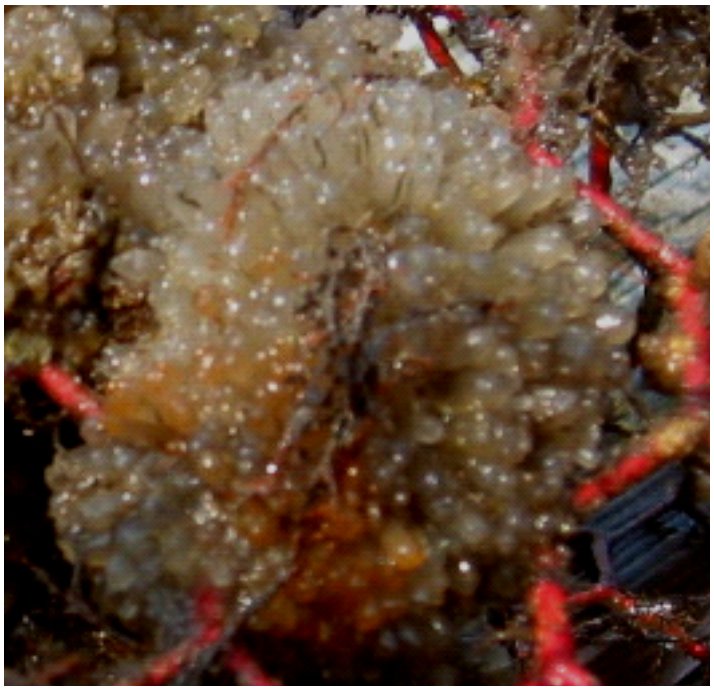

Fig. 26. Sea squirt, *Ecteinascidia turbinata*, attached to a crab trap in Panacea, Fl.

A total of 8 ecteinascidin compounds (Fig. 27, Table 7) have been isolated from the sea squirt and a total of 4 analogues (Fig. 28, Table 8) have been prepared as shown below.[96]

Table 7. Ecteinascidin compounds characterized by different R groups. The numbers shown in brackets represent the different structures for each compound shown below.[96] Molecular formula $(M+H-H_2O)^+$ determined by HRFABMS.

Et- compounds	Molecular formula	Molecular ion formula	R_1	R_2
Et-729 (**60a**)	$C_{38}H_{41}N_3SO_{11}$	$C_{38}H_{39}N_3SO_{10}$	H	OH
Et-722 (**59**)	$C_{39}H_{40}N_4O_9S$	$C_{39}H_{38}N_4SO_8$	H	OH
Et-736 (**59**)	$C_{40}H_{42}N_4O_9S$	$C_{40}H_{40}N_4SO_8$	CH_3	OH
Et-743 (**69b**)	$C_{39}H_{43}N_3O_{11}S$	$C_{39}H_{41}N_3SO_{10}$	CH_3	OH
Et-745 (**60c**)	$C_{39}H_{45}N_3SO_{11}$	$C_{39}H_{43}N_3SO_{10}$	CH_3	H_2
Et-759A (**60d**)	$C_{39}H_{43}N_3O_{12}S$	$C_{39}H_{41}N_3SO_{11}$	CH_3	OH
Et-759B (**60e**)	$C_{39}H_{43}N_3O_{12}S$	$C_{39}H_{41}N_3SO_{11}$	CH_3	OH
Et-770 (**60f**)	$C_{40}H_{42}N_4SO_{10}$	$C_{40}H_{42}N_4SO_{10}$	CH_3	CN
Et-776 (**60g**)	$C_{40}H_{45}O_{11}N_3S$	$C_{40}H_{46}O_{11}N_3S$	CH_3	OMe

* Et-759A/B: S-oxide

(**a**)

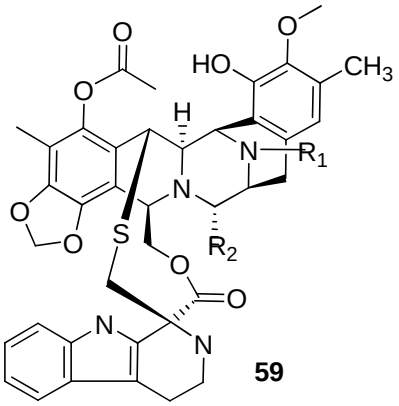

59

(**b**)

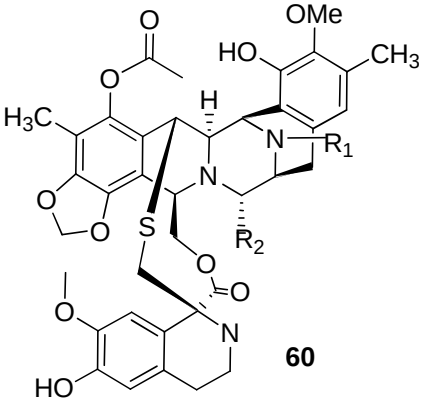

60

Fig. 27. The structures for the ecteinascidin compounds in Table 7.

Table 8. Ecteinascidin compounds characterized by different R groups. The numbers shown in brackets represent the structures for each compound shown below.[96] Molecular formula $(M+H-H_2O)^+$ determined by HRFABMS.

Et compounds	Molecular formula	Molecular ion formula	R_1	R_2	X	Y
Et-583 (c1)	$C_{29}H_{33}N_3SO_8$	$C_{29}H_{33}N_3SO_8$	H	OH	OCH_3	OH
Et-597 (c2)	$C_{30}H_{35}N_3SO_8$	$C_{30}H_{35}N_3SO_8$	CH_3	OH	OCH_3	OH
Et-594 (d1)	$C_{30}H_{30}N_2SO_9$	$C_{30}H_{30}N_2SO_9$	CH_3	OH	XY: O-CH_2-O-	
Et-596 (d2)	$C_{30}H_{32}N_2SO_9$	$C_{30}H_{32}N_2SO_9$	CH_3	OH	OCH_3	OH
Et-637 (e1)	$C_{30}H_{35}N_3SO_9$	$C_{30}H_{35}N_3SO_9$	CH_3	OH	XY: O-CH_2-O-	
Et-637-OBu (e2)	$C_{34}H_{40}N_2SO_{11}$	$C_{34}H_{40}N_2SO_{11}$	CH_3	OH	XY: O-CH_2-O-	

(**c**)

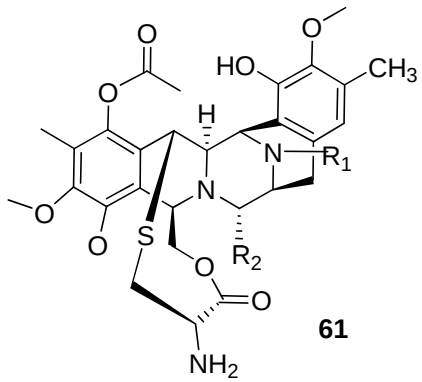

61

(c1: R = H; c2: R = CH_3)

(**d**)

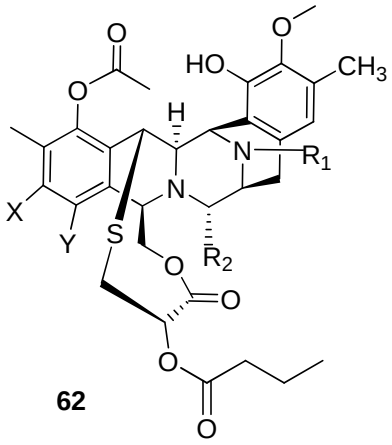

62

(d1: XY(C-CH_2-O); d2: X = OCH_3; Y - OH)

(**e1**) (**e2**)

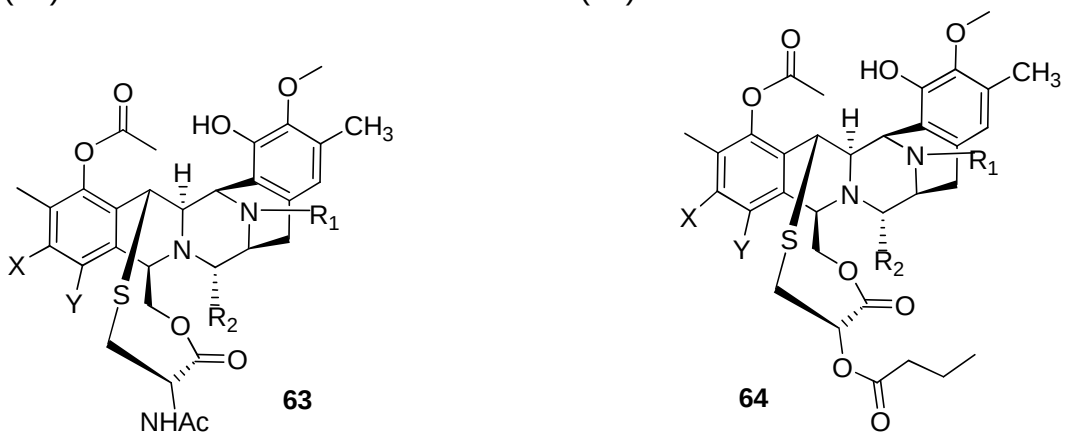

Fig. 28. The structures for the ecteinascidin analogues in Table 8.

Aside from the extraction of different ecteinascidin compounds and saframycin metabolites from the sea squirt, *Ecteinascidia turbinata,* other compounds have been isolated with potential antibiotic activity. Two of the antibacterial bisanthraquinone metabolites **65** and a cytotoxic artifact **66** (Fig. 29), were isolated from a cyanobacterium associated with the sea squirt. Both metabolites showed efficacy against *Staphylococcus aureus,* with an IC_{50} of 0.15−130 μM.[97] The identification of these metabolites from the sea squirt further supports the idea that these organisms ingest the bacteria responsible for the production of such medicinal agents.

(a) (b)

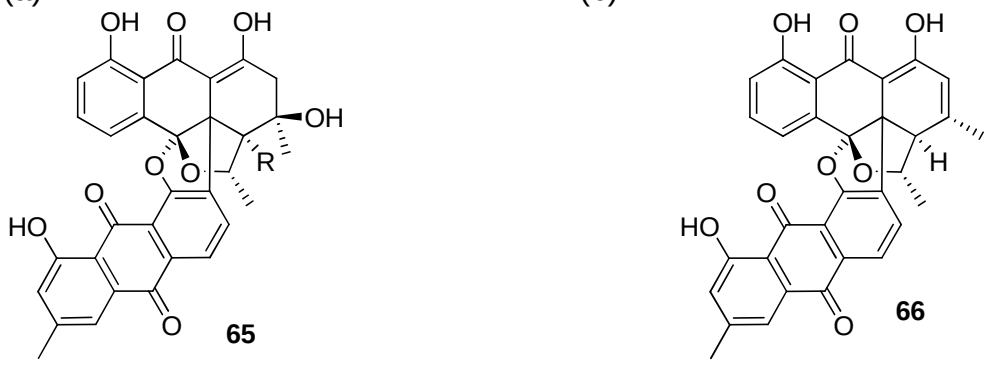

R1 = H; R2 = OH

Fig. 29. a) The two antibacterial metabolites identified by the change in R groups, and b) the cytotoxic artifact isolated from the cyanobacterium associated with the sea squirt, *Ecteinascidia turbinata*.[97]

1.3.1 Et-743

The total synthesis of Et-743 was carried out by Corey *et al*., in 1996.[98] Shortly after, a twenty one step semi-synthesis of the drug was achieved by Corey, Martinez *et al.*.[99] In 2002 another route to the total synthesis of Et-743 was achieved by Fukuyama *et al*..[100] In 2003, another group developed an asymmetric synthesis for the production of the ecteinascidin compounds by using a tyrosine derivative as the basic building block in an overall yield of 39%.[101]

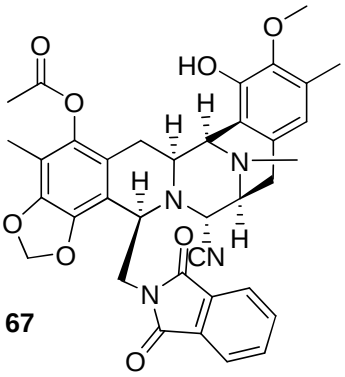

67

Fig. 30. Phthlascidin 650 ($C_{36}H_{34}N_4O_8$, 650.2371 g/mol), a synthetic analogue of Et-743, with anti-tumour properties. Phthlascidin an IC_{50} of 5 0.1–1 nM agonist.

Phthlascidin 650 **67** (Fig. 30), a synthetic analogue of Et-743, has been prepared by Corey *et al*., and shows similar cytotoxic effects to Et-743.[102] Since the discovery of Et-743, other ecteinascidin compounds have been identified, along with the production of different analogues of the drug, with some having greater activity than others, but Et-743 still remains the most potent.[93,103]

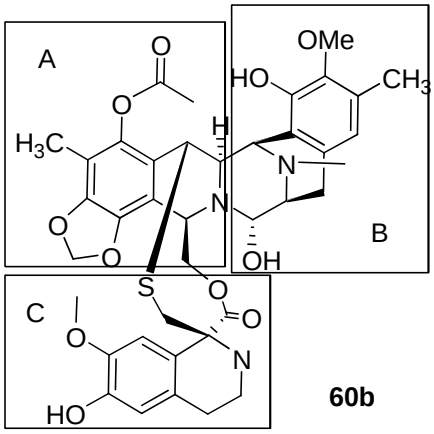

60b

Fig. 31. Et-743 separated into three building blocks (A, B and C).[104]

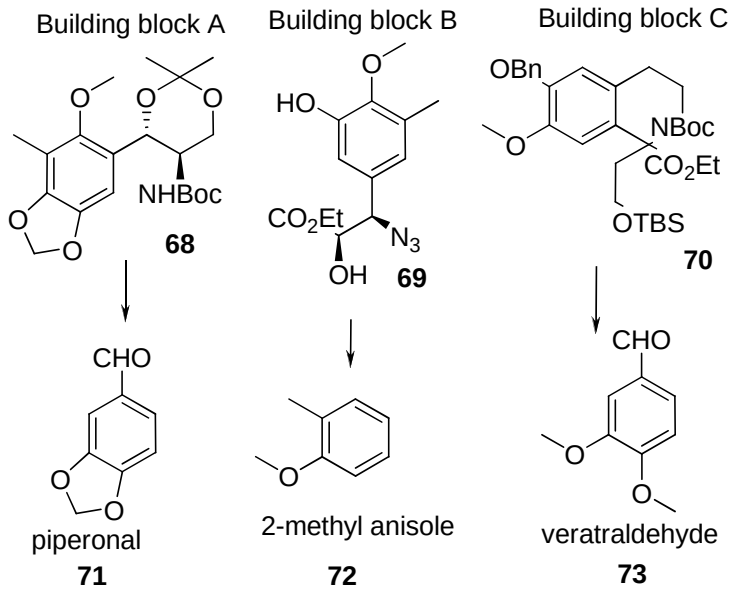

Fig. 32. The three precursors for each building block used for the synthesis of Et-743 by Chandrasekhar *et al*..[104]

A recent study was conducted to determine a new method of synthesizing Et-743 **60**, with the structure for Et-743 being considered as three blocks (A **68**, B **69**, C **70**) as shown in Fig. 31. Piperonal **71**, 2-methylanisole **72**, and veratraldehyde **73** were used as precursors to produce each building block respectively, as shown in Fig. 32.[104] This method could also be applied to other tetrahydroisoquinoline natural products such as Safracin **74** and Saframycin **75** (Fig. 33).[104]

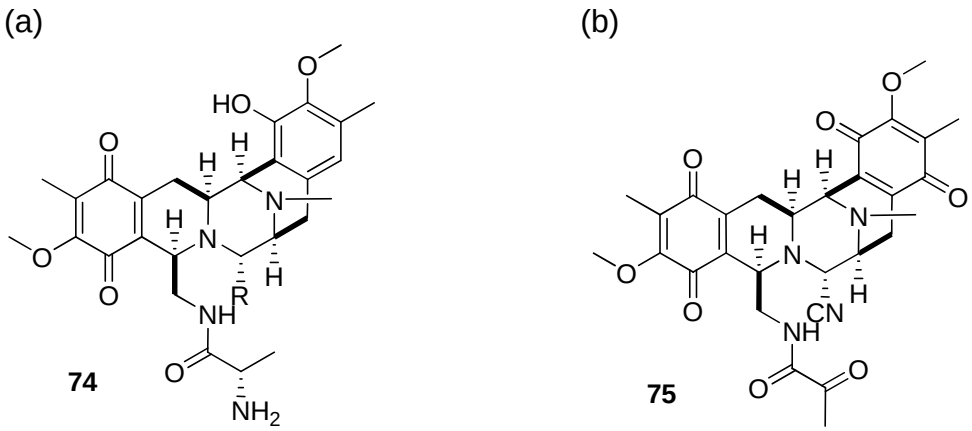

Fig. 33. a) Safracins A (R = H), safracin B (R = OH) and cyanosafracin (R = CN); b) Saframycin A. Both used as precursors for the production of the different ecteinascidin compounds.[104]

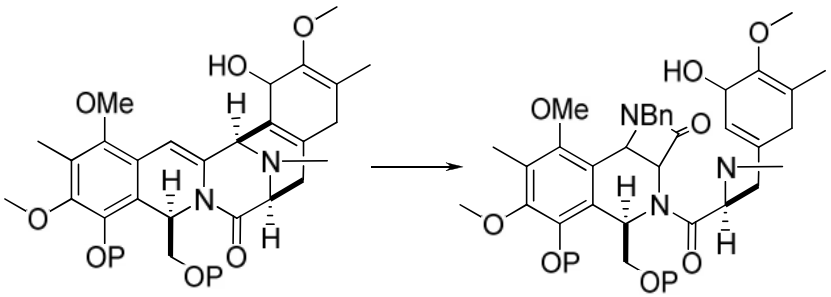

Fig. 34. The formation of the pentacyclic framework of the ecteinascidin compounds *via* β-lactam.

Other methods are also being used to reduce the number of synthetic steps for the production of the ecteinascidin compounds. In 2007, Williams *et al*., developed a method for the production of the pentacyclic framework **76** of the ecteinascidin compounds by using β-lactam **77** as a precursor (Fig. 34).[105] Methods used in the total synthesis, as mentioned above, include focusing on the pentacyclic structure of the different ecteinascidin compounds; since the basic framework for all the ecteinascidin compounds is the same, as shown in Fig. 27 and 28. The total synthesis still involves several steps in the preparation of the ecteinascidin compounds and their analogues, hence making the process unviable for economical use.[106]

1.3.2 Clinical trials

Since the discovery of Et-743, the drug has become by far the most advanced marine natural product in late stage phase II clinical trials and has already entered phase III clinical trials for the treatment of various tumours such as soft tissue sarcoma, melanoma, osteosarcoma, *etc*..[107]

A recent study was conducted in order to test the efficacy of administering Et-743 to patients with advanced soft tissue sarcoma, demonstrating significant success in treating patients with different forms of this type of tumour. Depending on the patient's condition, the overall progression free survival time and overall

survival rate after approximately one year was 42.6% and 72% respectively.[108] Data from treating myxoid liposarcoma signified that the median progression survival time was fourteen months with 88% of patients showing signs of progression free survival at six months after treatment.[109] Many studies have been unsuccessful in finding an effective agent to treat uterine leiomyosarcoma. Et-743 was administered to patients with uterine leiomyosarcoma showing a response rate of 32% and a survival rate of 8 months after treatment.[110]

The effectiveness of Et-743 *in vivo* was shown to be very successful against a human ovarian carcinoma xenograft.[111] Table 9 summarizes a few clinical trials that are currently recruiting patients in order to study the response of Et-743 as a sole agent and in combination with other drugs.[5] Table 10 summarizes the clinical trials that have been completed,[5] and Table 11 summarizes the clinical trials that are no longer recruiting patients.[5]

Table 9. A few clinical trials of Et-743 that are currently recruiting patients. [5]

Title, Location and Date	Purpose	Goals Set
Et-743 (Yondelis) in men with advanced prostate cancer Massachusetts General Hospital, Boston, MA Started: June 2002 Ended: April 2008 NCT00147212	Phase II trial to study the effectiveness of administering Et-743 for 3 hr/weekly to men with advanced prostate cancer.	To determine: 1. The response rate of the drug in patients. 2. The duration of response and time of progression of the drug over the designated time period.
Et-743 in men with advanced prostate cancer Massachusetts General Hospital, Boston, MA Started: January 2004 NCT00072670	Phase II study of Et-743 given to men with advanced prostate cancer.	To determine: 1. The safety and efficacy of the drug in patients. 2. The response rate of the drug. 3. The PSA (prostate specific antigen) levels in patients
To provide access to Trabectedin in patients with soft tissue sarcoma who have persistent or recurrent disease and who are not expected to benefit from currently available standard care treatment Santa Monica, CA Started: August 2005 End: May 2009 NCT00210665	Phase III study of Trabectedin administered to patients with locally advanced or metastatic soft tissue sarcoma.	To determine: 1. The survival rate of patients treated. 2. Any physical change through lab tests, heart rate, and any vital signs having taken the drug.
A study of the effectiveness of Trabectedin for the treatment of patients with specific subtypes of metastatic breast cancer Johnson & Johnson Pharmaceutical Research & Development, L.L.C Started: January 2007	Phase III trial studying the effectiveness and safety of administering Trabectedin to patients with breast cancer.	To determine: 1. The response rate of the drug in patients. 2. The survival and response rate of patients after the treatment period.

NCT00580112		
A study of the safety and effectiveness of Trabectedin for the treatment of localized myxoid / round liposarcoma Johnson & Johnson Pharmaceutical Research & Development, L.L.C Started: May 2007 NCT00579501	A phase II trial studying the effects of Trabectedin on (MRCL) when administered before the tumour is removed by surgery.	To determine: 1. The pathological response rate of the drug in patients.
Trabectedin in treating young patients with solid tumours that have relapsed or not responded to treatment Warren Grant Magnuson Clinical Center Bethesda, MD Started: June 2008 NCT00437047	Phase I trial studying the side effects and best dosage treatment of Trabectedin in young patients with solid tumours that have relapsed or not responded to treatment.	To determine: 1. The maximum tolerated dosage of the drug in children. 2. Any toxicity levels of the drug in patients.

Table 10. Clinical trials of Et-743 that have been completed. [5]

Title, Location, Date	Purpose	Goals Set
A safety study utilizing Yondelis and Doxorubicin in patients with soft tissue sarcoma Atlanta, GA Started: April 2005 NCT00102609	A phase I study of Yolendis and Doxorubicin in patients with recurrent or persistent soft tissue sarcoma.	To determine: 1. The proper dosage of both drugs when combined, using three different test concentrations.
Phase II study of Et-743 in patients with advanced ovarian cancer USC, Norris Comprehensive Cancer Center, Los Angeles, CA NCT00050414	Phase II trial to study the effectiveness of Et-743 in patients with advanced ovarian cancer.	To determine; 1. The safety of the drug in patients.

Ecteinascidin 743 in treating children with refractory solid tumours University of California San Diego Cancer Center, La Jolla, CA Started: October 2000 NCT00006463	Phase I study to determine the effectiveness of Et-743 in children with refractory solid tumours.	To determine: 1. The maximum tolerated dosage and dose limiting toxicity of the drug in patients. 2. The pharmacokinetics of the drug in patients 3. Any anti-tumour activity.
Ecteinascidin 743 in treating patients with malignant mesothelioma Dana-Farber Cancer Institute, Boston, MA Started: July 2001 NCT00027508	Phase II trial studying the effectiveness of administering Et-743 to patients with unresectable malignant mesothelioma.	To determine: 1. The response rate of drug in patients. 2. The toxicity levels of the drug. 3 The pharmacokinetics and pharmacodynamics of the drug in patients. 4. Overall survival rate, time until treatment failure and the quality of life of patients treated.
Phase II study of Et-743 in persistent or recurrent endometrial carcinoma USC, Norris Comprehensive Cancer Center, LA, CA NCT00050440	Phase II trial to determine the efficacy of Et-743 in patients with persistent or recurrent endometrial carcinoma.	To determine: 1. The safety and efficacy of the drug in patients.
Et-743 in patients with advanced breast cancer Torrance, CA Started: November 2003 Ended: May 2004 NCT00050427	Phase II study of Et-743 in patients with advanced breast cancer.	To determine: 1. The safety and efficacy of the drug in patients.

Table 11. Clinical trials of Et-743 that are no longer recruiting patients. [5]

Title, Location, Date	Purpose	Goals Set
The effectiveness of combining Doxil and Yondelis to Doxil alone, for patients with ovarian cancer Tucson, AZ Started: April 2005 End: November 2009 NCT00113607	A phase III study comparing the combination of Yolendis and Doxil to Doxil alone in patients with advanced relapse ovarian cancer.	To determine: 1. The overall survival rate in patients by combining both drugs in comparison to Doxil alone.
A study of Et-743 in patients with advanced liposarcoma or leiomyosarcoma Started: April 2003 Ended: February 2008 NCT00060944	Phase II trial studying the efficacy of Trabectedin in patients with advanced leiomyosarcoma or leiomyosarcoma.	To determine: 1. The safety and effectiveness of the drug in patients.
Ecteinascidin 743 in treating patients with advanced soft tissue sarcoma Ole Steen Nielsen, Study Chair, EORTC Soft Tissue and Bone Sarcoma Coop. Group NCT00003939	Phase II trial to determine the effectiveness of administering Et-743 in patients with advanced soft tissue sarcoma.	To determine: 1. The response rate in patients. 2. Any acute side effects of the drug in patients. 3. The therapeutic activity of the drug in patients.
Ecteinascidin 743 in treating patients with previously treated metastatic osteosarcoma Memorial Sloan-Kettering Cancer Center NY Started: December 1999 NCT00005625	Phase II trial to determine the effectiveness of Et-743 in patients previously treated for metastatic osteosarcoma.	To determine: 1. The response rate of patients treated. 2. The pharmacokinetics and pharmacodynamics of the drug in patients. 3. The toxicity levels of the drug in patients.

Ecteinascidin 743 in treating adults with advanced solid tumours Newcastle General Hospital, Newcastle upon Tyne, UK Started: February 1996 NCT00002904	Phase I study on the effectiveness of administering Et-743 to adults with advanced solid tumours.	To determine: 1. The pharmacokinetics of the drug in patients. 2. The maximum tolerated dosage of the drug in patients. 3. Any anti-tumour effects. 4. The qualitative and quantitative toxicity effects of the drug in patients.
Ecteinascidin 743 in treating patients with unresectable advanced or metastatic soft tissue sarcoma Memorial Sloan-Kettering Cancer Center, NY Started: February 2001 NCT00017030	A phase II study of Et-743 given to patients with unresectable advanced or metastatic soft tissue sarcoma.	To determine: 1. The overall survival rate of patients treated. 2. The pharmacokinetics and pharmacodynamics of drug. 3. The toxicity level of drug in patients.

1.3.3 Mechanism of action

Studies have shown that Et-743 binds to the minor groove of deoxyribonucleic acid (DNA), alkylating the second nitrogen on guanine, thus bending the molecule towards the major groove formation.[112,113] The proposed mechanism for the binding of Et-743 to DNA, alkylating the second nitrogen on guanine is shown in Fig. 36.[114] It is also shown that Et-743 **60b** forms hydrogen bonds with DNA as shown in Fig. 35.[114] In this process, only two subunits of Et-743 bind to the DNA strand, configuring the structure in the minor groove, resulting in interference with the DNA binding factor in cells.[115] Et-743 also inhibits the activity of NF-Y (nuclear transcription factor γ), which is activated by a specific coding sequence (CCAAT). When these results where compared to cell promoters lacking this CCAAT gene, no change in behaviour with Et-743 was detected.[116]

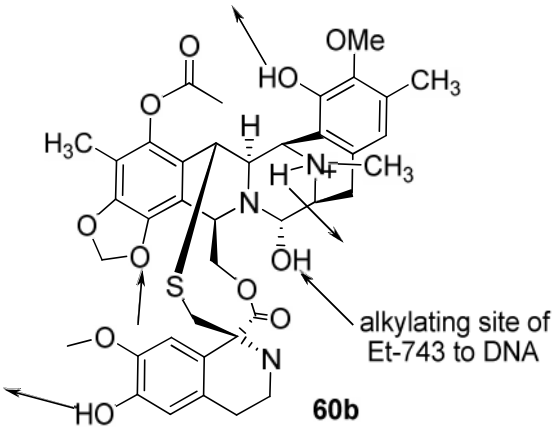

Fig. 35. Et-743 hydrogen binding sites to DNA. The arrows indicate the direction of hydrogen bond donors and acceptors.

At low concentrations, Et-743 inhibited the activity of topoisomerase 1 isomerases, which act on or change the topology of DNA.[117] The effectiveness of any anti-tumour activity of Et-743 is thus related to the transcription dependent growth arrest (at a concentration of 1-10 nM), as well as the transcription independent apoptosis of cells when Et-743 is administered at a concentration of 10-100 nM.[118]

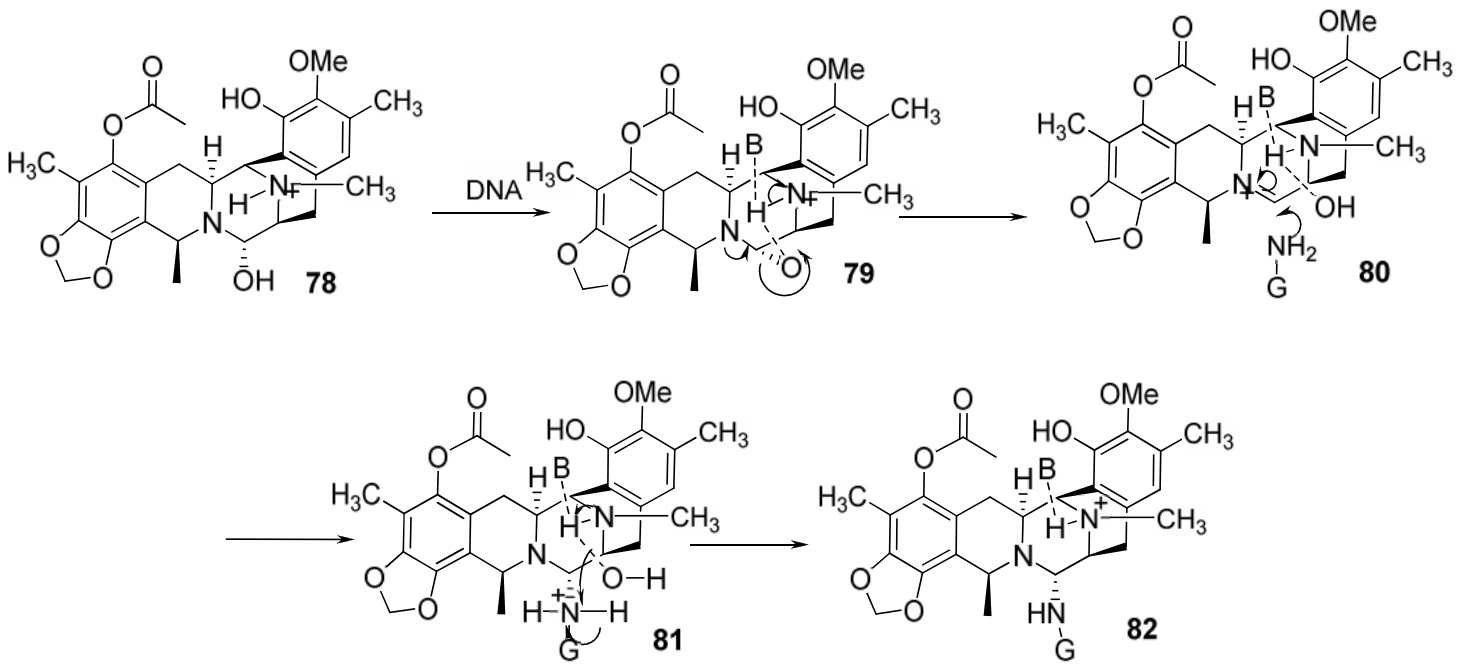

Fig. 36. The proposed mechanism of Et-743 alkylating the N2 of guanine **78**. The 12NH of the carbinolamine **79** catalyzes the dehydration of C21, yielding the iminium ion **80**. Nucleophilic attack by GN2 on **80** results in the expulsion of the transiently bound H_2O, which contains the proton released by guanine N2 **81**. The resulting adduct **82** retains a protonated N12. Hydrogen bonds are depicted by dotted lines, and **B** corresponds to a DNA base hydrogen bond acceptor.[114]

Recent studies were conducted to determine the DNA binding properties of Et-743 and different analogues (Et-745 **60c**, Et-637 **63** and Et-594 **62**). Results from gel retardation assays showed the ranking of the compounds (from most to least active, Fig. 28) as Et-743>Et-637>Et-594>Et-637-OBu **64** and finally Et-745. Et-743 showed extensive binding to DNA whereas Et-745 did not bind at all, suggesting no potency in configuring DNA in cancerous cells.[119]

Studies have also been conducted in order to further understand the molecular mechanism of Et-743 binding to DNA and the inhibition of DNA replication in cancerous cells. This investigation was conducted using yeast cells to determine the cytotoxicity levels. Yeast cells contain both BER (base excision repair) and NER (nucleotide excision repair), DNA repair mechanisms. In the presence of Et-743 cell death occurred, but cells that did not contain these DNA repair mechanisms showed resistance to Et-743.[120] This suggested that NER plays a pivotal role in targeting the drug in order to repair DNA. This prompted another study to further understand these recombinant repairs in yeast and mammalian cells. The ability of Et-743 to reconfigure the DNA into the minor groove is referred to as the NER pathway, which is recognised by XPG (a specific protein involved in NER) within the NER system, hence cells that lack NER are resistant to Et-743.

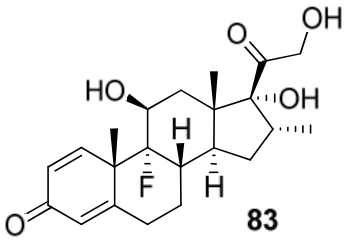

83

Fig. 37. Dexamethasone ($C_{22}H_{29}FO_5$, 392.1993 g/mol) used to decrease the hepatotoxicity of Et-743 in patients.

Recent clinical trials also showed that aside from Et-743's efficacy, high levels of the drug can lead to liver damage in patients. For this reason, dexamethasone **83** (DEX, Fig. 37) was given to patients, resulting in a significant

decrease in hepatotoxicity.[121] The effectiveness of DEX in reducing the toxicity of Et-743 in patients was mirrored by a 75% reduction in the level of hepatotoxicity in rats; an important consideration for further trials conducted *in vivo*.[122]

1.3.4 Problems with production

The problems facing on economic production of Et-743 are similar to those of bryostatin 1 (section 1.2.4). Approximately 1 metric ton of *Ecteinascidia turbinata* is needed to extract 1 g of the drug. Due to the high demand for the marine organism, several alternative methods are being used for the production of Et-743. PharmaMar has been extracting Et-743 from sea squirts using an aquatic culturing system, ensuring continuous drug production.[99] This method does not reduce the amount of the organism needed to produce grams of the drug. In 2000, a twenty one step semi-synthetic route was developed which is used in conjunction with cyanosafracin B **74** (Fig. 33), resulting in the production of Et-743.[98,99,123]

Since the discovery of Et-743, it has progressed the furthest of all MNPs in clinical studies against various cancers.[5] Et-743 is still extracted from tunicates found attached to rocks and mangrove roots in the Caribbean Sea, along the Florida coast and in the West Indies. Aquaculture systems for farming of the sea squirt are currently employed year round in order to provide the various clinical trials with continued supplies of the drug,[46] but the extraction process is a major drawback, resulting in low percentage yields and expensive production costs for the drug.

1.4 Paclitaxel (Taxol)

The pacific yew tree (*Taxus brevifolia*) is found along the coast of California, stretching from as far north as Alaska to southern California, and also in Idaho and Columbia. It is also found in Florida (Florida yew tree). The trees are protected under wild-life regulations, as they were previously extensively collected for the isolation of the active compound paclitaxel (Taxol).

Despite the historical use of the tree, for medicinal purposes, it was in the early 1960s that the anti-tumour compound, Taxol **84** (Fig. 38), was first identified and in 1971 that the structure of the compound was determined.[124,125] The total synthesis was not achieved until the early 1990s by Nicolaou *et al*.,[126] followed by a four step semi-synthesis by Holton *et al*., in 1994 (Fig. 39).[127] Other groups have since modified the synthesis of Taxol in the hope of increasing the yield.[128] With the discovery of Taxol from the Pacific yew tree, hundreds of other compounds such as Taxol C, taxane alkaloids, diterpenoids, lignans, and sugar derivates, *etc*., have been isolated from different yew trees.[129]

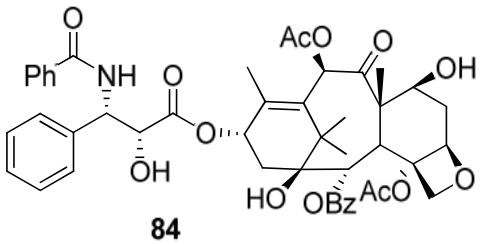

84

Fig. 38. Paclitaxel (Taxol), ($C_{47}H_{51}NO_{14}$, 853.3304 g/mol), an anti-cancer agent initially isolated from Pacific yew tree, *Taxus brevifolia.*

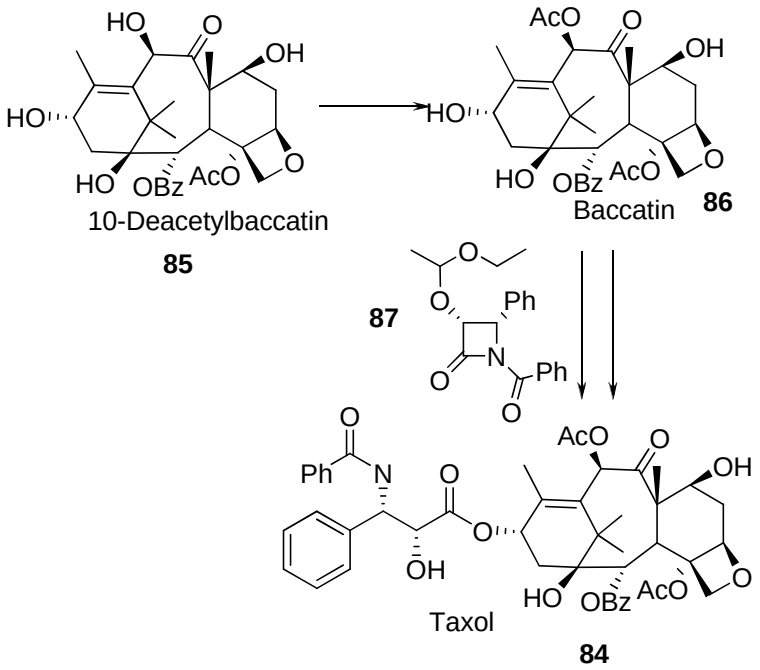

Fig. 39. The four step semi-synthesis of Taxol, using 10-Deacetylbaccatin as a precursor.

1.4.1 Clinical trials

Despite the initial identification and isolation of paclitaxel in the early 1970s phase I clinical trials were not conducted until 1984, with phase II trials beginning shortly after (between 1984 and 1986).[124] Since then, nearly one thousand clinical trials of paclitaxel have been conducted.[5] The initial clinical trials were first conducted using the drug as a sole agent against various cancers (ovarian, breast), then proceeding to synergistic administration with other medicinal agents.[5] Many trials have already been completed and achieved successful results *in vivo* and Table 12 summarizes some of the many clinical trials that have already been completed. Hundreds of trials are, however, still ongoing with many still in their initial stages. The first public record of paclitaxel in clinical trials became available in 1988 showing a 30% response rate in patients suffering from ovarian cancer.[130]

Recently, attempts have been made to modify the bioavailability of Taxol in patients, which is problematic due its large particle size (0.6-17 μm). The ability to solvate the drug for administration is difficult hence the rate of absorption in the

intestine is very low. The drug was placed under supercritical conditions with salicylic acid to reduce the particle size, thus facilitating the bioavailability of the drug in patients. Utilising this method led to a substantial reduction in the particle size of Taxol, from 0.6-17 μm to 0.3-1.7 μm.[131]

Other experiments in relation to the level of unbound and bound Taxol have also been recently reported, involving quantitative analysis of unbound and bound Taxol found in the plasma of patients after Abraxane (ABI-007) was administered. Results showed that paclitaxel had 88.8% efficacy in cells with merely 5% of the drug unbound to the plasma protein in patients.[132] Abraxane uses albumin, a human protein, to deliver Taxol into cells more readily than cremophor, a solvent used to aid in the administration of Taxol into patients.[133] Taxol has recently been used to stabilize microtubules in rats to restore facial nerves, allowing the movement of whiskers using only 10 μg/mL of Taxol.[134]

Table 12. A few completed clinical trials of paclitaxel as a sole agent and in combination with other natural products.[20]

Topic, Location, Date	Title	Goals set
Paclitaxel in (AIDS-KS): A phase II trial conducted by Baker Norton Pharmaceuticals Massachusetts General Hospital, AIDS Oncology Research, Boston, MA Started: Nov. 2nd, 1999 Ended: June 23rd, 2005 NCT00002189	Phase II trial of paclitaxel to treatment of patients with advanced refractory Kaposi's Sarcoma (AIDS-KS). (Related studies)[135]	To determine: 1. The response rate and tumour progression in patients. 2. Qualitative and quantitative toxicity levels of drug in patients.
Micellar paclitaxel for the treatment of severe psoriasis.[136] NCI Bethesda, MD Started: September 2000 Ended: October 2002 NCT00006276	Phase II trial studying the intravenous administering of micellar paclitaxel in patients with severe psoriasis.	To determine: 1. The safety and effectiveness of using paclitaxel to treat patients with psoriasis.
Flavopiridol and paclitaxel administered to treat patients with locally advanced or metastatic oesophageal cancer Memorial Sloan-Kettering Cancer Center, NY Started: July 2000 NCT00006245	Phase II trial studying the efficacy of Flavopiridol and paclitaxel in patients with refractory oesophageal cancer.	To determine: 1. The response rate and toxicity levels of both drugs in patients. 2. The quality of life of patients after treatment. 3. The pharmacokinetics of drug in patients.
Further study of giving ABI-007 and Taxol to patients with metastatic breast cancer Abraxis BioScience, Inc., Durham, NC Started: June 2001 Ended: July 2006 NCT00046527	Phase III trial to study the use of ABI-007 (a cremophor free, protein stabilized, nanoparticle paclitaxel) and Taxol to patients with metastatic breast cancer.	To determine: 1. The maximum tolerated dosage to be administered. 2. Any reduced infusion time or risks of hypersensitivity. 3. The pharmacokinetics of the drug in patients.

Administering paclitaxel with and without gemcitabine to women with advanced breast cancer Haematology/Oncology Group, Santa Rose, CA Started: July 2000 NCT00006459	Phase III trial study of administering gemcitabine with paclitaxel in comparison to paclitaxel alone, to patients with unresectable, locally recurrent or metastatic breast cancer.	To determine: 1. The overall survival rate of patients treated.
Carboplatin and paclitaxel administered with, and, without ISIS-3521 to treat patients with NSCLC ISIS Pharmaceuticals Inc., Carlsbad, CA Started: October 2000 NCT00017407	Phase III trial to study the therapeutic combination of administering carboplatin and paclitaxel, in comparison to carboplatin, paclitaxel and ISIS-3521 to treat patients with advanced, previously untreated NSCLC.	To determine: 1. The overall survival rate and response rate of drugs in patients. 2. The safety and duration of response in patients treated.
A pilot study of paclitaxel and radiation therapy for the treatment of locally advanced head and neck cancer National Cancer Institute Bethesda, MD Started: July 1995 Ended: June 2004 NCT00001442	Phase I trial studying the use of paclitaxel with radiation therapy to treat patients with locally advanced head and neck cancer.	To determine: 1. The toxicity level of drug in patients.
Paclitaxel, UFT and leucovorin administered to patients for the treatment of advanced gastric cancer Department of Oncology, National Taiwan University Hospital, Taipei, TWN Started: March 2003 Ended: June 2005 NCT00154778	Phase II trial studying the effectiveness and safety of administering paclitaxel, UFT and leucovorin to treat patients with advanced gastric cancer.	To determine: 1. The response rate and safety level of drugs in patients. 2. The time of progression in patients.

1.4.2 Mechanism of action

Paclitaxel interferes with the normal function of microtubules by binding to the β subunit tubulin, hence locking the microtubule and increasing stability. This prevents the mitosis of cells since the chain formation of microtubules is needed for the transportation of the cellular components for cell replication.[137] In doing so, Taxol effectively depletes the cell's present and triggers apoptosis. Due to Taxol's insolubility in water it is generally administered to patients in a formulation of a vehicle cremophor el micelles (a non-ionic surfactant used to equilibrate the emulsion of non-polar compounds into aqueous solutions).[138] In 1996, Han *et al*., conducted a study, indicating that Taxol binds to β-tubulin using the binding site as shown by the arrow (Fig. 40). This was determined by developing a fluorescent derivative of Taxol **88** (2-AB Taxol), to aid in detecting the binding site of the derivative to the β-tubulin. The results from this study showed that the C2 position as shown below is associated with the binding of taxol to β-tubulin.[139]

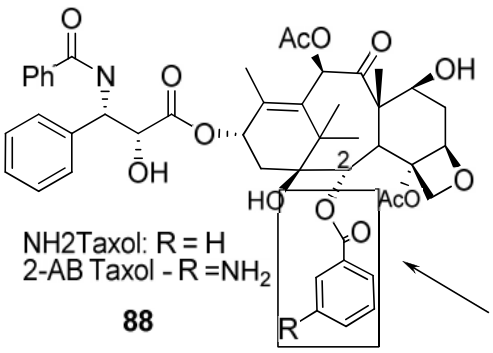

88

Fig. 40. The benzoyl group as shown binds to the β-tubulin.[139]

An increase in the dosage reaching the site of action is achieved by modifying Taxol or by formulating a complex method to allow the drug to reach its active site.[140,141,142] Bovine serum albumin (BSA), a proteinaceous microsphere, has been investigated for the potential transport of macromolecules within the bloodstream to the delivery site. With this in mind, a study was conducted to determine the delivery, release rate and anti-tumour activity of a Taxol-BSA

complex, in comparison to administering Taxol alone, to mouse multiple myeloma cells (MPC-11). The number of dead cells from each formulation was the same but the greater the concentration of Taxol in the microspheres the more effective the drug was against the myeloma cells. The reported success for the Taxol-BSA complex was attributed to the presence of mesitylene (an organic solvent) used in the preparation process.[142]

Using DNA electrochemical investigations, the mechanism of the DNA-drug interaction for Taxol was studied. Results from the electrochemical investigation showed a decrease of guanine in DNA as the concentration of Taxol increased, eventually reaching a level of saturation ($2.3x10^{7}$ M^{-1}). This decrease can be related to the binding of Taxol to the groove on the DNA strand.[143]

1.4.3 Production of Taxol

The isolation of Taxol from the bark of the Pacific yew tree resulted in a great demand for the drug. This caused many problems as the only means of isolation was by extracting the bark, where the highest concentration of the drug is found. In 1969, 1.20 ton of bark was collected; producing 10 g of pure Taxol and this was merely the beginning, with thousands of trees being felled for extraction purposes. Between 1977 and 1987 2.95 ton of bark was collected and used for clinical trials about to begin.[124] The yield from isolating Taxol from the bark of the yew tree is approximately 0.01% dry weight of bark. The vast number of trees that were sacrificed for *in vitro* and *in vivo* testing of paclitaxel caused major concerns for the protection and sustainability of the yew trees,[124] and protection orders forced the development of other methods to produce Taxol efficiently, on an economical level.

Other methods of purifying and isolating Taxol were subsequently investigated, resulting in higher percent yields.[144] In the 1990s the synthesis of

the drug was achieved, but the large number of steps made it very time consuming and the percentage yields were still low. A major breakthrough was achieved with a four step synthesis producing Taxol in an 80% yield.[127] Since then, other methods have been employed to produce Taxol. Currently Bristol Myers Squibb uses plant cell fermentation to grow the drug by cell culturing,[145] and in 2000 it was reported that the annual sales of Taxol was approximately 1.6 billion dollars.

Modification methods have been applied to the fermentation of cell culturing to produce Taxol.[146,147,148] A recent study showed that salicylic acid induced the production of Taxol in cultured cells of *Taxus chinensis* (Chinese yew tree). Results showed that high concentrations of salicylic acid induced the production of Taxol and resulted in it killing the cell cultures. However, quantitative studies showed that 20 g/mL of salicylic acid was enough to promote the production of Taxol to 1.626 mg/g dry weight, causing little or no damage to the cell cultures.[149]

It is now known that the production of Taxol is due to a fungus living in the yew tree.[150] Taxol has also been isolated from fungus collected from *Cupressus spp., Citrus medica* and *Taxus celebica* (Chinese yew tree).[151,152,153] Understanding the origin of Taxol may help devise a novel production method using an artificial method and techniques that have been devised for the production of the bryostatins and Et-743.

1.5 Work conducted

In order to understand the importance of finding an efficient method for the production of such complex natural drugs, it is imperative to first review studies that have already been conducted in order to identify the many problems that are currently affecting the isolation of MNPs. The numerous synthetic steps required

for the preparation of drugs such as bryostatin 1 and Et-743, resulting in low percentage yield of products, and the environmental consequences of harvesting marine organisms for the isolation of MNPs are two examples of the many problems affecting the availability of such drugs.

Subsequent chapters describe innovative and practical methods that have been developed in order to overcome the problems facing the availability of MNPs. This work is focused on two marine organisms, *Bugula neritina,* a marine bryozoan which produces the bryostatins, and *Ecteinascidia turbinata,* a sea squirt, which produces the ecteinascidin compounds, but some preliminary work has been started on the production of Taxol. Taxol as mentioned, is a terrestrial NP, however recent studies have shown that the production of Taxol is due to a fungus found at the root of the yew trees. For this reason, attempts have been started to apply the procedures used for the production of the bryostatins and Et-743 to that of Taxol, by modifying the properties to attract the fungi responsible for the production of the drug. This is important as it would provide an alternative method of producing the drug, and illustrate the efficacy of our method as a universal tool for the application of other NPs, both terrestrial and marine. The work related to the production of Taxol is mostly discussed in the suggested future works section of this thesis.

Detailed analysis of the environment (sediment), where these NPs are found, was necessary in order to identify and understand the conditions that promote the survival of these marine organisms and their ability to produce the compounds isolated from them. Results from this study instigated the application of a new technique of applying a chemical composition to an artificial surface to encourage the production of these NPs. It is suggested that this method could easily be applied to the production of other NPs, both terrestrial and marine, by simply modifying its constituents. Based on this proposition, several experiments

are currently being conducted, using this method, for the production of Taxol. Preliminary results are showing some success, suggesting the viability of these treated artificial surfaces as a means of cultivating and isolating Taxol as an alternative to synthetic methods alone. Taxol is currently produced in a four step synthesis process and is manufactured fairly efficiently by this method. Results regarding the production of any bryostatin compounds and ecteinascidin compounds are mentioned in their respective chapters.

As an adjunct to this, experiments involving the trans-esterification of bryostatin 1 were carried out to determine the effects of the drug under various conditions (37°C, ambient condition, and UV light), giving insight into its behaviour in the environment and in the body, respectively. Results from this showed that the compound does degrade to form $m/z < 927$ and compounds with $m/z > 927$. Two computational experiments were also conducted, involving the binding of the bryostatins and other MNPs to Fe^{3+}, resulting in the formation of a siderophore complex. From the results collected in this study, the data suggests that many of the compounds can form siderophore complexes and act as possible medicinal agents, as many appeared to have high dipole moment to surface volume (D/V) ratios similar to polar solvents; suggesting their ability to act as polar or non-polar agents when bound to Fe^{3+}.

With the computational study suggesting the ability of bryostatin 1-Fe^{3+} to act as a possible medicinal agent, cell line tests were conducted to determine its efficacy in comparison to bryostatin 1 alone. This new bryostatin-Fe^{3+} (fer-mer) compound was investigated against chronic myeloid leukaemia and human lung carcinoma cells in order to determine its effectiveness in comparison to bryostatin 1 alone. Data from both computational experiments was used to support the initial theoretical hypotheses that the fer-mer compound may act as a better medicinal agent than bryostatin 1 alone.

The subsequent chapters will focus on understanding the chemical and ecological environment within, and surrounding, *Bugula neritina* and *Ecteinascidia turbinata,* giving insight into the impact of the structure of the bryostatins and Et-743.[154,155,156,157] The development of a novel and efficient technique to collect the NPs from their host organism and surrounding sediment has been explored and an innovative method is proposed for the efficient and economical production of bryostatin, Et-743 and Taxol which could subsequently be adapted to other plant based or MNPs.

1.6 References

[1] Rudloe, Jack. The Sea Brings Forth. New York, NY: Alfred A. Knopf, 1968.

[2] P. Proksch, R. A. Edrada-Ebel, R. Ebel. V. Wray, and K. Steube. *Prog. Mol. Subcell. Biol.,* 2003, **(37)**, 117-42.

[3] R. W. Wallace. *Mol. Med. Today*, 1997, **3(7)**, 291-95.

[4] T. J. Manning, L. Noble, P. Groundwater, G. Abadi, W. Palen, J. Geddings, T. Irwin, N. Kasali, J. Colyer, F. Goodson, J. Smith, and J. Hester. (2007) A History of Bryostatin: A Prominent Marine Natural Product. D. K. Majumdar, J. N. Govil, V. K. Singh, R. K. Sharma. Recent Progress in Medicinal Plants: Vol. 15. Natural Products. Studium Press, Houston, TX.

[5] http://www.clinicaltrials.gov (January 14th 2009).

[6] D.J. Newman, and R.T. Hill. *J. Ind. Microbiol. Biotechnol*., 2006, **33(7)**, 539-44.

[7] J. Piel. *Curr. Med. Chem*., 2006, **13(1)**, 39-50.

[8] D. H. Williams, M. J. Stone, P. R. Hauck, and S. K. Rahman. *J. Nat. Prod*., 1989, **52(6)**, 1189-208.

[9] R. D. Firn, and C. G. Jones. *Nat. Prod. Rep*., 2003, **20(4)**, 382-91.

[10] W. C. Dunlap, C. N. Battershill, C. H. Liptrot, R. E. Cobb, D. G. Bourne, M. Jaspars, P. F. Long, and D.J. Newman. *Methods*, 2007, **42(4)**, 358-76.

[11] A. B. Friedrich, H. Merkert, T. Fendert, J. Hacker, P. Proksch, and U. Hentschel. *Mar. Biol.*, 1999, **134(3)**, 461-70.

[12] G. Toledo, W. Green, R. A. Gonzalez, L. Christoffersen, M. Podar, H. W. Chang, T. Hemscheidt, H. G. Trapido-Rosenthal, J. M. Short, R. R. Bidigare, and E. J. Mathur. *Oceanography*, 2006, **19(2)**, 120-25.

[13] T. L. Simmons, E. Andrianasolo, K. McPhail, P. Flatt, and W. H. Gerwick. *Mol. Cancer Ther*., 2005, **4(2)**, 333-42.

[14] G. R. Pettit, Y. Kamano, C. L. Herald, A. A. Tuinman, F. E. Boettner, H. Kizu, J. M. Schmidt, L. Baczynsky, K. B. Tomer, and R. J. Bontems. *J. Am. Chem. Soc*., 1987, **109(22)**, 6883-85.

[15] R. Bai, G. R. Pettit, and E. Hamel. *J. Biol. Chem*., 1990, **265(28)**, 17141-49.

[16] H. Luesch, R. E. Moore, V. J. Paul, S. L. Mooberry, and T. H. Corbett. *J. Nat. Prod*., 2001, **64(7)**, 907-10.

[17] L. M. West, P. T. Northcote, and C. N. Battershill. *J. Org. Chem*., 2000, **65(2)**, 445-49.

[18] K. A. Hood, L. M. West, B. Rouwe, P. Y. Northcote, M. V. Berridge, S. J. Wakefield, and J. H. Willer. *Cancer Res*., 2002, **62(12)**, 3356-60.

[19] http://www.niwa.co.nz/news-and-publications/publications/all/wa/14-3/sponge (June 20th 2009).

[20] A. R. Carroll, J. C. Coll, D. J. Bourne, J. K. MacLeod, T. M. Zabriskie, C. M. Ireland, and B. F. Bowden. *Aust. J. Chem*., 1996, **49(6)**, 659-67.

[21] X. Salvatella, J. M. Caba, F. Albericio, and E. Giralt. *J. Org. Chem*., 2003, **68(2)**, 211-15.

[22] J. L. Urdiales, P. Morata, I. Nunez de Castro, and F. Sanchez-Jimenez. *Cancer Lett*., 1996, **102(1-2),** 31-7.

[23] S. Sakemi, T. Ichiba, S. Kohmoto, G. Saucy, and T. Higa. *J. Am. Chem. Soc*., 1988, **110(14)**, 4851-53.

[24] J. Piel, D. Butzke, N. Fusetani, D. Hui, M. Platzer, G. Wen, and S. Matsunaga. *J. Nat. Prod.*, 2005, **68(3)**, 472-79.

[25] K. H. Lee, S. Nishimura, S. Matsunaga, N. Fusetani, S. Horinouchi, and M. Yoshida. *Cancer Sci.*, 2005, **96(6)**, 357-64.

[26] Woollacott, M. R., and L. R. Zimmer. Biology of Bryozoans. New York, NY: Academic Press Inc., 1997.

[27] Jackson, C. B. J., and K. F. McKinney. Bryozoan Evolution. Chicago: The University of Chicago Press, 1989.

[28] Woollacott, M. R., and L. R. Zimmer. Biology of Bryozoans. NY, NY: Academic Press Inc., 1997.

[29] J. D. Martin, Y. Ito, W. Homann, M. G. Haygood, and A. Butler. *J. Biol. Inorg. Chem*., 2006, **11(5)**, 633-41.

[30] J. S. Martinez, J. N. Carter-Franklin, E. L. Mann, J. D. Martin, M. G. Haygood, and A. Butler. *Proc. Natl. Acad. Sci. USA*, 2003, **100(7)**, 3754-59.

[31] G. R. Pettit, F. Gao, D. L. Herald, P. M. Blumberg, N. E. Lewin, and R. A. Nieman. *J. Amer. Chem. Soc.,* 1991, **113(17)**, 6693-95.

[32] H. U. Dahms, Q. F. Gao, and J. S. Hwang. *Aquaculture*, 2007, **265(1-4)**, 169-75.

[33] X. Yu, Y. Yan, and J. D. Gu. *Int. Biodeterior. Biodegradation*, 2007, **60(2)**, 81-9.

[34] G. R. Pettit, C. L. Herald, D. L. Doubek, D. L. Herald, E. Arnold, and J. Clardy. *J. Am. Chem. Soc*., 1982, **104(24)**, 6846-48.

[35] G. E. Keck, D. S. Welch, and Y. B. Poudel. *Tetrahedron Lett*., 2006, **47(47)**, 8267-70.

[36] M. Ball, B. J. Bradshaw, R. Dumeunier, T. J. Gregson, S. MacCormick, H. Omori, and E. J. Thomas. *Tetrahedron Lett*., 2006, **47(13)**, 2223-27.

[37] M. Kageyama, T. Tamura, M. H. Nantz, J. C. Roberts, P. Somfai, D. C. Whritenour, and S. Masamune. *J. Amer. Chem. Soc*., 1990, **112(20)**, 7407-8.

[38] A. J. Duplantier, M. H. Nantz, J. Roberts, R. P. Short, P. Somfai, and S. Masamune. *Tetrahedron Lett.,* 1989, **30(52)**, 7357-60.

[39] M. A. Blanchette, M. S. Malamas, M. H. Nantz, J. C. Roberts, P. Somfai, D. C. Whritenour, S. Masmune, M. Kageyama, and T. Tamura. *J. Org. Chem*., 1989, **54(12)**, 2817-25.

[40] J. Debrabander, K. Vanhessche, and M. Vandewalle. *Tetrahedron Lett.,* 1991, **32(24)**, 2821-24.

[41] D. A. Evans, P. H. Carter, E. M. Carreira, A. B. Charette, J. A. Prunet, and M. Lautens. *J. Am. Chem. Soc.,* 1999, **121(33)**, 7540-52.

[42] G. R. Pettit, D. Sengupta, C. L. Herald, N. A. Sharkey and P. M. Blumberg. *Can. J. Chem*., 1991, **69(5)**, 856-60.

[43] P. A. Wender, and V. A. Verma. *Org. Lett.*, 2006, **8(9)**, 1893-96.

[44] P. A. Wender, B. A. DeChristopher, and A. J. Schrier. *J. Am. Chem. Soc.,* 2008, **130(21)**, 6658-59.

[45] G. E. Keck, M. B. Kraft, A. P. Truong, W. Li, C. C. Sanchez, N. Kedei, N. E. Lewin, and P. M. Blumberg. *J. Am. Chem. Soc.,* 2008, **130(21)**, 6660-61.

[46] D. Mendola. *Biomol. Eng*., 2003, **20(4-6)**, 441-58.

[47] M. G. Haygood, and S. K. Davidson. *Appl. Environ. Microbiol*., 1997, **63(11),** 4612-16.

[48] S. Sudek, N. Lopanik, L. E. Waggoner, M. Hilderbrand, H. B. Liu, A. Patel, C. Anderson, D. H. Sherman, and M. G. Haygood. *J. Nat. Prod.,* 2007, **70(1)**, 67-74.

[49] S. K. Davidson, S. W. Allen, G. E. Lim, C. M. Anderson, and M. G. Haygood. *Appl. Environ. Microbiol.*, 2001, **67(10)**, 4531-37.

[50] M. Hildebrand, L. E. Waggoner, H. B. Liu, S. Sudek, S. Allen, C. Anderson, D. H. Sherman, and M. Haygood. *Chem. Biol.*, 2004, **11(11)**, 1543-52.

[51] G. R. Pettit, Y. Kamano, C. L. Herald, and M. Tozawa. *J. Am. Chem. Soc*., 1984, **106(22)**, 6768-71.

[52] G. R. Pettit, J. E. Leet, C. L. Herald, Y. Kamano, F. E Boettner, L. Baczynskyj, and R. A. Neiman. *J. Org. Chem*., 1987, **52(13)**, 2854-60.

[53] S. K. Davidson, and M. G. Haygood. *Bio. Bull.,* 1999, **196(3)**, 273-80.

[54] G. R. Pettit, and H. L. Cherry. *Euro. Patent Application*, 1984.

[55] M. A. Shah, and G. K. Schwartz. *Update Cancer Ther. I*, 2006, 311-32.

[56] J. E. Winegarden, A. M. Mauer, T. F. Gajewski, P. C. Hoffman, S. Krauss, C. M. Rudin, and E. E. Vokes. *Lung Cancer*, 2003, **39(2)**, 191-96.

[57] J. A. Koutcher, M. Motwani, K. L. Zakian, X. K. Li, C. Matei, J. P. Dyke, D. Ballon, H. H. Yoo, and G. K. Schwartz. *Clin. Cancer Res*., 2000, **6(4),** 1498-507.

[58] A. Rohner, U. Langenkamp, U. Siegler, C. P. Kalberer, and A. Wodnar-Filipowicz. *Leuk. Res.*, 2007, **31(10)**, 1393-402.

[59] F. Nezhat, S. Wadler, F. Muggia, J. Mandeli, G. Goldberg, J. Rahaman, C. Runowicz, A. J. Murgo, and G. J. Gardner. *Gynecol. Oncol.,* 2004, **93(1)**, 144-48.

[60] M. K. Sun, J. Hongpaisan, T. J. Nelson and D. L. Alkon. *Proc. Natl. Acad. Sci. USA*, 2008, **105(36)**, 13620-25.

[61] T. VanHuynh, G. Cole, R. Katzman, K. P. Huang, and T. Saitoh. *Arch. Neurol*., 1989, **46(11)**, 1195-99.

[62] R. Etcheberrigaray, E. Ito, K. Oka, B. TofelGrehl, G. E. Gibson, and D. L. Alkon, *Proc. Natl. Acad. Sci*. *USA*, 1993, **90(17)**, 8209-13.

[63] S. Govoni, S. Bergamaschi, M. Racchi, F. Battaini, G. Binetti, A. Bianchetti, and M. Trabucchi. *Neurology*, 1993, **43(12)**, 2581-86.

[64] A. Favit, M. Grimaldi, T. J. Nelson, and D. L. Alkon. *Proc. Natl. Acad. Sci. USA*, 1998, **95(10)**, 5562-67.

[65] R. Etcheberrigaray, E. Ito, C. S. Kim, and D. L. Alkon. *Science*, 1994, **264(5156)**, 276-79.

[66] W. Q. Zhao, L. Ravindranath, A. S. Mohamed, O. Zohar, G. H. Chen, C. G. Lyketsos, R. Etcheberrigaray, and D. L. Alkon. *Neurobiol Dis*., 2002, **11(1)**, 166-83.

[67] T. K. Khan, and D. L. Alkon. *Proc. Natl. Acad. Sci. USA*, 2006, **103(35),** 13203-07.

[68] J. T. Neary, T. Crow, and D. L. Alkon. *Nature*, 1981, **293(5834)**, 658-60.

[69] A. M. Kuzirian, H. T. Epstein, C. J. Gagliardi, T. J. Nelson, M. Sakakibara, C. Taylor, A. B. Scioletti, and D. L. Alkon. *Biol. Bull*. 2006, **210(3)**, 201-14.

[70] M. K. Sun, and D. L. Alkon. *Euro. J. Pharmacol*., 2008, **584(2-3)**, 328-37.

[71] D. L. Alkon, and J. Hongpaisan. *Proc. Natl. Acad. Sci. USA*, 2007, **104(49)**, 19571-76.

[72] M. K. Sun, and D. L. Alkon. *Euro. J. Pharmacol*., 2005, **512(1)**, 43-51.

[73] D. H. Wang, D. S. Darwish, B. G. Schreurs, and D. L. Alkon. *Behav. Pharmacol.*, 2008, **19(3)**, 245-56.

[74] http://www.alz.org/alzheimers_disease_facts_figures.asp (June 26th 2009).

[75] M. D. Fleming, S. K. Barrett, and H. D. Bear. *J. Surg. Res*., 1994, **57(1)**, 74-9.

[76] H. G. Jorgensen, E. K. Allan, J. C. Mountford, L. Richmond, S. Harrison, M. A. Elliot, and T. L. Holyoake. *Exp. Hematol*., 2005, **33(10)**, 1140-46.

[77] G. R. Pettit, J. S. Ramsdell, and A. H. Tashjian. *J. Biol. Chem*., 1986, **261 (36)**, 7073-80.

[78] J. A. McBain, G. R. Pettit, and G. C. Mueller. *Carcinogenesis*, 1988, **9(1)**, 123-29.

[79] M. Gschwendt, G. Fürstenberger, S. RoseJohn, M. Rogers, W. Kittstein, G. R. Pettit, C. L. Herald, and F. Marks. *Carcinogenesis*, 1988, **9(4)**, 555-62.

[80] R. M. Stone, E. Sariban, G. R. Pettit, and D. W. Kufe. *Blood,* 1988, **72(1)**, 208-13.

[81] J. L. Baryza, S. E. Brenner, M. L. Craske, T. Meyer, and P. A. Wender. *Chem. Biol*., 2004, **11(9)**, 1261-67.

[82] S. J Wang, Z. L. Wang, and S. Grant. *Mol. Pharmacol.,* 2003, **63(1)**, 232-42.

[83] J. Kortmansky, and G. K. Schwartz. *Cancer Invest*., 2003, **21(6)**, 924-36.

[84] C. S. Garcia, R. E. Curiel, J. M. Mwatibo, S. Pestka, H. F. Li, and I. Espinoza-Delgado. *J. Immunol.*, 2006, **177(4),** 2707-16.

[85] M. G. Kazanietz. *Mol. Pharmacol*., 2002, **61(5)**, 1265.

[86] M. K. Sun, and D. L. Alkon. *CNS Drug Reviews*, 2006, **12(1)**, 1-8.

[87] http://www.spacedu.com/protein_kinase_c_experiments.htm (June 26th 2009).

[88] R. Mutter, and M. Wills. *Bioorg. Med. Chem*., 2000, **8(8)**, 1841-60.

[89] J. Kortmansky, and G. K. Schwartz. *Cancer Invest*., 2003, **21(6)**, 924-36.

[90] A. S. Kraft, J. B. Smith, and R. L. Berkow. *Proc. Natl. Acad. Sci*. *USA*, 1986, **83(5)**, 1334-38.

[91] C. Asiedu, J. Biggs, M. Lilly, and A. S. Kraft. *Cancer Res*., 1995, **55(17)**, 3716-20.

[92] T. G. Bivona, S. E. Quantela, B. O. Bodemann, I. M. Ahearn, M. J. Soskis, A. Mor, J. Miura, H. H. Wiener, L. Wright, S. G. Saba, D. Yim, A. Fein, I. Perez del Castro, C. Li, C. B. Thompson, A. D. Cox, and M. R. Philips. *Mol. Cell*, 2006, **21(4)**, 481-93.

[93] K. L. Rinehart, R. Sakai, T. G. Holt, N. L. Fregeau, T. J. Perun, D. S. Seigler, G. R. Wilson, and L. S. Shield. *Pure Appl. Chem.,* 1990, **62(7)**, 1277-80.

[94] K. L. Rinehart, T. G. Holt, N. L. Fregeau, J. G. Stroh, P. A. Keifer, F. Sun, L. H. Li, and D. G. Martin. *J. Org. Chem*., 1990, **55(15)**, 4512-15.

[95] Y. Guan, R. Sakai, K. L. Rinehart, and A. H. J. Wang. *J. Biomol. Struct. Dyn.,* 1993, **10(5)**, 793-818.

[96] R. Sakai, E. A. JaresErijman, I. Manzanares, M. V. S. Elipe, and K. L. Rinehart. *J. Am. Chem. Soc*., 1996, **118(38)**, 9017-23.

[97] A. M. Socha, D. Garcia, R. Sheffer, and D. C. Rowley. *J. Nat. Prod*., 2006, **69(7)**, 1070-73.

[98] E. J. Corey, D. Y. Gin, and R. S. Kania. *J. Am. Chem. Soc*., 1996, **118(38)**, 9202-03.

[99] E. J. Martinez, and E. J. Corey. *Org. Lett*., 2000, **2(7)**, 993-96.

[100] A. Endo, A. Yanagisawa, M. Abe, S. Tohma, T. Kan, and T. Fukuyama. *J. Am. Chem. Soc.,* 2002, **124(23)**, 6552-54.

[101] W. Jin, and R. M. Williams. *Tetrahedron Lett.,* 2003, **44(25)**, 4635-39.

[102] E. J. Martinez, E. J. Corey, T. Owa, and S. Schreiber. *Proc. Natl. Acad. Sci. USA,* 1999, **96(7),** 3496-501.

[103] M. H. David-Cordonnier, C. Gajate, O. Olmea, W. Laine, J. de la Igiesia-Vincente, C. Perez, C. Cuevas, G. Otero, I. Manzanares, C. Bailly, and F. Mollinedo. *Chem. Biol*., 2005, **12(11)**, 1201-10.

[104] S. Chandrasekhar, N. R. Reddy, and Y. S. Rao. *Tetrahedron*, 2006, **62(51)**, 12098-107.

[105] G. Vincent, J. W. Lane, and R. M. Williams. *Tetrahderon Lett*., 2007, **48(21)**, 3719-22.

[106] Z. Z. Liu, Y. Wang, Y. F. Tang, S. Z. Chen, X. G. Chen, and H. Y. Li. *Bioorg. Med. Chem. Lett.*, 2006, **16(5)**, 1282-85.

[107] P. Proksch, R. A. Edrada, and R. Ebel. *Appl. Microbiol. Biotechnol*., 2002, **59(2-3)**, 125-34.

[108] R. Roylance, B. Seddon, A. McTiernan, K. Sykes, S. Daniels, and J. Whelan. *Clin. Oncol*., 2007, **19(8)**, 572-76.

[109] F. Grosso, R. L. Jones, G. D. Demetri, I. R. Judson, J. Y. Blay, A. L. Cesne, R. Sanfilippo, P. Casieri, P. Collini, P. Dileo, C. Spreafico, S. Stacchiotti, E. Tamborini, J. C. Tercero, J. Jimeno, M. D'Incalci, A. Gronchi, J. A. Fletcher, S. Pilotti, and P. G. Casali. *Lancet Oncol.,* 2007, **8(7)**, 595-602.

[110] D. Tewari, B. Saffari, C. Cowan, A. C. Wallick, M. Z. Koontz, and B. J. Monk. *Gynecol. Oncol.*, 2006, **102(3)**, 421-24.

[111] G. Valoti, M. I. Nicoletti, A. Pellegrino, J. Jimeno, H. Hendriks, M. D'Incalci, G. Faircloth, and R. Giavazzi. *Clin. Cancer Res.,* 1998, **4(8)**, 1977-83.

[112] Y. Pommier, G. Kohlhagen, C. Bailly, M. Waring, A. Mazumder, and K. W. Kohn. *Biochem*., 1996, **35(41)**, 13303-09.

[113] M. Zewail-Foote, and L. H. Hurley. *J. Med. Chem*., 1999, **42(14)**, 2493-97.

[114] F. C. Seaman, and L. H. Hurley. *J. Am. Chem. Soc.* 1998, **120(50)**, 13028-41.

[115] M. Bonfanti, E. La Valle, J. M. F. S. Faro, G. Faircloth, G. Caretti, R. Mantovani, and M. D'Incalci. *Anticancer Drug Des*., 1999, **14(3)**, 179-86.

[116] M. Minuzzo, S. Marchini, and M. Broggini. *Proc. Natl. Acad. Sci. USA*, 2000, **97(12)**, 6780-84.

[117] Y. Takebayashi, P. Pourquier, A. Yoshida, G. Kohlhagen, and Y. Pommier. *Proc. Natl. Acad. Sci. USA,* 1999, **96(13)**, 7196-201.

[118] C. Gajate, F. Y. An, and F. Mollinedo. *J. Bio. Chem*., 2002, **277(44)**, 41580-89.

[119] M. H. David-Cordonnier, C. Gajate, O. Olmea, W. Laine, J. de la Igiesia-Vincente, C. Perez, C. Cuevas, G. Otero, I. Manzanares, C. Bailly, and F. Mollinedo. *Chem. Biol*., 2005, **12(11)**, 1201-10.

[120] D. G. Soares, N. P. Poletto, D. Bonatto, M. Salvador, G. Schwartsmann, and J. A. P. Henriques. *Biochem. Pharmacol*., 2005, **70(1),** 59-69.

[121] M. Tavecchio, M. Simone, E. Erba, I. Chiolo, G. Liberi, M. Foiani, M. D'Incalci, and G. Damia. *Euro. J. Cancer*, 2008, **44(4)**, 609-18.

[122] J. K. Lee, E. M. Leslie, M. J. Zamek-Gliszezynski, and K. L. R. Brouwer. *Toxicol. Appli. Pharmacol.*, 2008, **228(1)**, 17-23.

[123] P. Cuevas, M. Perez, M. J. Martin, J. L. Chicharro, C. Fernandex-Rivas, M. Flores, A. Francesch, P. Gallego, M. Zarzuelo, F. de la Calle, J. Garcia, C. Polanco, I. Rodriquez, and I. Manzanares. *Org. Lett*., 2000, **2(16)**, 2545-48.

[124] V. Walsh, and J. Goodman. *Soc. Sci. Med.,* 1999, **49(9)**, 1215-25.

[125] M. C. Wani, H. L. Taylor, M. E. Wall, P. Coggon, and A. T. McPhail. *J. Am. Chem Soc.*, 1971, **93(9)**, 2325-27.

[126] K. C. Nicolaou, Z. Yang, J. J. Lui, H. Ueno, P. G. Nantermet, R. K. Guy, C. F. Clairborne, J. Renaud, E. A. Coulandouros, K. Paulvannan, and E. J. Sorensen. *Nature*, 1994, **367(6464)**, 630-34.

[127] R. A. Holton, Somoza, H. B. Kim, F. Liang, R. J. Biediger, P. D. Boatman, M. Shindo. C. C. Smith, S. Kim, H. Nadizedah, Y. Suzuki, C. L. Yao. P. Vu, S. H. Tang. P. S. Zhang, K. K. Murthi, L. N. Gentile, and J. H. Liu. *J. Am. Chem. Soc.*, 1994, **116(4)**, 1597-600.

[128] T. Enomoto, T. Morimoto, M. Ueno, T. Matsukubo, Y. Shimada, K. Tsutsumi, R. Shirai, and K. Kakiuchi. *Tetrahedron*, 2008, **64(18)**, 4051-59.

[129] V. S. Parmar, A. Jha, K. S. Bisht, P. Taneja, S. K. Singh, A. Kumar, Poonam, R. Jain, and C. E. Olsen. *Phytochemistry*, 1999, **50(8)**, 1267-304.

[130] R. C. Donehower, E. K. Rowinsky, L. B. Grochow, S. M. Longnecker, and D. S. Ettinger. *Cancer Treat. Rep*., 1987, **71(12),** 1171-77.

[131] N. Yildiz, S. Tuna, O. Doker, and A. Calimli. *J. of Supercritical Fluids*, 2007, **41(3)**, 440-51.

[132] E. R. Gardner, W. Dahut, and W. D. Figg. *J. Chromatogr. B Analyt. Technol. Biomed. Life Sci*., 2008, **862(1-2)**, 213-18.

[133] http://www.abraxane.com/ (June 21st 2009).

[134] M. Grosheva, O. Guntinas-Lichius, S. K. Angelova, S. Kuerten, A. Alvanou, M. Streppel, E. Skouras, N. Sinis, S. Pavlov, and D. N. Angelov. *Exp. Neurol.,* 2008, **209(1)**, 131-44.

[135] S. M. L. Aversa, A. M. Cattelan, L. Salvagno, G. Crivellari, G. Banna, M. Trevenzoli, V. Chiarion-Sileni, and S. Monfardini. *Crit. Rev. Oncol. Hematol.,* 2005, **53(3)**, 253-65.

[136] A. Ehrlich, S. Booher, Y. Becerra, D. L. Borris, W. D. Figg, M. L. Turner, and A. Blauvelt. *J. Am. Acad. Dermatol*., 2004, **50(4)**, 533-40.

[137] N. Kumar. *J. Biol. Chem.,* 1981. **256(20),** 435-41.

[138] M. Fransson, and H. Green. *Euro. J. Pharm. Sci*., 2008, **33(2)**, 128-37.

[139] Y. Han, A. G. Chaudhary, M. D. Chordia, D. L. Sackett, B. PerezRamirez, D. G. I. Kingston, and S. Bane. *Biochemistry*, 1996, **35(45)**, 14173-83.

[140] J. S. Choi, and B. W. Jo. *Int. J. Pharm*., 2004, **280(1-2)**, 221-27.

[141] L. P. Cavalcanti, O. Konovalov, and H. Haas. *Chem. Phys. Lipids*, 2007, **150(1)**, 58-65.

[142] O. Grinberg, M. Hayun, B. Sredni, and A. Gedanken. *Ultrason. Sonochem*., 2007, **14(5)**, 661-66.

[143] A. Mehdinia, S. H. Kazemi, S. Z. Bathaie, A. Alizadeh, M. Shamsipur, and M. F. Mousavi. *Anal. Biochem*., 2008, **375(2)**, 331-38.

[144] J. H. Kim. *Process Biochem*., 2004, **39(11)**, 1567-71.

[145] http://www.epa.gov/greenchemistry/pubs/pgcc/winners/gspa04.html (June 26th 2009).

[146] J. S. Cheng, C. Lei, J. C. Wu, and Y. J. Yuan. *J. Biotechnol*., 2008, **133(1)**, 96-102.

[147] A. Y. Khosroushahi, M. Valizadeh, A. Ghasempour, M. Khosrowshahli, H. Naghdibadi, M. R. Dadpour, and Y. Omidi. *Cell Biol. Int.,* 2006, **30(3)**, 262-69.

[148] J. S. Cheng, D. M. Yin, S. Y. Li, and Y. J. Yuan. *Enzyme Microb. Technol*., 2006, **39(6)**, 1250-57.

[149] Y. D. Wang, J. C. Wu, and Y. J. Yaun. *Cell Biol. Int*., 2007, **31(10)**, 1179-83.

[150] A. Stierle, G. Strobel, and D Stierle. *Science*, 1993, **260(5105)**, 214-16.

[151] R. S. Kumaran, J. Muthumary, and B. K. Hur. *Eng. Life Sci.,* 2008, **8(4)**, 438-46.

[152] R. S. Kumaran, J. Muthumary, and B. K. Hur. *J. Biosci. Bioeng.,* 2008, **106(1)**, 103-06.

[153] B. V. S. K. Chakravarthi, P. Das, K. Surendranath, A. A. Karande, and C. Jayabaskaran. *J. Biosci.*, 2008, **33(2)**, 259-67.

[154] T. J. Manning, M. Land, E. Rhodes, L, Chamberlin, J. Rudloe, D. Phillips, T. T. Lam, J. Purcell, H. J. Cooper, M. R. Emmett, and A. G. Marshall. *Nat. Prod. Res*., 2005, **19(5)**, 467-91.

[155] T. Manning, T. Umberger, S. Strickland, D, Lovingood, R. Borchelt, M. Land, D. Phillips, and J. C. Manning. *Int. J. Environ. Anal. Chem*., 2003, **83(10)**, 861-66.

[156] T. J. Manning, E. Rhodes, M. Land, R. Parkman, and A. G. Marshall. *Nat. Prod. Res*., 2006, **20(6)**, 611-28.

[157] T. J. Manning, E. Rhodes, R. Loftis, D. Phillips, D. Demaria, D. Newman, and J. Rudloe. *Nat. Prod. Res*., 2006, **20(5)**, 461-73.

CHAPTER 2

A composition of chemicals used as an artificial source

for the production of the bryostatins

2.1 Introduction

Within recent decades**,** the ocean has become an increased target for the identification and isolation of new compounds with possible medicinal activity.[1,2] The isolation of numerous NPs has shown much success in clinical trials against various cancers, such as prostate, kidney, ovarian, leukemia, *etc*..[3] Further studies of these NPs and others have been limited due to: 1) environmental concerns of collecting marine organisms; 2) their seasonal availability; 3) the time consuming process; and/or, 4) labor intensive isolation techniques currently used. Alternative methods, such as synthetic techniques, have been determined and aquaculture farming of marine organisms has been conducted, in the hope of developing a feasible method to produce economically these natural products. Despite continuous efforts, no practical method has so far materialized for the feasible production of any bryostatin compounds.

Agar is a type of gel designed to support the growth of bacteria in a controlled environment.[4] Many different agars are used for the production of bacteria, each depending on the bacteria of interest.[5] For example, mannitol salt agar is a growth medium which contains high concentrations of sodium chloride, used specifically for the growth of *Staphylococci spp.*. By using this agar, the growth of other bacteria are inhibited due to the high concentrations of sodium chloride present.[6] Another example is the production of a potato carrot agar, a semi-selective medium, for the isolation of *Alternaria spp., Epicoccum spp.,* and *Phoma spp.* from soil and plant samples. The medium consisted of 10 g/L of potato and carrot as a base and manganese(II) chloride, which was used to isolate selectively the bacteria of interest by inhibiting the growth of other species of bacteria in the soil and plant samples.[7]

Nutrient agars containing peptone, amino acids and carbon sources, are also used for the production of microorganisms. Despite this remarkable tool to

aid in the growth of bacteria, many bacteria are still unable or impossible to grow under controlled conditions. With recent developments by other groups, new speculations regarding the true source of marine organisms have suggested the correlation of marine bacteria to marine organism containing MNP's.[8,9,10,11] For this reason, the concept of an agar medium, was applied to the production of marine bacteria, using a chemical compilation developed.

In order to develop the chemical composition that was subsequently used, initial analysis of the environment of these marine organisms was conducted in order to understand the conditions in which these marine organisms live and the properties of the environment that can aid in the production of such compounds. In this regard, initial studies for developing a novel method for the economical production of the bryostatins was instigated by first understanding the environment of its host organism. This involved a thorough investigation and chemical analysis of the marine environment where *Bugula* is found.[12,13,14,15] Based on results from these studies, a composition of chemicals was used to develop an artificial growth medium, in an attempt to mimic the composition of the host marine organism. This artificial growth medium would serve as an artificial surface to cultivate and isolate the marine bacterium responsible for the production of the bryostatins. Previous studies have shown traces of bryostatin 1 in several marine organisms other than *Bugula,* further supporting the postulate that a marine bacterium is responsible for the production of the bryostatins.[12-15]

Bugula neritina has also reportedly been found in areas along the coast of England and for this reason a small scale experiment was conducted off the coast of Sunderland, UK, using the same artificial medium. The artificial growth medium (as tablets) was placed in three designated locations for an allocated time to initiate the broth assessment. The purpose of this experiment was to determine if any bacterial growth along the coast of England would show

prominence for the production of any bryostatin compounds. Successful results showing the production of different bryostatin compounds from either US or UK locations would revolutionize the availability and reproducibility of natural products for pharmaceutical industries and companies demanding such products.

2.2 Experimental Section

In each experiment, the chemical composition was applied either as a paste or packed into a tablet form. Sample extracts collected from each experiment were compared to bryostatin 1 standard. Samples were analyzed in positive mode by a LC-MS system, with a gradient solvent system consisting of 0.1% formic acid and methanol, in a 95:5 ratio, respectively, with a run time of 30 min and a flow rate of 1 mL/min. A C18 Luna column (Sigma Aldrich, 250 mm by 4.6 mm, 5 µm) was used to analyze all samples. Some samples were also analyzed using the MALDI-TOF-MS (Matrix assisted laser desorption ionization, time of flight mass spectrometry) at the University of Georgia Mass Spectrometry Facility (Athens, Georgia, USA). A matrix consisting of 50:50 water and acetonitrile with 0.1% TFA (trifluoroacetic acid) was used to run the samples in this study. All samples analyzed via LC-MS were conducted at chemiSpec, University of Sunderland (Sunderland, UK) and at the USDA (United States Department of Agriculture, Tifton, Georgia, USA), respectively. High resolution mass spectrometry (HRMS) data were collected by the University of Warwick (Warwick, UK). The samples analyzed by HRMS were conducted using a nanoLC-ESI-MS with the NanoAcquity/Q-ToF instrumentation (Waters). The reference compound used was the [Glu^1]-Fibrinopeptide B (human F3261, Sigma), infused at 0.5 µL/min sampled for 1 s each minute of data collection.

2.2.1 Mineral paste, Gulf of México (February 2006)

The chemicals (Table 1) were combined and applied as a paste to both sides of two artificial surfaces (grids). Each surface contained a strip of zinc sandwiched between two strips of copper (Fig. 1). The grids were placed in the water on February 11th 2006, at 10:00 a.m., and removed after 6 hr in the water. The grids were air dried, then stored at 4°C before being placed at Alligator Point, Florida (25° 36’ 0" N, 81° 14’ 28" W). Each grid was positioned inside a PVC tube, with holes drilled in each side to allow water to flow freely. Each end of the tube was covered with a screen to prevent anything from entering: each set of traps (a total of 2) were tightly secured to a weighted support as shown in Fig 2. After immersion for 6 hr, the grids from each trap were removed and placed into two large pails containing salt water.

One pail was placed at RT (room temperature, 23°C) and the other was stored at 4°C. On May 8th 2006, at 9:00 a.m., 12 wk after the grids were placed at 4°C, a white film was removed from the surface of the water and extracted into 30 mL of ethanol (Fisher Scientific) then stored at 4°C. After 24 hr, the ethanol was placed under vacuum to dryness. A second extraction of the white film into 30 mL of methanol (Fisher Scientific) was carried out, then placed at 4°C. After 48 hr the methanol was placed under vacuum to dryness.

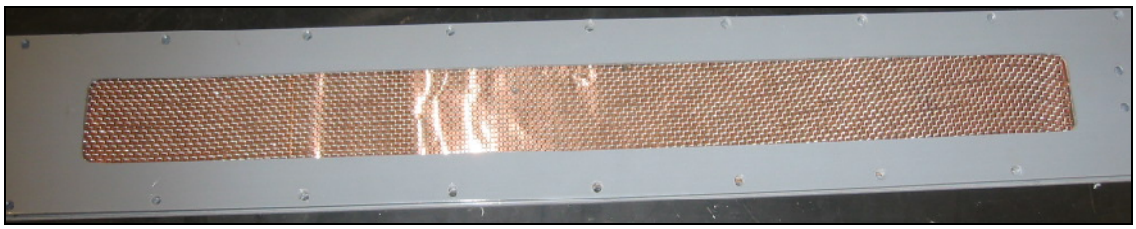

Fig 1. The reassembled grid after placing strips of copper on each side**.**

Fig 2. The trap design of the grids inside the PVC pipes before being placed in the water.

Table 1. The chemical composition used to produce the tablets.

Chemicals	**Amount used (g)**	**Company**	**Product code**
Calcium carbonate	100.004	Fisher Scientific	S71922
Iron (III) chloride	3.000	Fisher Scientific	FL-01-0784
Iron (np)[a]	0.05	Nanophase	0800
CuO (np)	0.01	Nanophase	EXP0502
$CuCl_2$	0.123	Sigma-Aldrich	221783-500G
Instant ocean	1.000	Marine Labs	SS3-50
Marine buffer	0.500	SeaChem	UPC# 000116034708
Sodium acetate	0.400	Fisher Scientific	S210-500
Squalene	0.500 (10 drops)	Sigma-Aldrich	S3626-100 mL
Peptone	1.000	Fisher Scientific	BP1420-100
Glycerine	1.003	Fisher Scientific	G33-500
Stearic acid	0.400	Aldrich	175366-1Kg
Octanoic acid	0.215 (10 drops)	Acros Organics	167261000
Docosanoic acid	0.799	Aldrich	216941-5G
Amino acid tablets	1.411 (1 tablet)	GNC	750612
Sugar	1.000	Pure Cane Dixie Crystals	S133E06A-PA
Chitin[b]	4.09	Gulf of México	N/A
Sand	3.017	N/A	I116-500
Distilled water	35 mL	N/A	N/A

[a] np – nano particle
[b] chitin - shrimp shells

A second experiment was later conducted using the method mentioned above. However, a chemical (cement) was applied to adhere the paste to each side of the grids. A total of 5 grids were prepared and placed at Alligator Point, FL. The grids were placed under the exact conditions (location, time period in water, and conditions in the laboratory *etc*.) as previously. Results from the experiments were analyzed as mentioned in section 2.2.

2.2.2 Mineral paste, Gulf of México (May 2007)

On March 12th 2007, at 10:00 a.m., another experiment was conducted using the combined chemicals listed in Table 2; a modified composition of those given in Table 1. Dry combinations of chemicals (20 g) were packed into 15 plastic vials with a hole in the top of each vial to allow the passage of water. All 15 vials were placed in a bacterial chamber filled with calcium carbonate pellets and iron chloride (Fig. 3), then submerged at Alligator Point, Florida. On March 31st 2007, at 12:00 p.m., the container was removed from the water at Alligator Point, Fl. The water from each vial was replaced with 30 mL of methanol-DTPA (diethylene triaminepentaacetic acid) solution before vials were stored at RT.

Table 2. The chemical composition used to produce the tablets.

Chemical	Amt used	Company	Product code
$CaCO_3$	500 g	Fisher Scientific	S71922
$FeCl_36H_2O$	10 g	Fisher Scientific	FL-01-0784
Marine Buffer	2 g	Sea Chem	UPC# 000116034708
Instant Ocean	2 g	Marine Labs	SS3-50
Sodium acetate	2 g	Fisher scientific	S210-500
Sodium nitrate	2g	Fisher scientific	
Sodium sulfate	1 g	Fisher scientific	AC21875-0250
Peptone	2 g	Fisher scientific	BP1420-100
Amino Acid	10 tablets	Fisher Scientific	S71922
Fish Oil	10 tablets	GNC	750612
Multi-Vitamin	10 capsules	Equate	N/A
Vitamin A & D	10 capsules	Spring Valley	N/A
Vitamin C	10 tablets	Spring Valley	N/A
Sugar	20 g	Pure Cane Dixie Crystals	S133E06A-PA
Glycerin	2 mL	Fisher scientific	G33-500
Stearic acid	1 g	Sigma Aldrich	175366-1Kg
Squalene	2 mL	Fisher scientific	AC20747-1000
Octanoic acid	2 mL	Fisher scientific	167261000

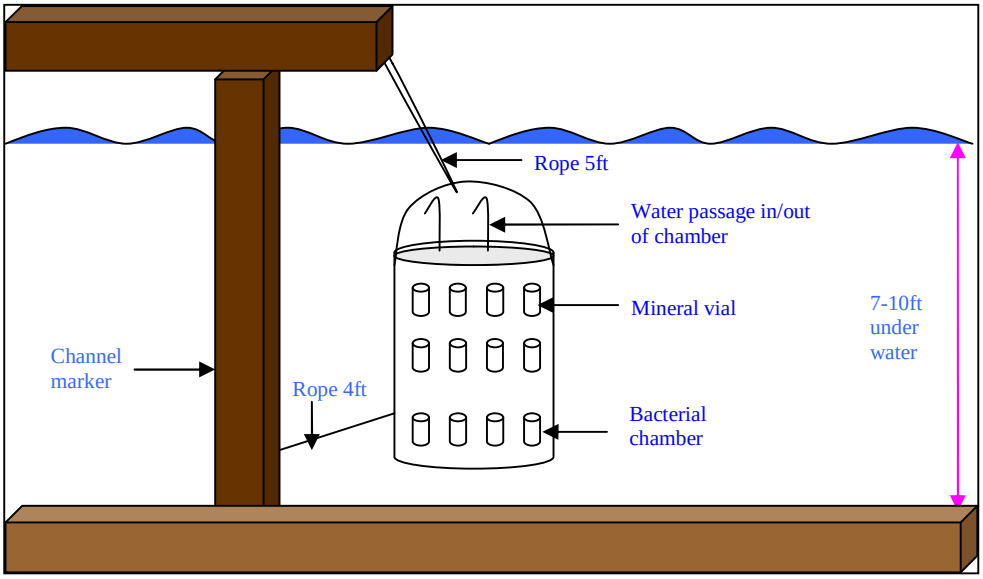

Fig. 3. A 2-dimensional image of the chamber (section 2.2.2).

2.2.3 Mineral paste, Gulf of México (June 2008)

On June 15th 2008, at 12:00 p.m., the combined chemicals listed in Table 2 were compressed into tablets (average weight of 10 g), and then placed into 50 mL plastic vials with two holes in each vial for water to flow through. A total of 10 vials, each containing 4 tablets, were placed at Alligator Point, Florida, for 1 wk and removed on June 22nd 2008, at 12:00 p.m.. Vials were then transferred into containers with water from Alligator Point and placed at 4°C for 48 hr, then moved to RT for 4 ½ wk of the broth assessment. The broth was checked twice a week; which entailed the removal of a white film from the surface of the water that was extracted into 80 mL of anhydrous methanol (Fisher Scientific), followed by the addition of 10 g of mineral paste compilation (Table 2) to the container. The methanol extract was filtered using 5 µm filter paper and placed into a vacuum to dryness. Total dry weight of crystals collected (1.85 g) was later analyzed (section 2.2).

2.2.4 Mineral paste, UK coast (November 2006)

On November 3rd 2006, at 5:00 p.m., three locations off the North East coast (Sunderland Marina (54º 55'N, 01º 22' W), Hartlepool Marina (54º 41' N,

01º 11' W) and Hartlepool Fish Quay (54° 41′ 26.56″ N, 1° 12′ 39.79″ W) were selected for this study. Tablets were prepared (section 2.2.1). A total of 6 vials, each containing 2 tablets, were placed at each location for 1 wk. Samples were collected on November 11th 2006, at 10:00 a.m., then collected in pails of sea water and stored at RT (18°C) for 4 wk to determine cultivation of bacterial growth. The film produced after 4 wk was collected from the surface of the water and was extracted into anhydrous methanol. The sample was analyzed by LC-MS at chemiSpec.

2.3 Results

All the results collected were compared to the LC-MS and MALDI-MS of a bryostatin 1 reference standard (Figs. 4 and 5) respectively. Due to low detection limitations for each peak from the samples in this study, no further evidence could be obtained to conclusively support or disprove the correlation of the peaks identified with their possible bryostatin representations.

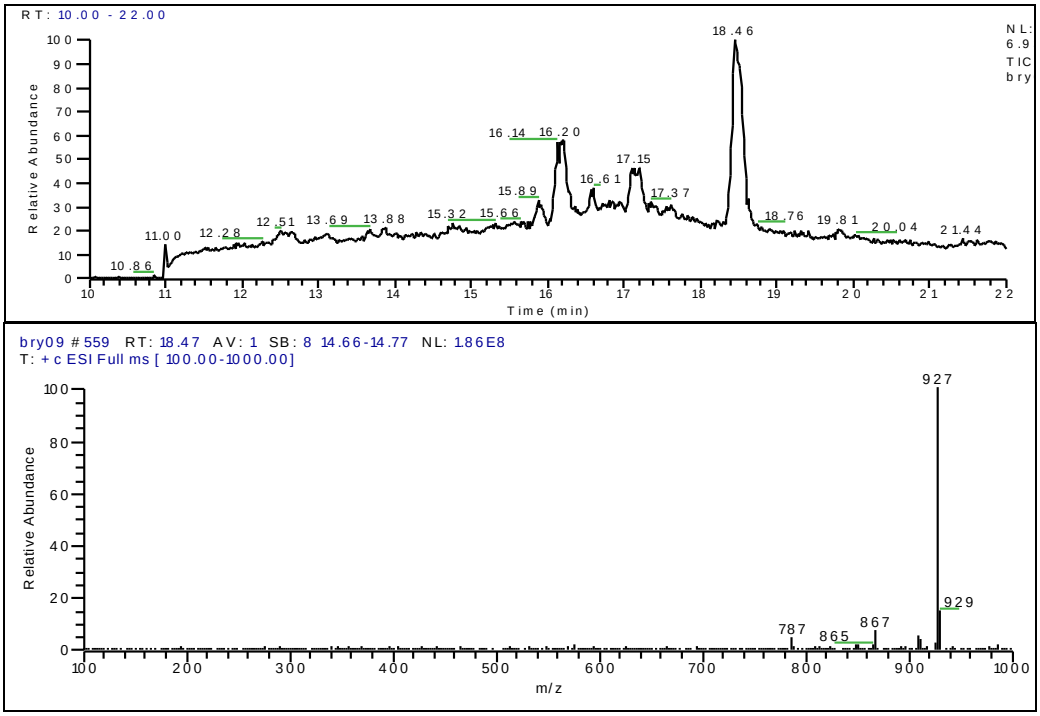

Fig. 4. LC-MS of bryostatin 1 standard ($C_{47}H_{68}NaO_{17}$, *m/z* 927, retention time 18.46 min).

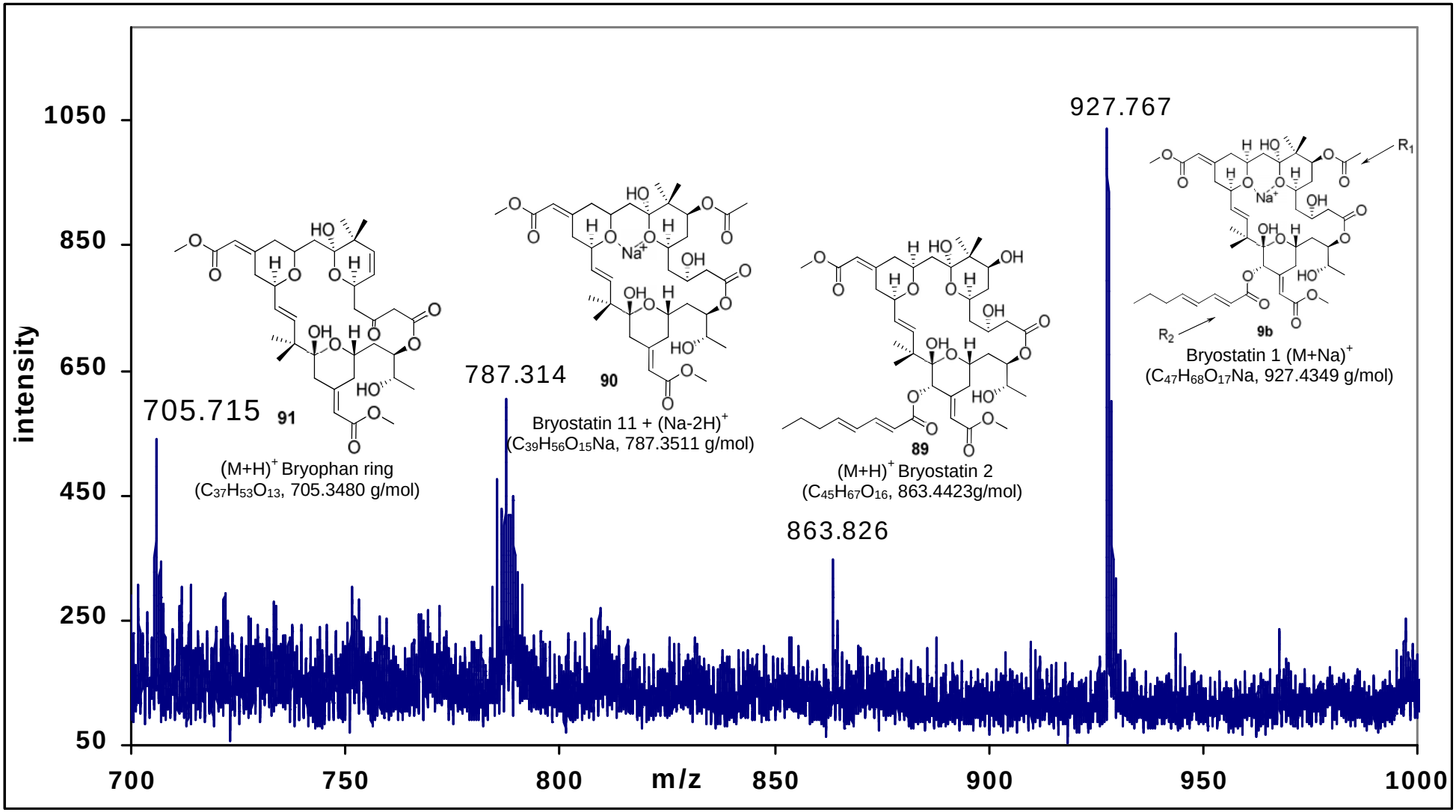

Fig 5. MALDI-MS of bryostatin 1 standard (10 µg) in 5 mL anhydrous methanol.

The above illustration shows how bryostatin 1 fragments in the mass spectrometer to give the peaks as shown. There are twenty bryostatin compounds that have been isolated from *Bugula neritina*, each bryostatin compound differs by the R_1 and R_2 group positions as shown above. Bryostatin 1+ Na^+ adduct **9b** ($C_{47}H_{68}O_{17}Na$, 927.4349 g/mol) loses $C_2H_3O^{\cdot}$ ion with a *m/z* of 863.826 $(M+H)^+$. This peak can therefore be correlated to bryostatin 2 $(M+H)^+$ **89,** which has a formula of ($C_{45}H_{67}O_{16}$, 863.4423 g/mol). Due to the intensity of this peak, it is suggested that only a fraction of the bryostatin 1 molecule loses acetyl to show the formation of the peak as shown.

In much of the MALDI-MS data that has been conducted for bryostatin 1, consistent fragment is always shown: the peak with a *m/z* of 789 $(M+Na)^+$ **90** sometimes seen as 787 $(M-2H+Na)^+$ peak. As shown above, the species of mass 789 can be formed by the loss of the carboxylate group (R_2 group), which can be correlated to the bryostatin 11+Na^+ adduct ($C_{39}H_{58}O_{15}Na$, 789.3668 g/mol).

The basic structure for all of the bryostatin compounds is the bryophan ring $(M+H)^+$ **91** ($C_{37}H_{53}O_{13}$, 705.3481 g/mol). The loss of the R_1 and R_2 groups gives the basic structure of the bryophan ring (i.e. the acetate group at R_1 position and the C8 chain at the R_2 position). The formation of this ring gives a stable product, as many of the ester groups are susceptible to hydrolysis or degradation. As shown above, bryostatin 1 fragments to give a *m/z* of 705.715, which could correlate to the bryophan ring $(M+H)^+$. Of all the bryostatin compounds that have been isolated from *Bugula*, bryostatin 1 has the most potency as a medicinal agent. The fragments of bryostatin 1 shown in Fig. 5 are used as a reference to support further the postulated species, identified by their *m/z*, found for the samples in this study, and to allow correlation to the bryostatin compounds they might represent.

2.3.1 Mineral paste, Gulf of México (February 2006)

The purpose of this study was to develop an artificial medium that would attract marine bacteria presumed to be responsible for the production of any bryostatin compounds in the *Bugula* ecosystem. Observations from the pail containing grids at 4°C noted the formation of a white film on the surface of the water. The pail placed at RT (23°C) showed no sign of a white film and was therefore deemed unsuccessful. Having compared the results from pails stored at RT with those at 4°C, it is suggested that marine bacteria are responsible for the production of the white film collected from the pail at 4°C and that they are likely to grow and live longer in a colder environment as opposed to 23°C. In general, bacteria tend to initially grow and reproduce rapidly, but eventually die in the environment. This is due to many factors, such as 1) lack of a food source or nutrients; 2) too many toxins produced by the bacteria; 3) temperature (some bacteria prefer colder temperatures while others prefer warmer conditions); and, 4) oxygen concentrations, to name only a few.[16] The thick, white film collected off the surface from the water after 12 wk was extracted in ethanol and dried in a vacuum for analysis. The crystals collected are shown in Fig. 6 and mass spectral data of the ethanol extract from the white film (Fig. 7). None of the peaks shown in Fig. 7 can be correlated to any bryostatin compound.

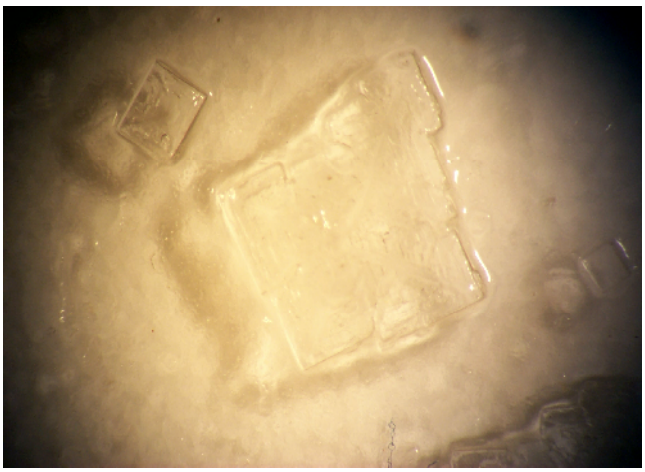

Fig. 6. Crystal collected from the extraction of white film produced from the broth at 4°C.

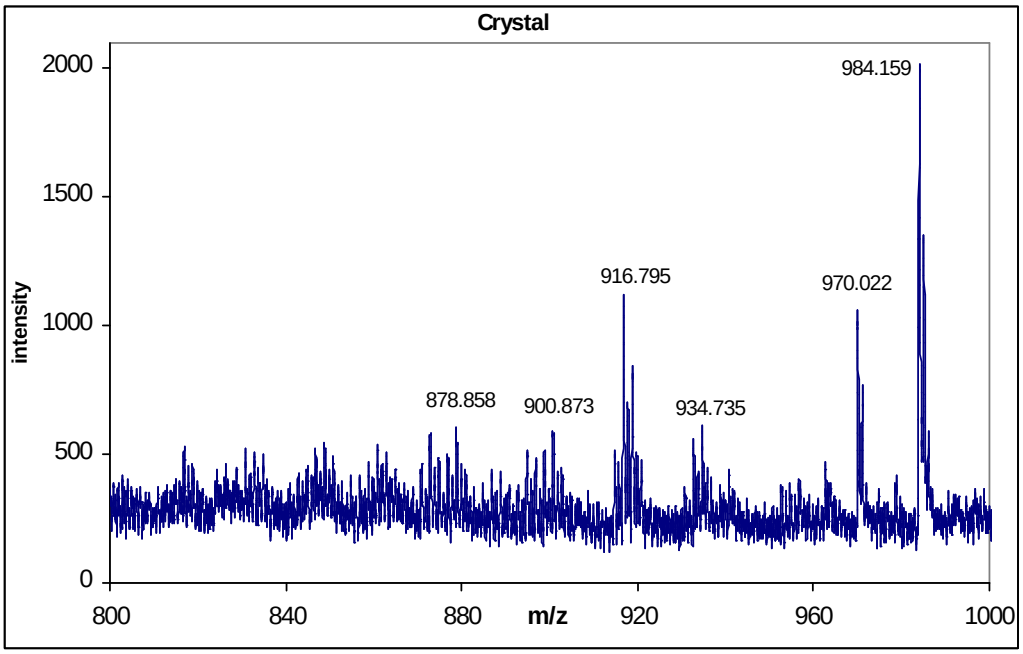

Fig. 7. Mass spectral data of crystal collected from the small scale growth.

2.3.2 Mineral paste, Gulf of México (May 2007)

In this study, the chemicals from Table 1 were modified as shown in Table 2 in order to improve the cultivation and continuous growth of marine bacteria isolated from the ocean. Food sources (amino acids, multi vitamins, and fish oil, *etc*.) were added as growth factors to attract and maintain the marine bacteria on the surfaces while placed in the water. After the 3 wk period, the mineral paste, calcium carbonate pellets and water in the bucket appeared black in color, emitting a pungent odor. The solvent extracted from each vial appeared golden yellow in color and after 48 hr all the vial contents were combined and analyzed by LC-MS (Fig. 8). The *m/z* of 927 shown below shows the presence of bryostatin 1, despite the shift in retention time from 18.45 min to 17.52 min, which can be due to a change in temperature or other properties when the sample was analyzed.

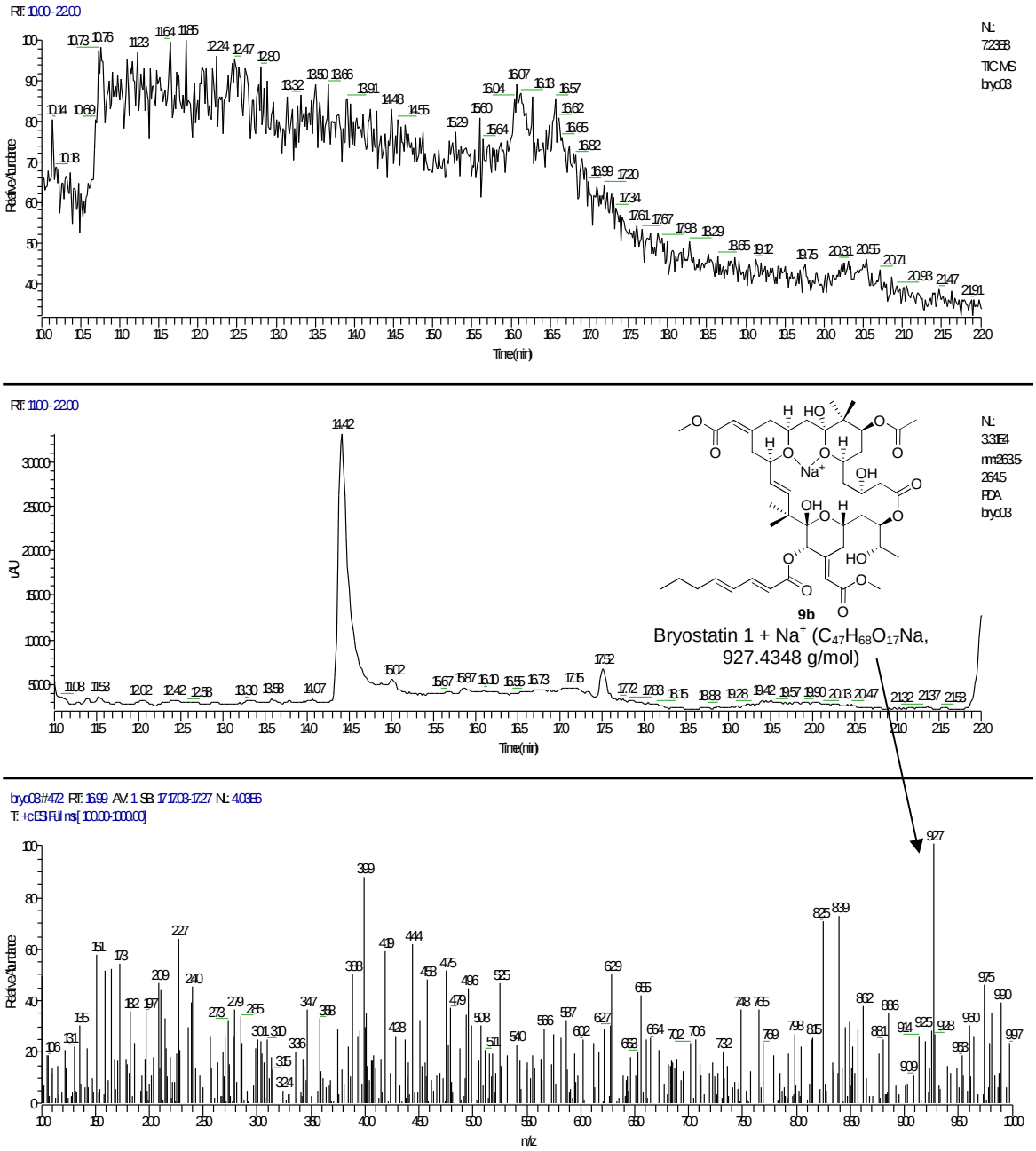

Fig 8. LC-MS of mineral paste extracted into methanol.

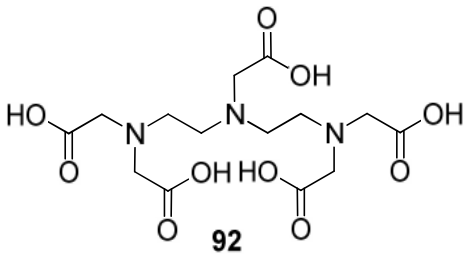

Fig. 9. Structure of DTPA ($C_{14}H_{23}N_3O_{10}$, 393.1378 g/mol)

DTPA **92** (Fig. 9.) is a chelating agent used as a soil extractant to remove metals, such as Fe^{3+}, Na^{+}, Ca^{2+}, and Zn^{2+}, *etc*., from the sediment.[17] In the extraction process, DTPA was used as a means of extracting the compounds

easier. Bryostatin 1 was used as a control in the mass spectrometry studies and is almost exclusively observed as a Na^+ adduct Typically the bryostatins are observed as Na^+ adducts, unless an aminocarboxylate such as EDTA (ethylenediaminetetraacetic acid) or DTPA is utilized in the extraction.

2.3.3 Mineral paste, Gulf of México (June 2008)

After 1 wk in the water, most of the tablets appeared black in color and after 2 days at RT, the tablets were completely black. A gelatinous film seen on the surface of the water after 5 day at RT was removed and extracted into 80 mL of anhydrous methanol during the 4 ½ wk broth assessment. The dry weight of crystals (1.72 g) was analyzed by HRMS as shown in Fig. 10 and 11.

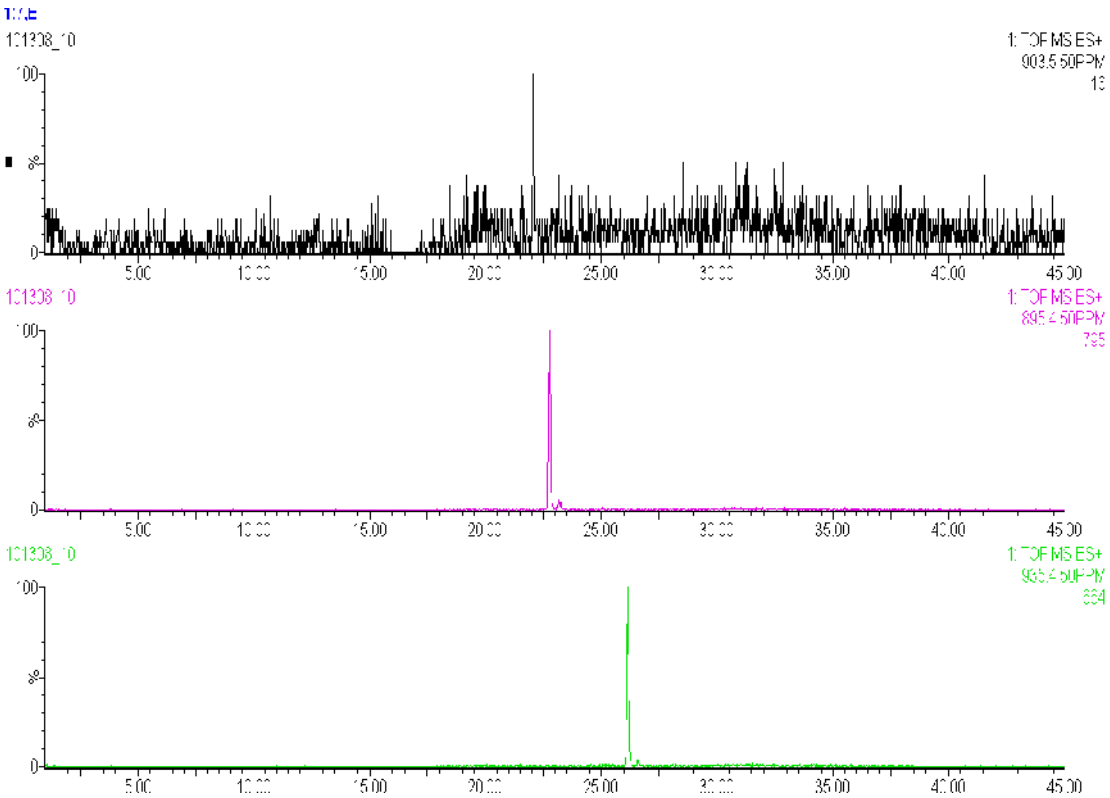

Fig 10. The extract ion chromatogram for peaks identified from the white film.

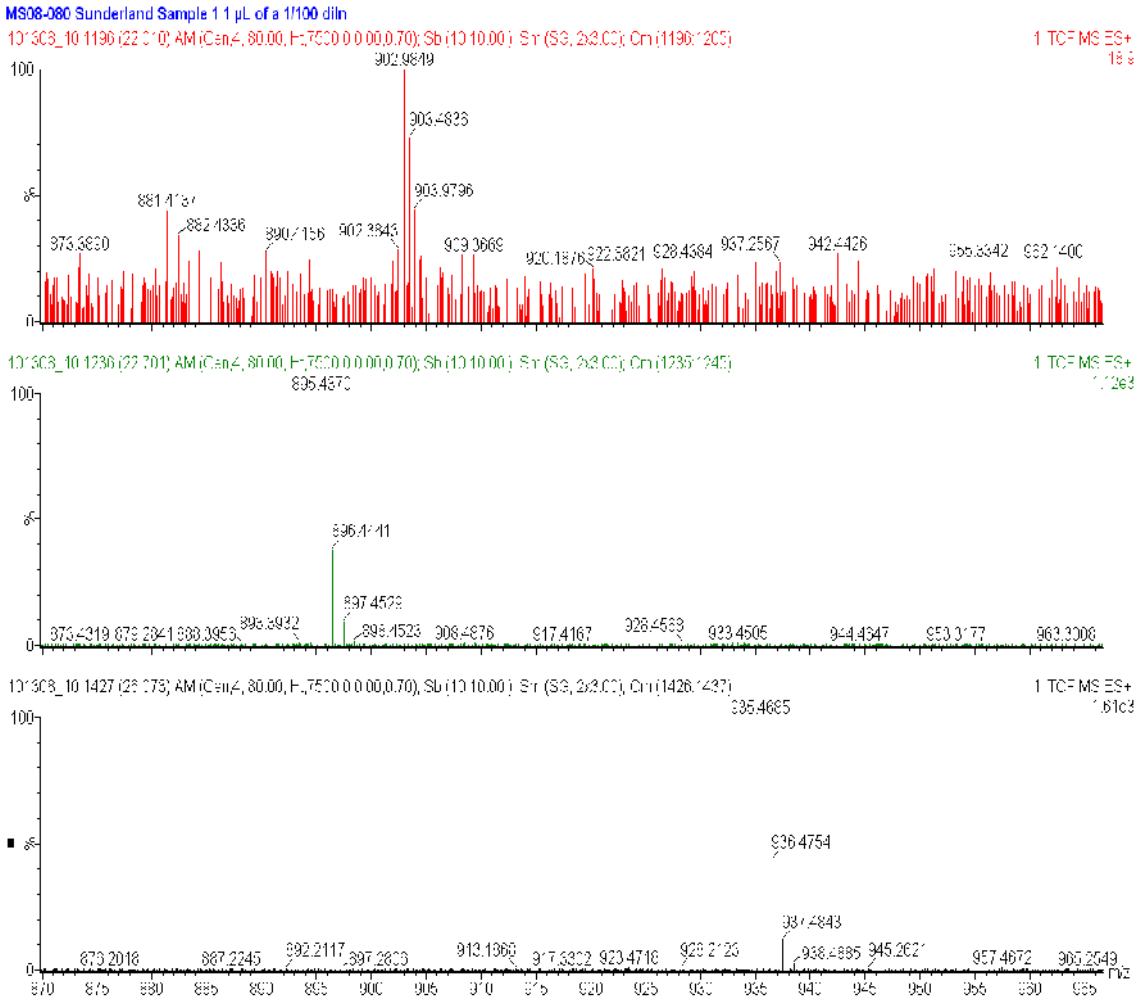

Fig. 11. High resolution mass spectra of the extract ions shown in Fig. 10.

a)

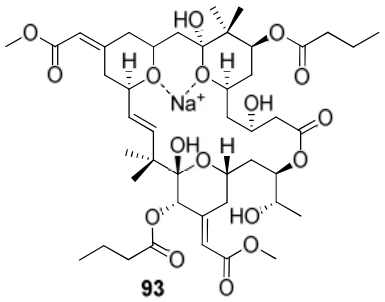

93

$(M+Na)^+$ Bryostatin 8+Na^+
($C_{45}H_{68}O_{17}Na$, 903.4348 g/mol)

b)

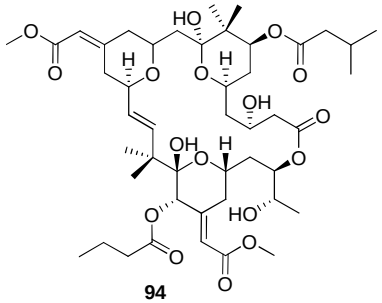

94

$(M+H)^+$ Bryostatin 4
($C_{46}H_{71}O_{17}$, 895.4685 g/mol)

c)

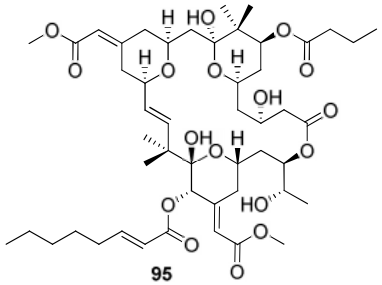

95

$(M+H)^+$
($C_{49}H_{75}O_{17}$, 935.4998 g/mol)

Based on the data collected from the white film, Fig. 11 shows three peaks that may be correlated to three different bryostatin compounds. These peak are: a) *m/z* at 902.9849 $(M+Na)^+$, which may be Bryostatin 8 + Na^+ **93** ($C_{45}H_{68}O_{17}Na$, 903.4348 g/mol), b) *m/z* at 895.4370 $(M+H)^+$, which may be bryostatin 4 **94** ($C_{46}H_{71}O_{17}$, 895.4685 g/mol), and c) *m/z* at 935.4685 $(M+2H)^+$, which may be bryostatin 12 **95** ($C_{49}H_{75}O_{17}$, 935.4998 g/mol). Based on the HRMS data collected, the peaks (Fig. 11) each showed an error of approximately 30 ppm when compared to the possible bryostatin compounds that each could represent. For example, the calculated mass accuracy of bryostatin 4 is (895.4685, $M+H)^+$ and bryostatin 12 is (935.4998, $M+2H)^+$. The acceptable marginal difference is 10 ppm. In the mass spectrometer, different radicals can form to give different masses $(M+H)^+$ $(M+2H)^+$, $(M-H)^+$ and $(M-2H)^+$.[18] These radicals occur naturally in the mass spectrometer and can therefore be accounted for in relation to the peaks shown above. Aside from the bryostatin compound that the peak at *m/z* of 903 might represent, it was observed that the *m/z* at 903 shown in Fig. 11 splits by a *m/z* of 0.5, which suggests the possibility that the compound with a *m/z* of 903 may be a dimer bound together by a Na^+ adduct.

2.3.4 Mineral paste, UK coast (November 2006)

After 1 wk in seawater, only tablets from the vials placed at Hartlepool Marina were black in colour, suggesting the presence of bacterial growth. After 2 wk at RT, the formation of a thin gelatinous surface film was noticeable in the containers with samples from Hartlepool Marina and Hartlepool Fish Quay. By the 4^{th} wk, a white gelatinous film completely covered the surface of the sample pails from Hartlepool Marina and the Fish Quay, each was removed and extracted into 20 mL anhydrous methanol (Fisher Scientific). Further purifications were conducted by TLC (thin layer chromatography, 5.08cmX1.27cm, silica gel

60) plates, using a 30/70 mixture of petroleum ether and ethyl acetate as the mobile phase. This separation technique showed two distinct bands, under uv light, which were removed from the silica plate and placed in methanol. All the results from this experiment were unsuccessful in detecting any bryostatin compounds from the samples collected at each location.

2.4 Discussion

Many marine organisms are believed to produce these biologically active compounds 1) as a chemical defense mechanism (prey, predator or compete for territory due to the overgrowth of species), 2) as a secondary method for survival, or 3) as secondary metabolites**.**[19,20,21,22] Secondary metabolites are organic compounds produced by marine organisms that have no effect on the growth, development and reproduction of marine organisms. However, many secondary metabolites are believed to be created by modified primary metabolite enzymes or by using substrates of primary metabolite origin. Primary metabolites in contrast to secondary metabolites, are important for the growth, development and reproduction of organisms.[23] For example, okadic acid **1**, a NP originally isolated from sponges, *Halichondria okadai* and *Halichondria melanodocia,* is responsible for most diarrheic shellfish poisoning related illnesses in humans. The significance of okadic acid is unclear in the sponges from which it has been isolated; however, it has been shown to help the marine sponge, *Lubomirskia baicalensis*, tolerate extremely cold conditions.[19]

Many of the marine organisms that have shown activity as medicinal agents are filter feeders (*e.g. Ecteinascidia turbinata* and *Bugula neritina*) and therefore contain high levels of marine viruses and bacteria, (suspected to be the primary source in the production of marine natural products). Attempts have been made to determine which particular bacterium is responsible for the production of

the bryostatins and the ecteinascidin compounds; however no conclusive evidence has yet been established.[8-11] Nonetheless, some groups have shown that the production of these drugs can be correlated to the presence of photosymbiont in the marine organisms, which can be cultured to produce the drugs more efficiently.[24,25]

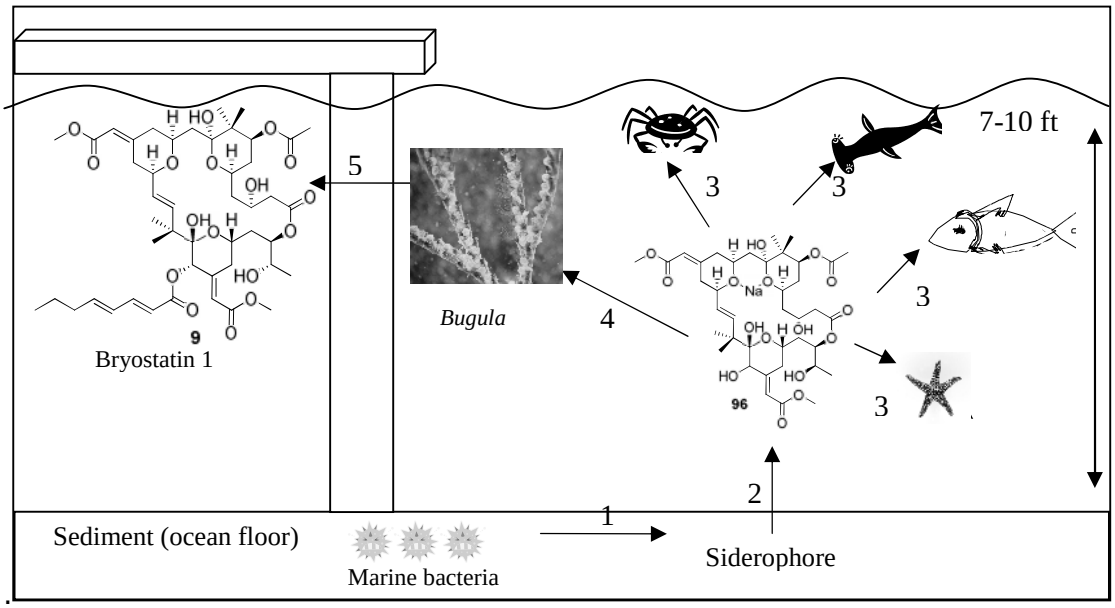

Fig. 12. A 2-dimensional image showing the ubiquity of bacteria within the marine ecosystem.

Previous work by this group has shown that natural products (*e.g.* bryostatins) are ubiquitous in the ecosystem in which the marine organism is found.[12-14] From this study and others (*e.g.* environmental study), it can be concluded that these marine organisms filter in the bacteria that are responsible for the production of these natural products (Fig. 12). The specificity and uniqueness of any particular marine organism is believed to be dependent upon the environmental preferences of a particular bacterium, as it selects a suitable host to live in and produce such compounds.

The chemicals used in the assessment of this study were based on detailed analysis of the marine organism, *Bugula neritina*, and the ecosystem in which it is found.[12-14] The importance of the chemicals can be placed into four

categories. Firstly, the surface of *Bugula* has shown to contain high levels of calcium carbonate and extraction of the marine organism has shown high concentration of nano particles (Fe, CuO); indicating that the bacteria found within the organism thrives on these components. The ecosystem of the marine organism has a high deposit of limestone (approximately 40%) as well, which accounts for the main component of our chemical composition to be calcium carbonate. These chemicals were therefore used as a means to attract the bacteria, due to the perceived high affinity for the compounds. The concentrations shown in Tables 1 and 2 were based on previous study showing the concentration values of iron, copper an calcium in the marine ecosystem.[14] Concentration levels of iron and copper found in *Bugula* are higher than any other living creature can tolerate.

Secondly, to cultivate and isolate the bacteria, it is necessary to replicate the contents of the ocean in efforts to mimic the environment of the bacteria. For this reason marine buffer and Instant Ocean were used. Marine buffer consists of a combination of different salts of magnesium, sodium, and potassium, *etc*., in the form of carbonates, chlorides, sulfates, and borates, *etc*., which are important to maintain the pH (8.3) of the environment.[26] Instant Ocean contains synthetic sea salts which contain traces of the elements needed for natural sea water, as found in the marine environment, necessary for animal growth.[27] Many of these salts are important for bacteria, for example, potassium salts function as a cofactor for certain enzymes and magnesium salts function as a cofactor for certain enzymatic reactions *etc*..[28] The addition of sodium acetate, sulfate and nitrate was rationalized as additional salts that are important for bacterial growth. The total percentage of salts used only accounts for approximately 0.8% dry weight of the chemical composition.

Thirdly, the vitamins, amino acids, fish oil, peptone, sugar, and glycerin were all used as a form of food source and nutrients to promote growth and development of the bacteria. Peptone is used in agars (nutrient agars) to stimulate the growth of bacteria. Sugar and glycerin are used as forms of carbohydrate as an energy source for bacteria. Vitamins are important as bacteria need the organic molecules (containing C, H, O, N, S, and P, *etc*.) and vitamins in order for enzymes to function.[28, 29] For example, vitamin B_{12} was a coenzyme, methyl form cobalamine, and vitamin K is a coenzyme form.[28,29] Amino acids are the building blocks of proteins, important for metabolism and nutrition. Proteins are important for cell signaling and the cell cycle. These are important as the plasma membrane of bacteria consists of a protein lipid bi-layer, and the cell wall is made of peptidoglycan, which is a polysaccharide chain with cross-links peptide with D-amino acids.[28,29] The concentration values of vitamins, and amino acids, *etc*., used were based on the necessity of those chemicals for bacterial growth. For example, a total of 6 grams of peptone is generally used as a source of amino acids, nitrogen, sulfur and phosphorus.[28,29] In this study, 2 grams of peptone were used and the 4 grams in correspondence included the amino acid tablets that were used to give a total of 6 gram; which accounts for a total of 1.2% dry weight of the chemical composition.

Fourthly, chemicals such as squalene, stearic acid, octanoic acid, and docosanoic acid are all carboxylic acids used due to their earlier observation in a sediment study that was conducted of the marine environment.[13,14] The importance of these carboxylic acids and hydrocarbons to marine bacteria is still being determined; however, properties of squalene and stearic acid, important to bacteria, have been determined. Squalene is a natural organic compound, found in shark liver oil, which is used as a biosynthetic precursor for steroid and bile acid synthesis in bacteria and sea squirts among other functions.[30] Stearic acid

is a saturated fatty acid found naturally in animal, fat and vegetable oil. It is important for cell culturing for the bio-manufacture of protein, important for the cell structure of the cell wall in bacteria.[31] The concentrations of the acids used are in proximity to values found in a previous study.[14] The total percentage of squalene and stearic acid used accounts for approximately 0.6% dry weight of the chemical compilation. Together, the chemical compilation served as an appropriate medium to cultivate the bacteria, as these chemicals are naturally found in the ecosystem of *Bugula*.[14]

Data collected from Alligator Point strongly suggest success in capturing marine bacteria from the ecosystem of the marine organism. With promising preliminary results from using this method in the Gulf of México, the technique was also implemented off the coast of Sunderland. *Bugula neritina* has previously been found off the coast of England, and for this reason three trial locations with high levels of heavy metals were chosen. Two of these sites showed encouraging, but inconclusive, results.[32]

Bugula neritina is a seasonal marine organism, found between the months of October to April, and is temperature dependent (18-22°C); however, the marine organism has been found during the summer time in the Gulf of México. It is important to note that the data collected from the three experiments conducted at Alligator Point, Florida varied, which may be due to the change in water temperature when each experiment was conducted. For example, the temperature of the water in February (section 2.3.1) was 17°C and the peaks shown in Fig. 7 suggest no correlation to any bryostatin compounds. However, the average water temperature for samples placed in March (section 2.3.2) was 23°C and results collected from this sample show a *m/z* of 927 (Fig. 8), which suggest the isolation of bryostatin 1. The average water temperature for the samples placed in June (section 2.3.3) was 25°C with results from the artificial

medium showing two peaks at *m/z* of 903 and 895 (Fig. 11) which could correlate to bryostatin 8+Na^+ and bryostatin 4 respectively, as mentioned earlier. It should also be noted that *Bugula* was also found attached to the containers which were placed in the water in section 2.2.3.

Since the artificial mediums from the studies conducted (section 2.2.1 - 2.2.3) were all placed at the same location, it is suggested that there are two factors that account for the variation in the data collected, which are: 1) the temperature of the water when the samples were placed, and 2) how long the artificial medium was placed in the water. For this reason, it is suggested that such factors may also explain the presence of the twenty different bryostatin compounds that have been isolated from the marine organism. Other factors for the identification of these 20 compounds are believed to be dependent on the geographical location of the marine organism, season and depth of collection.[33] For example, bryostatin 4 is extracted from *Bugula* found in the Gulf of México, Gulf of California and Gulf of Sagami.[33] Bryostatin 12 and 13 are extracted from *Bugula* collected off the Eastern Pacific Ocean.[34] Bryostatin 14 and 15 were extracted from *Bugula* found in the Gulf of México and Eastern Pacific Ocean (California).[35] Bryostatins 16-18 are extracted from *Bugula* found in the Gulf of México.[36]

This study clearly shows that the origin of production of these compounds is related to bacteria found in the marine organism. Sufficient evidence showing the likely production of the essential bacteria in the laboratory demonstrates the relevance of bacterial growth enough to explore further using this technique for producing these compounds on a large scale.

2.5 Conclusion

In conclusions it can be stated:

1) The chemical composition in comparison to agar media, posed much success in isolating marine bacteria from the *Bugula's* ecosystem, consistent with the seasonal availability of the marine organism in the area.

2) Despite inconclusive evidence to determine the production of any bryostatin compounds using this method, results showing the production of marine bacteria in the broths strongly suggest that the bacteria merely looks for a host suitable for survival and colonization.

3) *Bugula* was not seen or looked for at the three designated sites used in the UK; nonetheless, the mineral paste compilation indicated a possible cultivation of bacteria.

4) Both experiments show substantive evidence that methods other than synthetic techniques, aquaculture and genetic identification of bacteria can be used in the production and isolation of NPs.

5) By modifying the technique used, this method can be useful in overcoming problems currently affecting the production of MNPs.

2.6 References

[1] Y. W. Chin, M. J. Balunas, H. B. Chai, and A. D. Kinghorn. *AAPS J*., 2006, **8(2)**, E239-53.

[2] G. M. Cragg, D. J. Newman, and S. S. Yang. *J. Nat. Prod*., 2006, **69(3)**, 488-98.

[3] http://www.clinicaltrials.gov (January 16th 2009).

[4] Madigan, M., and J. Martinko. Brock Biology of Microorganisms. 11th Edition, Prentice Hall., 2005.

[5] Ryan, K. J., and C. G. Ray. Sherris Medical Microbiology. 4th Edition, McGraw Hill., 2004.

[6] G. H. Chapman. *J. Bacteriol*., 1945, **50(2)**, 201-03.

[7] J. L. Sorensen, J. M. Mogensen, U. Thrane, and B. Andersen. *Int. J. Food Microbiol*., 2009, **130(1)**, 22-6.

[8] M. G. Haygood, and S. K. Davidson. *Appl. Environ. Microbiol*., 1997, **63(11),** 4612-16.

[9] M. G. Haygood, E. Schmidt, S. Davidson, and J. Faulkner. *J. Mol. Microbiol. Biotechnol*., 1999, **1(1)**, 33-3.

[10] S. K. Davidson, and M. G. Haygood. *Bio. Bull.,* 1999, **196(3)**, 273-80.

[11] S. K. Davidson, S. W. Allen, G. E. Lim, C. M. Anderson, and M. G. Haygood. *Appl. Environ. Microbiol.*, 2001, **67(10)**, 4531-37.

[12] T. J. Manning, M. Land, E. Rhodes, L, Chamberlin, J. Rudloe, D. Phillips, T. T. Lam, J. Purcell, H. J. Cooper, M. R. Emmett, and A. G. Marshall. *Nat. Prod. Res*., 2005, **19(5)**, 467-91.

[13] T. Manning, T. Umberger, S. Strickland, D, Lovingood, R. Borchelt, M. Land, D. Phillips, and J. C. Manning. *Int. J. Environ. Anal. Chem*., 2003, **83(10)**, 861-66.

[14] T. Manning, M. Land, E. Rhodes, R. Loftis, C. Tabron, G. Abadi, L. Golden, H. J. Cooper, T. T. Lam, A. G. Marshall, D. R. Phillips, and J. Rudloe. *Ga. J. Sci*., 2005, **63**, 97-114.

[15] T. J. Manning, C. Hardeman, K. Olsen, E. Rhodes, R. Parkman, M. Land, Michael, S. M. North, K. Riddle, and D. Phillips. *Chemical Educator*, 2004, **9(5)**, 276-80.

[16] Campbell, N. A., J. B. Reece, and B. Cummings. Biology. 7th Edition, Pearson., 2004.

[17] A. R. Coscione, C. A. de Abreu, and G. C. G. dos Santos. *Scientia Agricola*., 2009, **66(1)**, 64-70.

[18] Hillenkamp, F., and J. Peter-Katalinić. MALDI MS: A practical guide to instrumentation, methods and applications. Wiley-VCH., 2007.

[19] V. J. Paul, K. E. Arthur, R. Ritson-Williams, C. Ross, and K. Sharp. *Biol. Bull.*, 2007, **213(3)**, 226-51.

[20] J. Piel. *Curr. Med. Chem.*, 2006, **13(1)**, 39-50.

[21] L. X. Zhang, R. An, J. P. Wang, N. Sun, S. Zhang, J. C. Hu, and J. Kuai. *Curr. Opin. Microbiol.*, 2005, **8(3)**, 276-81.

[22] G. E. Lim-Fong, L. A. Regali, and M. G. Haygood. *Appl. Environ. Microbiol*. 2008, **74(11)**, 3605-09.

[23] http://www.chemie.de/lexikon/e/Secondary_metabolite/ (May 14th 2009).

[24] W. C. Dunlap, C. N. Battershill, C. H. Liptrot, R. E. Cobb, D. G. Bourne, M. Jaspars, P. F. Long, and D. J. Newman. *Methods*, 2007, **42(4)**, 358-76.

[25] A. B. da Rocha, R. M. Lopes, and G. Schwartsmann. *Curr. Opin. Pharmacol.*, 2001, **1(4)**, 364-69.

[26] http://www.seachem.com/Products/product_pages/MarineBuffer.html (May 15th 2009).

[27] http://www.instantocean.com/InstantOcean.home (May 12th 2009).

[28] http://www.textbookofbacteriology.net/index.html (May 22nd 2009).

[29] Black, J. G. Microbiology: Principles and explorations. 5th Edition. John Wiley and Sons Inc., 2002.

[30] K. E. Bloch. *Crit. Rev. Biochem.*, 1979, **7(1)**, 1-5.

[31] http://www.sigmaaldrich.com/life-science/cell-culture/learning-center/media-expert.html (May 22nd 2009).

[32] J. A. Mackie, M. J. Keough, and L. Christidis. *Mar. Biol.*, 2006, **149(2)**, 285-95.

[33] G. R. Pettit, Y. Kamano, C. L. Herald, and M. Tozawa. *J. Am. Chem. Soc*., 1984, **106(22)**, 6768-71.

[34] G. R. Pettit, J. E. Leet, C. L. Herald, Y. Kamano, F. E Boettner, L. Baczynskyj, and R. A. Neiman. *J. Org. Chem*., 1987, **52(13)**, 2854-60.

[35] G. R. Pettit, F. Gao, D. Sengupta, J. C. Coll, C. L. Herald, D. L. Doubek, J. M. Schmidt, J. R. Vancamp, J. Rudloe, and R. A. Neiman. *Tetrahedron*. 1991, **47(22)**, 3601-10.

[36] G. R. Pettit, F. Gao, P. M. Blumberg, C. L. Herald, J. C. Coll, Y. Kamano, N. E. Lewin, J. M. Schmidt, and J. Chapuis. *J. Nat. Prod*., 1996, **59(3)**, 286-89.

CHAPTER 3

Artificial surfaces treated with a composition of chemicals for the production of the bryostatins

3.1 Introduction

The bryostatins are MNPs that were originally isolated from the bryozoa, *Bugula neritina*. Since the isolation of bryostatin 1 in the 1980s, nineteen other bryostatin compounds have been isolated from *Bugula,* which are found all over the world. For example, bryostatin 4 is extracted from *Bugula* found in the Gulf of México, Gulf of California and the Gulf of Sagami.[1] It takes approximately fourteen tons of *Bugula* to extract approximately eighteen grams of bryostatin 1, while the current method of production involves a 65 step synthetic process. Bryostatin 1 is the most studied bryostatin and it is currently in a number of clinical trials for the treatment of various cancers such as kidney, prostate, ovarian, leukaemia and is also being looked at as a possible treatment for Alzheimer's disease.[2] For this reason, it is essential that an economical method is developed which would facilitate more trials and the treatment of greater numbers of patients.

It has been suggested that the true source of the NP is of bacteria found in the marine organism.[3,4,5] Studies conducted by Manning *et al*., have also shown a ubiquitous component responsible for the compound as traces of bryostatins have been found in various marine organisms in the *Bugula* ecosystem.[6,7,8] Additional work has also been conducted, showing the chemical properties of the ecosystem where the marine organism is found and the marine organism itself.[7,9] From these studies the development of an artificial medium for the production of the bryostatins was developed. The chemical composition of this medium is similar to that of the ecosystem and the marine organism; this replicating the components of the ocean and the organism in an artificial environment.

As mentioned, other groups have suggested the presence of marine bacteria as the source for the production of the bryostatins. In the laboratory,

agar media are usually used for the cultivation of bacteria in an artificial environment, with different media used for the cultivation of specific bacteria.[10] This chemical composition, based on the marine ecosystem of *Bugula*, serves as an alternative to agar media. It has been reported that 99% of naturally occurring microorganisms are almost impossible to cultivate in the laboratory and have yet to be identified.[11] For those that do grow in the laboratory, agar media are used to aid in the growth and production of the bacteria. Different agar media are used to provide nutrients, and the additional chemicals necessary for specific bacteria to grow. The chemical composition also contains the necessary nutrients and chemicals which have been identified in the marine environment in which the marine organism resides.

Based on studies (chapter 2) suggesting the efficacy of the artificial medium, this study was conducted to improve its efficacy for the isolation of the bacteria of choice. The artificial surfaces used were coated (treated) with the chemical composition in order to determine the overall efficacy and the most feasible artificial surface for economical production. The artificial surfaces (polyurethane, sawdust and cellulose sponge) used in this study were prepared and processed as described below. The results from this study would thus provide sufficient means to isolate and produce the marine natural products needed, as well as providing further proof of the real source of production for the NP. Initial results suggest the production of different bryostatin compounds in most of the artificial surfaces used.

3.2 Experimental Section

The artificial surfaces were treated using the chemical composition as initially described in section 2.2.2. The surfaces were coated (treated) in a two step process as shown in Tables 1 and 2. In both steps sponges (Dick Blick Art

Materials, 32901-0000), *Bugula* (provided by the Gulf Specimen Marine lab in Panacea, Fl.), and sawdust were coated by submerging the surfaces in each solution for total of 4 hr, while polyurethane strips were coated by submerging the strips in each solution for 8 hr. After the allocated time, the surfaces were removed and air dried, before coating them in the second solution. After both coatings were applied, the surfaces were air dried at room temperature (RT) then packed into bacterial amplification chambers (BACs) as shown in Fig. 1. Initial traps consisted of 5 BACs: two for polyurethane; two for sponges; and a control containing both a strip of untreated polyurethane (1 ft) and two untreated sponges, each separated by a strip of zinc (Fig. 2). The amount of *Bugula*, sawdust and chitin used in this study were not quantified. The weight of the artificial surface were not determined before and after coating with the chemical composition used.

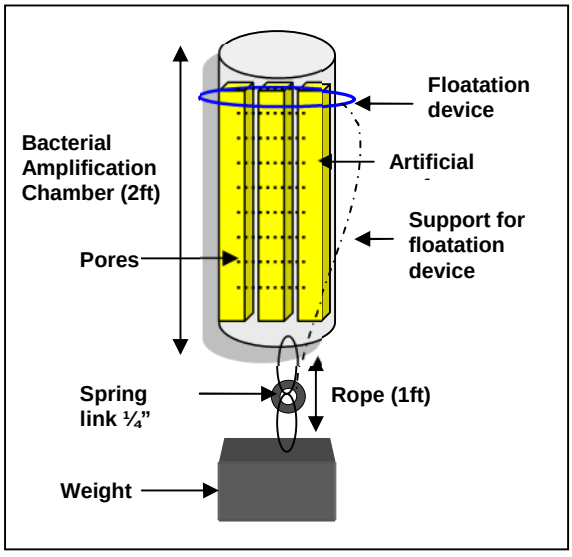

Fig. 1. An inside view of a bacterial amplification chamber.

Table 1. Surfaces were first treated with the listed chemicals. A total of 4 strips of polyurethane, and 2 strips of cellulose sponge were treated, as detailed below.

Chemicals	**Amount used**	**Company**	**Product code**
Calcium carbonate	20 g	Fisher Scientific	S71922
Iron Chloride	10 g	Fisher Scientific	FL-01-0784
Instant Ocean	2 g	Marine Labs	SS3-50
Distilled Water	700 mL	N/A	N/A

Table 2. The chemicals used for the second coating of the artificial surfaces. A total of 32 strips of polyurethane and 16 strips of cellulose sponge per 4 L containers.

Chemical	Amount used	Company	Product code
$CaCO_3$	5 g	Fisher Scientific	S71922
$FeCl_36H_2O$	2 g	Fisher Scientific	FL-01-0784
Amino Acid	10 tablets	Fisher Scientific	S71922
Fish Oil	10 tablets	GNC	750612
Multi-Vitamin	10 capsules	Equate	N/A
Vitamin A & D	10 capsules	Spring Valley	N/A
Vitamin C	10 tablets	Spring Valley	N/A
Sugar	15 g	Pure Cane Dixie Crystals	S133E06A-PA
Marine Buffer	2 g	Sea Chem	UPC# 000116034708
Sodium acetate	2 g	Fisher scientific	S210-500
Peptone	2 g	Fisher scientific	BP1420-100
Sodium sulfate	1 g	Fisher scientific	S421-1
Glycerin	2 mL	Fisher scientific	G33-500
Stearic acid	1 g	Sigma Aldrich	175366-1Kg
Squalene	2 mL	Fisher scientific	AC20747-1000
Octanoic acid	2 mL	Fisher scientific	167261000
Distilled water	4 L	N/A	N/A

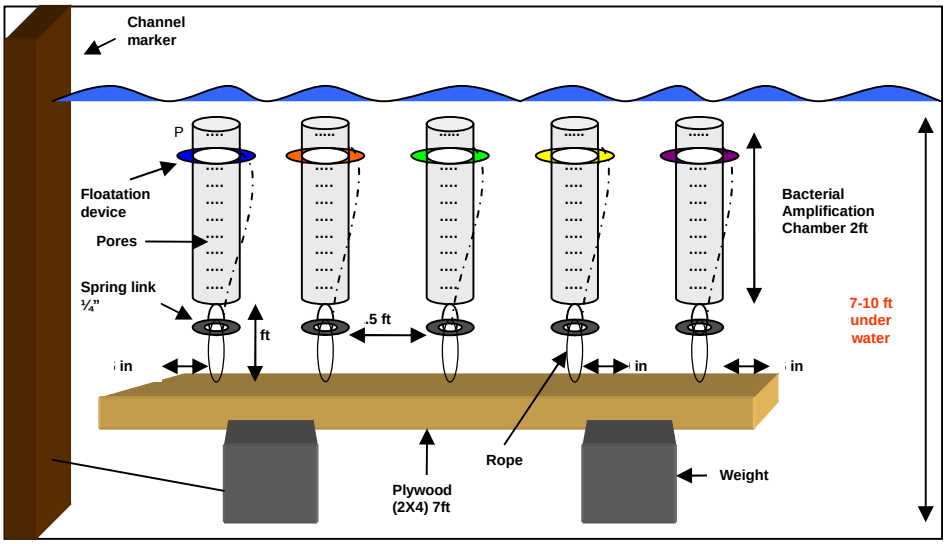

Fig. 2. A 2 dimensional design of the prototype used for the broth assessments: BACs were placed at three designated locations in Florida.

The BACs were placed in Alligator Point Yacht Basin, Alligator Point, Florida (25° 36’ 0" N, 81° 14’ 28" W) and Turkey Point (29° 54’ 0.9" N, 84° 30’ 0.7" W), St. Teresa, Florida, USA. A total of 74 sponges and 60 polyurethane strips were used in this study. The traps were checked twice a month to determine that bacterial growth on the media was taking place. After the allocated

time period (Table 3), the artificial surfaces were removed from the BACs and placed in containers filled with sea water from their respective location. The containers were placed at 4°C for 48 hr then placed at RT for the broth assessment.

The extraction procedures are mentioned in section 3.2.1-3.2.3. Samples from all the experiments were analyzed by MALDI-TOF-MS and LC-MS as described in section 2.2. Samples from all the broths were collected, processed and analyzed (section 3.2.4) using a Scanning Electron Microscope (SEM), Valdosta State University, Valdosta, GA (USA). Additional images for each broth from each location, additional spectra for each broth assessment, and additional SEM images can be found on the enclosed DVD.

3.2.1 Artificial surfaces

Table 3. The different artificial surfaces (AS) used, the cultivation period in the water, and the assessment period of the broths at RT.

AS	Location	Year	Water	Broth growth
1	Alligator Point, Fl.	February 24th, 2007 at 12:00 p.m. to May 17th, 2007 at 10:00 a.m.)	11 ½ wk	12 wk
2	Alligator Point, Fl.	May 17th, 2007 at 10:00 a.m. to May 27th, 2007 at 11:00 a.m.	10 day	10 wk
3	Alligator Point, Fl.	May 27th, 2007 at 1:30 p.m. to June 18th, 2007 at 5:00 p.m.	3 wk	8 wk
4	Alligator Point, Fl.	February 24th, 2007 at 12:00 p.m. to May 17th, 2007 at 10:00 a.m.)	11 ½ wk	12 wk
5	Alligator Point, Fl.	June 18th, 2007 at 5:00 p.m. to June 25th, 2007 at 12:00 p.m.	1 wk	7 wk
6	Alligator Point, Fl.	June 15th, 2008 at 1:00 p.m. to June 22nd, 2008 at 1:00 p.m.	1 wk	4 ½ wk
7	Panacea, Fl.	June 15th,2008 at 2:00 p.m. to June 22nd, 2008 at 2:00 p.m.	1 wk	4 ½ wk
8	St. Teresa, Fl.	February 24th, 2007 at 1:00 p.m. to May 17th, 2007 at 11:00 a.m.)	11 ½ wk	12 wk

1. Two BACs containing treated sponges (4, 19.1cmx11.4cmx5.08cm) respectively.
2. Three BACs containing treated sponges (10, 7.62cmx2.54cmx2.54cm) and packed with chitin (shrimp shells) as fillers respectively.
3. One BAC containing treated sponges (10, 7.62cmx2.54cmx2.54cm), and packed with the marine organism, *Bugula neritina*, (Gulf Specimen Marine Lab) as fillers.
4. Six BACs containing treated polyurethane strips (10, 12.7cmx2.54cmx2.54cm) respectively. Two chambers were placed at Alligator Point, two were placed at Panacea, Fl. and two at St. Teresa, Florida.
5. Four BACs, two containing treated sawdust and one containing sawdust and sponge and one containing treated sawdust and sponge respectively. A total of (10, 7.62cmx2.54cmx2.54cm) sponges were placed in the chamber containing sponge.
6. Three BACs containing treated sponges (total of 7, 19.1cmx11.4cmx5.08cm) respectively.
7. Three BACs containing treated sponges (total of 7, 19.1cmx11.4cmx5.08cm) respectively.
8. Two BACs containing treated sponges (total of 4, 19.1cmx11.4cmx5.08cm) respectively.

3.2.2 Extraction of white film

Analysis of each container after 48 hr at RT showed the formation of a white film on the surface of the water. This film was removed from each container biweekly, extracted into 40 mL anhydrous methanol (Fisher Scientific) and then stored at 4°C. Biweekly assessments of the broths were followed by the addition of 10 g of mineral paste composition (section 2.2.2, Table 2) to each container. After the complete assessment (growth assessment of bacteria at RT as mentioned in section 3.2, Table 3) of the surfaces at RT, the extracts collected were filtered, using a 5 µm filter paper followed by a 0.2 µm filter paper.

3.2.3 Extraction of artificial surfaces

After the assessment period (time period for the grow-out of the broths at RT, Table 3), the artificial surfaces from each container were removed and prepared for extraction. Surfaces were air dried at RT for 24 hr, then placed in 100 mL of methanol containing 2 g of sodium sulfate for 48 hr. The extract was filtered using a 5 µm filter paper then placed at 65°C for 72 hr to remove the methanol. Crystals were analyzed and correlated with the white film extracts collected from their respective containers.

3.2.4 Preparative procedure for SEM analysis

The white film collected from each broth assessed and the AS used in the broths, as mentioned in section 3.2.1, were analyzed by SEM. Samples were collected on July 16th 2007, at 10:00 a.m., and prepared as mentioned below. Samples were analyzed on the SEM, from July 17th 2007 to July 25th 2007.

Each sample (white film and AS) was removed from the broths and placed directly into a chemical fixative consisting of 1% glutaraldehyde in 0.2 M sodium cacodylate buffer, pH 7.2 for 4 hr. After 4 hr, the samples were washed by

replacing the fixative with fresh buffer 3 times at 15 min intervals, without exposing the samples to air. The buffer was then replaced with deionized water until the sample was immersed in 100% deionized water only. The samples were then dehydrated using 95% ethanol. A 10% gradation series of ethanol (10, 20 to 90%) using 95% ethanol was used with each series added for 10 min, until the samples were in 100% absolute ethanol respectively. This process was repeated again, to replace samples in ethanol, with 100% acetone, necessary for critical point drying.

Once in acetone, the samples were placed in plastic containers then placed in a critical point drier. After critical point drying, samples were mounted on a stub then coated with argon. The stubs were then placed in the vacuum chamber of the SEM and analyzed. The preparative procedures for the SEM mentioned above were conducted as indicated by the Biology Department at Valdosta State University, Valdosta, GA, USA, where the samples were analyzed.[12]

3.3 Results and Discussion

Artificial surfaces were checked twice a month to determine the timescale of bacterial growth from the three designated locations. After 2 wk, surfaces from all three locations showed no sign of bacterial growth. However, 4 wk after the start date, samples from St. Teresa Bay and Alligator Point were black in color and reduced in size when compared to the control sponges (untreated). Untreated AS placed in both locations retained their original appearance after 12 ½ wk, as shown in Fig. 3.

Most of the AS (sponge, sawdust and *Bugula*) that were used in this study turned completely greenish black in colour, were reduced in size, slimy and gave off a pungent odor, after being placed in the water. The BACs containing sponge

and chitin (shrimp shells) showed no presence of chitin after 10 days in the water. The sponges left in the container alone were greenish black in colour, reduced in size, slimy and gave off a pungent odor. The *Bugula* placed in the BACs with the treated sponges was still present when the BACs were removed, after the allocated time in the water. The *Bugula* was black in color; similar in appearance to the sponges in the chamber. In all the BACs containing the controls, there was no change in appearance, size, colour or texture compared to the untreated surfaces (sponge and polyurethane), as shown in Fig. 3.

Fig. 3. Sponges shown above were placed at St. Teresa Bay, Florida for 13 wk. The treated sponge (top) appears green/black in color while the untreated sponge (bottom) still retained its original appearance.

The strips of polyurethane were not as effective as the other AS used. After 4 wk the surface of the polyurethane strips appeared partially black on the surface, however the bacterial growth was not as pronounced as shown on the other surfaces. After 13 wk the appearance of the polyurethane strips in all three locations was consistent, showing limited bacteria growth. After 2 wk at RT, the surfaces still remained the same, and the water was clear and odourless (Fig. 4). Despite the partial black appearance on sections of the polyurethane, this artificial surface was not successful in collecting any marine bacteria from either location, as opposed to the other artificial surfaces used, while in the laboratory,

for the broth assessment at RT, no indication of bacterial growth was seen. The white film formed on the surface of the other containers was not seen in the container containing the polyurethane strips collected from each location, as shown below.

Fig. 4. Treated polyurethane strips placed at Panacea, Fl. for 13 wk.

The three surfaces used were selected in order to establish which would serve as the most successful surface, when coated with the artificial media. Previous work by Yasumoto-Hirose *et al*., showed that polyurethane treated with various agar media and placed in seawater was successful in cultivating marine bacteria.[13] Applying this concept to the chemical composition used by this group, polyurethane strips were treated then placed in the stated locations. Throughout the 13 wk period, bimonthly analysis of traps showed no signs of bacterial growth, especially in comparison to the other two artificial supports. Results from the polyurethane blocks left at RT for 12 ½ wk were also unsuccessful.

These results questioned the credibility of using polyurethane as a potential artificial surface as the other two artificial surfaces showed more promise in cultivating the bacteria from *Bugula* ecosystem. This suggestion is

based upon the success of the other surfaces that we used in this study; of which all showed the presence of bacterial growth when analyzed by SEM (Fig. 14).

After 48 hr of placing all the containers at RT, a white film covered the water layer in each container and areas of the sponges protruding above the water layer as shown in Fig. 5. This white film was seen on the surface of the water, in each container, and was continuously present throughout the broth assessment. These results were consistent for the artificial surfaces placed at all three locations.

Fig. 5. White film is shown after 48 hr at RT from a broth containing treated sawdust placed at Alligator Point, Florida for 1 wk.

The chemicals used in this study were based on detailed analysis of the marine organism, *Bugula neritina*, and the ecosystem in which it is found.[8,9] As mentioned earlier, this chemical composition was developed to replace the use of agar media which is normally used for the cultivation of bacteria in the laboratory. As previously stated, approximately 99.9% of bacteria are almost impossible to grow in the laboratory using agar media.[11] Being based on the properties of the ecosystem, the chemical composition would serve as a replica of that environment and therefore aid in the cultivation and isolation of marine bacteria.

For example, the surface of *Bugula* has been shown to contain high levels of calcium carbonate, and extraction of the marine organism has shown high concentration of nano particles (Fe, CuO); suggesting that the bacteria found within the organism thrive on these components.[9] The ecosystem of the marine organism also has a high deposit of limestone (approximately 40%), which accounts for the main component of our chemical composition being calcium carbonate.

Secondly, to cultivate and isolate the bacteria, it is necessary to replicate the contents of the ocean in an attempt to mimic the environment of the bacteria. For this reason, marine buffer and Instant Ocean were used. Many of these salts are important for bacteria. For example, potassium salts function as a cofactor for certain enzymes, and magnesium salts function as a cofactor for certain enzymatic reactions *etc*..[14]

The vitamins, amino acids, fish oil, peptone, sugar, and glycerin were all used as nutrients in order to promote the growth and development of the bacteria. Vitamins are important as bacteria need the organic molecules in order for enzymes to function.[14,15,16] For example, vitamin B_{12} was a coenzyme, methyl form cobalamine, and vitamin K is a coenzyme form.[14]

Next, chemicals such as squalene, stearic acid, octanoic acid, and docosanoic acid are all carboxylic acids used due to the initial findings in a study that was conducted by Manning *et al.*, of the marine environment.[8,9] Stearic acid is a saturated fatty acid found naturally in animal, fat and vegetable oil. It is important for cell culturing for the bio-manufacture of protein, and important for the cell structure of the cell wall in bacteria.[17]

The purpose of analyzing the surfaces in the broths, aside from the white film collected was to compare the data to that from the white film extracted from the surface of the water in each container, and to determine whether the

compounds of interest were actually in the white film, or in the artificial surfaces. Based on the data collected both the surfaces and the white film gives peaks that can be correlated to different bryostatin compounds. As shown in the tables below, many of the peaks can be seen in more than one broth. This is important as it shows a consistency in the data from the different surfaces placed in the same location, and that the surfaces used are promising and all are efficient for use as artificial surfaces. The main difference between the artificial surfaces was the percentage of bacteria cultivated, for example, increasing the surface area from blocks of cellulose sponge to using strands of sawdust, increased the yield of the bacteria collected.

Tables 4 and 5 both show a summary of the peaks from the MALDI-MS and LC-MS analysis of each sample. The structures shown next to the tables are suggestive structures for the peaks that could correlate to the different bryostatin compounds. Examples of MALDI-MS data are shown in Fig. 6-11. Spectral peaks from samples collected were compared to a bryostatin 1 standard[12] (Fig. 6). Based on the fragmentation pattern of bryostatin 1, structural formulae for the dominant peaks were postulated with reference to data collected in chapter 6. The twenty bryostatin compounds that have been isolated each differ only by the R_1 and R_2 groups, as shown in Fig. 6.

Table 4. The artificial surfaces which produced a white film over a 9 wk period in the laboratory. Spectral peaks, both MALDI-MS and LC-MS, are shown. The highlighted *m/z* values have been used to suggest the bryostatin compounds each might represent.

Peaks (m/z)	Container[1]	Container[2]	Container[3]	Container[4]	Container[5]	Container[6]
705	☑					
714		☑	☑	☑		
733	☑	☑			☑	
743						☑
752						☑
761	☑			☑		☑
789		☑	☑		☑	☑
798		☑			☑	
805						☑
874				☑	☑	
889			☑	☑		
895	☑					
903				☑	☑	
912		☑			☑	
925		☑			☑	
959	☑	☑				
998		☑				☑

1. Sponges from Alligator Point.
2. Sponges from St. Teresa Bay.
3. Sponges and chitin from Alligator Point.
4. Sponges and *Bugula neritina* from Alligator Point (Fig. 11).
5. Sponges and sawdust from Alligator Point (Fig. 10).
6. Sawdust from Alligator Point.

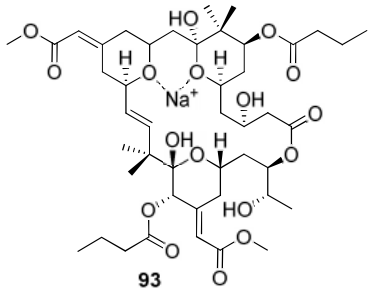

93

$(M+Na)^+$ Bryostatin 8+Na^+
($C_{45}H_{68}O_{17}Na$ m/z 903.4348 g/mol)

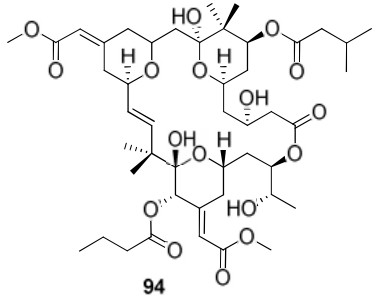

94

$(M+H)^+$ Bryostatin 4
($C_{46}H_{71}O_{17}$, 895.4685 g/mol)

Table 5. Spectral peaks from extracts collected from artificial surfaces heated to 65°C, from both MALDI-MS and LC-MS analysis. The highlighted *m/z* values have been used to suggest the bryostatin compounds each might represent.

Peaks (m/z)	Container[7]	Container[8]	Container[9]	Container[10]	Container[11]	Sample[12]
705		☑		☑		☑
713	☑		☑	☑	☑	
733			☑	☑	☑	
755		☑	☑		☑	
761	☑		☑	☑	☑	
789		☑	☑	☑	☑	☑
808		☑				
851				☑		
875	☑					
889					☑	
928			☑	☑	☑	☑
943						☑
962		☑	☑			
998		☑	☑			

7. Sponges from Alligator Point (Fig. 8).
8. Sponges from St. Teresa Bay
9. Sponges and chitin from Alligator Point.
10. Sponges and *Bugula neritina* from Alligator Point (Fig. 7).
11. Sponges and sawdust from Alligator Point.
12. Control sample was bryostatin 1 standard in methanol (Fig. 6)

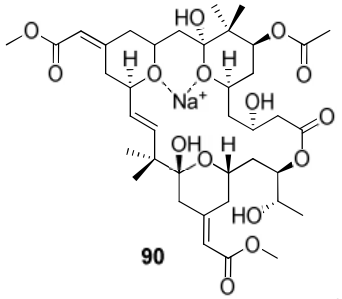

Bryostatin 11 + $(Na - 2H)^+$
($C_{39}H_{56}O_{15}Na$, 787.3511 g/mol)

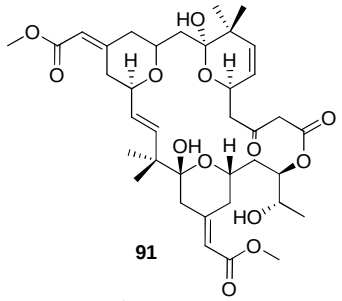

$(M+H)^+$ Bryophan ring
($C_{37}H_{53}O_{13}$, 705.3480 g/mol)

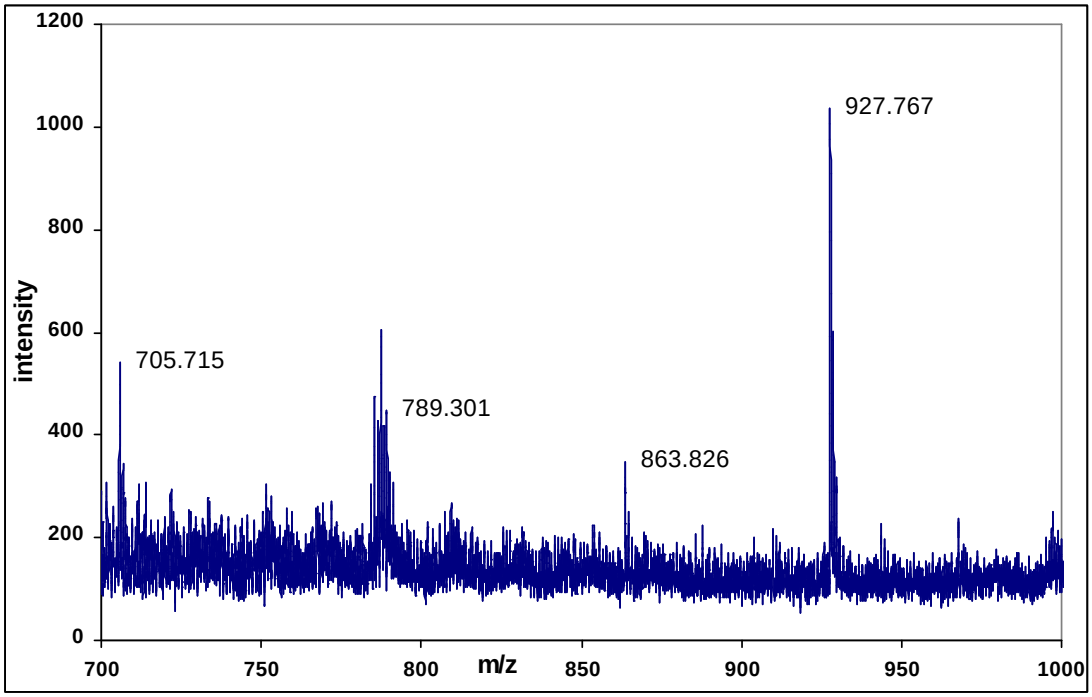

Fig. 6 MALDI-MS of bryostatin 1 standard in anhydrous methanol. Bryostatin 1+ Na^+ adduct ($C_{47}H_{68}O_{17}Na$, 927.4348 g/mol). The structures shown below correlate to the *m/z* peaks shown in Fig. 6.

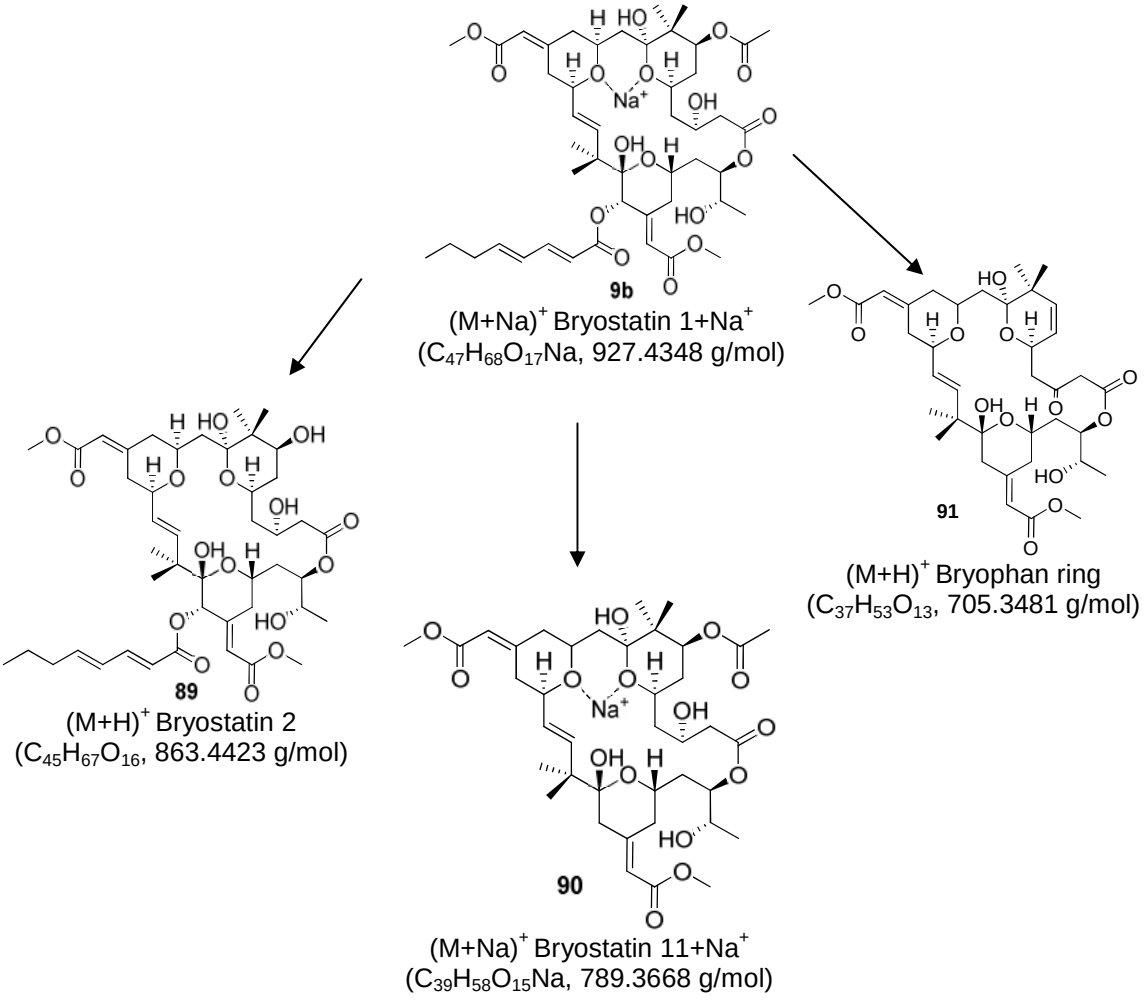

The above illustration shows how bryostatin 1 fragments in the mass spectrometer can give the peaks shown above. There are twenty bryostatin compounds that have been isolated from *Bugula neritina*, each bryostatin compound differs by the R_1 and R_2 group positions as shown above. Bryosatin 1+ Na^+ adduct **9b** ($C_{47}H_{68}O_{17}Na$, 927.4348 g/mol) loses $(C_2H_3O^{\cdot})^{\cdot}$ radical at the R_1 position to give an *m/z* of 863.826 $(M+H)^+$. This peak can therefore be correlated to bryostatin 2 **89** $(M+H)^+$ which has a formula of ($C_{45}H_{67}O_{16}$, 863.4423 g/mol).

In many of the MALDI-MS data that has been obtained for bryostatin 1, a consistent fragment that is always shown, is the peak with a *m/z* of 789 $(M+Na)^+$. As shown above the mass at 789 is formed by the loss of the carboxylate group (R_2 group) which can be correlated to bryostatin 11+Na^+ adduct **90** ($C_{39}H_{58}O_{15}Na$, 789.3668 g/mol).

The basic structure for all the bryostatin compounds is the bryophan ring **91** (M^+: $C_{37}H_{52}O_{13}$, 704.4302 g/mol). The loss of the R_1 and R_2 groups gives the basic structure of the bryophan ring (*e.g.* the acetate group at R_1 position and the C8 chain at the R_2 position). As shown above, bryostatin 1 fragments to give an *m/z* of 705.715 which suggests the bryophan ring $(M+H)^+$. Of all the bryostatin compounds that have been isolated from *Bugula* bryostatin 1 has the greatest potency as a medicinal agent. The fragments of bryostatin 1 shown in Fig. 6 are used as a reference to further support the postulations of the *m/z* values found for the samples in this study.

Studies by Pettit *et al*., have shown that the exposure of bryostatin 1 to various conditions can lead to the degradation of bryostatin 1.[18] Some of the mass peaks found within the samples suggested different bryostatin compounds or other related compounds found in *Bugula neritina*. The peaks shown in Fig. 6 can also be correlated to the fragmentation pattern of the bryostatin 1. It should

also be noted, however, the compounds shown could also be biosynthetic precursors for the production of bryostatin 1.[19,20]

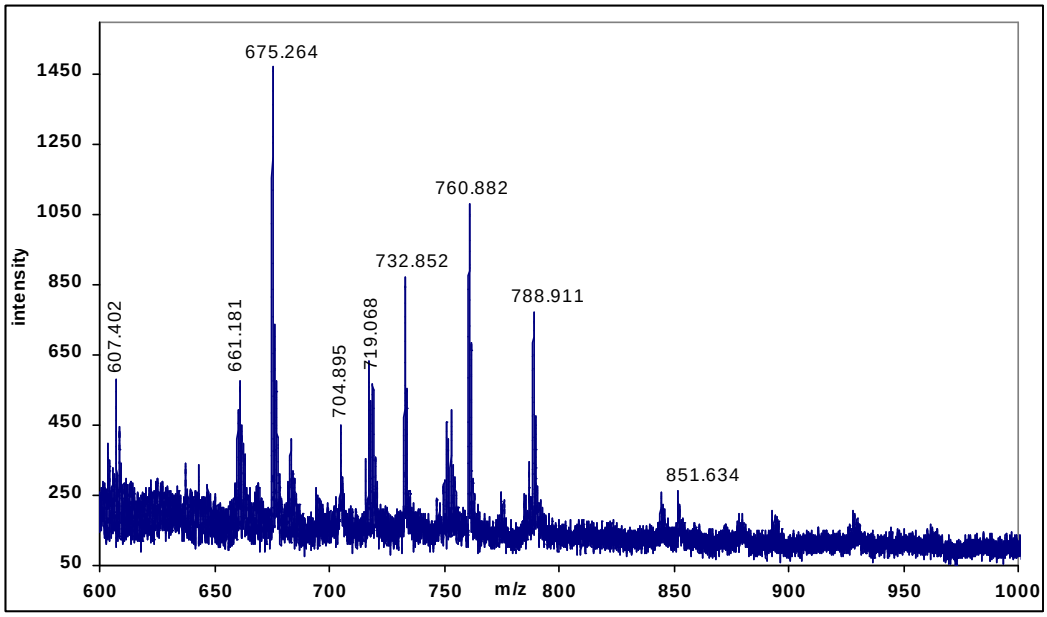

Fig. 7. MALDI-MS of sponge extract removed from the broth containing *Bugula* and sponge. The extract was heated at 65°C for 72 hr.

(a) (b)

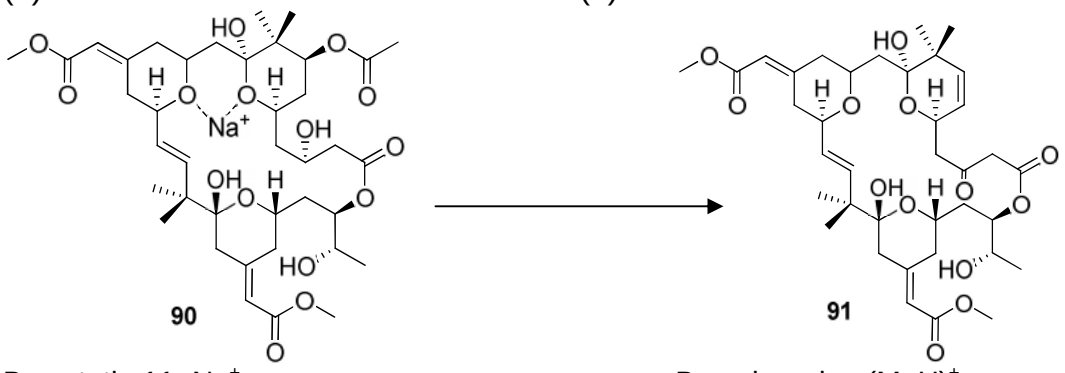

Bryostatin 11+Na^+
($C_{39}H_{58}O_{15}Na$, 789.3668 g/mol)

Bryophan ring $(M+H)^+$
($C_{37}H_{53}O_{13}$, 705.3480 g/mol)

As shown in Fig. 7, the peak at *m/z* 705.715 $(M+H)^+$ suggests the bryophan ring **91** of the bryostatins (M^+: $C_{37}H_{52}O_{13}$, 704.3402 g/mol). The bryophan ring form the basic structure of all the bryostatin compounds, for this reason the isolation of the bryophan ring can be a precursor to the production of bryostatin 1.[21]

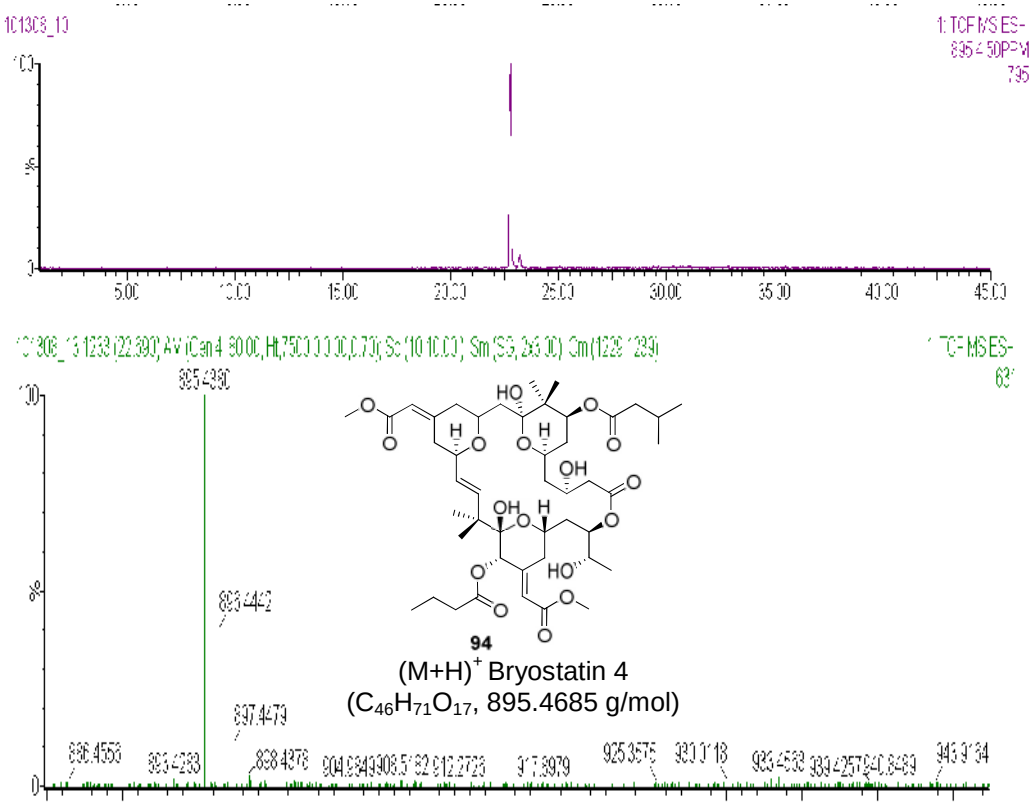

Fig. 8. The extract ion chromatogram of a peak analyzed by HRMS. The sample is a sponge extract at RT for artificial surfaces placed at Alligator Point, Fl. in June 2008.

The extract was divided equally into two containers; one was placed at 65°C while the other was placed at RT to dry. A dry weight of crystal extracts (1.12 g) was collected from white film over 4 wk period. A total of 21 sponges were extracted into 1L of methanol. The dry weight of crystals collected from the heated sponge extract was 25.23 g with 24.79 g from the extract placed at RT. Results from HRMS (Fig. 8) show the extract ion chromatogram at *m/z* of 895.4, a peak consistent with results cited in chapter 2. The peak at m/z 895 $(M+H)^+$ can be correlated to bryostatin 4 **94** (M^+: $C_{46}H_{70}O_{17}$, 894.4607 g/mol). The margin of error for the peak in correlation to bryostatin 4 is 34 ppm, with the acceptable error usually being 10 ppm. This may be due to the instrument not being calibrated properly.

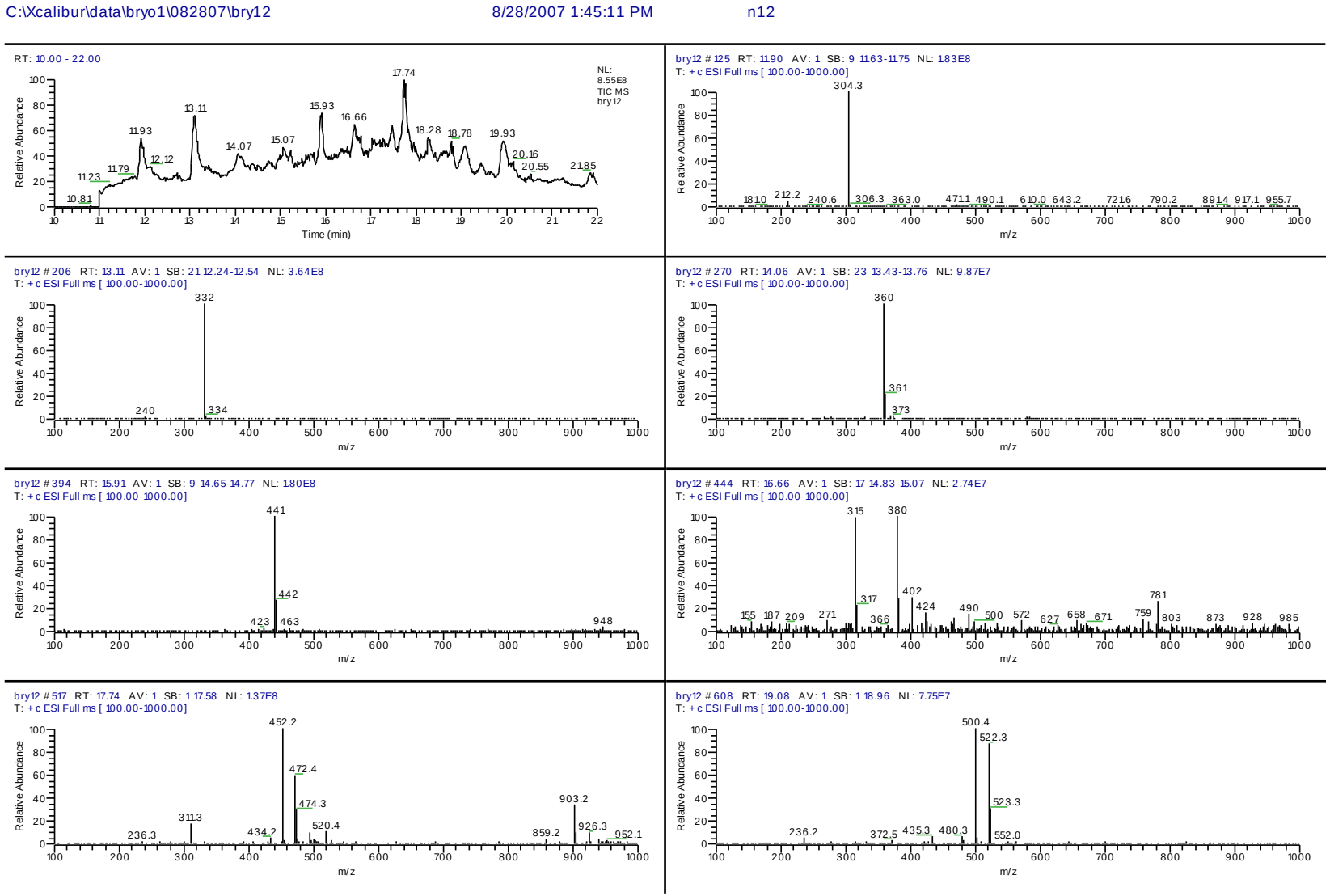

Fig. 9. LC-MS of white film collected from the surface of water, in the container containing sawdust and sponge placed at Alligator Point, Fl.

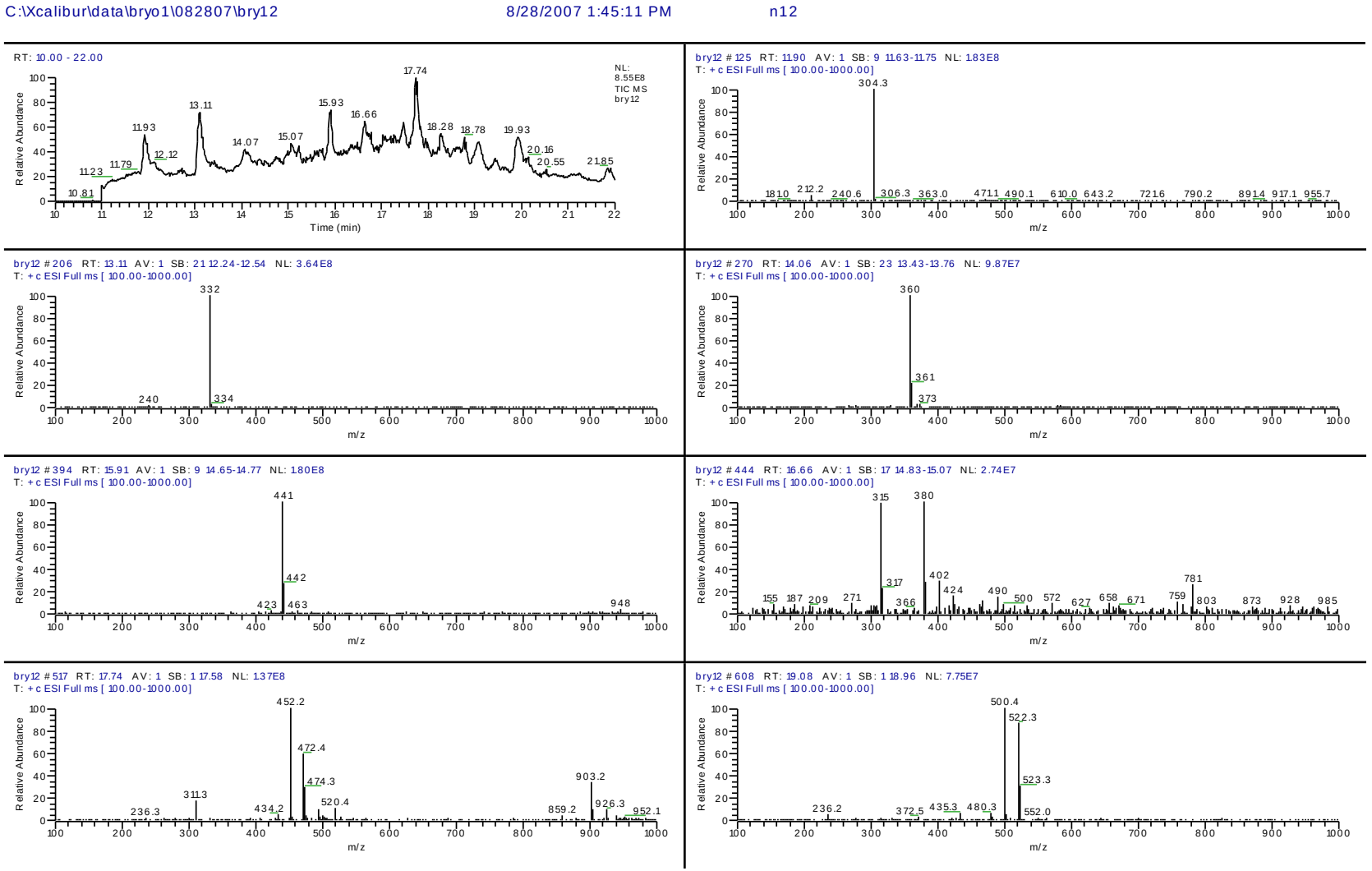

Fig. 10. LC-MS of white film collected from the surface of water, in the container containing *Bugula* and sponge placed at Alligator Point, Fl.

In Figs. 9 and 10 below, one peak at an *m/z* of 903 $(M+Na)^+$ is seen in both samples at a RT of 17.74 minutes. It is suggested that this peak may correlate to bryostatin 8 + Na^+ **93** ($C_{45}H_{68}O_{17}Na$, 903.4348 g/mol) as shown in Fig. 11. The LC-MS data from both samples correlate to two different treated AS, (sawdust and sponge; *Bugula* and sponge), that were used in the study, with both placed at Alligator Point, Florida.

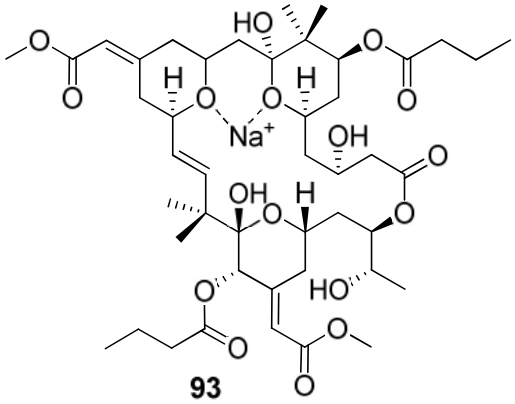

Fig. 11. Bryostatin 8 + Na^+ adduct ($C_{45}H_{68}O_{17}Na$, 903.4348 g/mol)

Both surfaces were placed at different times in the water; chambers containing *Bugula* and sponge were placed in the water from May 27th 2007, at 1:30 p.m. to June 18th 2007, at 5:00 p.m., and the chambers containing sawdust and sponge were placed in the water from June 18th 2007, at 5:00 p.m. to June 25th 2007, at 12:00 p.m.. This strongly suggests a ubiquitous component that was isolated during that time period in which the treated surfaces were *in situ*. Analysis of the surfaces from both locations, by SEM, shows the presence of numerous bacteria as shown in Fig. 14.

Fig. 12. Artificial surfaces where checked on April 14th 2007 at 2:00 p.m., the presence of *Bugula* was seen on the PVC pipes containing the treated surfaces.

Bugula is a seasonal and temperature dependent marine organism. It is generally found attached to boats and other substrates during the months of October to April (18-22°C); however, *Bugula* was found attached to the PVC pipes which were used to store the AS while the surfaces were placed at Alligator Point, Fl. *Bugula* was seen attached to the PVC pipes during the months of April to June 2007, and June 2008, while the surfaces were placed in the water (Fig. 12). The presence of *Bugula* suggests that the bacteria isolated from the marine environment may have also been present in the *Bugula* attached to the PVC pipes; however this was never verified as the *Bugula* attached to the PVC pipes were not analyzed. From the graph shown in Fig. 13 below, it is clearly seen that the change in water temperature which may be correlated to the data collected (Tables 4 and 5). In Tables 4 and 5, a peak with an *m/z* of 789 is seen in many of the different AS that were placed at Alligator Point, Fl. at different time periods. This peak with an *m/z* of 789 may correlate to bryostatin 11+ Na^+ as mentioned earlier. However, many of the other peaks vary in the times the surfaces were placed in the water. For example, in June 2008, the AS placed at Alligator Point, Fl., showed a peak at an *m/z* of 895 which may correlate to bryostatin 4; a peak which was not seen in the other surfaces used at the allocated times shown in Table 3.

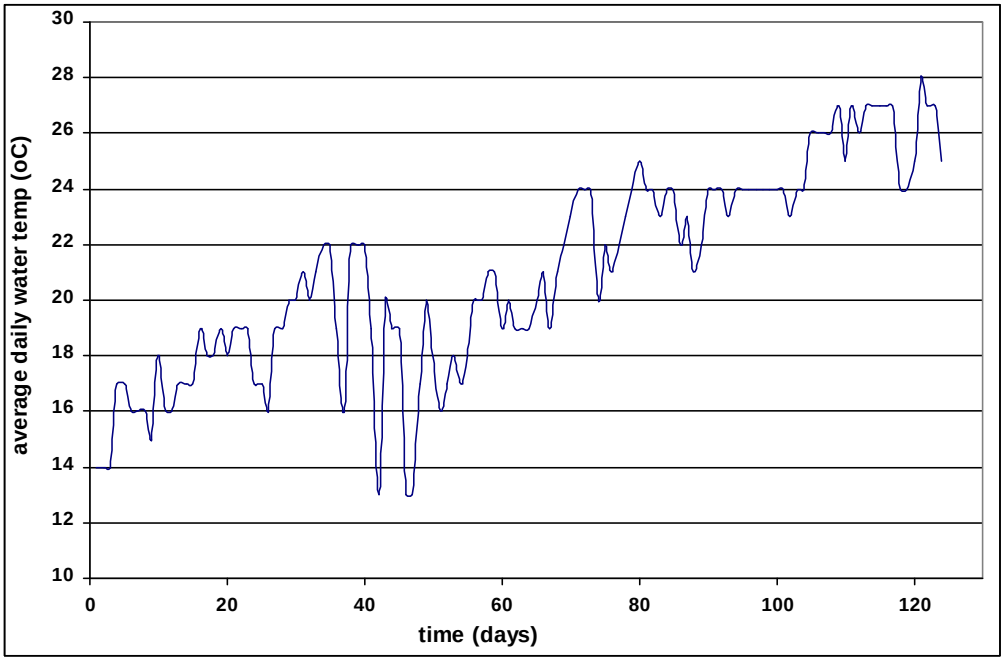

Fig. 13. Daily recorded water temperature of Alligator Point, Florida where the surfaces were placed from February to June.

It is important to note that, since the artificial mediums from the studies conducted (section 3.2.1) were all placed at the same location, it is suggested that there are three factors that account for the variation in the data collected, which are: 1) the temperature of the water when the samples were placed, 2) how long the treated artificial surfaces were placed in the water, and 3) the broth assessment period of the surfaces at RT. It is also suggested that such factors may also account for the presence of the twenty different bryostatin compounds that have been isolated from the marine organism.

3.4 Symbiont bacteria

Results from all the bacterial broths in this study showed that with the right medium and the optimum conditions, the desired bacterium can be cultivated. Despite the lack of any further analysis to determine the specific bacteria responsible for bryostatin production, SEM images from each broth were collected. Surfaces and white film from each container were processed and viewed under the microscope, showing vast numbers of bacteria in each (Fig.

14). Most of the bacteria in Fig. 14 are bacilli (rod-shaped), which are approximately two micron in size. However, cocci (spherical) bacteria are also seen, which are approximately one micron in size.[16]

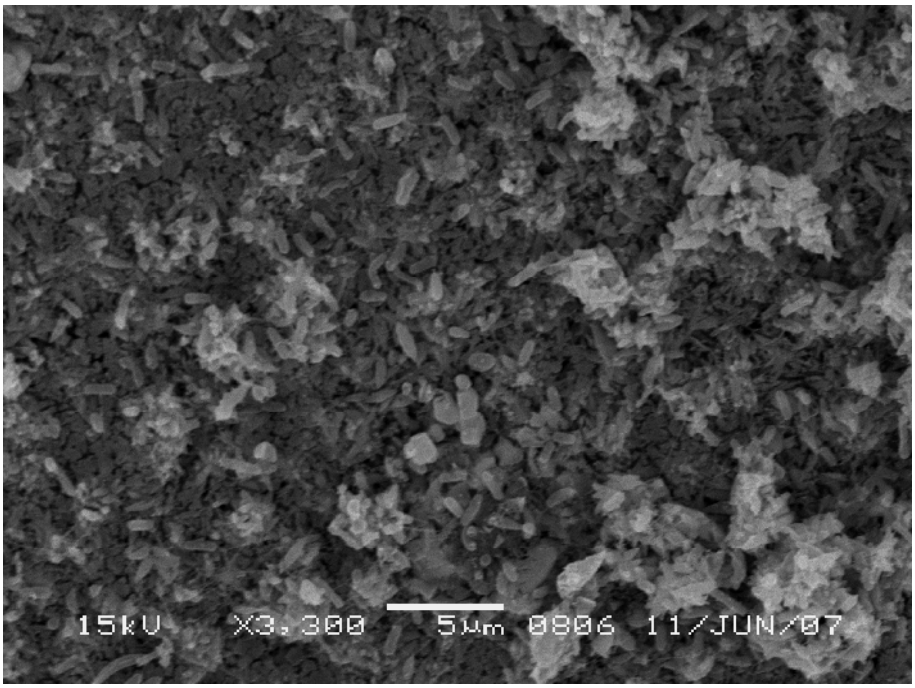

Fig. 14. An SEM image of the white film collected from BACs containing treated artificial surfaces placed at St. Teresa Bay, Fl.

As shown in Fig. 14 most of the bacteria are found in clusters, which is also known as a biofilm. A biofilm is a structured community of microorganisms encapsulated within a self-developed polymeric matrix and adherent to a living or inert surface.[22] Single-celled organisms generally exhibit two distinct modes of behaviour. One type of biofilm is the familiar free floating, or planktonic, form in which single cells float or swim independently in some liquid medium. The formation of a biofilm begins with the attachment of free-floating microorganisms to a surface.[23] These first colonies adhere to the surface initially through weak, reversible van der Waals forces. If the colonies are not immediately separated from the surface, they can anchor themselves more permanently using cell adhesion structures such as pili.[23] Bacteria living in biofilms display a complex arrangement of cells and extracellular components, forming secondary structures

such as micro-colonies, through which there are networks of channels to enable better diffusion of nutrients.[24]

3.5 Conclusion

Despite significant improvements in finding a cost efficient method to produce this NP, some inconsistencies in the cultivation of the marine bacteria were apparent, resulting in inconclusive evidence for the support for the production of any bryostatin compounds.

In summary, results from the artificial surfaces used showed that:

1. The chemical composition used was successful in capturing marine bacteria from *Bugula's* ecosystem.

2. Despite the very close comparability of certain *m/z* values (34 ppm), the HRMS data for the samples fell above the accepted error limit of 10 ppm for absolute identification.

3. Low detection levels also presented problems for further studies; hence the spectral data cannot support or disprove irrefutably the production of the bryostatin compounds that the masses could represent.

3.6 References

[1] G. R. Pettit, Y. Kamano, C. L. Herald, and M. Tozawa. *J. Am. Chem. Soc*., 1984, **106(22)**, 6768-71.

[2] http://www.clinicaltrials.gov/ (January 24th 2009).

[3] S. Sudek, N. Lopanik, L. E. Waggoner, M. Hilderbrand, H. B. Liu, A. Patel, C. Anderson, D. H. Sherman, and M. G. Haygood, *J. Nat. Prod.,* 2007, **70(1)**, 67-74.

[4] M. Hildebrand, L. E. Waggoner, H. Liu, S. Sudek, S. Allen, C. Anderson, D. H. Sherman, and M. Haygood. *Chem. Biol*., 2004, **11(11)**, 1543-52.

[5] Y. W. Chin, M. J. Balunas, H. B. Chai, and A. D. Kinghorn. *AAPS J*., 2006, **8(2)**, E239-53.

[6] T. Manning, T. Umberger, S. Strickland, D, Lovingood, R. Borchelt, M. Land, D. Phillips, and J. C. Manning. *Int. J. Environ. Anal. Chem*., 2003, **83(10)**, 861-66.

[7] T. J. Manning, M. Land, E. Rhodes, L, Chamberlin, J. Rudloe, D. Phillips, T. T. Lam, J. Purcell, H. J. Cooper, M. R. Emmett, and A. G. Marshall. *Nat. Prod. Res*., 2005, **19(5)**, 467-91.

[8] T. J. Manning, E. Rhodes, M. Land, R. Parkman, and A. G. Marshall. *Nat. Prod. Res*., 2006, **20(6)**, 611-28.

[9] T. Manning, M. Land, E. Rhodes, R. Loftis, C. Tabron, G. Abadi, L. Golden, H. J. Cooper, T. T. Lam, A. G. Marshall, D. R. Phillips, and J. Rudloe. *Ga. J. Sci*., 2005 **63**, 97-114.

[10] Madigan, M., and J. Martinko. Brock Biology of Microorganisms. 11th Edition, Prentice Hall., 2005.

[11] P. Hugenholtz, B. M. Goebel, and N. R. Pace. *J. Bacteriol*., 1998, **180(18)**, 4765-74.

[12] http://www.valdosta.edu/~rgoddard/bugs/bug.htm (July 16th 2007).

[13] M. Yasumoto-Hirose, M. Nishijima, M. K. Ngirchechol, K Kanoh, Y. Shizuri, and W. Miki. *Mar. Biotechnol*., 2006, **8(3)**, 227-37.

[14] http://www.textbookofbacteriology.net/index.html (May 22nd 2009).

[15] Atlas, R. M. Microbiology: Fundamental and applications. 2nd Edition, Macmillan Publishing Company, 1988.

[16] Black, J. G.. Microbiology: Principles and exploration. 5th Edition, John Wiley and Sons Inc., 2002.

[17] http://www.sigmaaldrich.com/life-science/cell-culture/learning-center/media-expert.html (May 22nd 2009).

[18] G. R. Pettit, F. Gao, D. L. Herald, P. M. Blumberg, N. E. Lewin, and R. A Neiman. *J. Am. Chem. Soc.*, 1991, **113(17)**, 6693-95.

[19] R. Mutter, and M. Willis. *Bioorg. & Med. Chem*., 2000, **8(8)**, 1841-40.

[20] G. Abadi, T. J. Manning, D. Phillips, P. Groundwater, and L. Noble. *Nat. Prod. Res.,* 2008, **22(10)**, 865-78.

[21] Hillenkamp, F., and J. Peter-Katalinić. MALDI MS: A practical guide to instrumentation, methods and applications. Wiley-VCH., 2007.

[22] S. S. Branda, A. Vik, L. Friedman, and R. Kolter. *Trends Microbiol*., 2005, **13(1),** 20-26.

[23] S. S. Branda, J. E. Gonzalez-Pastor, S. Ben-Yehuda, R. Losick, and R. Kolter. *Proc. Natl. Acad. Sci. U S A*, 2001, **98(20)**, 11621-26.

[24] R. Donlan. *Emerg. Infect. Dis*., 2002, **8(9)**, 881-90.

CHAPTER 4

Artificial surfaces treated with a composition of chemicals for the production of Et-743

4.1 Introduction

The anti-tumour drug Ecteinascidin 743 **60b** (Fig. 1), also known as Yolendis or Trabectedin, is a MNP extracted from the sea squirt, *Ecteinascidia turbinata.*[1,2,3] Since the isolation of the compound from the marine organisms in the 1970s, Et-743 has become by far the most advanced compound in late stage phase II clinical trials and has already entered phase III clinical trials for the treatment of various cancers such as soft tissue sarcoma, osteosarcoma, melanoma, and prostate cancer, *etc*..[4]

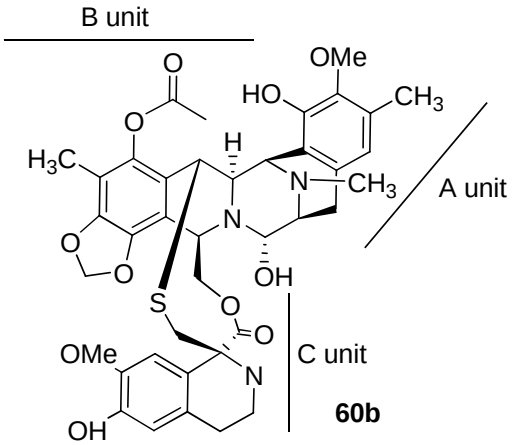

Fig. 1. The structure of Et-743 ($C_{39}H_{43}N_3SO_{11}$, 761.2613 g/mol).

Despite the efficacy of Et-743 as a potential anti-tumour agent, the overall success of the drug is restricted due to its limited supply. For this reason, the need for an economical method to produce compounds such as Et-743 is imperative. A 45 step synthesis of the compound was achieved in 1996 by Corey *et al*., however the numerous steps are time consuming and the overall yields are low.[5] Other attempts, such as aqua-culturing of the marine organism has been developed as an alternative method for the production of the drug, however the percentage yields from this, are again still low.[6] The synthesis of a synthetic analogue of Et-743, Phthlascidin 650 **67** (Fig. 2), has also been achieved by Corey *et al*., and this shows similar cytotoxic effects as Et-743.[7]

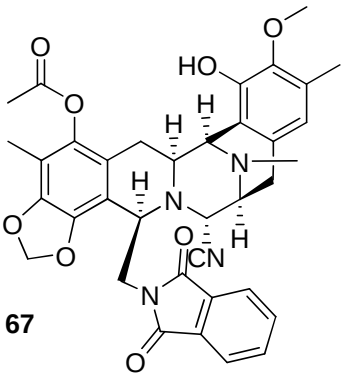

67

Fig. 2. Phthlascidin 650 ($C_{36}H_{34}N_4O_8$, 650.2371 g/mol), a synthetic analogue of Et-743, with anti-tumour properties.

Since the discovery of Et-743, other ecteinascidin compounds have been identified, along with the synthesis of different analogues of the drug, with some having greater activity than others. However, Et-743 is still the most potent.[8,9] Recently, Safracin B **74** (Fig. 3) was isolated from the bacteria, *Pseudomonas fluorescens*, and this is now used to prepare Et-743 in a 21 step semi-synthesis,[10,11,12,13] but the overall percentage yields of Et-743 by this method are still low.

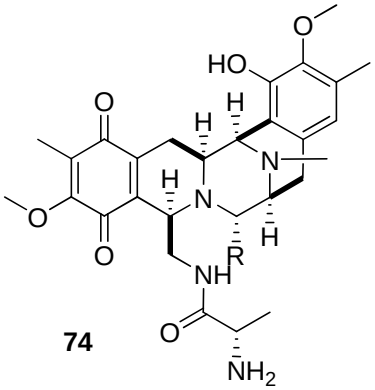

74

Fig. 3. Safracin B ($C_{28}H_{36}N_4O_7$, 540.2578 g/mol), a compound produced by *Pseudomonas fluorescens* used for the production of Et-743.[12]

Despite several alternative methods that have been used in an attempt to improve the overall yields for the production of the compound, no method has thus far proved valuable. Previous work has shown that Et-743 is not only found in the sea squirt, but the active compound is also ubiquitous in the environment where the organism resides.[14,15] Since then, the original source of the drug has

been continuously questioned. From the ubiquity of the compound in the ecosystem of the marine organism, it has been suggested that marine bacteria could be responsible for the production of the marine organism. Marine organisms such as sea squirts are filter feeders and can easily ingest marine bacteria. It has also been suggested that many marine organisms use marine bacteria to produce primary and secondary metabolites for various reasons that are still being determined.[16,17,18,19]

In the laboratory, the primary method for the isolation and cultivating of marine bacteria uses an agar medium. Agar is a gel medium which contains all the necessary growth factors needed for bacteria to grow.[20,21] Despite the innovation of the use of agar media, many bacteria are still impossible to grow in an artificial setting, unless the properties necessary for the bacteria growth are determined. In this study, the concept of using an agar medium was implemented into the development of a chemical composition, which consisted of the chemicals and growth factors similar to those in an agar medium, but without the use of any agar. The chemicals were selected based on previous studies conducted which analyzed the sediment and properties of the ecosystem of the organism, in order to determine the conditions in which the sea squirts resides.[15]

This chemical composition, was applied to the artificial surfaces (as detailed in section 3.2) by coating the surface with the chemicals, then placing the surfaces in locations where the sea squirt is present, in order to determine if the production of Et-743 from its ecosystem would be possible. The treated surfaces, having been coating with a composition of chemicals, have properties similar to that of the ecosystem and the marine organism. This may therefore be a beneficial tool to mimic the host organism and a suitable means for the isolation of the source responsible for the production of Et-743.

With previous work, as mentioned, showing the compound present in the marine environment; BACs containing treated AS (sponges) were placed in Panacea, Florida and Lido Key, Florida where the sea squirt is found. Aside from placing the AS at these locations, sediment and sea squirt from Panacea was also collected to investigate the presence of any ecteinascidin compounds in the Gulf of México. Mass spectral results from both locations strongly suggest peaks corresponding to two ecteinascidin compounds, however low detection levels could not give a definite mass accuracy to conclusively support the correlation of the data sets.

4.2 Experimental Section

All the samples in this study were analyzed as mentioned earlier (section 2.2). Et-743 standard was donated by the NCI (Bethesda, Maryland). Artificial surfaces (sponges) were treated as previously (section 3.2). Extraction procedures are detailed in sections 3.2.1-3.2.3. Additional SEM images of the white film collected from each broth and images of the surfaces initially removed from the water can be found on the enclosed DVD. Preparative procedures for the contents analyzed by SEM are as given in section 3.3.4. Tables 1 and 2 show the correlation of the different R groups for the different ecteinascidin compounds that have been isolated from the sea squirt.

4.2.1 Extraction (Panacea and Lido Key, Fl., 2007)

The broths were assessed at RT (room temperature) for a total of 4 wk (Lido Key sponges) and 12 ½ wk (Panacea sponges). Sponges were treated and packed into three BACs which were placed in Lido Key, Florida (27° 18’ 2.7648" ºN, -82° 34’ 5.5302" W) and Panacea, Florida (30° 1’ 44" N, 84° 23’ 56"W) respectively. The cultivation period for traps placed at Lido Key for 5 days (July

2nd 2007, at 10:00 a.m. to July 7th 2007, at 11:00 a.m.) and at Panacea 13 wk (February 24th 2007, at 11:00 a.m. to May 17th 2007, at 9:00 a.m.). After the allocated time period, the surfaces were transported to the laboratory in containers of sea water from each respective location.

4.2.2 Extraction (Panacea, Fl., 2008)

On June 15th 2008, at 2:00 p.m., the sponges prepared as mentioned in section 3.2 were placed in the Gulf of México at Panacea, Fl. The sponges (21, 19.1cmx11.4cmx5.08cm) were packed into three chambers and placed at Panacea, Florida for 1 wk and removed on June 22nd 2008, at 2:00 p.m.. The surfaces were then transported to the laboratory, containing water from the same location. The broth assessment was carried out for a total of 4 ½ wk as mentioned in sections 3.2.2 and 3.2.3. The solvent extracts from both and the surfaces were placed in a vacuum until dry. The crystals collected from both extracts (white film and surfaces) were extracted into anhydrous methanol (Fisher Scientific) and analyzed as mentioned in section 2.2.

4.2.3 Sea squirt extraction (Panacea, Fl., 2008)

Sea squirt was collect from crab traps at Panacea on June 2006 and June 2008. Sea squirts collected on June 17th 2006, at 11:00 a.m. were air dried at RT then placed in 30 mL of anhydrous methanol. The sample extract was filtered using a 0.2 µm filter then analyzed. Sea squirt (600 g wet weight) collected on June 22nd 2008, at 2:00 p.m. from the same location was air dried at RT, then extracted into 300 mL anhydrous methanol. The sample extract was filtered using a 5 µm filter paper followed by a 0.2 µm filter then analyzed as mentioned in section 2.2.

4.3 Results and Discussion

After 4 wk in the water, the treated surfaces (Panacea, Florida; section 4.2.1) appeared partially black in colour, reduced in size and gave off a strong pungent odor suggesting bacterial growth. The untreated surfaces retained their original appearance (Fig. 4). At RT, containers from both locations showed the formation of a white film visible on the surface of the water after 2 days (Fig. 5). Results from all the extracts collected in this study, were compared to the Et-743 standard (Figs. 6 and 8).

Fig. 4. Treated and untreated sponges shown above were both placed at Panacea, Florida (section 4.2.1). Images of both sponges were taken at the 8 wk mark during the 14 wk period in the water.

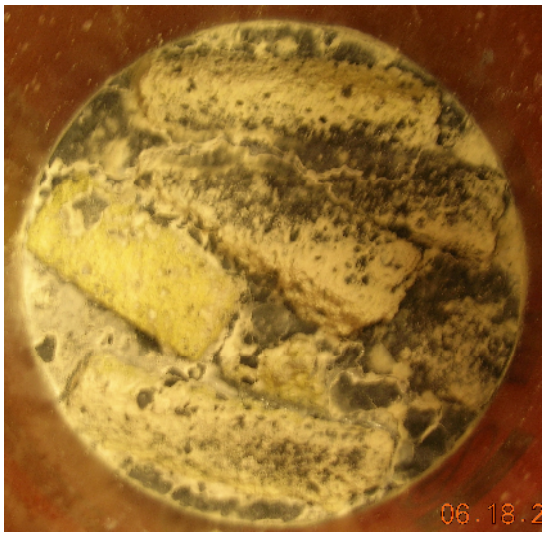

Fig. 5. The formation of the white film on the surface of the water during the broth assessment at RT (8 wk).

According to Rinehart *et al*., the molecular weight of Et-743 **60b** is (M^+: $C_{39}H_{43}N_3SO_{11}$, 761.2613 g/mol,), however, when dehydrated the compound has a mass of (M^+: $C_{39}H_{41}N_3SO_{10}$, 743.2507 g/mol,).[3,22,23] This explains why the

standard shows peak with *m/z* of 744 **97** and a smaller peak with an *m/z* of 762. The peak at m/z 776 $(M+H)^+$ **60g** correlates to the dioxyecteinascidin 743 extracted naturally in the standard (Fig. 8).

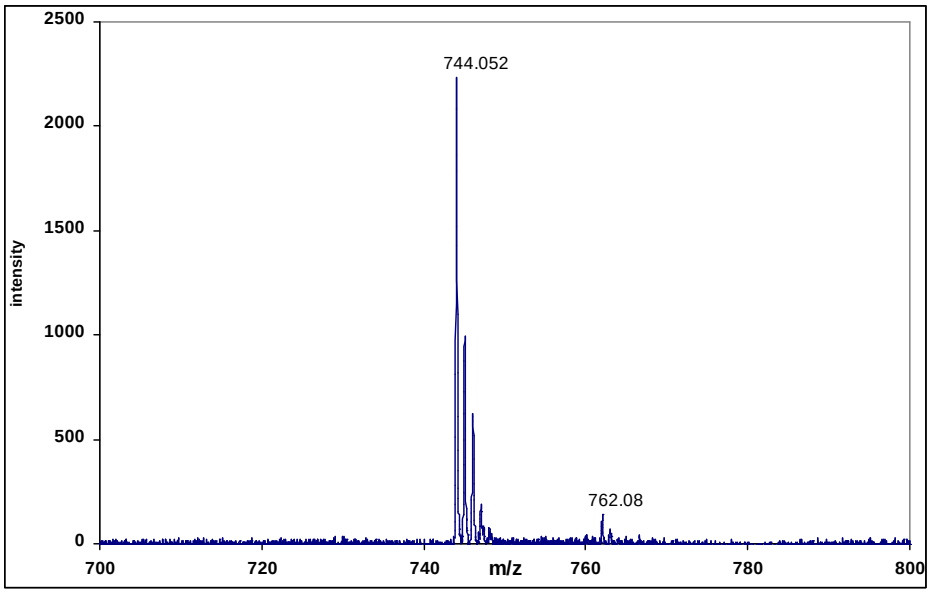

Fig. 6. MALDI-MS of an Et-743 standard in 2-propanol. Et-743 (Fig. 8) has a mass of 762.2613 g/mol $(M+H)^+$. When dehydrated (Fig. 7), it has a mass of 744.2585 g/mol **97** ($[M+H-H_2O]^+$, $C_{39}H_{42}N_3SO_{10}$).

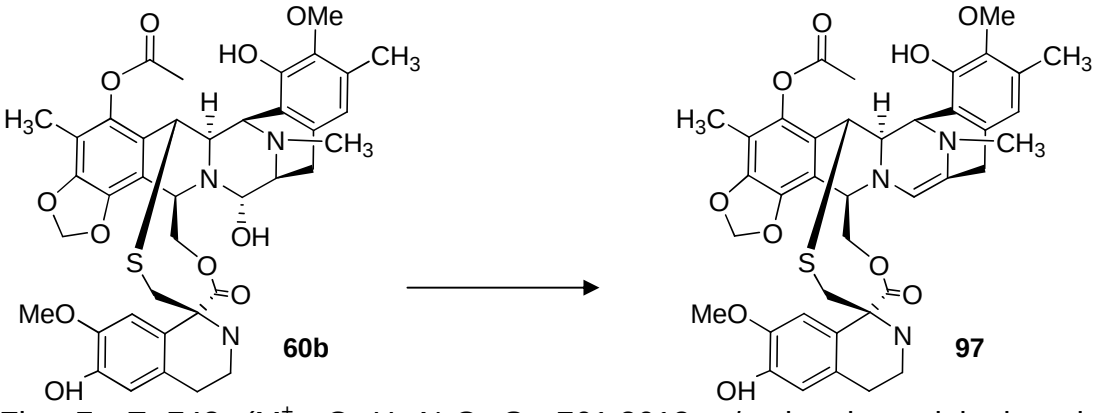

Fig. 7. Et-743 (M^+: $C_{39}H_{43}N_3O_{11}S$, 761.2613 g/mol, when dehydrated M^+: $C_{39}H_{41}N_3O_{10}S$, 743.2507 g/mol).

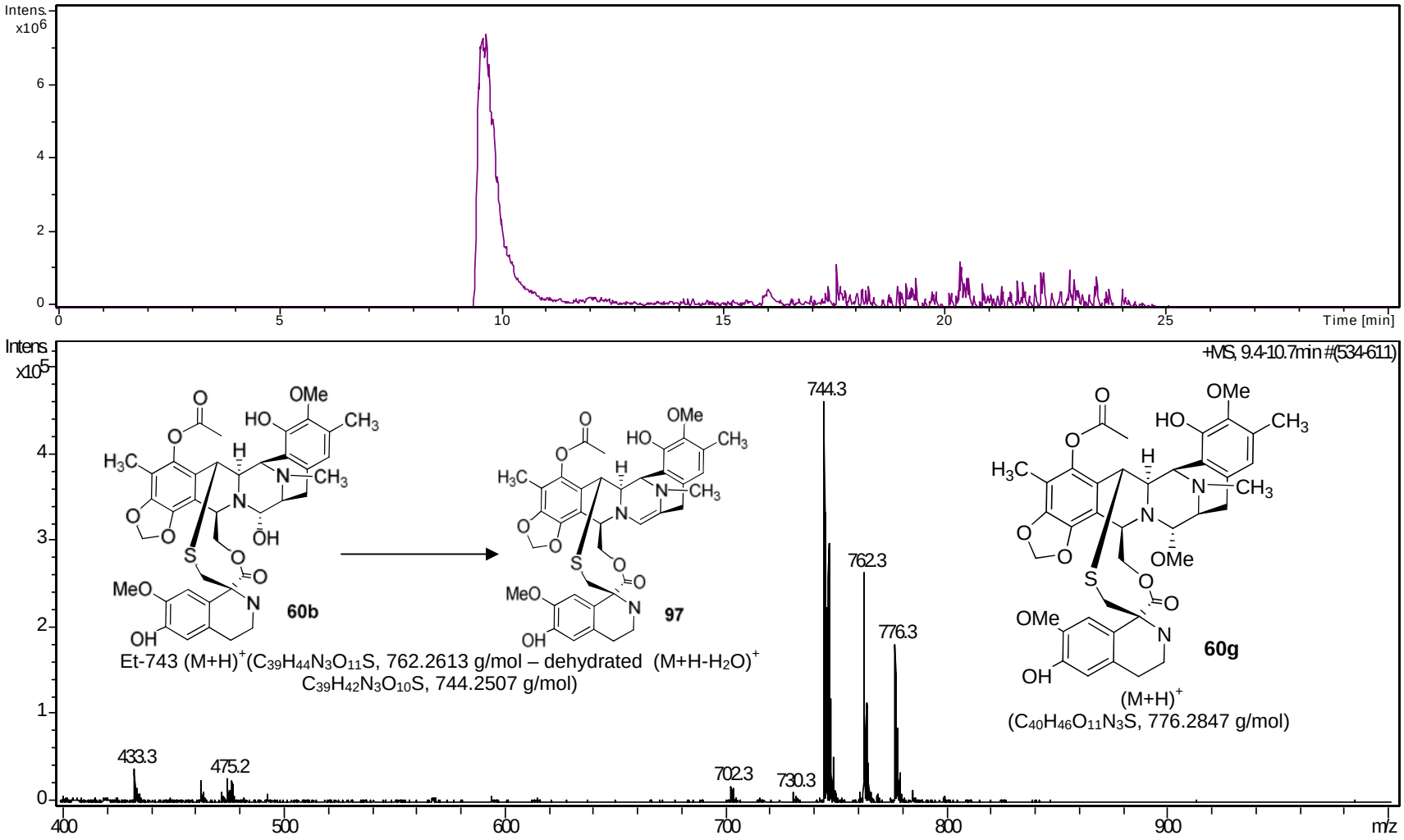

Fig. 8 LC-MS of Et-743 $(M+H-H_2O)^+$ standard **60b**. As shown, peaks with *m/z* at 744 $(M+H-H_2O)^+$ **97**, 762 $(M+H)^+$ and 776 [dioxyexteinascidin 743, $(M+H)^+$] **60g** at a retention time of 9.5 to 10.4 min.

There are eight known ecteinascidin compounds that have been extracted from the sea squirt and four synthetic compounds that have been prepared as shown in Tables 1 and 2.[22,23] The difference between each is defined by their R groups, as shown in Tables 1 and 2. Et-743 is primarily extracted from the sea squirt, *Ecteinascidia turbinata*.[1-3]

Table 1. Ecteinascidin compounds characterized by different R groups. The numbers shown in brackets represent the different structures for each compound shown below.[23] Molecular formula $(M+H-H_2O)^+$ determined by HRFABMS.

Et- compounds	Molecular formula	Molecular ion formula	R_1	R_2
Et-729 (**60a**)	$C_{38}H_{41}N_3SO_{11}$	$C_{38}H_{39}N_3SO_{10}$	H	OH
Et-722 (**59**)	$C_{39}H_{40}N_4O_9S$	$C_{39}H_{38}N_4SO_8$	H	OH
Et-736 (**59**)	$C_{40}H_{42}N_4O_9S$	$C_{40}H_{40}N_4SO_8$	CH_3	OH
Et-743 **(60b)**	$C_{39}H_{43}N_3O_{11}S$	$C_{39}H_{41}N_3SO_{10}$	CH_3	OH
Et-745 (**60c**)	$C_{39}H_{45}N_3SO_{11}$	$C_{39}H_{43}N_3SO_{10}$	CH_3	H_2
Et-759A (**60d**)	$C_{39}H_{43}N_3O_{12}S$	$C_{39}H_{41}N_3SO_{11}$	CH_3	OH
Et-759B (**60e**)	$C_{39}H_{43}N_3O_{12}S$	$C_{39}H_{41}N_3SO_{11}$	CH_3	OH
Et-770 (**60f**)	$C_{40}H_{42}N_4SO_{10}$	$C_{40}H_{42}N_4SO_{10}$	CH_3	CN
Et776 (**60g**)	$C_{40}H_{45}O_{11}N_3S$	$C_{40}H_{46}O_{11}N_3S$	CH_3	OMe

* Et-759A/B: S=oxide

(**a**)

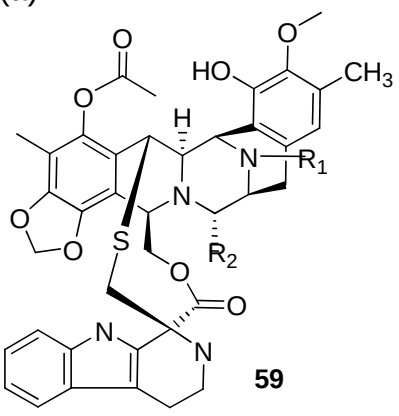

59

(**b**)

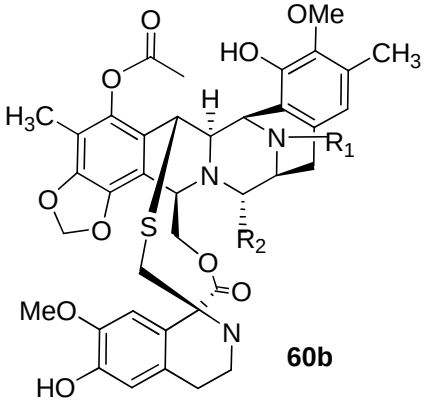

60b

Table 2. Ecteinascidin compounds characterized by different R groups. The numbers shown in brackets represent the different structures for each compound shown below.[23] Molecular formula $(M+H-H_2O)^+$ determined by HRFABMS.

Et compounds	Molecular formula	Molecular ion formula	R_1	R_2	X	Y
Et-583 (**61c**)	$C_{29}H_{33}N_3SO_8$	$C_{29}H_{33}N_3SO_8$	H	OH	OCH_3	OH
Et-597 (**61c**)	$C_{30}H_{35}N_3SO_8$	$C_{30}H_{35}N_3SO_8$	CH_3	OH	OCH_3	OH
Et-594 (**62d**)	$C_{30}H_{30}N_2SO_9$	$C_{30}H_{30}N_2SO_9$	CH_3	OH	XY: O-CH_2-O-	
Et-596 (**62d**)	$C_{30}H_{32}N_2SO_9$	$C_{30}H_{32}N_2SO_9$	CH_3	OH	OCH_3	OH
Et-637 (**63e1**)	$C_{30}H_{35}N_3SO_9$	$C_{30}H_{35}N_3SO_9$	CH_3	OH	XY: O-CH_2-O-	
Et-637-OBu (**64e2**)	$C_{34}H_{40}N_2SO_{11}$	$C_{34}H_{40}N_2SO_{11}$	CH_3	OH	XY: O-CH_2-O-	

(**c**)

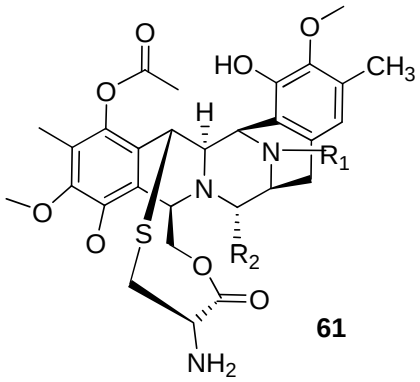

61

(A1: R = H; A2: R = CH_3)

(**d**)

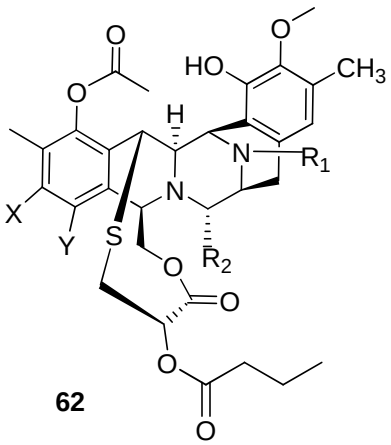

62

(B1 – XY(C-CH_2-O); B2 – X = OCH_3; Y - OH)

(**e1**)

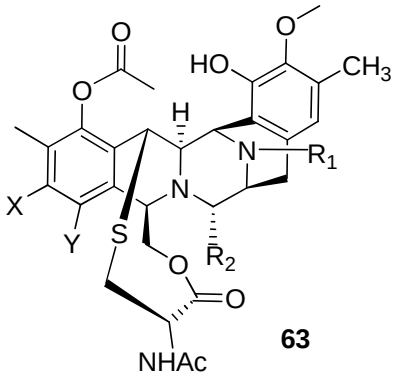

63

(**e2**)

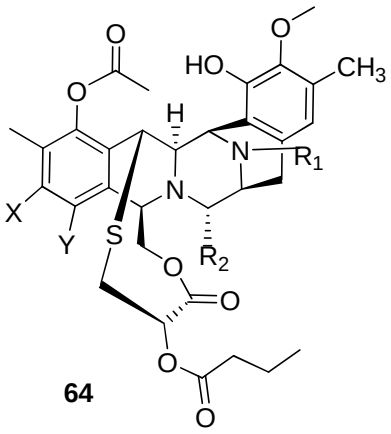

64

Fig. 28. The structures for the ecteinascidin analogues in Table 8.

In the Et-743 standard other peaks related to different ecteinascidin compounds were identified which could arise due to impurities the extraction process. For example, in Fig. 9 the peak with *m/z* of 771 $(M+H)^+$ **60f**, corresponds to Et-770 (M^+: $C_{40}H_{42}N_4SO_{10}$, 770.2616 g/mol).

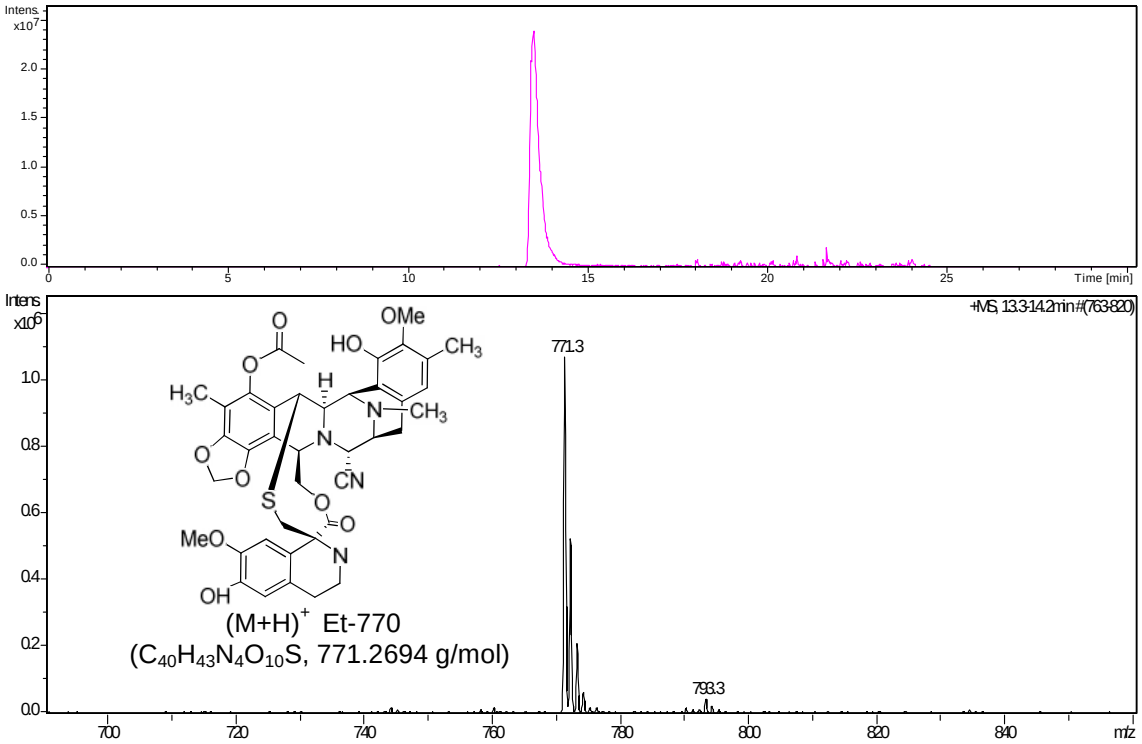

Fig. 9. LC-MS of Et-743 standard showing impurities within sample.

4.3.1 Treated surfaces (Panacea, Fl., 2007)

The white film (Fig. 10) from samples collected every 48 hr over an 8 wk period and extracted as mentioned in section 3.2.2. The MALDI-MS data from the extracted sponges heated to 65°C for 72 hr is shown in Fig. 11. In Fig. 10, an *m/z* of 760.859 $(M+H)^+$ is shown which could correspond to Et-759 A/B **60d/e** with a molecular formula of $C_{39}H_{41}N_3O_{11}S$, 759.2456 g/mol. Results from Panacea, Florida showed some consistency with mass spectral peaks collected from artificial surfaces placed in Lido Key, Florida (Fig. 12). Sea squirts collected from Panacea (Fig. 13) also gave a peak with an *m/z* of 760 $(M+H)^+$ consistent with the data from bacterial growth collected from the artificial surfaces and the Et-743 standard (Fig. 6 and 8).

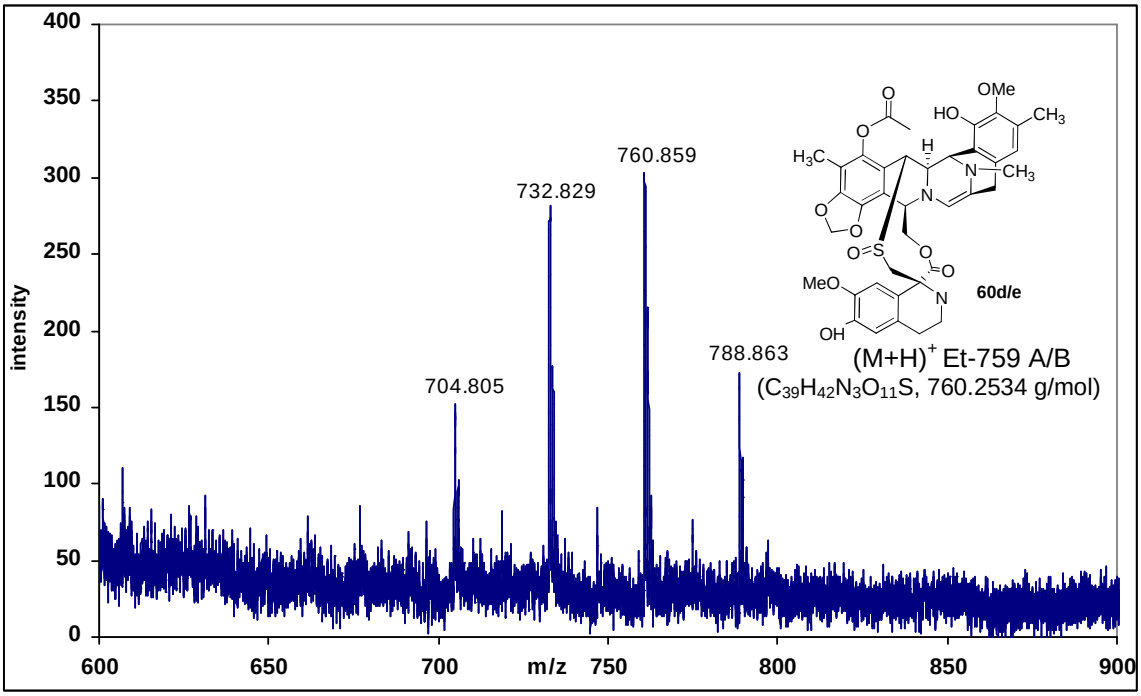

Fig. 10. MALDI-MS of the white film collected over a 12 ½ wk period from treated surfaces placed at Panacea, Florida.

Data obtained from the extracts heated to 65°C and those not heated were similar. The consistent correlations between the two data sets were helpful in understanding the effects of temperature, if any, on the NP. Firstly, the stability of the compound prevented the molecule from degrading when the extract was heated to 65°C. Secondly, the structure does not have a bryophan ring, therefore the stability of the compound is greater than bryostatin 1, whose bryophan ring has many ester bonds that can be easily broken.[24]

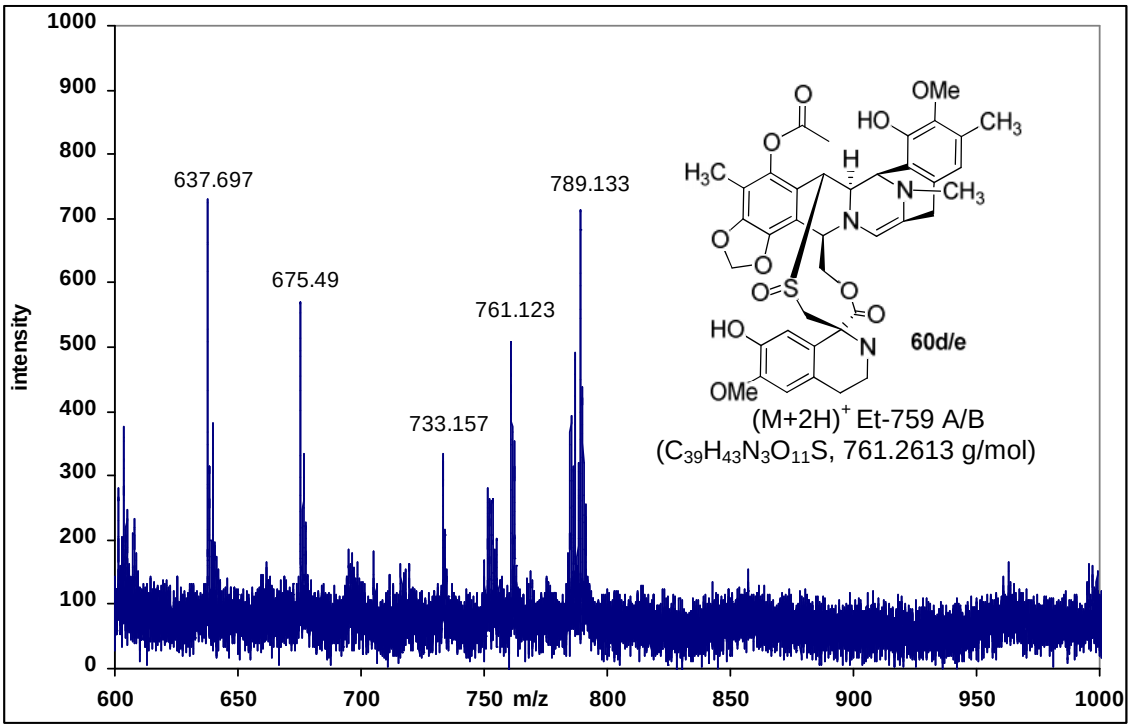

Fig. 11. MALDI-MS of sponge extract heated to 65°C for 72 hr.

4.3.2 Treated surfaces (Lido Key, Fl., 2007)

After 1 wk, all treated surfaces appeared black in colour and after 1 wk at RT a white film was visible on the surface of the water. Data analysis of the film was taken after 6 wk of production (Fig. 12). As shown in Fig. 12, the peak with an *m/z* of 760. 882 correspond to Et-759 A/B **60d/e** with a molecular formula of $C_{39}H_{41}N_3O_{11}S$, 759.2456 g/mol. This peak is also seen in samples collected from Panacea, Florida [Fig. 10, 760.859 $(M+H)^+$] and is also present in the sea squirt (original source of the ecteinascidin compounds) as shown in Fig. 13. This correlation strongly suggests the isolation of Et-759A/B from the ecosystem of the marine organism.

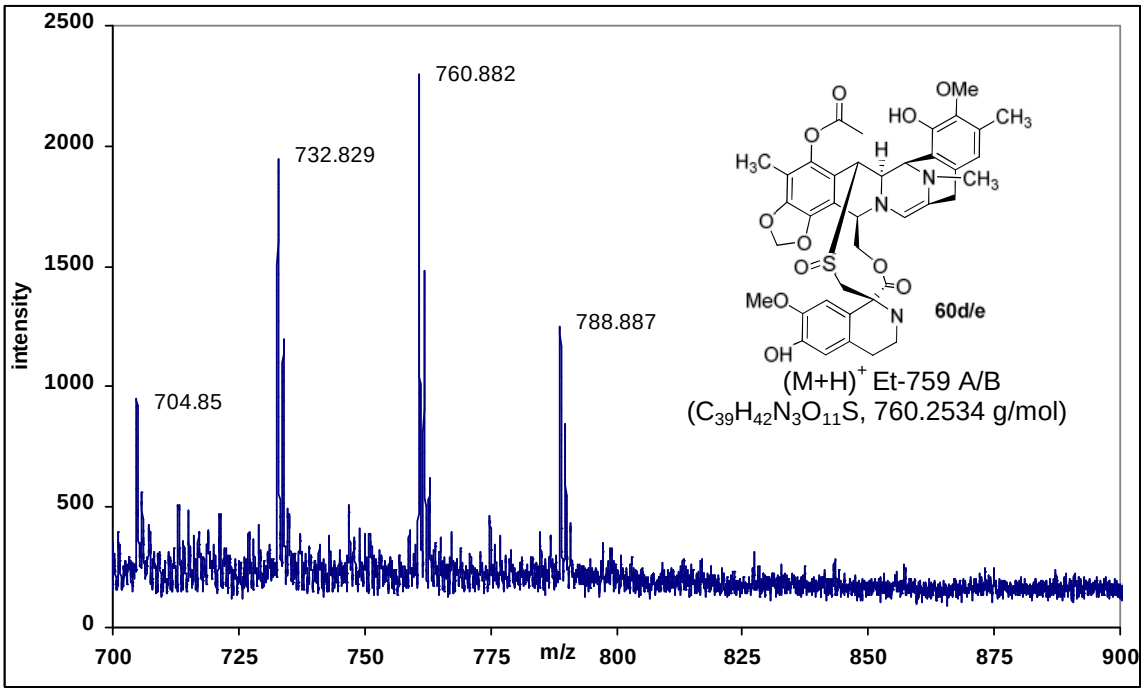

Fig. 12. MALDI-MS of the white film collected over a 4 wk period from surfaces placed at Lido Key, Florida.

4.3.3 Treated surfaces (Panacea, Fl., 2008)

After 1 wk in the water, the treated surfaces were black in colour, reduced in size and gave off a pungent smell, similar to the surfaces mentioned in section 4.3.1. The dry weight of crystals collected in section 3.2.2 was 0.76 g. Dry weights of crystals collected from sponge extract heated and not heated were 25.41 g and 22.57 g respectively. Analysis of all the extracts showed no indication of any ecteinascidin compounds in any of the extracts collected.

4.3.4 Sea squirt extraction (Panacea, Fl., 2008)

Ecteinascidia turbinata, originally found in the West Indies, was shown to contain Et-743, however other locations where the sea squirt is found have also showed levels of the NP to be present.[25] Previous work has shown that Et-743 is ubiquitous in the ecosystem of the sea squirt, with traces of Et-743 having been found in red mangroves in the Florida Keys.[14] Sea squirt collected in June 2006 was analyzed by MALDI-MS. Results showed no significant correlation to any

ecteinascidin compounds. Sea squirt extract collected in June 2008 was first analyzed by LC-MS (Fig. 13) and then analyzed by HRMS as shown in Fig. 14 and 15.

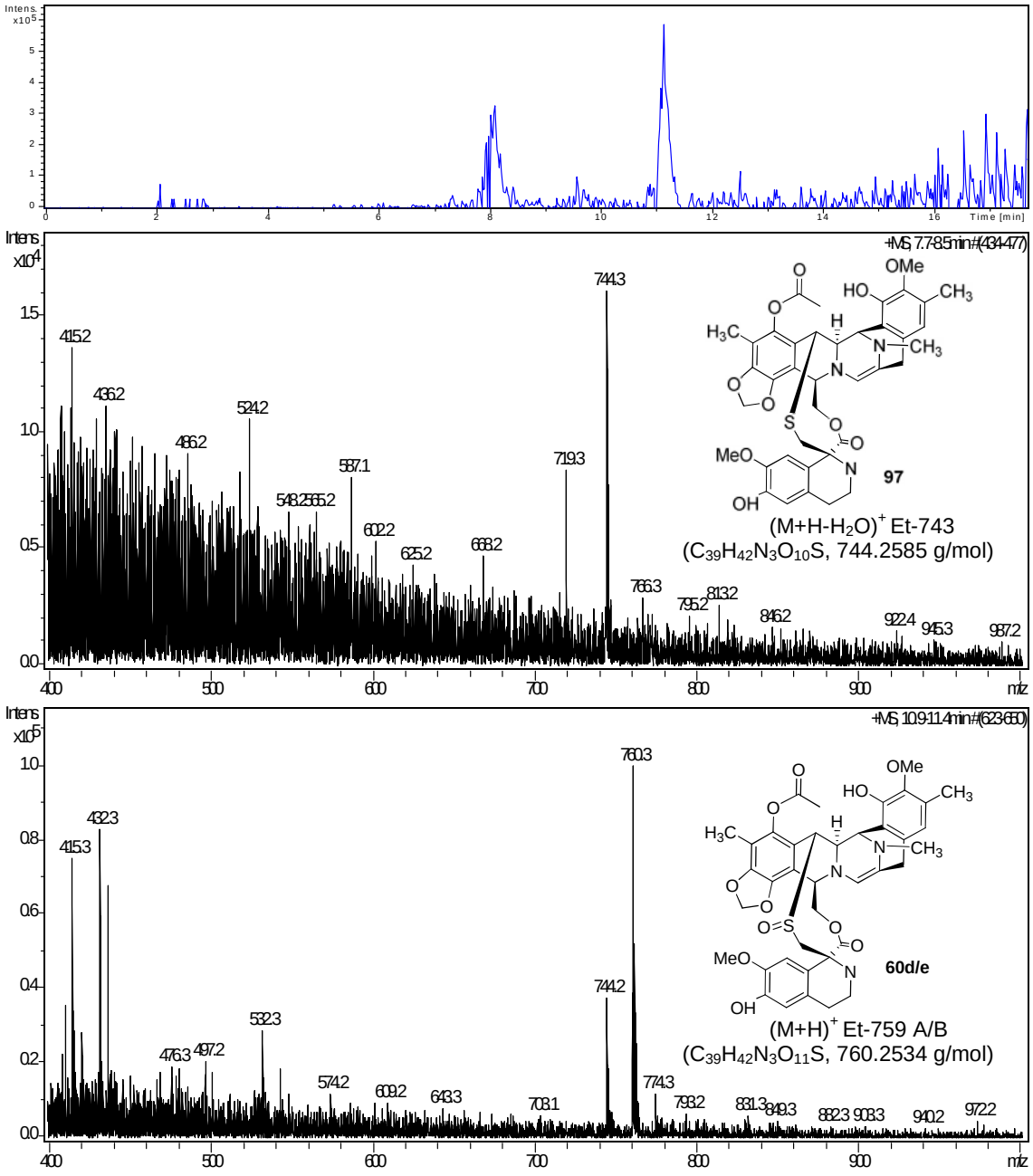

Fig. 13. Extract of *Ecteinascidin turbinata* collected from Panacea, in June 2008.

The sea squirt extract as shown in Fig. 13 shows two peaks at a *m/z* of 744 $(M+H)^+$ **97** and 760 $(M+H)^+$ **60d/e**. This correlation is important as the compound was initially isolated from the sea squirt collected in the West Indies. Detection levels for the *m/z* at 744.3 (Fig. 13) was too low to obtain a mass accuracy. However, the peak at *m/z* of 760.3 as mentioned is suggested to be Et-

759A/B. The HRMS for Et-759A/B **60d/e** as shown below is is (M^+: 759.2698 g/mol) however the correlation of the peak in Fig. 14 to Et-759 A/B has a HRMS value of (M^+: 759.2456 g/mol), showing an error of 21 ppm, with the acceptable error limit being 10 ppm.

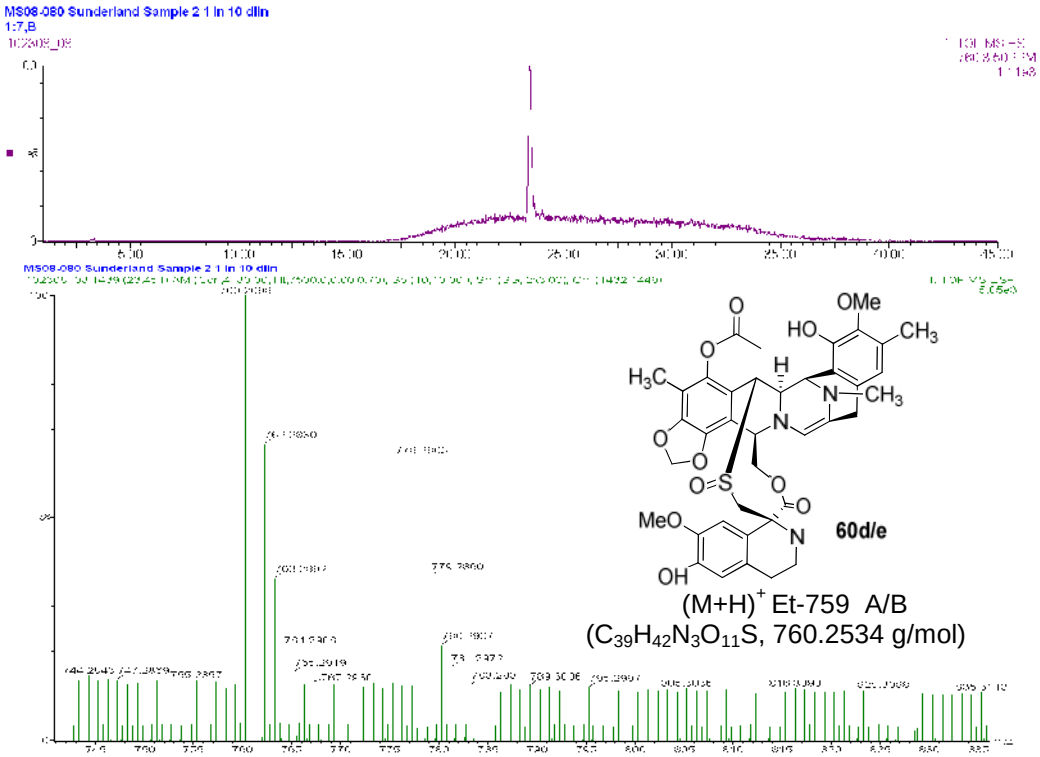

Fig. 14. HRMS of sea squirt extract as mentioned in Fig. 13.

An LC-MS (uv-vis) comparison of the extract and the Et-743 standard (Fig. 15) shows an overlap of the peak at a retention time of 10 minutes. The presence of this peak in both samples strongly suggests the possibility of it being Et-759A/B. The other peaks in the standard, other than Et-743 are mostly likely impurities of the compound collected during the isolation of the sea squirt. An additional study was conducted by injecting equal volumes of both the Et-743 standard and the sea squirt extract as a mixture and analyzed by LC-MS shown in Fig. 15. This mixture was then compared to Et-743 standard alone to show a more distinct overlap of the peaks in support of the correlation of the peak to Et-

759A/B **60d/e**. In The MALDI-MS it is natural for ions to occur in the form of $(M+H)^+$, $(M+2H)^+$, $(M-H)^+$ and $(M-2H)^+$.[26]

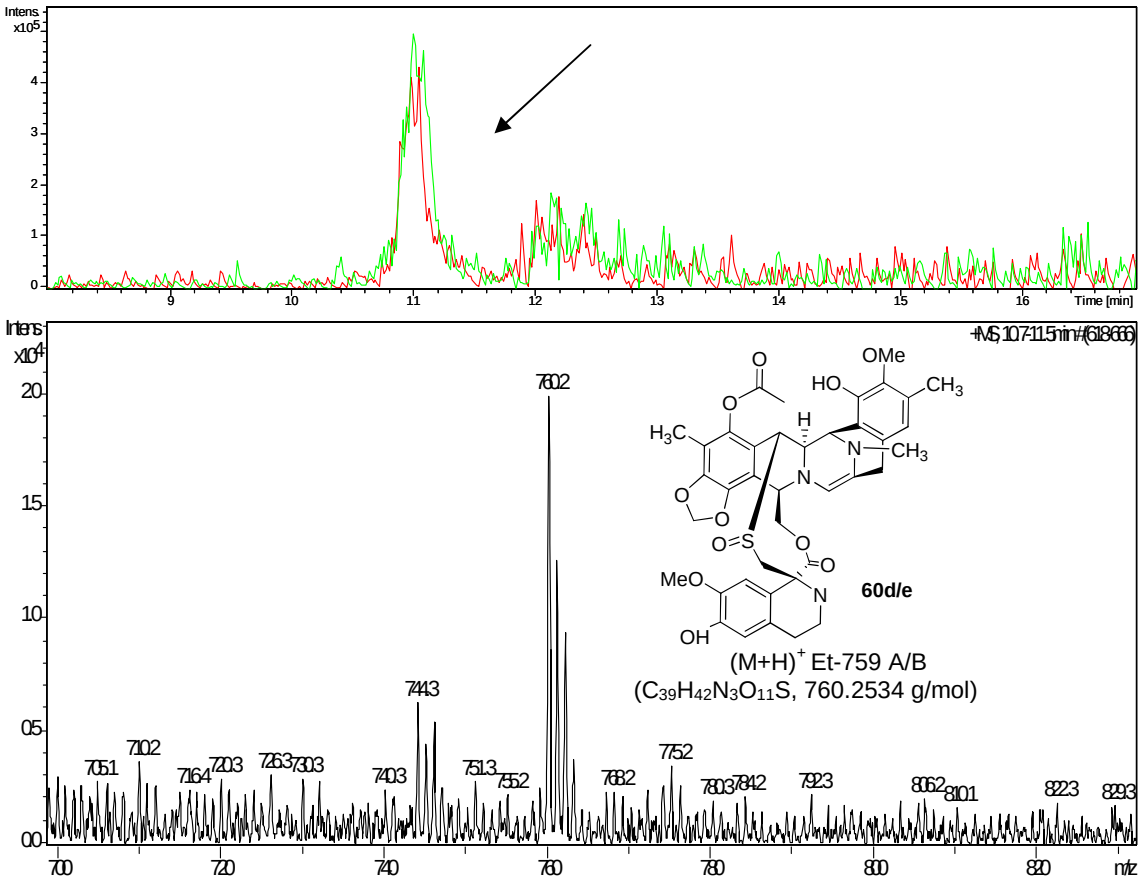

Fig. 15 LC-MS of Et-743 standard and sea squirt extract injected as a mixture. The green peak represents the sea squirt extract and the red represents the standard.

4.3.5 Symbiont bacteria

There is no conclusive proof of the primary source responsible for the production of Et-743, however evidence suggests that the marine symbiont, *Candidatus endoecteinascidia frumentensis* type 1 strain is a strong candidate as it is the only bacterium found to be associated with the sea squirt found in both the Mediterranean Sea and the West Indies.[27,28] Direct sequencing of the gene from the type 1 strain after PCR (polymerase chain reaction) amplification to obtain DNA data, indicated the importance of the marine symbiont in the sea squirt found in both locations.[28]

In an artificial environment, it is hard to grow bacteria. Less than 1% of bacteria that have been identified are either impossible or very hard to grow.[29] The broths that were accessed from both locations suggest that marine bacteria can grow in the laboratory however it is important to know the conditions at which they thrive in order to aid in their continuous production. No attempts were made to determine whether the chemical composition, developed for the broths, could also be useful for the cultivation of the bacterium *Candidatus endoecteinascidia frumentensis*. In agreement with the work of other groups, based on SEM images collected from the broths placed in both locations, it is proposed that marine bacteria are responsible for the production of Et-743 and this claim is supported by the ubiquity of the compound in the locations mentioned. No conclusive data on the specific bacterium has yet been obtained.

Data analysis of bacterial broths from the artificial surfaces placed in both locations suggests that the chemical composition used to treat the surfaces has met with some success in capturing marine bacteria. It is tentatively suggested that the bacterium captured and cultivated from the artificial surfaces may be *Candidatus endoecteinascidia frumentensis*.[28] The identification of the same bacterial strains in the different stages of the sea squirt provides some correlation between the presence of the bacteria in the ecteinascidin compounds and the ecosystem of the marine organism.[28]

Despite the fact that marine bacteria cultivated from the artificial surfaces were not studied further to determine the specific bacterial strain, SEM images from both broths at RT showed much evidence of bacteria in the white film, as well as on the surfaces themselves. Most of the bacteria, Fig. 16, are bacilli (rod-shaped) and are approximately two microns in size. However, some filamentous (thread-like) and cocci (spherical) bacteria are also seen, which are approximately five microns and one microns in size, respectively. Bacterial

filamentation is a defect in the completion of replication and is observed in bacteria responding to various stresses. This may happen, for example, while responding to extensive DNA damage through the SOS response system. Nutritional change may also cause bacterial filamentation. Shapes of bacteria in SEM image bacillus (rod) coccus (round) filamentous (thread like).[21,30]

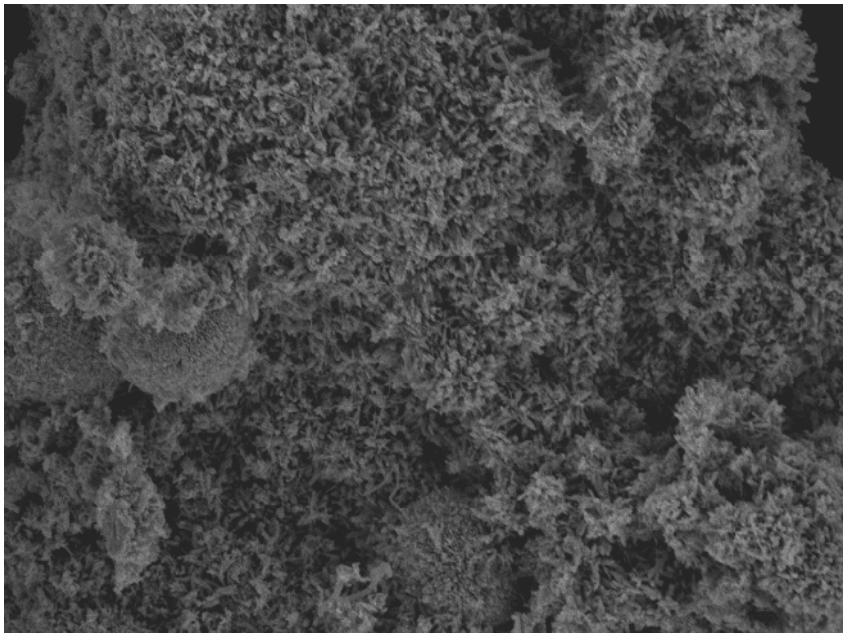

Fig. 16**.** SEM image of sponge removed from the broth at RT over the 4 wk assessment period. Sponges were located at Lido Key, Fl for 1 wk.

As shown in Fig. 16 most of the bacteria seen under the SEM are found in clusters also known as a biofilm, which is a structured community of microorganisms enclosed within a polymeric matrix, found either adherent to a living or inert surface.[31] One type of biofilm which is suggested to be present in the broths is familiar free floating, or planktonic biofilm, which form as single cells that float or swim independently in some liquid medium.[32] The SEM images of the white film, could be biofilms of bacteria clustered together (Fig. 16), which was collected from the surface of the water from the broths assessed in this study. Biofilms are formed by the attachment of free-floating microorganisms to a surface, or liquid surface. For the attachment to take place, colonies initially adhere to the surface by weak, reversible van der Waals forces; those that are

not immediately separated from the surface more permanently by pili, which are cell adhesion structures.[33] Micro-colonies are formed when bacteria form complex arrangements of cells and extracellular components while living in biofilms. This is done through networks of channels which allow for better diffusion of nutrients.[33]

In relation to this suggestion, MALDI-MS and LC-MS data from the extracts collected from the artificial surfaces were compared to an Et-743 standard, with preliminary results suggesting correlations to ecteinascidin compounds. The two locations used are both prominent sites where the sea squirt is found. Despite the geographical assumption and seasonality of the marine organism, *Ecteinascidia turbinata* is known to contain levels of Et-743 only in sea squirts found in the Caribbean, Mediterranean and along the Southern Coast of Florida.

4.4 Conclusion

The use of artificial surfaces was successful in capturing the marine bacteria from both locations where the sea squirt is found. Preliminary results showed the reliability of this technique for the production of other NPs, which could be achieved by merely modifying the chemical composition necessary for the cultivation of the specific bacterium of choice. Since the current method of producing the drug is neither appropriate nor sustainable, this novel technique could prove a promising cost effective and economical solution for the production of Et-743. Despite the mass spectra showing the possible production of different ecteinascidin compounds, low detection levels prevented further mass accuracy determination to either support or disprove the identifications of Et-743 and its analogues.

4.5 References

[1] K. L. Rinehart, T. G. Holt, N. L. Fregeau, P. A. Keifer, G. R. Wilson, T. J. Perun, R. Sakai, A. G. Thompson, J. G. Stroh, L. S. Shield, D. S. Seigler, L. H. Li, D. G. Martin, C. J. P. Grimmelkhuijen, and G. Gade. *J. Nat. Prod*., 1990, **53(4)**, 771-92.

[2] K. L. Rinehart, T. G. Holt, N. L. Fregeau, J. G. Stroh, P. A. Keifer, F. Sun, L. H. Li, and D. G. Martin. *J. Org. Chem*., 1990, **55(15)**, 4512-15.

[3] K. L. Rinehart, R. Sakai, Y. Guan, and A. H. J. Wang. *Proc. Natl. Acad. Sci. USA,* 1992, **89(23)**, 11456-60.

[4] http://www.clinicaltrials.gov/ (January 25th 2009).

[5] E. J. Corey, D. Y. Gin, and R. S. Kania. *J. Am. Chem. Soc*., 1996, **118(38)**, 9202-03.

[6] http://www.pharmamar.com/yondelis.aspx (June 25th 2009).

[7] E. J. Martinez, E. J. Corey, T. Owa, and S. Schreiber. *Proc. Natl. Acad. Sci. USA,* 1999, **96(7),** 3496-501.

[8] K. L. Rinehart, R. Sakai, T. G. Holt, N. L. Fregeau, T. J. Perun, D. S. Seigler, G. R. Wilson, and L. S. Shield. *Pure Appl. Chem.,* 1990, **62(7)**, 1277-80.

[9] M. H. David-Cordonnier, C. Gajate, O. Olmea, W. Laine, J. de la Igiesia-Vincente, C. Perez, C. Cuevas, G. Otero, I. Manzanares, C. Bailly, and F. Mollinedo. *Chem. Biol*., 2005, **12(11)**, 1201-10.

[10] Y. Ikeda, H. Idemoto, F. Hirayama, K. Yamamoto, K. Iwao, T. Asao, and T. Munakata. *J. Antibiot.*, 1983, **36(10)**, 1279-83.

[11] E. J. Martinez, and E. J. Corey. *Org. Lett*., 2000, **2(7)**, 993-96.

[12] A. R. Duckworth, G. A. Samples, A. E. Wright, and S. A. Pomponi. *Aquaculture*, 2004, **241(1-4)**, 427-39.

[13] C. Cuevas, M. Pérez, M. J. Martín, J. L. Chicharro, C. Fernández-Rivas, M. Flores, A. Francesch, P. Gallego, M. Zarzuelo, F. de la Calle, J. García, C. Polanco, I. Rodríguez, and I. Manzanares. *Org. Lett.,* 2000, 2(16), 2545-48.

[14] T. J. Manning, E. Rhodes, M. Land, R. Parkman, and A. G. Marshall. *Nat. Prod. Res*., 2006, **20(5)**, 461-73.

[15] T. J. Manning, M. Land, E. Rhodes, L, Chamberlin, J. Rudloe, D. Phillips, T. T. Lam, J. Purcell, H. J. Cooper, M. R. Emmett, and A. G. Marshall. *Nat. Prod. Res*., 2005, **19(5)**, 467-91.

[16] V. J. Paul, K. E. Arthur, R. Ritson-Williams, C. Ross, and K. Sharp. *Biol. Bull.*, 2007, **213(3)**, 226-51.

[17] J. Piel. *Curr. Med. Chem.*, 2006, **13(1)**, 39-50.

[18] L. X. Zhang, R. An, J. P. Wang, N. Sun, S. Zhang, J. C. Hu, and J. Kuai. *Curr. Opin. Microbiol.*, 2005, **8(3)**, 276-81.

[19] G. E. Lim-Fong, L. A. Regali, and M. G. Haygood. *Appl. Environ. Microbiol*. 2008, **74(11)**, 3605-09.

[20] Madigan, M., and J. Martinko. Brock Biology of Microorganisms. 11th Edition, Prentice Hall, 2005.

[21] Black, J. G. Microbiology: Principles and explorations. 5th Edition, John Wiley and Sons Inc., 2002.

[22] K. L. Rinehart. *Med. Res. Rev.,* 2000, **20(1)**, 1-27.

[23] R. Sakai, E. A. JaresErijman, I. Manzanares, M. V. S. Elipe, and K. L. Rinehart. *J. Am. Chem. Soc*., 1996, **118(38)**, 9017-23.

[24] J. C. Baer, J. A. Slack, and G. R. Pettit. *J. Chrom*., 1989, **467(1)**, 332-35.

[25] J. L. Carballo. *Rev. Biol. Trop*., 2000, **48(2-3)**, 365-69.

[26] Hillenkamp, F., and J. Peter-Katalinić. MALDI MS: A practical guide to instrumentation, methods and applications. Wiley-VCH, 2007.

[27] A. E. Perez-Matos, W. Rosado, and N. S. Govind. *Antonie van Leeuwenhock*, 2007, **92(2)**, 155-64.

[28] C. Moss, D. H. Green, B. Perez, A. Velasco, R. Henrıquez, and J. D. McKenzie. *Mar. Biol*., 2003, **143(1)**, 99-110.

[29] http://www.textbookofbacteriology.net/nutgro.html (May 22nd 2009).

[30] Talaro, K. Park, and A. Talaro. Foundations in Microbiology. 3rd Edition, McGram-Hall Companies, 1999.

[31] S. S. Branda, A. Vik, L. Friedman, and R. Kolter. *Trends Microbiol*., 2005, **13(1),** 20-26.

[32] S. S. Branda, J. E. Gonzalez-Pastor, S. Ben-Yehuda, R. Losick, and R. Kolter. *Proc. Natl. Acad. Sci. USA*, 2001, **98(20)**, 11621-26.

[33] R. Donlan. *Emerg. Infect. Dis*., 2002, **8(9)**, 881-90.

CHAPTER 5

Sediment extractions for the isolation of the bryostatins

5.1 Introduction

Alternative sources for NP from the sea have been an increasingly important investment over the past fifty years. However, many problems, such as harvesting marine organisms, isolating drugs and tedious synthetic steps, all limit the production of NPs for the pharmaceutical industry. For this reason, other alternative methods have since been attempted to overcome such problems. For many years, diverse groups (industrial, and agricultural, *etc*.) have conducted studies on sediment from the environment, focusing on a variety of research areas for diverse reasons.[1,2,3,4] For example, a recent study conducted by Giltrap *et al*., focused on chemical properties of marine sediment at three locations in Ireland. Results from this study, showed the concentration of metals such as copper, lead, nickel, and zinc, *etc*., and organic contaminants such as anthracene, dichlorodiphenyltrichloroethane, naphthalene and, endosulphan A, *etc*., were detected in the sediment; indicating the toxicity levels of these compounds in the water.[5]

There are many different types of microorganisms found in sediment and the ocean with beneficial functions such as: 1) the capability to produce predominant populations of actinomycetes, which are believed to be responsible for the production of marine natural products isolated from marine invertebrates; 2) the presence of nitrobacteria, to remove nitrogen ions from water; 3) the presence of non toxic gamma positive bacteria, ubiquitous in the environment, with bioactive properties; and 4) the presence of lactobacteria such as *Lactobacillus acidophilus,* used to disintegrate lignin and cellulose, which are generally difficult to decompose. The microorganisms mentioned above are a few examples of the different types of marine organisms found in sediment and water, each with a specific function.[6]

For this reason, there has been an increasing interest in studying sediment for the isolation of NPs or marine bacteria with medicinal potential.[7,8,9] A study was conducted by Adesina *et al*., on the composition of soil bacteria in various countries in Europe, to determine any *in vitro* activity. This showed that 18.3% of the bacteria had *in vitro* properties as anti-fungal agents.[8]

A recent study conducted by Cetecioğlu *et al*., showed that the diversity of marine bacteria in sediment, collected from different locations in the Marmara Sea, is significantly based on the depth at which the sediment samples were collected and of chemicals such as sulfur, iron, and manganese. Results also showed that the archaeal communities (52 archaeal species), were more diverse than bacterial diversity (48 bacteria species) in all the sites that were used in the study.[10] Studies conducted by Manning *et al*., analyzing sediment samples from the Gulf of México, have also shown high concentrations of different metals.[11] This data was also correlated to marine bryozoa in the area and marine bacteria within *Bugula neritina*, in order to further understand the conditions the organism resides in and the environment where it is collected.

With many investigations showing the ubiquity of marine bacteria in sediment and correlation of the production of natural products to marine bacteria, a new study was conducted primarily focusing on sediment in the ecosystem of *Bugula neritina*. This was designed to test the viability of isolating bryostatin compounds from *Bugula's* natural environment. Detailed analyses of sediment in the *Bugula* locality have previously detected traces of various bryostatin compounds. This prompted four separate studies, concentrating on sediment from Alligator Point, Florida. Successful extraction of compounds of interest from the sediment would support the idea that one ubiquitous component (*e.g.* a marine bacterium) is responsible for the production of the NPs. Results from this study would hopefully support and correlate to the findings discussed in previous

chapters; designing and developing artificial surfaces in combination with the mineral paste composition, to attract marine bacteria in the ecosystem of *Bugula neritina*.

5.2 Experimental section

5.2.1 Sediment extraction (March 2006)

February 2nd 2006, at 9.00 a.m., sediment (wet mass 506.41 g) from Alligator Point Marina, Florida was collected and stored at 4°C. On March 8th 2006, at 9.00 a.m., the sediment was processed and extracted as described. A 1 L solution of 0.06 M HNO_3 (Fisher Scientific) was slowly added to the sediment; the extract was stirred and left to settle. After 3 hr the top layer (water) was discarded and replaced with an equal volume of water in the sediment container, along with 50 mL of 0.1 M NaOH (Fisher Scientific). The sample was stirred and left to settle. After 0.50 hr, the top layer (water) was discarded and a 1 L solution of 0.005 M EDTA (ethylenediaminetetraacetic acid, Fisher Scientific) was added to the sediment and stirred for 48 hr.

After 48 hr, the sediment was filtered then placed under vacuum to dryness (dry weight of 203.49 g). To the dried sediment, 150 mL of pentanol (Fisher Scientific) was added and at 2 day intervals replaced with another 150 mL of pentanol until a total of 1.5 L of pentanol was used. The extract collected was filtered, using a 5 µm filter paper, followed by a 0.2 µm filter. The pentanol extracts from each interval were combined and the sediment in the container was filtered and dried producing a dry weight of 141.16 g (Table 1).

A 1 L solution of 0.01 M EDTA adjusted to pH of 2-3 with 0.1 M HCL (Fisher Scientific) was added to 1 L of the pentanol extract and stirred (Fig. 1). After 48 hr, the foam between both layers was removed and placed under vacuum to dryness. The pentanol layer was added to a 1 L solution of 2.30 g of

$FeCl_3$ (Fisher Scientific), 44 mL of 0.1 M NaOH, plus an additional 0.55 g of NaOH pellets. This pentanol-iron (III) chloride solution was stirred for 48 hr. The foam layer between the pentanol-iron (III) chloride mixture was removed by centrifugation and dried.

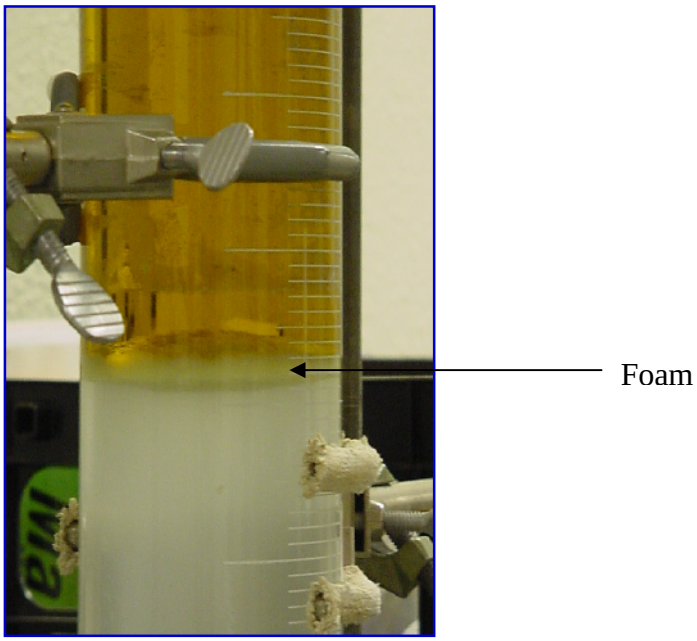

Fig. 1. Mixtures of 1L of pentanol extract and 1L of EDTA solution resulted in the formation of a foam suspension between both layers.

5.2.2 Sediment extraction (May 2006)

On May 9th 2006, at 9.00 a.m., a wet weight of 1.17 kg of sediment was used for a second extraction of sediment collected from Alligator Point, Florida. This sediment was removed from the same container containing sediment as used in section 5.2.1. Volumes of acid and base were used, as in section 5.2.1. The total dry weight of the sediment before extracting into 1.5 L of pentanol was 369.63 g. The total mass of the dry sediment after extracting into pentanol was 271.74 g. A total of 0.66 g of white powder (foam) was collected, as in section 5.2.1, from this extraction process.

5.2.3 Sediment extraction (June 2006)

On June 19th 2006, at 9.00 a.m., a total of 5.5 L of pentanol was used to extract approximately 9.611 kg of sediment collected from Alligator Point, Florida. Three litres of 0.16 M HCL was periodically added to the sediment over a 5 day period, after which the top layer (water) was removed and a 4 L solution of 0.03125 M NaOH was added to the sediment. A total of 2 L of the pentanol extract-EDTA solution was used to isolate white powder (foam) for analysis. The detailed amount of pentanol added and removed over the course of the extraction procedure is given in Table 4. The purification procedures (sections 5.2.4) were used for the remaining 2 L of extract collected.

5.2.4 Purification of sediment extract

Two techniques, detailed below, were used to determine the most suitable purification method using the sediment extraction collected (section 5.2.3). The primary goal was to isolate any compounds that could signify the presence of any bryostatin compounds.

5.2.4.1 Column Chromatography

Silica (Fluka) was packed into a 10" column then flushed using 75 mL of petroleum ether (Aldrich), followed by 20 mL of the pentanol extract. The pentanol extract was then flushed with petroleum ether (200 mL of 40/60) followed by 150 mL of methanol (Sigma Aldrich), which was used to separate the different bands. The first fractions collected were the excess petroleum and remaining pentanol from the column. Finally the methanol fraction was collected, which was evaporated to dryness. The second, third and final fractions were analyzed by LC-MS to determine the success of separating the components from the pentanol extract.

A second modified column was prepared using basic alumina oxide (BDH Laboratory Supplies) instead of silica, and hexane (Sigma) instead of petroleum ether. The 10" column was initially flushed with 150 mL of hexane, followed by 20 mL the pentanol extract. The pentanol extract on the column was then flushed with 100 mL of hexane followed by 90 mL of methanol. Each fraction was collected separately and analyzed by LC-MS.

Attempts were made to prepare an iron bonded 8-hydroxyquinoline silica column.[12,13] In the process of preparing the 8-hydroxyquinoline silica column, the compound did not bind to the silica to form a siderophore medium for the isolation of the bryostatins. This method was not pursued further.

5.2.4.2 Ionic liquids

Ionic liquids are liquids comprised of 99.9% ions, often referred to as molten salts such as ammonium, imidazolium, *etc*., with melting points less than 100°C. In a liquid-liquid extraction using ionic liquids, these solvents ideally bind the compound of interest by changing its polarity.[14]

5.2.4.2.1 1-Butyl-2,3-dimethylimidazolium hexafluorophosphate

Ionic liquid, 1-butyl-2,3-dimethylimidazolium hexafluorophosphate **101** (Sigma Aldrich), was heated at 34°C to melt the salt. The molten salt (1 g) was added to 5 mL of the pentanol extract, placed in a water bath (34°C) for 10 min and sonicated for 30 min at 30°C. The top layer (pentanol extract) was removed and 5 mL of deionized water was added to the ionic liquid (lower layer) and the mixture was sonicated again for 15 min. The water was removed and 5 mL of methanol was added to the ionic liquid. The sample was placed in a cold bath (-86°C) for 30 min. The crystal formed (dry weight 0.0035 g) was removed by

suction filtration using a 5 µm filter paper. The methanol-ionic liquid mixture was evaporated to dryness.

5.2.4.2.2 *N, N*-Dimethylethanolammonium propionate

The Ionic liquid method using *N,N*-dimethylethanolammonium propionate **100** (Bioniqs) was used with a few adjustments. The ionic liquid (5 mL) was added to 5 mL of pentanol extract and sonicated for 30 min. The bottom layer (ionic liquid) was placed in 5 mL of deionized water and sonicated again for 20 min. After sonication, the two layers collected were analyzed by LC-MS.

5.2.5 Sediment extraction (June 2008)

On June 15th 2008, at 12.00 p.m., two collections of sediment from Alligator Point, Florida, were assessed. The first collection (600 g) was processed using experimental procedures given in section 5.2.1; however, anhydrous methanol (Fisher Scientific) was substituted for pentanol and once the methanol extracts were collected and filtered, the sample was placed under vacuum to dryness.

The second collection was a raw extraction, collected by filtering the sediment to dryness (dry weight 600 g) and extracting into 1 L anhydrous methanol. Crystal extracts, collected from both samples, after solvent removal, were analysed by LC-MS. Sediment collected was stored at 4°C until June 16th 2008, at 9:00 a.m., when the processing of the sediment extracts for each batch (600 g of dry sediment for processed and 600 g dry sediment for non processed) began.

5.3 Results and Discussion

All extractions collected were compared to a bryostatin 1 standard (Fig. 2) donated by the NCI in Bethesda, Maryland. All the samples were analyzed as in section 2.2. Bryostatin 1 has two absorbance values at 233 nm and 262 nm. The absorbance value at 262 nm was used to analyze all extracts conducted in this study, as well as the absorbance value of 660 nm for any indication of chlorophyll. An ultraviolet-visible spectroscopy (uv-vis) was used to determine the absorbance values of the extracts at the wavelengths mentioned above.

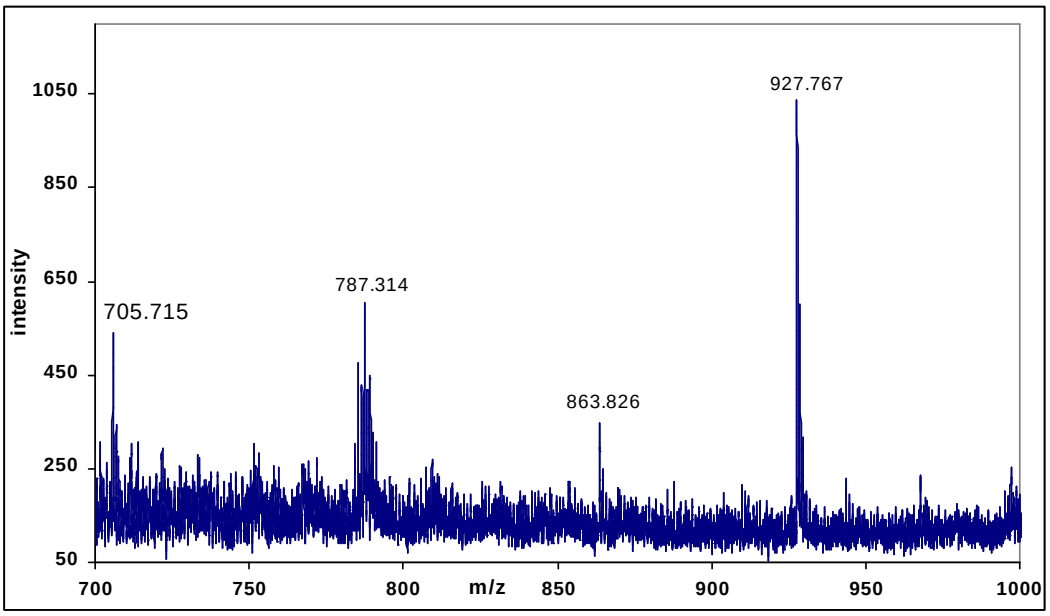

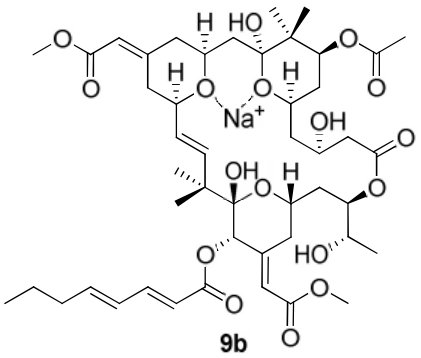

$(M+Na)^+$ Bryostatin 1+Na^+
($C_{47}H_{68}O_{17}Na$, 927.4349 g/mol)

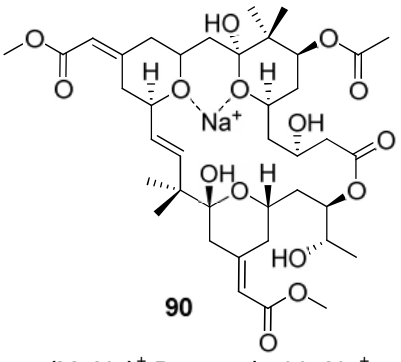

$(M+Na)^+$ Bryostatin 11+Na^+
($C_{39}H_{58}O_{15}Na$, 789.8724 g/mol)

Fig. 2. Bryostatin 1 standard with Na^+ adduct ($C_{47}H_{68}O_{17}Na$, 927.4349 g/mol).

Having extracted sediment from Alligator Point, Fl. at different time periods, findings strongly suggested that the bacterium producing the NP can be

found in the *Bugula* environment all year round; with higher concentrations from October to May. However, this also showed that different compounds were detected at different times in the year. Concentrations in the collections made during the summer season are not as pronounced. For example, in Fig. 11 there does not seem to be any peaks that could be correlated to any bryostatin compounds. One reason for this would be that the bacteria are temperature dependent and thrive better in colder conditions; when the water is approximately 18-22°C. Based on this, it can be construed that the marine organism is merely used as a host for the bacterium, which would explain the seasonal availability of the drug. Another family of NPs, macrolactin a-f, has been isolated from sediment collected in their host environment.[15, 16]

The use of pentanol in the study, adversely affected further analyses due to the high viscosity of the solvent. For this reason, several separating techniques were evaluated to determine the best method of isolating the compounds from the solvent; however, no method proved practical. The four sediment extractions showed preliminary success in isolating compounds that could be correlated to different bryostatin compounds but no conclusive evidence could be obtained due to low detection levels

5.3.1 Sediment extraction (March 2006)

A total of 10 collections from the sediment sample were made. Table 1 shows the amount of pentanol collected from each extraction over a 3 wk period. The white foam collected from the pentanol-EDTA layer had dry weight of 2.31 g (Fig. 3). The pentanol extract (Fig. 4) shows several peaks consistent with previous results from the artificial mediums and surfaces analyses. Table 1 shows the amount of pentanol added and removed at every 2 day interval.

Table 1. Pentanol collected and uv-vis data for each sample extraction.

Pentanol (mL)	Amt retrieved (mL)	Absorbance (263 nm)	Absorbance (660 nm)
150	36	1.525	0.0488
300	209 (inc. 36)	0.90	0.0308
450	330 (inc. 209)	0.59	0.0490
600	503 (inc. 330)	0.46	0.0203
750	619.50 (inc. 503	0.52	0.0395
900	778 (inc. 619.50)	0.35	0.0382
1050	905.50 (inc. 778)	0.376	0.0315
1200	1020.50 (inc. 905.50)	0.280	0.0271
1350	1160.50 (inc. 1020.50)	0.164	0.0198
1500	1290 (inc. 1160.50)	0.110	0.010

From the 150 mL of pentanol that was added in the initial addition only 36 mL was collected. This may be due to the absorption of the pentanol into the sediment. From the 1.5 L of pentanol used in the extraction process, only 1290 mL was collected from the sediment; an indication of how much was absorbed into the sediment. Despite the fact that the sediment was filtered to dryness, to remove any additional pentanol added during the extraction process, at least 210 mL was unaccounted for due to absorption into the sediment. Bryostatin 1 has a characteristic uv-vis absorbance at 262 nm and chlorophyll at 660 nm. Table 1 shows the gradual decrease at both absorbance values, suggesting the removal of components of interest at these wavelengths.

Table 2. Solubility test of white powder (0.02 g) in various solvents

Solvents	Results
Hexane	Clear solution – powder settled at the bottom of the test-tube.
Pentanol	Solution turned cloudy – powder settled at the bottom of t-tube
Ethanol	Solution turned cloudy – powder settled at the bottom
Water	Solution turned cloudy – powder settled at the bottom
0.1M HCL	Solution turned cloudy – powder suspended in the acid
0.1M NaOH	Solution clear – powder completely dissolved in the base

Fig. 3. Image of the dried white foam collected from the pentanol-EDTA mixture.

In the pentanol-EDTA mixture, EDTA was used as a surfactant to remove any organic compounds bound to any metals present in the pentanol extract. Surfactants reduce the surface tensions of systems resulting in the foam (white powder) that was collected between both solvent layers (Fig. 1). A solubility test of the white powder from the pentanol-EDTA mixture was also carried out using various solvents (Table 2). The appearance of the white powder in hexane suggests that it has properties consistent with polar compounds; since hexane is non-polar, polar compounds are insoluble in non-polar solvents. In water and ethanol, two polar solvents, the powder formed a suspension making the solvent cloudy, suggesting polar properties; the non-polar components of the compound settled at the bottom of the test-tube. The solubility of the white powder in 0.1 M NaOH indicated that components of the powder could contain a mixture of carboxylic acids or compounds with carboxylic acid side chains.

The mass spectrum of the pentanol extract (Fig. 4) was compared to the powder (Fig. 5). The method shows the successful isolation of the compounds of interest. Further analysis to determine the mass accuracy for the peaks shown in (Fig. 5) proved difficult as the powder contained too many ions.

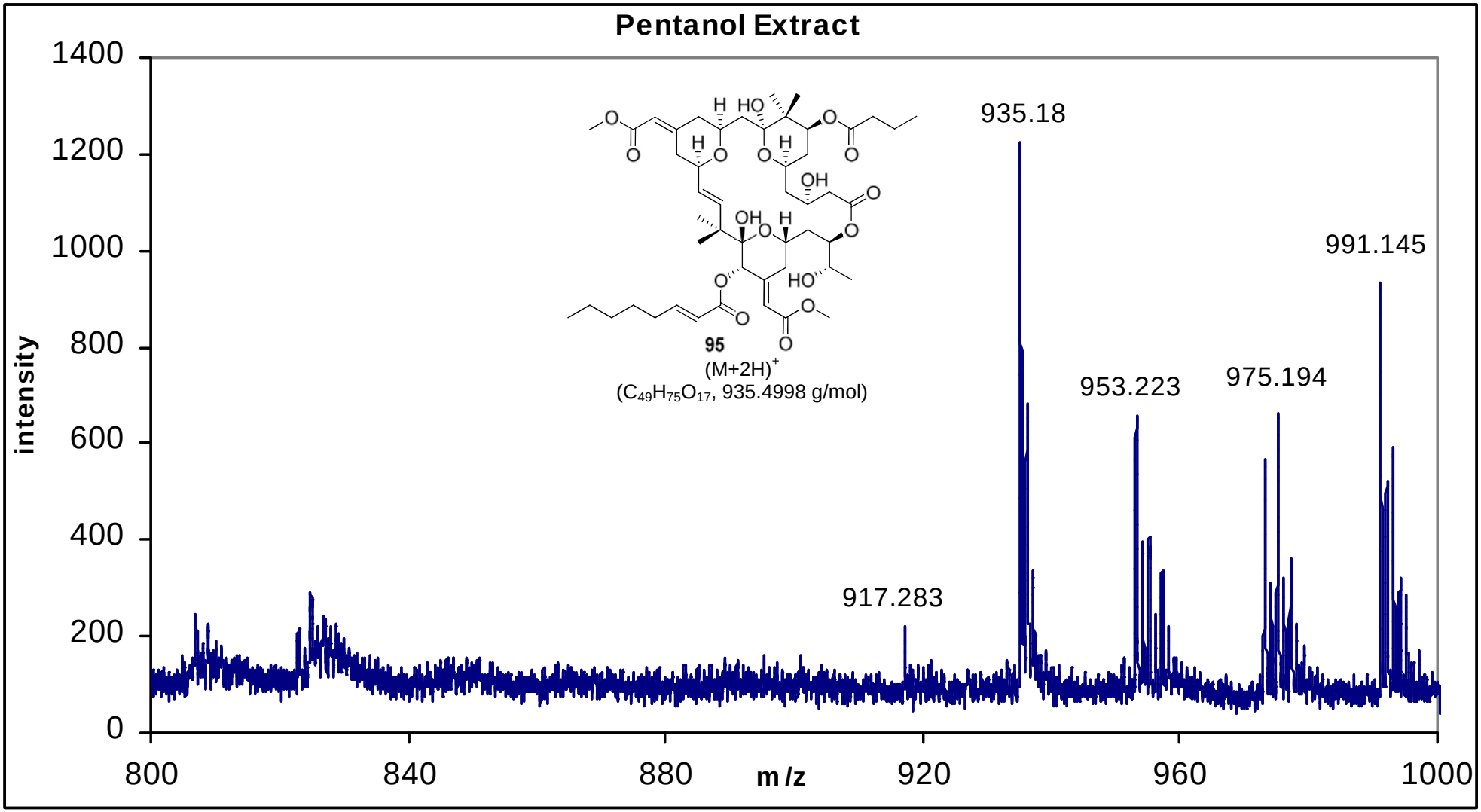

Fig, 4. Mass spectrum of the pentanol extract.

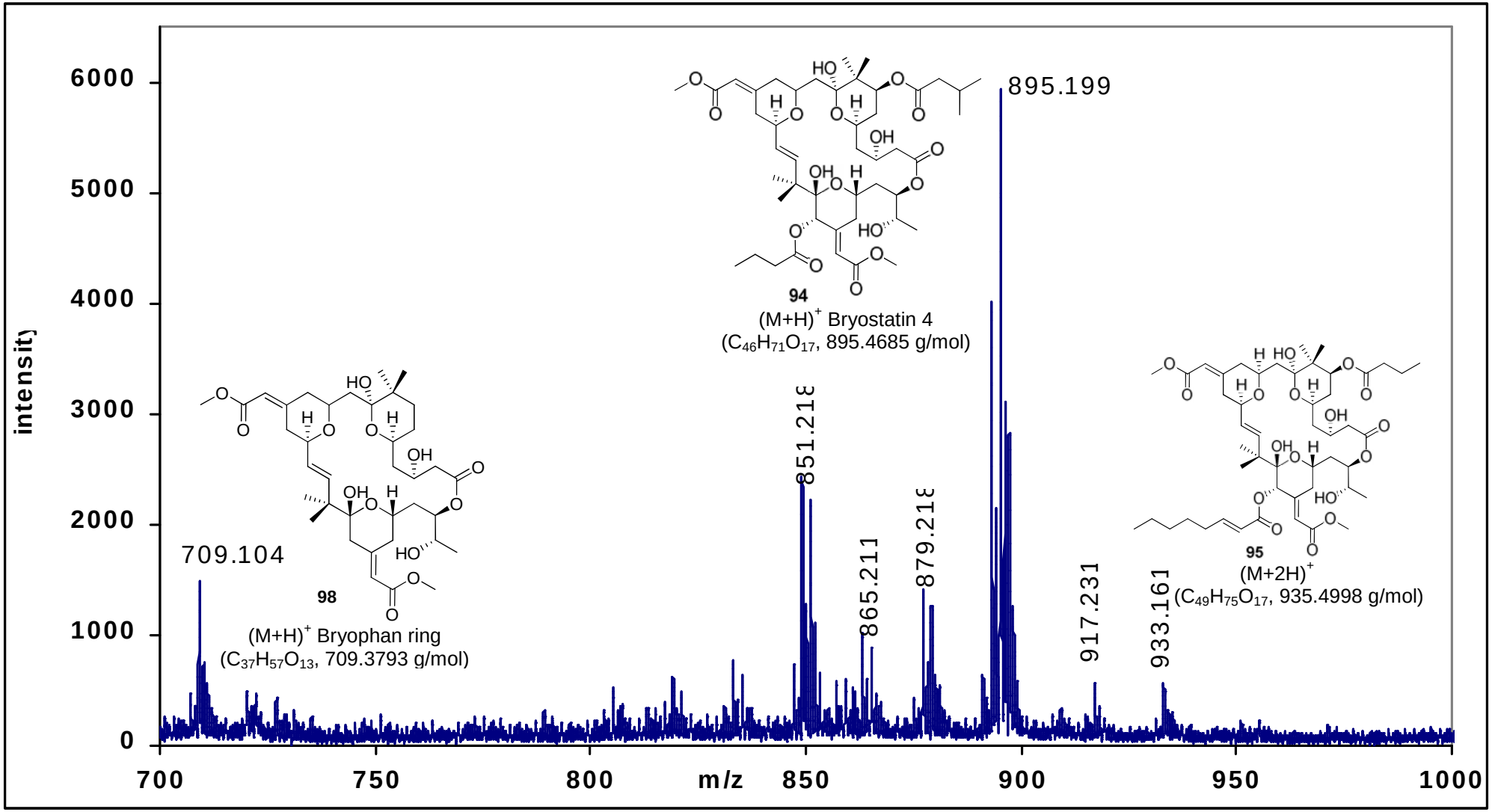

Fig. 5. Mass spectrum of the white powder in a positive ion test in TFA (trifluoroacetic acid).

Fig. 4 shows a peak at *m/z* 935 $(M+2H)^+$, and Fig. 5 shows two peaks at *m/z* 709 $(M+H)^+$ and *m/z* 895 $(M+H)^+$, all of which could suggestively be correlated to the bryostatin 12 **95** (M^+: $C_{49}H_{72}O_{17}$, 933.1032 g/mol), bryophan ring **98** (M^+: $C_{37}H_{56}O_{13,}$ 708.3715 g/mol) of the compound and bryostatin 4 **94** (M^+: $C_{46}H_{70}O_{17}$, 894.4607 g/mol), respectively. In Fig. 4 the peak at *m/z* 935 can be correlated to an $(M+2H)^+$ as this can generally occurs within the mass spectrometer.[17] This peak could therefore similarly correlate to bryostatin 12, as mentioned above. This suggests that the white powder may also contain organic compounds**.**

5.3.2 Sediment extraction (May 2006)

Data relating to the 10 fractions collected over a 3 wk period (section 5.3.1) is shown in Table 3. The pentanol extraction collected was analyzed (Fig. 6) and compared to the results of the white powder (Fig. 7).

Table 3. Pentanol collected and uv-vis data for each sample extraction.

Pentanol (mL)	Amt retrieved (mL)	Absorbance at 262 nm
150	38	0.8452
300	148 (inc. 33)	0.6050
450	289 (inc. 148)	0.4213
600	413 (inc. 289)	0.3713
750	558 (inc. 413)	0.2169
900	693 (inc. 558)	0.1941
1050	827 (inc. 693)	0.1386
1200	965.50 (inc. 827)	0.1259
1350	1088.50 (inc. 965.50)	0.0743
1500	1264 (inc. 1088.50)	0.0846

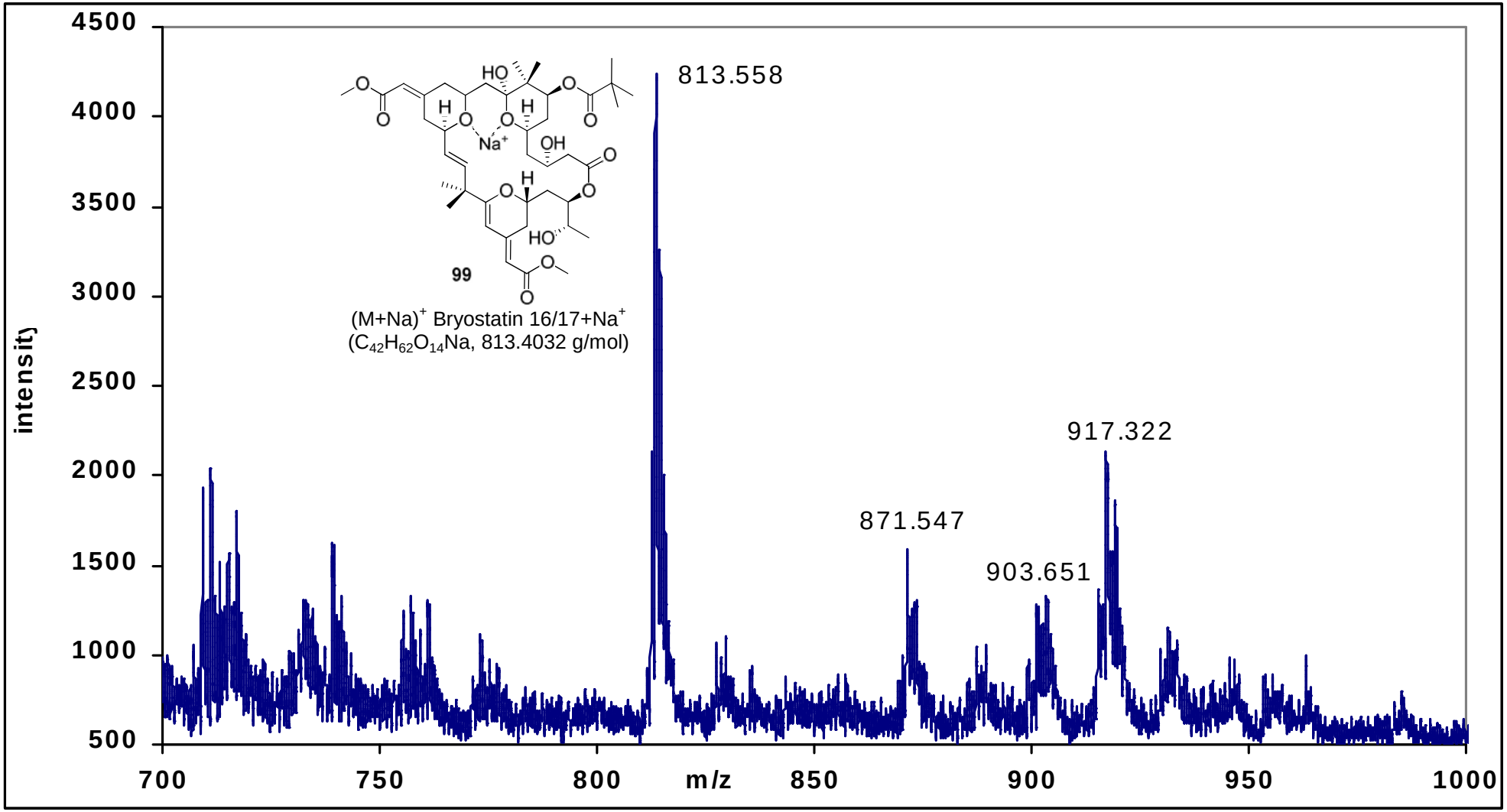

Fig. 6. MALDI-MS of pentanol extract (section 5.2.2).

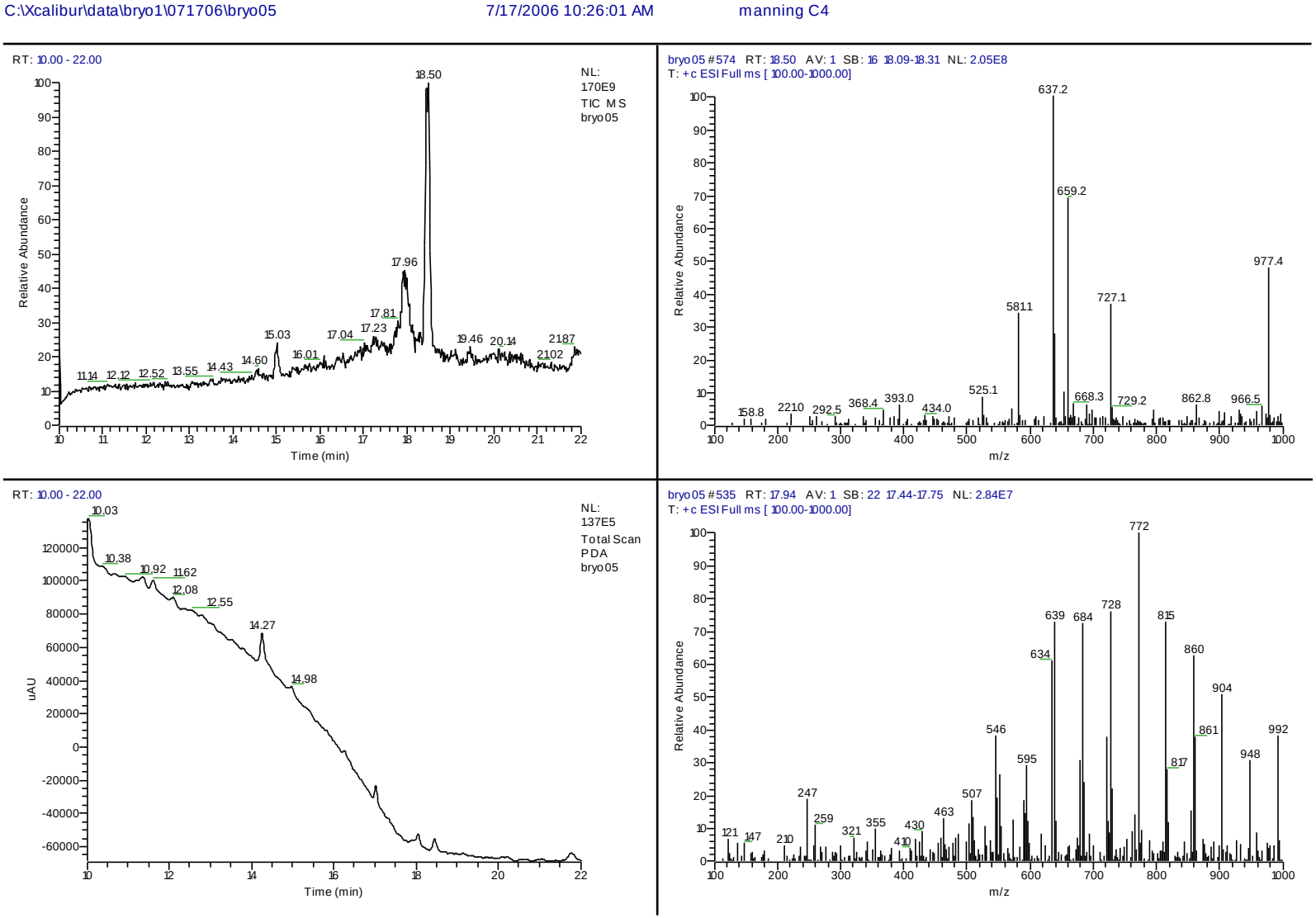

Fig. 7. LC-MS data of white powder from the sediment extraction (section 5.2.2).

The initial volume of pentanol seemed to be substantially absorbed by the dry sediment, with only 38 mL of pentanol removed after adding 150 mL originally. From the 1.5 L of pentanol added in total, 236 mL was absorbed into the sediment. Despite filtering to remove any additional pentanol, it was still retained within the sediment. The uv-vis absorbance values at 262 nm showed a decrease over time which suggests almost complete extraction from the sediment over the 3 wk period.

The peak at *m/z* 813 (Fig. 6), could be correlated to bryostatin 16/17+Na^+ **99** ($C_{42}H_{62}O_{14}Na$, 813.4032 g/mol). Aside from the possible bryostatin compounds shown in the data, Fig. 7 shows the presence of a polymer in the LC-MS with a consecutive loss of 44 g/mol. Polymers are large molecules consisting of repeated units. The consecutive loss of a species with *m/z* 44 correlates to the loss of a repeating unit from the polymer. It is suggested that the source of polymer found in the sediment extraction is due to specific bacteria in the sediment degrading polymer sources in the ocean, as shown by Pan *et al*..[18]

5.3.3 Sediment extraction (June 2006)

Table 4 shows the amount of pentanol that was added to the sediment, how much was collected, how often the extractions were taken and the uv-vis absorbance values suggestive of bryostatin 1. The white powder collected from the pentanol-EDTA layer in this extraction had dry weight of 5.41 g. Analysis of the pentanol extract (Fig. 8) shows two peaks at *m/z* 812.943 $(M+Na)^+$, *m/z* 903 $(M+Na)^+$ and *m/z* 787.486 $(M+Na)^+$ that could be correlated to bryostatin 16/17+Na^+ **99** ($C_{42}H_{62}O_{14}Na$, 813.4032 g/mol), bryostatin 8+Na^+ **94** ($C_{45}H_{68}O_{17}Na$, 903.4348 g/mol) and Bryostatin 11+Na^+-2H^+ **91** ($C_{39}H_{56}O_{15}Na$, 787.5311 g/mol) respectively.

Table 4. Data relating to the large scale pentanol extraction.

Date added	Pentanol added (mL)	Date removed	Amt retrieved (mL)	Uv-vis Abs. 260 nm
30/6/06	2000	4/7/06	1350	0.96906
4/7/06	1350	17/7/06	1125	1.5382
17/7/06	1125	6/8/06	1000	0.8198
6/8/06	1000	14/8/06	700	0.67905

A total of 5.5 L of pentanol was used in the extraction process and only 4.174 L was collected. A loss of 1.325 L is unaccounted for due to absorption into the sediment. Despite efforts to dry the sediment to remove any additional pentanol, only what is accounted for was collected. The final extraction showed an absorbance value of 0.6790 which did indicate that more pentanol could have been used to remove any additional components being absorbed during the extraction process. Bryostatin 1 has a distinctive uv-vis absorbance of 262 nm, and these results demonstrate a possibility of isolation. Many organic compounds have absorbance values similar to that of bryostatin; the absorbance value at 262 nm was merely used as a suggestive tool to show the isolation of organic compound(s) from the sediment.

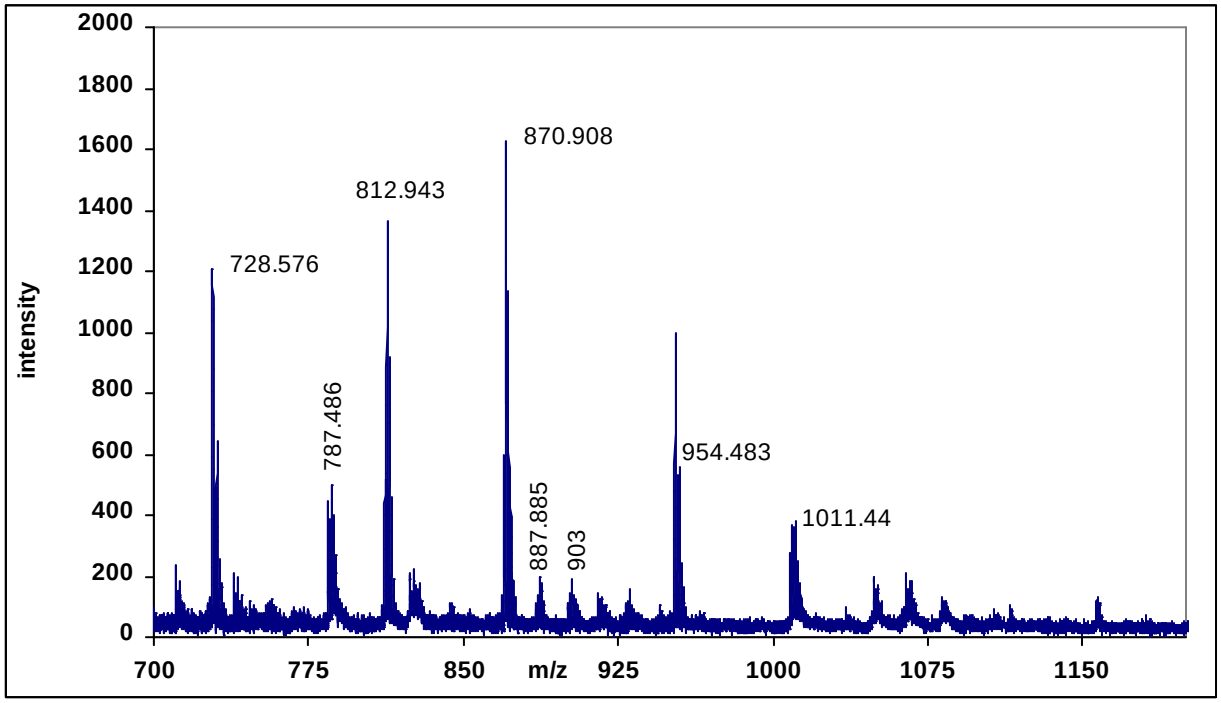

Fig. 8. MALDI-MS of sediment extract collected.

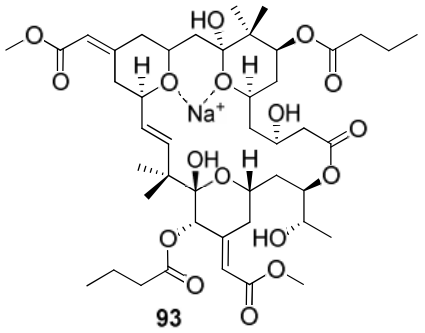

93

$(M+Na)^+$ Bryostatin 8+Na^+
($C_{45}H_{68}O_{17}$, 903.4348 g/mol)

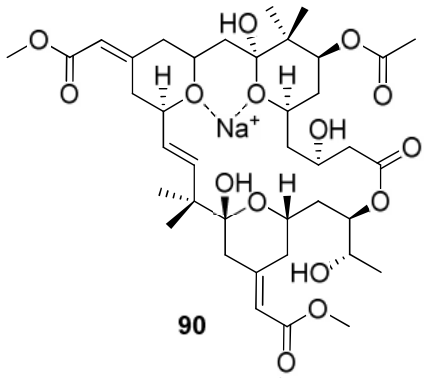

90

$(M+Na-2H)^+$
($C_{39}H_{56}O_{15}Na$, 787.3511 g/mol)

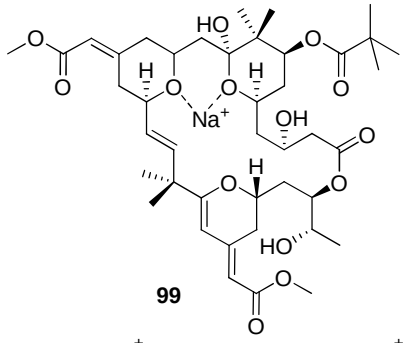

99

$(M+Na)^+$ Bryostatin 16/17+Na^+
($C_{42}H_{62}O_{14}Na$, 813.4032 g/mol)

5.3.3.1 Column chromatography

Results from both column chromatography techniques were unsuccessful in isolating the compounds from the liquid extract due to the high viscosity of the pentanol solvent. Despite the considerable volumes of solvent used to flush the column, traces of pentanol were always present in the final fraction collection.

The separating methods (basic alumina oxide and silica column chromatography) were efficient at separating the chlorophyll from the pentanol extract. However, due to the particulates and traces of pentanol still present in the final collections, alternative techniques were sought to establish a better method of extracting the compounds for further analysis.

The purpose of adding iron(III) chloride to the sediment extract collected (section 5.2.1), was to test whether compounds in the solvent would bind to iron(III), thus facilitating a separation from the solvent. Sodium hydroxide was used to make the solution basic, as a basic pH is needed for organic compounds to bind Fe^{3+}. Computational data to support this postulation is described in chapter 7.

Data from previous work has shown that bryostatin 1 has the capability to act as a siderophore by binding Fe^{3+}, forming a hexavalent complex. Taking into account the ability for this to occur, this method was expected to be a viable prospect for removing any possible bryostatin compounds from the pentanol solution. The extraction of doxorubicin using Fe^{3+} loaded 8-hydroxyquinoline bonded silica has been shown to be a suitable method for recovering the NP.[19] However, this promising method could not be used due to difficulties in preparing the column; hence, the formation of a bryostatin-Fe^{3+} complex, and subsequent separation, was not possible.

.5.3.3.2 Ionic liquids

Neither ionic liquid (Fig. 9 and 10) tested was shown to be suitable for the isolation of the bryostatins from the pentanol extract. The crystals formed when the ionic liquid-methanol mixture was cooled to -86°C were not analyzed, as high pressure liquid chromatography (HPLC) data showed that the compounds were still present when compared to the original pentanol solution.

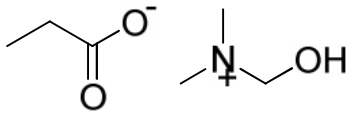

100

Fig. 9. The structure of the ionic liquid *N*-*N*-dimethylethanolammonium propionate.[20]

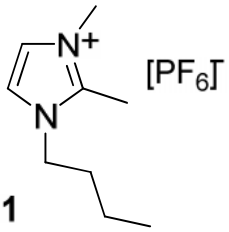

101

Fig. 10. The structure of the ionic liquid 1-butyl-2,3-dimethylimidazolium hexafluorophosphate.[20]

Ionic liquids are a relatively new method for substituting solvents with high volatility and immiscibility in water, *etc*.. The purpose of using ionic liquids in this work was to modify the charge of the compounds in the pentanol extract, resulting in a change in polarity. The most common ionic liquid, 1-butyl-2,3-dimethylimidazolium hexafluorophosphate **101** (Fig. 10), was used in an attempt to remove the organic compounds from the pentanol solution. The addition of water would make the compound hydrophobic, hence, facilitating collection via precipitation of the sample into the water layer, due to the change in polarity. However, the hydrophobic effect of the initial ionic liquid used was unsuccessful.

An alternative ionic liquid was chosen that would be immiscible in water, but not pentanol, and hence would allow easier removal of the bryostatin from the

sample. Using ionic liquids for natural product extraction has been shown to be a useful method when used for the extraction of artemisinin.[21,22] The extraction of artemisinin using hexane was compared to the ionic liquids *bis* (methoxyethyl)ammonium *bst* (bistrifluoromethylsulfonamide) and dimethylethanol ammonium octanoate. The ionic liquid method was shown to be four times better than hexane for the extraction of artemisinin.[21]

As this technique proved successful for artemisinin, its application was also considered; however, the results realized minor flaws. The second ionic liquid was also unsuccessful in removing the compounds from the pentanol extract. The major disadvantage of using ionic liquids is that each ionic liquid is specific towards particular compounds, therefore determining the most suitable salt for liquid-liquid isolation of compounds in the pentanol extract would be both time consuming and costly. In effect, the most suitable salt could only be determined if the supply company themselves conducted the study.[20]

5.3.4 Sediment extraction (June 2008)

The ecosystem of *Bugula* contains high levels limestone, hence acid (0.1 M HCL) was added to the sediment to remove any excess calcium carbonate. Previous study by Manning *et al*.,[23] noted the presence of numerous carboxylic acids in the ecosystem where *Bugula* is found; 0.1 M NaOH was therefore used to remove any carboxylic acids in the sediment. The use of EDTA **102** for processing the samples was to remove any metals present. EDTA is an iron chelating agent used to complex metals such as Ca^{2+}, Zn^{2+} and Fe^{3+} (Fig. 11).[24] The crystals collected from the raw extraction had a dry mass of 14.28 g and the crystals collected from the processed extraction had a dry mass of 3.95 g. Mass spectral results from both extractions are shown in Fig. 12.

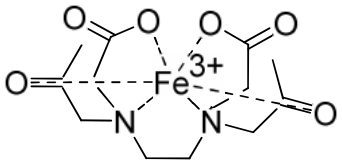

102

Fig. 11. The iron chelating agent EDTA bound to Fe^{3+} ion.

Despite the fact that the concentration of acid, used as a preparative step, was not high, it is difficult to state whether the addition of acid did impact the compound, *e.g.* by subsequently reducing the percentage of bryostatin compounds extracted from the sediment fractions. It is impossible to fully disprove that the addition of HNO_3 had any effect on instigating the degradation of bryostatin compounds present in the samples. The lack of any bryostatin compounds in either batches of sediment precludes any evidence of samples being compromised. However, comparison of the peaks shown in the uv-vis chromatogram of both sediment samples (Fig. 12a) shows the overlap of three different peaks at retention times of 15.7 to 16.3 min, 18.4 to 19.3 min and 19.4 to 19.9 min, respectively.

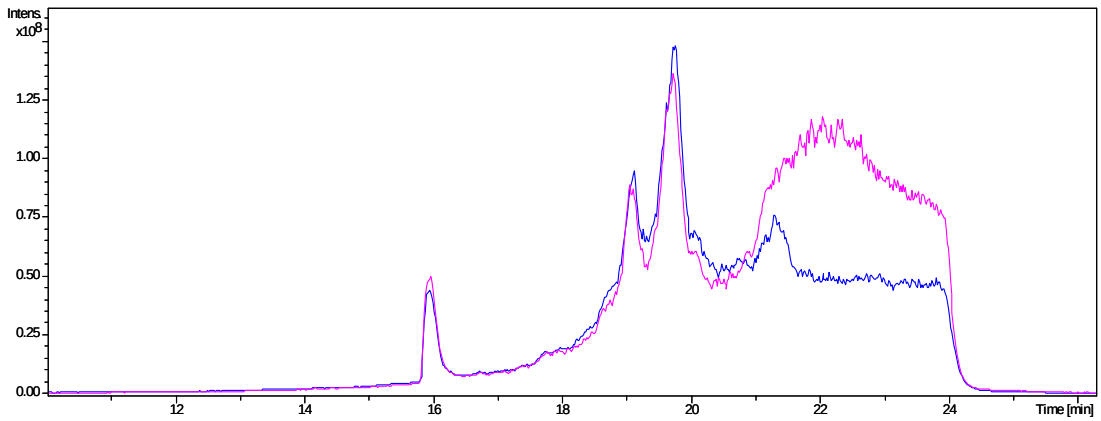

Fig. 12a. LC-MS. chromatograms demonstrating correlation between processed (blue) and raw (pink) sediment extracts from Alligator Point, Fl.

The overlapping peak at a RT of 15.7-16.3 min (Fig. 12a) shows the same mass correlation (Fig. 12b), suggesting that the addition of acid for the processed extraction of the sediment did not compromise that particular compound.

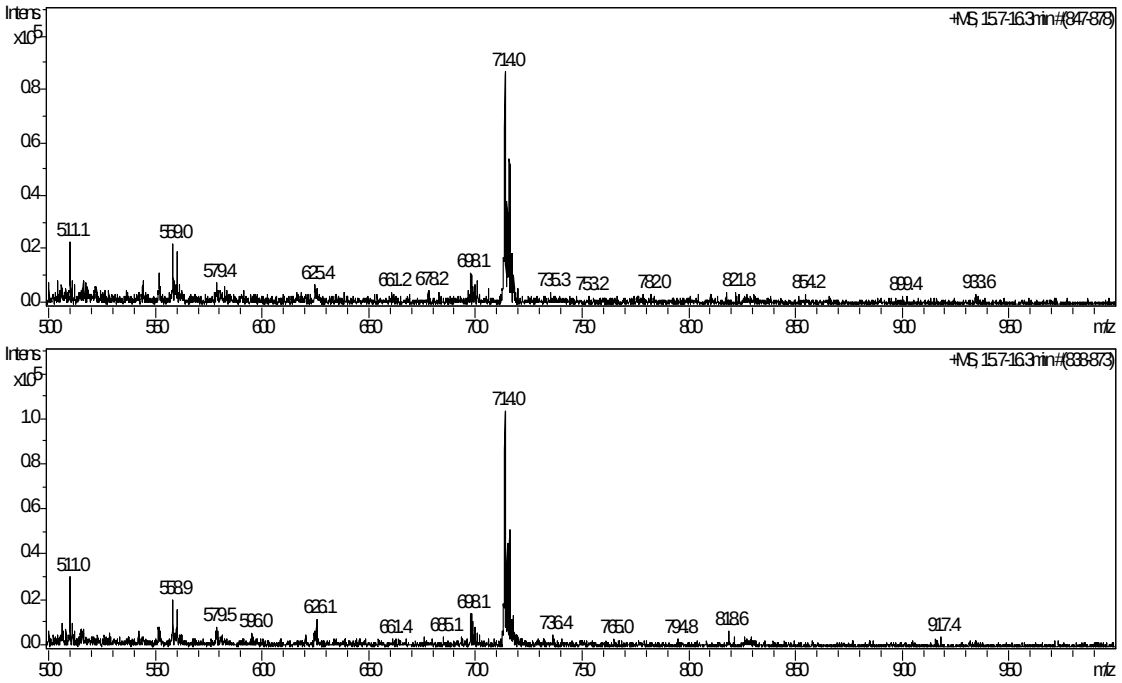

Fig. 12b. Mass spectra of the peak at RT 15.7 to 16.3 min (Fig. 12a). The first mass spectrum shows processed sediment extract the second mass spectrum shows the raw sediment extract.

The overlap of the peak at a RT of 18.9 to 19.3 min implies the presence of polymers in the sample, showing the consecutive loss of *m/z* of 44 g/mol. Both mass spectral peaks (Fig. 12c) show a correlation in the polymers present. The presence of polymers in the sediment can be expected due to the degradation of polymer based material in the ocean by bacteria.[19] However, a slight difference between both spectra, due to the presence of other peaks that are only seen in the processed sample versus the raw sediment extract (Fig. 12c). In Fig. 12c the peaks at *m/z* of 763, 786, 899 and 907 are all observed in the processed sediment but not seen in the raw extraction process; however, none of the peaks have any correlation to any of the bryostatins.

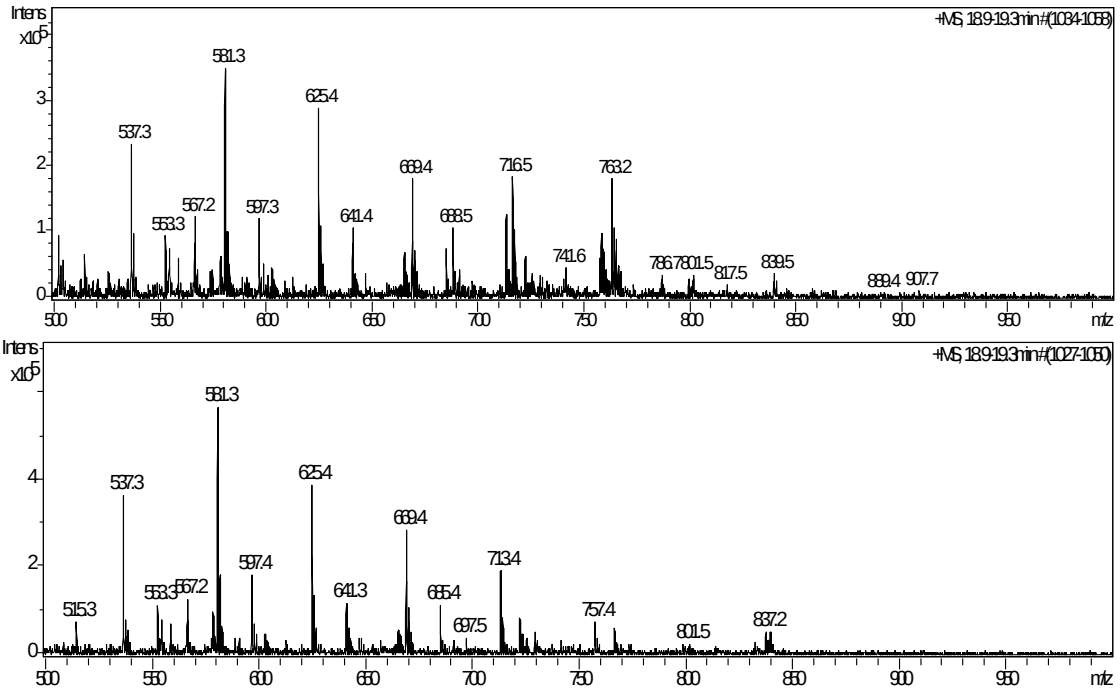

Fig. 12c. Mass spectra of the peak at RT of 18.9 -19.3 min (Fig. 12a). The first mass spectrum shows processed sediment extract the second mass spectrum shows the raw sediment extract.

Fig. 12d points to the presence of polymers in both sediment samples, showing the consecutive loss of *m/z* of 44 g/mol. Other peaks seen in both samples were not analyzed, as none suggested the presence of bryostatin compounds. The presence of these peaks in the processed sample and not the raw sediment may be due to the formation of by-product compounds. This suggests that the processing of the sediment may indeed have some impact on other unidentified compounds in the sediment.

The broad peak, between 20-23 min in the uv-vis chromatogram in Fig. 12a, suggests the presence of various compounds in the extracts as shown below, including the peak at *m/z* of 803; while the processed sediment shows a distinct peak with a *m/z* of 803 while the (Fig. 12e).

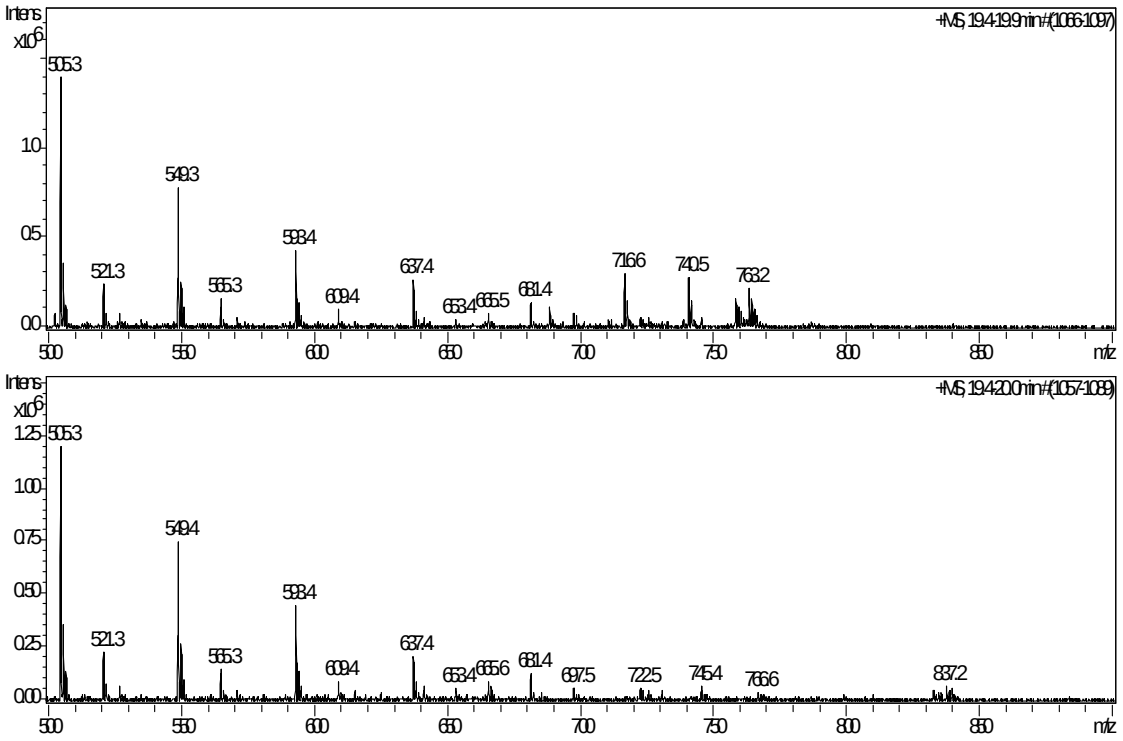

Fig. 12d. Mass spectra for peak at RT of 19.4-19.9 min, (Fig. 12a). The first mass spectrum shows processed sediment extract the second mass spectrum shows the raw sediment extract.

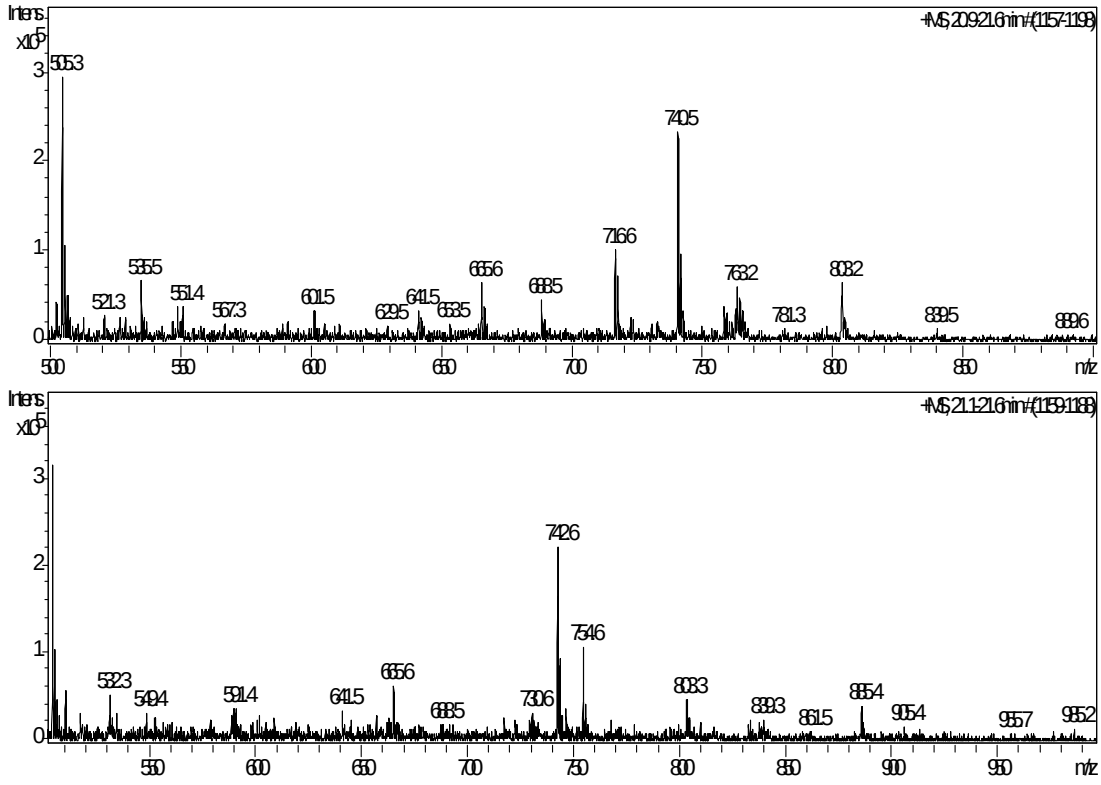

Fig. 126. Mass spectra for peak at RT of 20-23 min, (Fig. 12a). The first mass spectrum shows processed sediment extract the second mass spectrum shows the raw sediment extract.

The results from all the extractions were optimistic in demonstrating that sediment found in the *Bugula* environment could be an alternative source for obtaining bryostatin compounds economically in larger quantities. The extractions collected, and white powder removed, from the extracts all showed peaks that are possible correlations to several bryostatin compounds. The result from extraction of sediment for the isolation of other NPs has also been successful in other published studies. This method can be optimised to provide another innovative and efficient means of obtaining marine natural products.

5.4 Conclusion

In conclusion it can be stated that:

1) The sediment extractions showed a strong indication of the isolation of compounds that could be correlated to various bryostatin compounds. However, due to low detection levels, no conclusive evidence could be obtained to support or disprove the postulations.

2) Many of the mass spectral peaks identified in the sediment extraction were also seen when artificial media and surfaces for the isolation of such compounds from the ecosystem of *Bugula neritina* were investigated. (described in previous chapters).

3) The consistency in data from all the analyses carried out strongly suggests some correlation between the marine organisms collected in the environment where *Bugula* is found, and the marine bacterium believed to be responsible for the production of the bryostatins.

5.5 References

[1] R. Jaffe, A. I. Rushdi, P. M. Medeiros, and B. R. T. Simoneit. *Chemosphere*, 2006, **64(11)**, 1870-84.

[2] G. Mille, M. Guiliano, L. Asia, L. Malleret, and N. Jalaluddin. *Chemosphere*, 2006, **64(7)**, 1062-73.

[3] D. Acevedo-Figueroa, B. D. Jiménez, and C. J. Rodríguez-Sierra. *Environ. Pollut*., 2006, **141(2)**, 336-42.

[4] M. J. Simpson, B. Chefetz, A. P. Deshmukh, and P. G. Hatcher. *Mar. Environ. Res*., 2005, **59(2)**, 139-63.

[5] M. Giltrap, A. Macken, B. McHugh, R. Hernan, K. O' Rourke, E. McGovern, B. Foley, and M. Davoren. *Chemosphere*, 2009, **76**, 357-64.

[6] Q. Zhou, K. Li, X. Jun, and L. Bo. *Bioresour. Technol.*, 2009, **100(16)**, 3780-86.

[7] P. Trivedi, A. Pandey, and L. M. S. Palni. *Microbiol. Res.,* 2008, **163(3)**, 329-36.

[8] M. F. Adesina, A. Lembke, R. Costa, A. Speksnijder, and K. Small. *Soil Biol. Biochem*., 2007, **39(11)**, 2818-28.

[9] T. J. Manning, E. Rhodes, M. Land, R. Parkman, and A. G. Marshall. *Nat. Prod. Res*., 2006, **20(6)**, 611-28.

[10] Z. Cetecioğlu, B. K. Ince, M. Kolukirik, and O. Ince. *Mar. Pollut. Bull.*, 2009, **58(3)**, 384-95.

[11] T. J. Manning, M. Land, E. Rhodes, L. Chamberlin, J. Rudloe, D. Phillips, T. T. Lam, J. Purcell, H. J. Cooper, M. R. Emmett, and A. G. Marshall. *Nat. Prod. Res*., 2005, **19(5)**, 467-91.

[12] J. M. Hill. *J. Chromatogr*., 1973, **76(2)**, 455-58.

[13] M. T. W. Hearn, and M. Zachariou. *J. Chromatogr*., 1992, **599(1-2)**, 171-77.

[14] G. Absalan, M. Akhond, and L. Sheikhian. *Talanta*, 2008, **77(1)**, 407-11.

[15] K. Gustafson, M. Roman, and W. Fenical. *J. Am. Chem. Soc*., 1989, **111(19)**, 7519-24.

[16] J. S. Martinez, G. P. Zhang, P. D. Holt, H. T. Jung, C. J. Carrano, M. G. Haygood, and A. Butler. *Sci*., 2000, **287(5456)**, 1245-47.

[17] Hillenkamp, F., and J. Peter-Katalinić. MALDI MS: A practical guide to instrumentation, methods and applications. Wiley-VCH, 2007.

[18] L. Pan, J. G. Gu, B. Yin, and S. P. Cheng. *Int. Biodeterior. Biodegradation*, 2009, **63(1),** 24-29.

[19] E. Vandervlis, H. Irth, U. R. Tjaden, and J. Vandergreef. *Anal. Chim*., 1993, **271(1)**, 69-75.

[20] http://www.bioniqs.co.uk/ (June 21st 2009).

[21] http://www.mmv.org/IMG/pdf/Extraction_Ionic_Liquids.pdf (June 21st 2009).

[22] A. A. Lapkin, P. K. Plucinski, and M. Cutler. *J. Nat. Prod*., 2006, **69(11)**, 1653-64.

[23] T. J. Manning, T. Umberger, S. Strickland, D. Lovingood, R. Borchelt, M. Land, D. Phillips, and J. C. Manning. *Int. J. Environ. Anal. Chem.*, 2003, **83(10)**, 861-66.

[24] W. B. Xia, H. Gao, X. H. Wang, C. H. Zhou, Y. G. Liu, T. Fan, and X. Wang. *J. Hazard. Mater.*, 2009, **164(2-3)**, 936-40.

CHAPTER 6

Naturally occurring esterification reactions and hydrolysis of bryostatin 1

6.1 Introduction

Since the isolation of bryostatin 1 **9a** in the 1980s, nineteen other bryostatin compounds have been isolated from the marine organism, as shown by Manning *et al.*, believed to be responsible for the production of the natural product.[1] Each bryostatin compound differs by the different R_1 and R_2 groups as shown in (Fig. 1). Many of the bryostatin compounds have been found in specific locations around the world. For example, bryostatin 4 is extracted from *Bugula* found in the Gulf of Mexico, Gulf of California and Gulf of Sagami.[2] Bryostatin 12 and 13 are extracted from *Bugula* collected off the Eastern Pacific Ocean.[3]

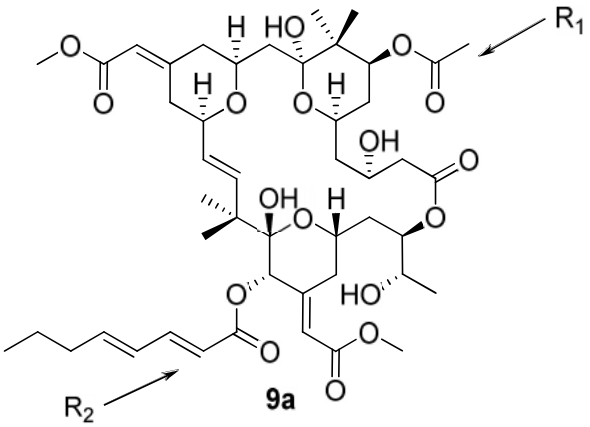

Fig. 1. Bryostatin 1 ($C_{47}H_{68}O_{17}$, 904.4451 g/mol) has two variable groups on the bryophan ring, an acetate group at R_1 and a C_8 group at R_2, which distinguishes the twenty bryostatin compounds that have been isolated from *Bugula*.

Several studies by Haygood *et al*., have collected data suggesting the true source of the NP to a specific bacterium found in the marine organism.[4,5,6,7] This group has also suggested that the different types of bryostatins are suggestively related to the different types of bacterial genetics found in the marine organism.[6] From all the bryostatins that have been isolated, bryostatin 1 has shown to be the most efficient medicinal agent. Bryostatin has been in over thirty phase I and II clinical trials for various cancers such as kidney, prostate, breast and ovarian cancer; and it is currently being looked at as a possible treatment for Alzheimer's

Disease.[8] Bryostatin 1 has shown much efficacy as a medicinal agent *in vitro*; however, it fails slightly as an efficient agent *in vivo*.

In this study, it is suggested that the different bryostatin compounds can be derived by naturally occurring esterification reactions rather than species dependency or bacterial genetics. Many carboxylic acids, such as octanoic acid (OA), exist in the marine environment; for this reason, OA was selected.[9] The esterification or reverse ester reactions of bryostatin 1 ($C_{47}H_{68}O_{17}$) and OA ($C_8H_{16}O_2$) as reactants, were used to determine the possible derivatization of different bryostatin compounds.[10] Results suggested that larger compounds ([bryo]-$(C_8H_{16}O_2)_x$ where x = 1, 2, 3 etc.) can form by reacting OA with bryostatin 1, under various conditions.

Due to the different configurations possible as a result of the esterification and reverse reactions, the hydrolysis of bryostatin 1 was also analysed. Different media were prepared to determine the impact of hydrolysis on the ester bonds on the bryophan ring. This determination is vital, first since bryostatin 1 is extracted from an aquatic environment and second due to its potential *in vivo*. This may help with understanding and determining the impacts of bryostatin 1 when administered *in vivo*; and whether or not the concentration of bryostatin compounds would be initially higher than currently measured, due to prolonged exposure to water after the organism is harvested.[9]

6.2 Experimental

6.2.1 Hydrolysis of bryostatin 1

The hydrolysis of bryostatin 1 was conducted using uv-vis, to determine the kinetics of the mixture, by measuring the absorbance values over a designated time

period. Bryostatin 1 (20 µg, B-7431, Boston, Massachusetts) was dissolved in 1.5 mL of pentanol (Fisher Scientific) and, over a two day period, the uv-vis absorption was measured 3 times a day. On the third day, 50 µL of RO (reverse osmosis) water was added to the pentanol sample. Absorbance values of the mixture were measured every 3 min for 4 hr, after which it was measured every 5 min for 1 hr, then every 10 min for another hour. After a total of 6 hr, the absorbance was measured every 3-5 hr to ensure that the reaction had gone to completion.

6.2.2 Esterification of bryostatin 1

Bryostatin 1 (10 µg, B-7431, Boston, Massachusetts) stored at 4°C was later diluted in 20 mL anhydrous ethanol (A405-20, Fisher Scientific). Different samples were prepared containing OA (167261000, Acros Organics stock), 0.1 M NaOH (SS276-1, Fisher Scientific), 0.1 M HCL (SA45-1, Fisher Scientific), $FeCl_3 6H_2O$ (I-88, Fisher Scientific) and 18 Mohm RO water.

Six sets of samples containing bryostatin 1 were prepared, three containing Fe^{3+} and three without Fe^{3+}. Each set contained six samples: 1). octanoic acid and bryostatin, 2). OA, a base and bryostatin 1, 3). OA, an acid and bryostatin 1, 4). bryostatin 1 only, 5). a base and bryostatin 1, 6). an acid and bryostatin 1. With the first batch of three sets; the first set was placed in the dark at ambient conditions (22-24°C) for 96 hr, the second set was placed under an ultraviolet lamp for 24 hr and the third set of samples was placed in an oven at 37°C for 48 hr. The same conditions outlined above were used for the second batch of three sets of samples containing iron(III) chloride respectively. All samples were stored at 4°C after the experiments were conducted, until they could be analyzed.

Analysis was achieved by MALDI TOF-MS, University of Georgia Mass Spectrometry Facility (Athens, Georgia, USA). LC-MS data was obtained from the US Dept. of Agriculture, Tifton (GA, USA) and the University of Sunderland (Sunderland, UK).

6.3 Results and Discussion

6.3.1 Hydrolysis of bryostatin 1

After two day in pentanol, no change in the absorbance measurements was observed. However, after 50 µL of water was added, the characteristic spectral feature for bryostatin 1 (wavelength = 262 nm) started to decrease at a constant rate, with most of the change occurring during the first couple of hours. This constant decrease for the first hr is shown in (Fig. 2). This decomposition or reduction in the concentration of the bryostatin 1 can be correlated to mass spectral data (Tables 1-4). The concentration and absorbance intensity of the hydrolysis of bryostatin, is expressed as a function of the initial concentration of bryostatin 1, over the three day period, is shown (Fig. 2).[10]

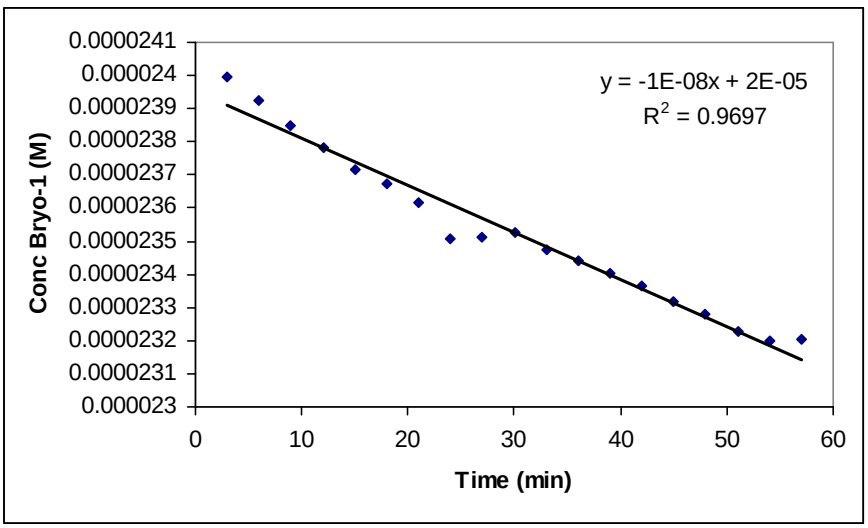

Fig. 2. The uv-vis absorbance of bryostatin 1 showing its hydrolysis in aqueous pentanol.

The purpose of looking at these substitutions was to show that bryostatin 1 does break down in its marine environment and/or in the body, resulting in the smaller, more stable bryophan structure, which could explain its performance *in vivo*. The use of water as part of the solvent, as shown in Table 1, resulted in the increased degradation of the compound into several smaller molecular weight species 927 g/mol as shown below. For example, the loss of the carboxylate group ($C_8H_{15}OO^{\cdot}$) results in the *m/z* of 787 $(M+Na-2H)^+$ **90** as shown in Table 1. The peak at *m/z* 867 $(M+H)^+$ **104**, suggests the displacement of the acetate group with a hydroxyl group at the R_1 position and the hydrogenation of the carboxylate group at the R_2 position on bryostatin 1. The peak at *m/z* of 909 $(M+Na-H_2O)^+$ **105**, as suggested is the loss of H_2O from bryostatin 1+Na^+ adduct **9b** (927-H_2O, 909 g/mol).

Table 1. LC-MS analysis of bryostatin 1 standard, in different matrices, at a retention time of 18.5 min. (± 0.1 min). The letters in superscript represent the structure that correlates with the highlighted peaks as shown in Fig. 3 below.

Sample	Solvent	Additional additives	Peaks observed m/z
Standard	Methanol/formic acid	-	851, **867**$^{(b)}$, **909**$^{(d)}$, **927**$^{(c)}$
1	95% ethanol, 5% water	-	581, 637, 659, 695, 727, 752, 768, **787**$^{(a)}$, 809, 865, **867**$^{(b)}$, 896, **927**$^{(c)}$, 978
2	32% ethanol, 68% water	0.0075 M HCl	581, 637, 659, 729, 753, **867**$^{(b)}$, **909**$^{(d)}$, 949, 985
3	32% ethanol, 68% water	0.1% Instant Ocean	581, 637, 659, 727, **787**$^{(a)}$, **867**$^{(b)}$, **909**$^{(d)}$, **927**$^{(c)}$, 978, 993
4	32% ethanol, 68% water	0.1 % $FeCl_3$	581, 637, 659, 727, **787**$^{(a)}$, 814, 829, **867**$^{(b)}$, 869, **909**$^{(d)}$, **927**$^{(c)}$, **957**$^{(e)}$, 978
5	32% ethanol, 67% pentanol, 1% water	0.1% Instant Ocean	581, 637, 659, 727, 779. **787**$^{(a)}$, **867**$^{(b)}$, **909**$^{(d)}$, **927**$^{(c)}$, **957**$^{(e)}$, 979
6	32% ethanol, 36% water, 32% pentanol	Small piece of *Bugula neritina* (calcified surface)	581, 637, 659, 727, 779. **787**$^{(a)}$, **867**$^{(b)}$, **909**$^{(d)}$, **927**$^{(c)}$, **957**$^{(e)}$, 979

(a)

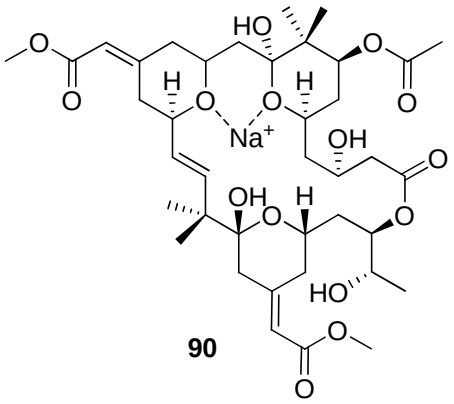

90

Bryostatin 11+Na $(M+Na-2H)^+$
($C_{39}H_{56}O_{15}Na$, 787.3511 g/mol)

(b)

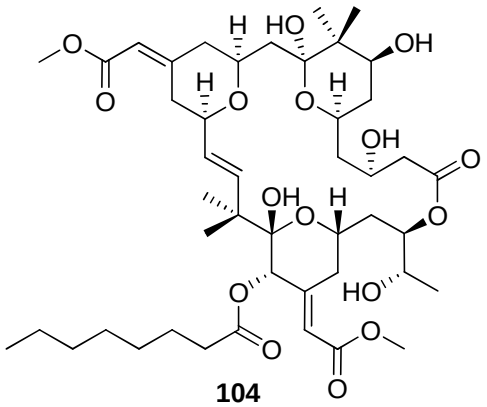

104

$(M+H)^+$
($C_{45}H_{71}O_{16}$, 867.4736 g/mol)

(c)

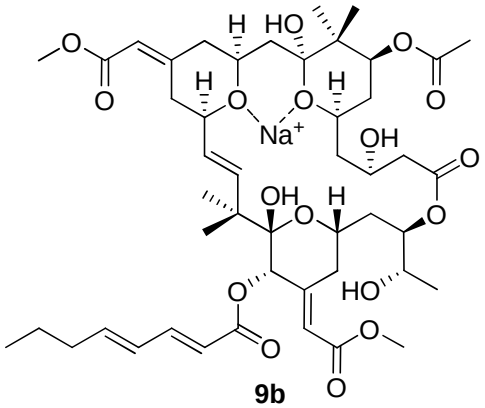

9b

Bryostatin 1 $(M+Na)^+$
($C_{47}H_{68}O_{17}Na$, 927.4348 g/mol)

(d)

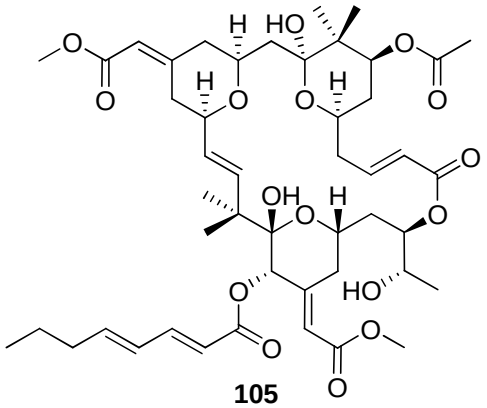

105

Bryostatin 1 $(M+Na-H_2O)^+$
($C_{47}H_{66}O_{16}Na$, 909.4243 g/mol)

(e)

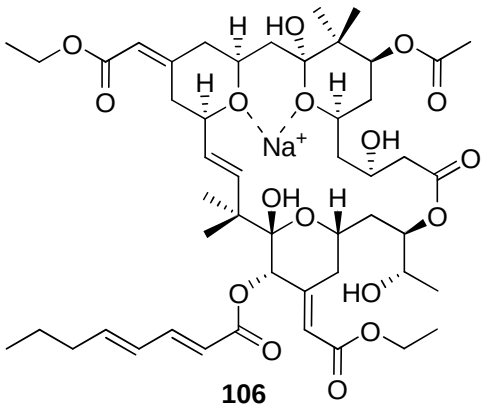

106

$(M+Na+2H)^+$
($C_{49}H_{74}O_{17}Na$, 957.4818 g/mol)

Fig. 3 a-e. The degradation of bryostatin 1 dissolved in different solvents correlating with consistent peaks within each. The formation of larger molecular specie is also shown in 3e.

This impact on bryostatin 1 as a medicinal agent is emphasized considering that the human body consists of approximately 70% water. The half-life of the drug in the blood stream (0.81 hr) should be considered a critical measurement to better understand its potential in the body.[11,12] The decrease in absorbance appeared to be proportional to the decrease in the concentration values of bryostatin 1.

An additional experiment, using bryostatin 1 standard exposed to water was conducted under various conditions, (pH and ionic strength) and then analyzed by LC-MS (Table 1). A number of smaller molecular species were observed in all samples, suggesting that ester bonds may be a key element in the hydrolysis, or reverse esterification reactions, of bryostatin compounds when placed in water or hydrophilic solutions. These observations could be significant for medicinal and harvesting/extraction applications.[9,10] For example, bryostatins have been identified in marine sediment from the *Bugula* ecosystem located in the Gulf of México, suggesting that the marine bacteria that produce the bryostatins reside there.[1] Molecular species measured from this environment,[1] show some consistency with the *m/z* masses outlined in Table 2.

6.3.2 Esterification of bryostatin 1

The tables below summarize the peaks identified in all the samples that were analyzed. Additional spectra of the samples analyzed can be found on the enclosed DVD. Bryostatin 1 (Fig. 4) has numerous ester bonds, making the compounds unstable and prone to degradation or hydrolysis reactions. This makes the molecule susceptible to cleavage under various conditions and the possibility of esterification reactions to occur.[13] For most samples (Tables 2-5), the mass spectral features

show both a degradation of bryostatin 1 to smaller species (*m/z* < 927) and the formation of larger species.

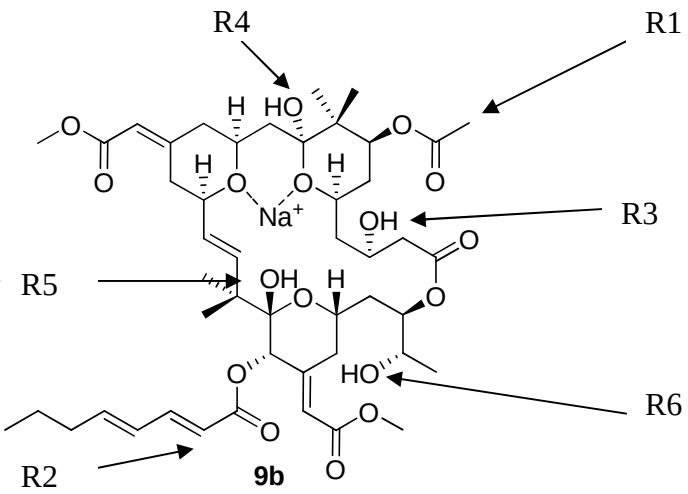

Fig. 4. Bryostatin 1 + Na^+ adduct **9b** ($C_{47}H_{68}O_{17}Na$, 927.4348 g/mol). R represents the possible sites where substitution reactions may occur in the presence of OA, forming ester bonds.

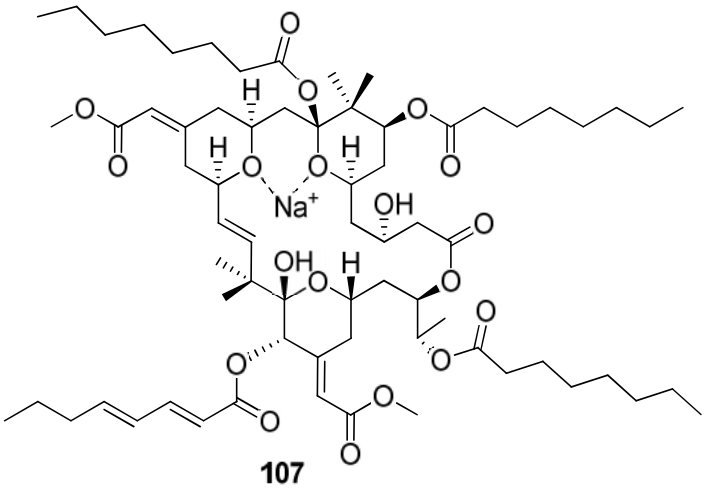

Fig. 5. Multiple substitution of the bryophan ring by OA produces much larger molecular species, for example (Table 2, 3(a, b) $(M+Na)^+$ $C_{69}H_{112}NaO_{19}$, 1267.7690 g/mol) **107**.

Table 2. Values (*m/z*) for bryostatin without Fe $^{3+}$. The numbers in brackets after the masses (e.g. 789(1)) correspond to peak numbers in Tables 4 and 5.[10] Examples of suggestive structures for the highlighted peaks shown in below.

Condition	Sample[a] (*m/z*)	Sample[b] (*m/z*)	Sample[c] (*m/z*)	Sample[d] (*m/z*)	Sample[e] (*m/z*)	Sample[f] (*m/z*)
1. No light	**789(2)**, **809(4)**, 847(7), 978(16), 998(18), 1196(24), 1267(26)	**789(2)**, **809(4)**, 927(11), 978(16), 998(18), 1267(26)	**789(2)**, **796 (3)**, 909(10), 972 (15) 998(18), 1007(19), 1057(21), 1196 (24)	**789(2)**, **809(4)**, 998(17), 1057(21)	**789(2)**, **809(4)**, 847(7), 978(16), 1057(21), 1267(26)	909 (10), 927(11), 956(14), 1007(19), 1026(20)
2. UV lamp	**789(2)**, **796 (3)**, **809(4)**, 927(11), 998(18), 1007(19), 1196(24)	**789(2)**, **796 (3)**, 874 (8) 932(12), 1007(19)	**789(2)**, 927(11), 978(16), 1007(19), 1026(20), 1233(25), 1141(23)	**789(2)**, **809(4)**, 824(5), 847(7), 889(9), 927(11), 978(16), 998(18)	**789(2)**, **809 (4)**, 927(11), 998(18), 1267 (26)	727(1) 847(7), 889(9), 927(11), 1141(23)
3. 37°C	**789(2)**, **809(4)**, 847(7), 927(11), 998(18), 1057(21), 1267(26)	**789(2)**, 847(7), 982(17), 998(18), 1196(24), 1267(26)	**796 (3)**, **809 (4)**, 889(9) 927(11),	**789(2)**, 847(7), 927(11), 978(16), 998(18), 1007(19) 1057 (21)	**789(2)**, 874 (8) 932(12), 978(16), 1141(23)	**789(2)**, 825(5), 927(11), 978(16), 1026(20), 1057(21)

[a] $5.52*10^{-7}$ M bryostatin 1, $1.53*10^{-4}$M OA.
[b] $5.52*10^{-7}$ M bryostatin 1, $2.38*10^{-3}$M HCl, $1.5*10^{-4}$M OA.
[c] $5.52*10^{-7}$ M bryostatin 1, $2.38*10^{-3}$M NaOH, $1.5*10^{-4}$M OA.
[d] $5.52*10^{-7}$ M of bryostatin 1.
[e] $5.52*10^{-7}$ M bryostatin and $2.44*10^{-3}$M HCl.
[f] $5.52*10^{-7}$ M bryostatin and $2.44*10^{-3}$M NaOH.

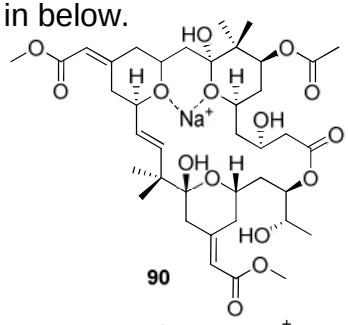

Bryostatin 11 + Na^+
($C_{39}H_{58}O_{15}Na$, 789.3667 g/mol)

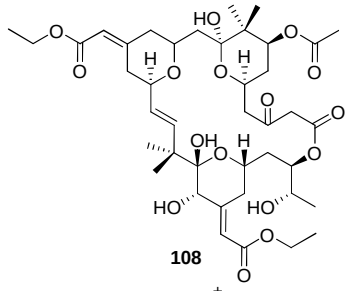

$(M+H)^+$
($C_{41}H_{61}O_{16}$, 809.3954 g/mol)

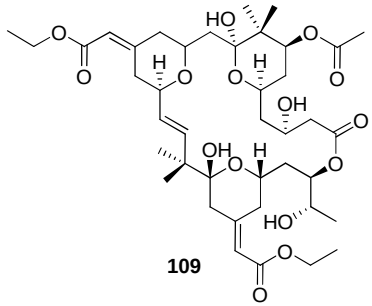

$(M+2H)^+$
($C_{41}H_{64}O_{15}$, 796.4239 g/mol)

The degradation of bryostatin 1 (Fig. 6a) can result from reverse esterification by: (6b) the hydrolysis of the carboxylate at the R_2 position ($C_7H_{15}COO\text{-}R_2 \rightarrow C_7H_{15}COO^- + HO\text{-}R_2$), (6c) the reduction of the hyxdroxyl group at the R_2 position (ROH → R-H), or by (6d) dehydration ($R_1\text{-}CHOH\text{-}C\text{-}R_2 \rightarrow R_1\text{-}CH{=}CH\text{-}R_2 + H_2O$).[10] The synthesis to form larger species (*m/z* > 927) can result from (e) esterification (R-OH + OA → R –OOC-C_7H_{15}) or (f) hydration reactions ($R_1\text{-}CH{=}CH\text{-}R_2 + H_2O \rightarrow R_1\text{-}CHOHCH\text{-}R_2$).[10] Even though the exact structures cannot be determined from the mass spectral data alone, many empirical formulae shown in the tables above strongly suggest the possible existence of some of the products. Figures 7-9 represent the mass spectra for different samples, respectively, as mentioned in Tables 2 and 3.

Spectral characteristics showing the gain or loss of 2H shown in Fig. 7 illustrates a single peak at 927, but also shows other spectral features. The $(M\text{-}2H)^+$ is a frequent attribute resulting in the m/z 787 ($789\text{-}2H^+$) **90**. In the MALDI-MS, it is normal for radical to be formed giving different masses [$(M+H)^+$, $(M+2H)^+$, $(M\text{-}H)^+$ and $(M\text{-}2H)^+$] as shown in the samples above. [14] The MALDI-MS process itself had no significant effect on the formation of peaks obtained from samples. If this had been the case bryostatin 1 standard would have the identical spectral peak profile to that of the samples analysed.

Results from previous experiments show the degradation of bryostatin consistent with data collected from this study, illustrating that bryostatin 1 can react with its own components under various conditions.[7] It is also suggested that reverse esterification can result in the loss of a C_8 group from one bryophan ring, which can esterify a position on another bryophan ring to form a larger species (Table 4), with the possibility of other large species, as shown in Tables 2-5.

(a)

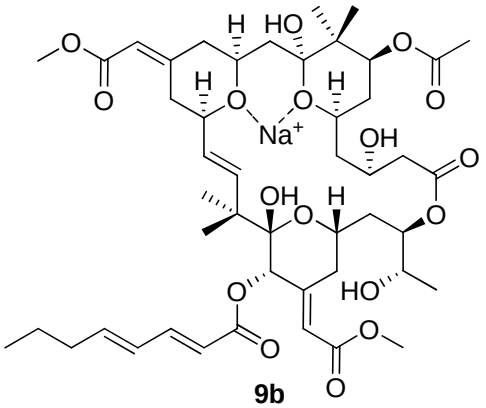

9b

(b)

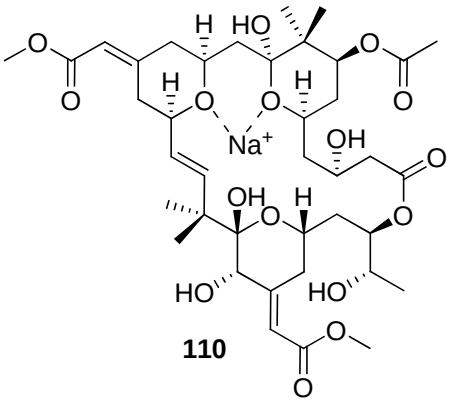

110

(c)

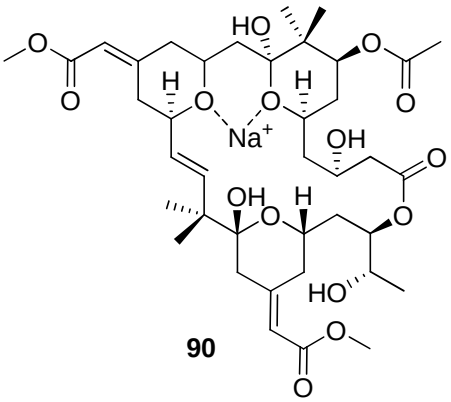

90

(d)

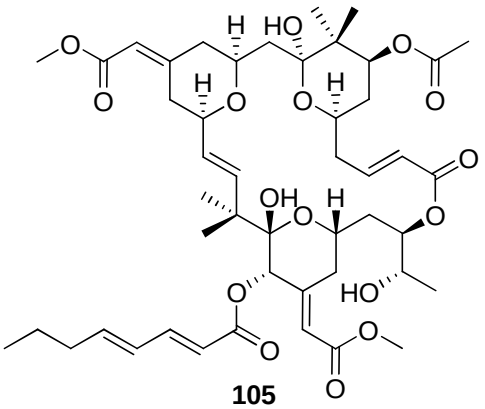

105

(e)

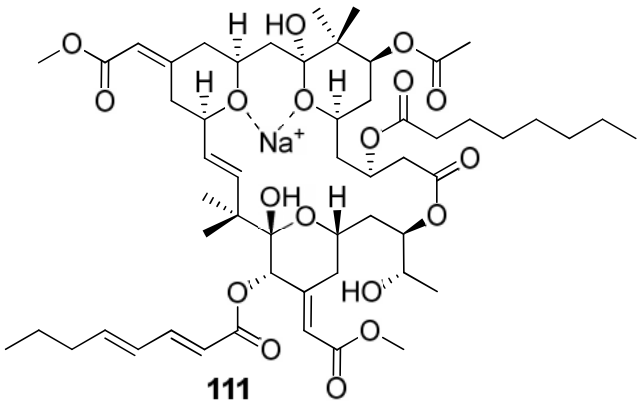

111

(f)

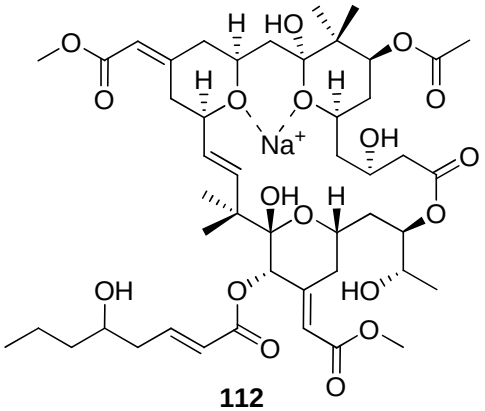

112

Fig. 6. (a) Bryostatin 1+Na^+ adduct **9b** ($C_{47}H_{68}O_{17}Na$, 927.4348 g/mol). (b) the hydrolysis of the carboxylate group from bryostatin 1 gives a structure with a mass of ($C_{39}H_{58}NaO_{16}$, 805.3617 g/mol) **110**. (c) the reduction of the hyxdroxyl group gives a structure of ($C_{39}H_{58}NaO_{15}$, 789.3667 g/mol) **90**. (d) The dehydration of bryostatin 1+Na^+ adduct ($C_{47}H_{68}O_{17}Na$, 927.4348 g/mol) resulting in the formation of m/z 909 $(M+Na)^+$ **105** ($C_{47}H_{66}O_{16}Na$, 909.4243 g/mol), (e) The OA molecule can undergo an ester reaction with one of the bryophan's R-OH groups resulting in a *m/z* of 1057 **111** ($C_{55}H_{86}NaO_{18}$, 1057.5706 g/mol), (f) The hydration of bryostatin 1+Na^+ resulting in the formation of *m/z* at 945 **112** ($C_{47}H_{70}NaO_{18}$, 945.4454 g/mol).[10]

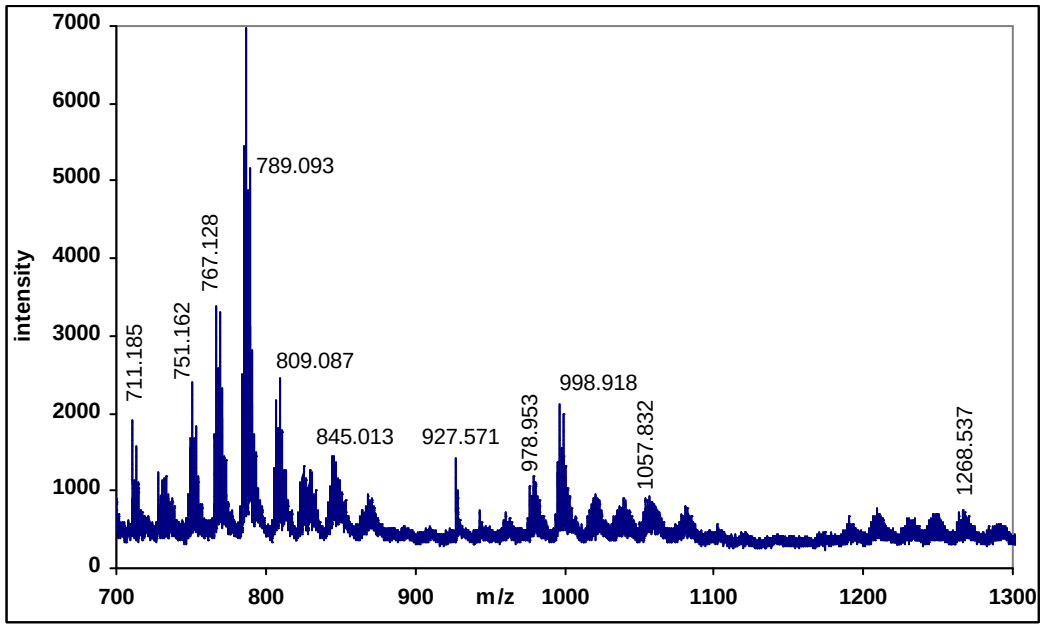

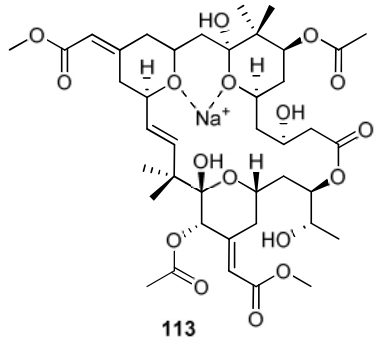

$(M+Na)^+$ Bryostatin 7+Na^+
($C_{41}H_{60}O_{17}Na$, 847.3722 g/mol)

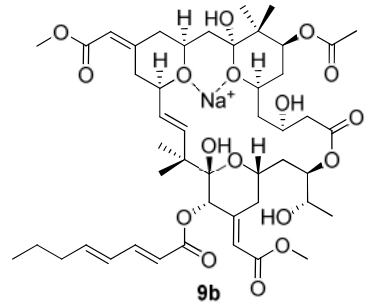

$(M+Na)^+$ Bryostatin 1+Na^+
($C_{47}H_{68}O_{17}Na$, 927.4348 g/mol)

Fig. 7. The reaction involving sample 3d shows the parent ion (*m/z* of 927) as well as a number of degradation products (<927) and larger structures that can be attributed to the attachment of OA attaching (Fig. 4). The structures shown are suggestive correlations to some of the peaks in the above mass spec.

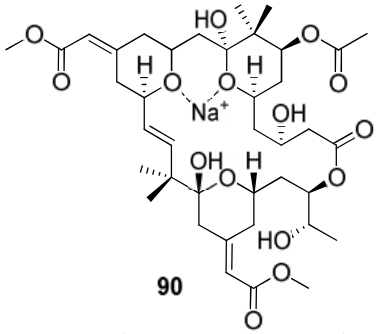

$(M+Na)^+$ Bryostatin 11+Na^+
($C_{39}H_{58}O_{15}Na$, 789.3668 g/mol)

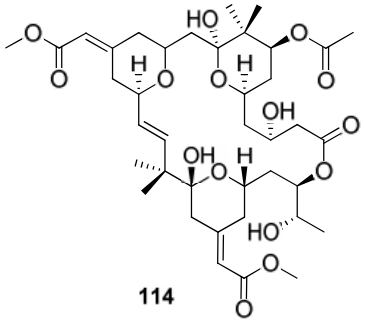

$(M+H)^+$ Bryostatin 11
($C_{39}H_{59}O_{15}$, 767.3848 g/mol)

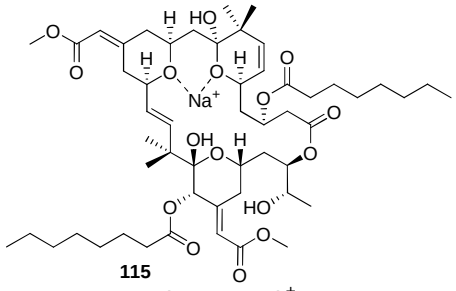

$(M+Na+H)^+$
($C_{53}H_{83}O_{16}Na$, 998.5573 g/mol)

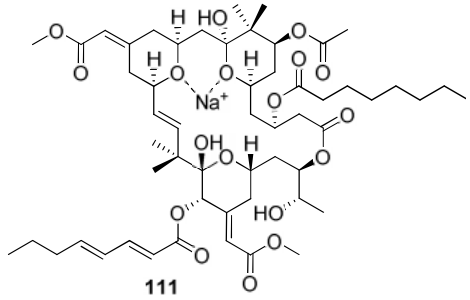

$(M+Na)^+$
($C_{55}H_{86}O_{18}Na$, 1057.5706 g/mol)

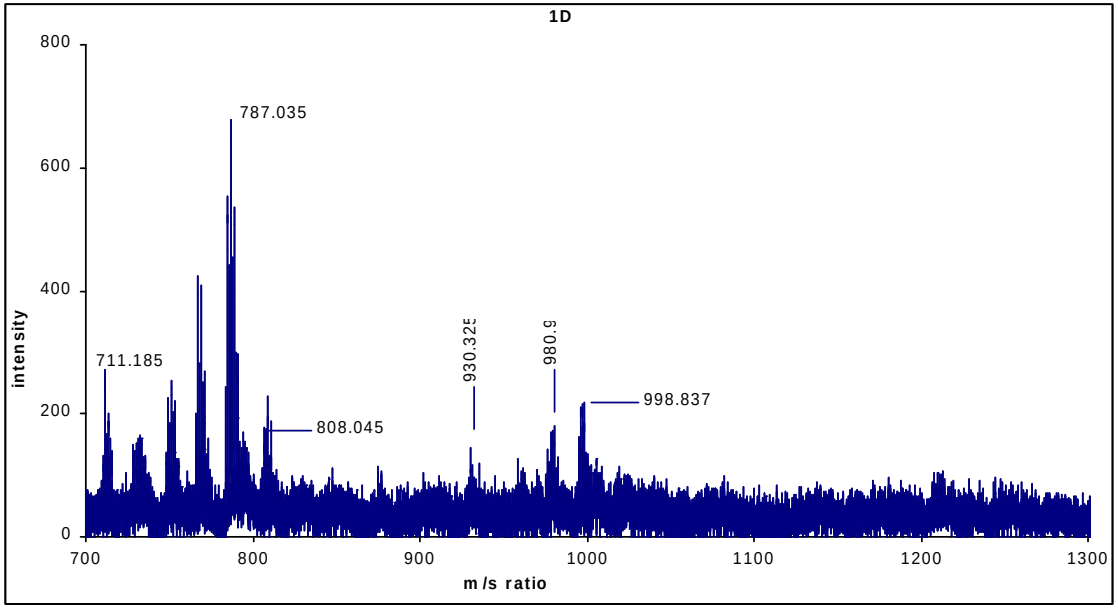

Fig. 8. Mass spectrum of sample 1d (Table 2).

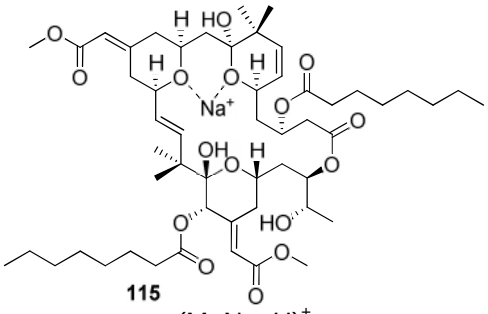

115

$(M+Na+H)^+$

$(C_{53}H_{83}O_{16}Na, 998.5573 g/mol)$

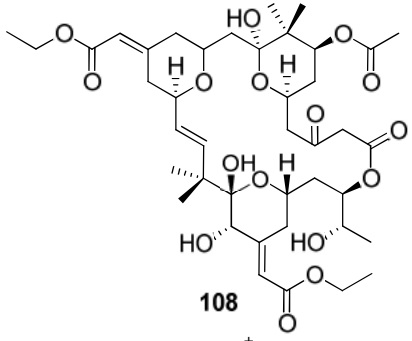

108

$(M+H)^+$

$(C_{41}H_{61}O_{16}, 809.3954 g/mol)$

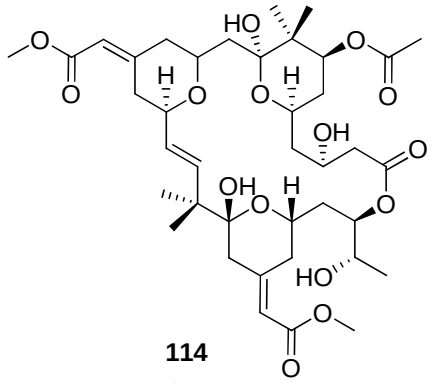

114

$(M+H)^+$ Bryostatin 11

$(C_{39}H_{59}O_{15}, 767.3848 g/mol)$

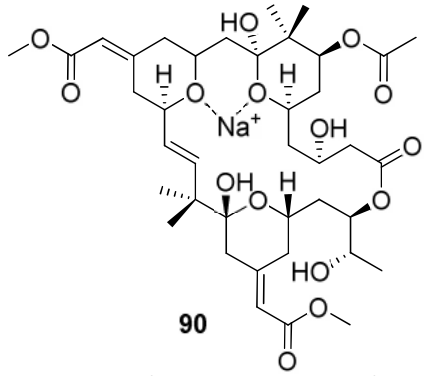

90

$(M+Na)^+$ Bryostatin $11+Na^+$

$(C_{39}H_{58}O_{15}Na, 789.3668 g/mol)$

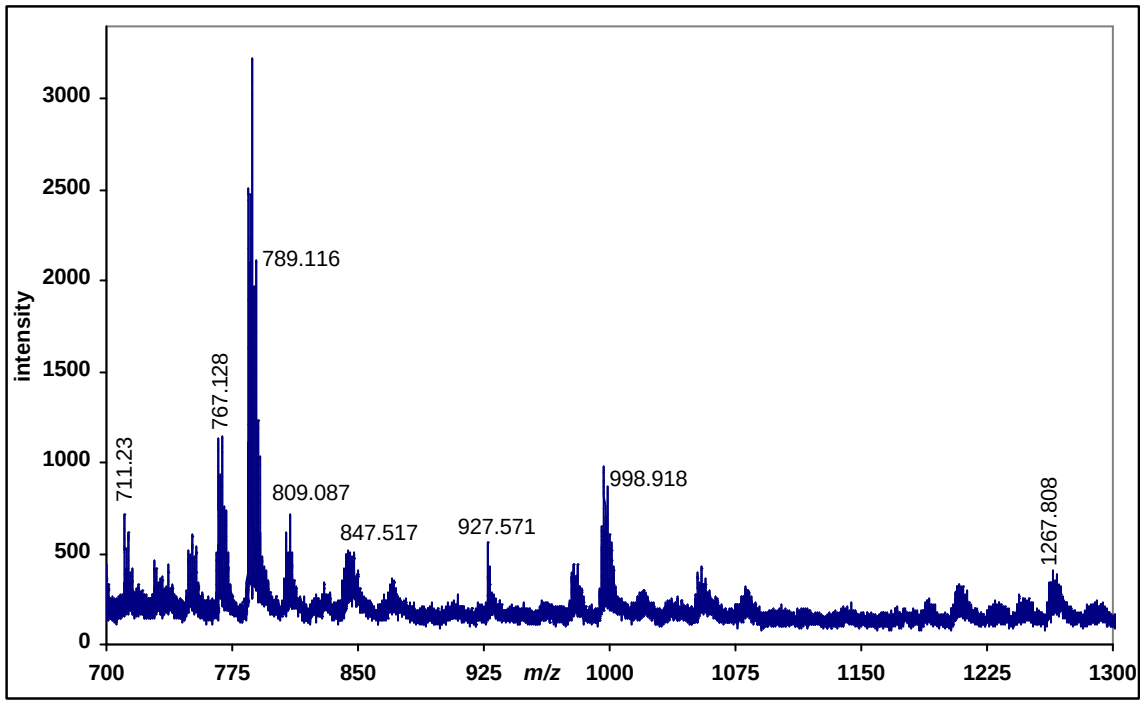

Fig. 9. Mass spectrum of sample 2e (Table 2).

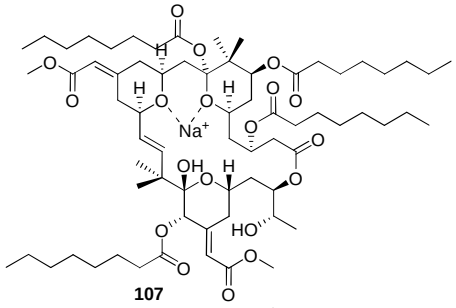

107

$(M+Na)^+$

($C_{69}H_{112}O_{19}Na$, 1267.7690 g/mol)

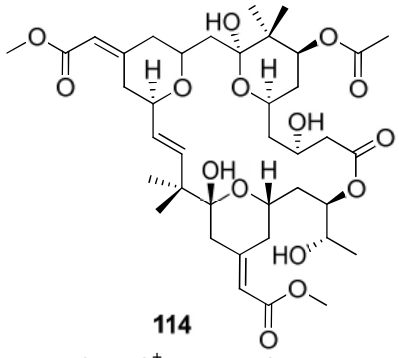

114

$(M+H)^+$ Bryostatin 11

($C_{39}H_{59}O_{15}$, 767.3848 g/mol)

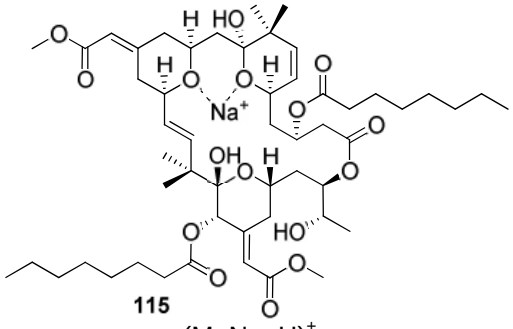

115

$(M+Na+H)^+$

($C_{53}H_{83}O_{16}Na$, 998.5573 g/mol)

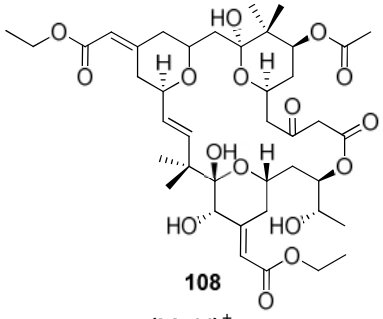

108

$(M+H)^+$

($C_{41}H_{61}O_{16}$, 809.3954 g/mol)

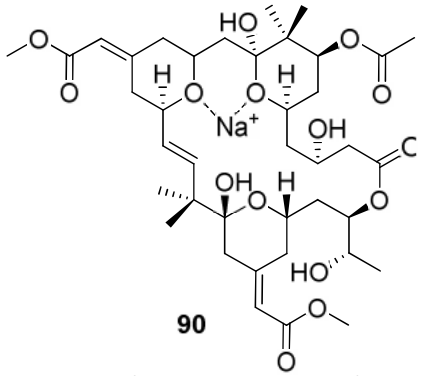

90

$(M+Na)^+$ Bryostatin 11+Na^+

($C_{39}H_{58}O_{15}Na$, 789.3668 g/mol)

Table 3. Values (*m/z*) for bryostatin samples that contain Fe^{3+}. The numbers in brackets after the masses (e.g. 789(1)) correspond to empirical formulae in Tables 4 and 5.[10] Examples of suggestive structures for the highlighted peaks are shown below.

Condition	Sample[g] (*m/z*)	Sample[h] (*m/z*)	Sample[i] (*m/z*)	Sample[j] (*m/z*)	Sample[k] (*m/z*)	Sample[l] (*m/z*)
4. No light	789(2), 809(4), 978(16), 998(18), 1057(21)	789(2), 809(4), 824(5), 998(18), 1102(22), 1389(34)	789(2), 809(4), 978(16), 998(18), 1114(29)	789(2), 809(4), 927(11), 998(18), 1026(20)	789(2), 809(4), **889(9)**, 1026(20), 1102(22), 1227(32)	789(2), 809(4), 909 (10), 927(11), 941(13), 1141(30)
5. UV	789(2), 809(4), 927(11), 998(18), 1026(20)	789(2), 809(4), 956(14), 998(18), 1026(20)	789(2), 809(4), 941(13)	789(2), 809(4), 941(13), 998(18), 1007(19), 1114(29)	789(2), 927(11), 962(27), 1057(21)	789(2), 847(7), 927(11), 1057(21), 1302(33)
6. 37°C	789(2), 809(4), 956(14), 962(27), 998(18)	789(2), 809(4), 847(7), 941(13), 998(18)	831(6),	789(2), 809(4), 927(11), 985(28), **1141(23, 30)** 1205(31)	909 (6), 927 (11), 1102(22), 1205(31)	789(2), 809(4), 927(11). 998(18), 1196 (24)

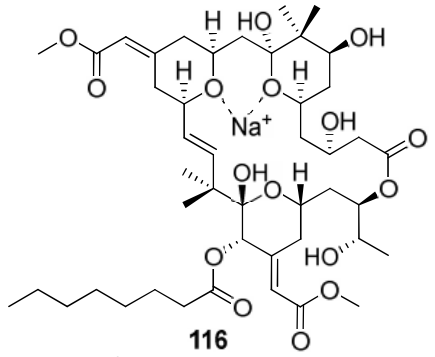

116

$(M+Na)^+$ ($C_{45}H_{70}O_{16}Na$, 889.4556 g/mol)

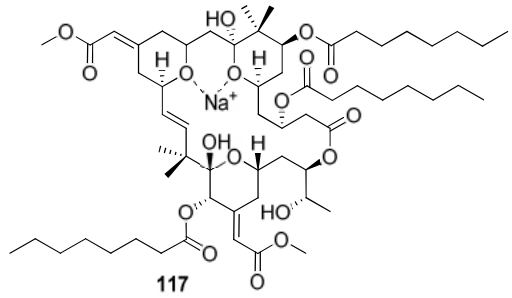

117

$(M+Na)^+$ $C_{61}H_{98}O_{18}Na$, 1141.6645 g/mol)

[g] $5.52*10^{-7}$M bryostatin 1, $1.50*10^{-4}$M OA, $1.19*10^{-4}$M Fe^{3+} solutions.
[h] $5.52*10^{-7}$M bryostatin 1, $1.46*10^{-4}$M OA, $1.17*10^{-4}$M Fe^{3+}, $2.32*10^{-4}$M HCl.
[i] $5.52*10^{-7}$M bryostatin 1, $1.46*10^{-4}$M OA, $1.17*10^{-4}$M Fe^{3+}, $2.32*10^{-4}$ M NaOH.
[j] $5.52*10^{-7}$M bryostatin 1, $1.22*10^{-4}$M Fe^{3+}.
[k] $5.52*10^{-7}$M bryostatin 1, $1.19*10^{-4}$M Fe^{3+}, $2.38*10^{-3}$M HCl.
[l] $5.52*10^{-7}$M bryostatin 1, $1.19*10^{-4}$M Fe^{3+}, $2.38*10^{-3}$M NaOH

Table 4. Values (*m/z*) corresponding to bonds formed with octanoic acid and at the various sites as showed in Fig. 4. The peak numbers below correlate with each (*m/z*) value that can be identified in different experimental conditions as shown in Tables 2 and 3.[10] Structures for the highlighted peaks are as shown.

Peak	R1	R2	R3	R4	R5	m/z	Emp Formula
1	OH	H				727	$C_{37}H_{56}O_{14}$
2	$C_2H_3O_2$	H				789	$C_{39}H_{58}NaO_{15}$
3	CH_3COO	H				796	$C_{41}H_{64}O_{15}$
4	CH_3COO	OH				809	$C_{41}H_{61}O_{16}$
5	$C_2H_3O_2$	$C_2H_3O_2$				825	$C_{41}H_{61}O_{17}$
6	CH_3COO	OH				**831**	$C_{41}H_{60}NaO_{16}$
7	$C_2H_3O_2$	$C_2H_3O_2$				847	$C_{41}H_{60}NaO_{17}$
8	OH	$C_8H_{15}O_2$				874	$C_{45}H_{70}NaO_{15}$
9	OH	$C_8H_{15}O_2$				889	$C_{45}H_{70}NaO_{16}$
10	$C_2H_3O_2$	$C_8H_{11}O_2$				909	$C_{47}H_{72}O_{16}$
11	$C_2H_3O_2$	$C_8H_{11}O_2$				**927**	$C_{47}H_{68}NaO_{17}$
12	$C_2H_3O_2$	$C_8H_{15}O_2$				932	$C_{47}H_{73}NaO_{17}$
13	$C_3H_5O_2$	$C_8H_{11}O_2$				941	$C_{48}H_{70}NaO_{17}$
14	$C_8H_{15}O_2$	$C_8H_{13}O_2$				956	$C_{53}H_{80}O_{15}$
15	H	$C_8H_{15}O_2$	$C_8H_{11}O_2$			**973**	$C_{53}H_{80}O_{16}$
16	$C_8H_{15}O_2$	$C_8H_{15}O_2$				978	$C_{53}H_{84}O_{16}$
17	$C_2H_3O_2$	$C_8H_{11}O_2$	$C_3H_5O_2$			983	$C_{50}H_{72}O_{18}$
18	H	$C_8H_{15}O_2$	$C_8H_{15}O_2$			998	$C_{53}H_{83}NaO_{16}$
19	$C_8H_{15}O_2$	$C_8H_{11}O_2$				1007	$C_{53}H_{76}NaO_{17}$
20	OH	$C_8H_{12}O_3$	$C_8H_{15}O_2$			1027	$C_{53}H_{82}NaO_{18}$
21	$C_2H_3O_2$	$C_8H_{15}O_2$		$C_8H_{15}O$		1057	$C_{55}H_{86}NaO_{18}$
22	H	$C_8H_{15}O_2$	$C_8H_{15}O$	$C_8H_{15}O$		1102	$C_{61}H_{98}O_{17}$
23	OH	$C_8H_{15}O_2$	$C_8H_{15}O_2$	$C_8H_{15}O$		1141	$C_{61}H_{98}NaO_{18}$
24	$C_8H_{13}O_2$	$C_2H_3O_2$	$C_8H_{15}O$	$C_8H_{15}O_2$		1196	$C_{63}H_{98}NaO_{20}$
25	H	$C_8H_{11}O_2$	$C_8H_{15}O$	$C_8H_{15}O$	$C_8H_{15}O_2$	1233	$C_{69}H_{110}NaO_{17}$
26	$C_8H_{15}O_2$	$C_8H_{15}O_2$	$C_8H_{15}O$	$C_8H_{15}O$		1267	$C_{69}H_{112}Na0_{19}$

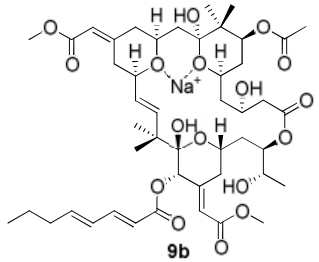

Bryostatin 1 + Na^+
($C_{47}H_{68}O_{17}Na$, 927.4348 g/mol)

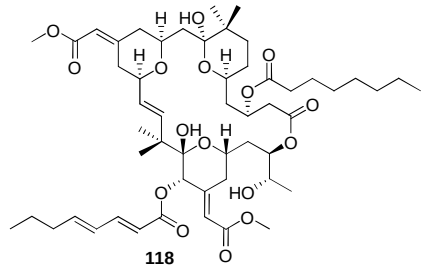

$(M+H)^+$ ($C_{53}H_{81}O_{16,}$ 973.5519 g/mol)

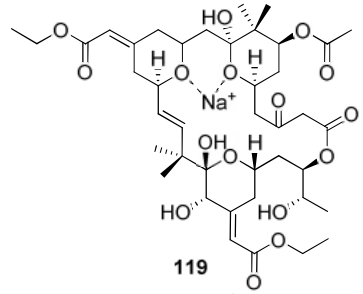

$(M+Na)^+$
($C_{41}H_{60}O_{16}Na$, 831.3773g/mol)

In the above table, R1-R5 corresponds to the possible sites for esterification or transesterification as shown in Fig. 4.

Table 5. The (*m/z*) values below correspond to the Fe^{3+} complex and substitution reactions at the various binding sites shown in Fig. 10. The peak numbers below correlate with each (*m/z*) which can be identified in different experimental conditions, shown in Tables 2 and 3.[10] The structures below are suggestive based on the highlighted peaks.

Peak	R1	R2	R3	R4	R5	m/z	Empirical Form
27	$C_2H_3O_2$	$C_8H_{15}O_2$				**962**	$C_{47}H_{70}FeO_{17}$
28	$C_2H_3O_2$	$C_8H_{15}O_2$				**985**	$C_{47}H_{70}FeNaO_{17}$
29	$C_2H_3O_2$	OH	$C_8H_{15}O_2$	$C_8H_{15}O_2$		1114	$C_{55}H_{85}FeNaO_{18}$
30	H	$C_8H_{11}O_2$	$C_8H_{15}O_2$	$C_8H_{15}O_2$		1141	$C_{61}H_{96}FeO_{16}$
31	H	$C_8H_{11}O_2$	$C_8H_{15}O_2$	$C_8H_{15}O_2$		1206	$C_{63}H_{99}FeNaO_{17}$
32	$C_8H_{15}O_2$	$C_8H_{15}O_2$	$C_8H_{15}O_2$	$C_8H_{15}O_2$		**1227**	$C_{69}H_{110}O_{18}$
33	$C_8H_{15}O_2$	$C_8H_{15}O_2$	$C_8H_{15}O_2$	$C_8H_{15}O_2$		**1302**	$C_{69}H_{112}FeO_{19}$
34	$C_8H_{15}O2$	$C_8H_{11}O_2$	$C_8H_{15}O_2$	$C_8H_{15}O_2$	$C_8H_{15}O_2$	**1389**	$C_{77}H_{122}NaO_{20}$

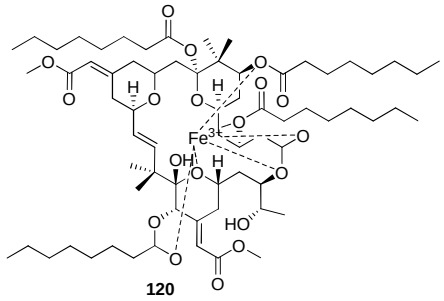

120

$(M+Fe)^+$

($C_{69}H_{114}FeO_{19}$, 1302.7298 g/mol)

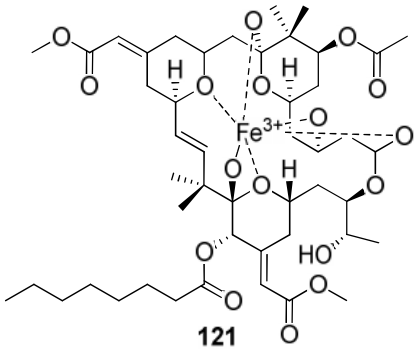

121

$(M+Fe)^+$

($C_{47}H_{70}FeO_{17}$, 962.3956 g/mol)

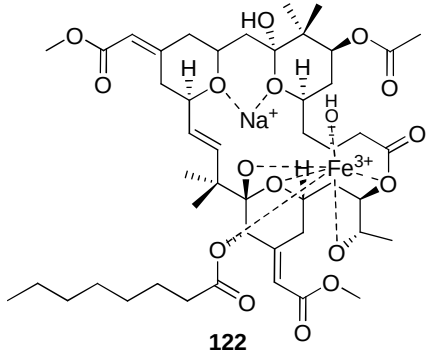

122

$(M+Fe+Na+H)^+$

($C_{47}H_{70}FeNaO_{17}$, 985.3854 g/mol)

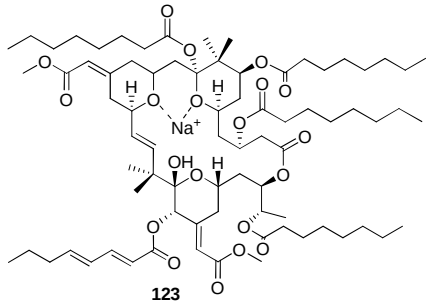

123

$(M+Na)^+$

($C_{77}H_{122}NaO_{20}$, 1389.8421 g/mol)

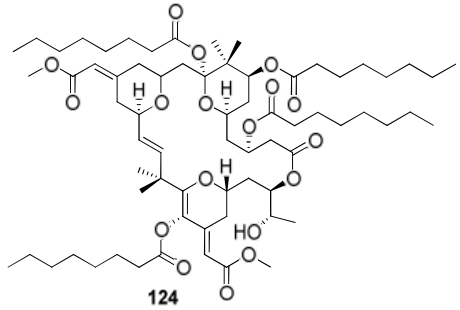

124

$(M+H)^+$

($C_{69}H_{111}O_{18}$, 1227.7765 g/mol)

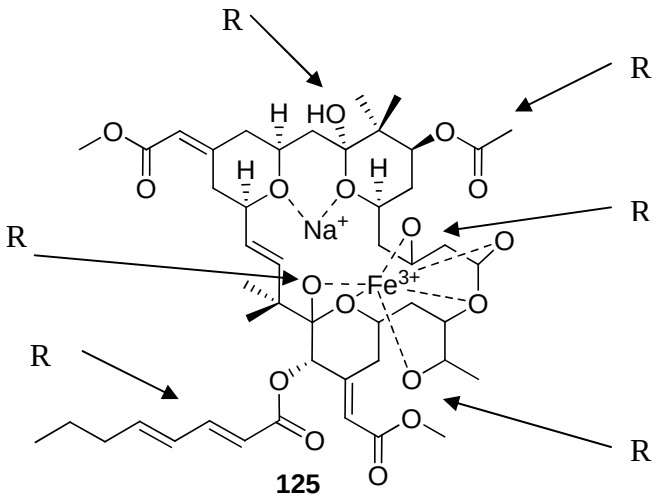

125

Fig. 10. A possible structure for bryostatin 1 binding to Na^+ and Fe^{3+} [$(M+Fe+Na+H)^+$, **125** $C_{47}H_{66}FeNaO_{17}$, 981.3541 g/mol]. The R groups represent the possible binding sites where substitution reactions may occur.

Bryostatin is believed to have properties similar to siderophores produced by marine bacteria. Siderophores are iron chelating compounds released by marine organisms to bind metals such as Fe^{3+} that cannot be ingested by the organism itself.[15,16] These organisms can then ingest the complex by an active transport mechanism. For this reason, iron(III) chloride was added to the samples (Table 3 and 5) to show the possible binding of Fe^{3+} to bryostatin 1 under various conditions. Samples 4g, 6j and 6l (37°C) from Table 3, all show the formation of molecular species at a *m/z* of 1390, 1350 and 1374, respectively, suggesting the binding of Fe^{3+}, along with some esterification reactions of C_8 on bryostatin 1. Also, experiment 6i (Table 3) showed that bryostatin 1 and its various products were no longer present.[10] In the presence of Fe^{3+} (Fig. 11 and 12) the bryostatins are not seen, thus questioning whether or not the production of an insoluble complex was formed and/or the complex had bonded to the reaction vessel. A recent study showing the polymerization of a DOPA derivative using Fe^{3+} resulted in the formation of a strong hydrophobic molecule.[17]

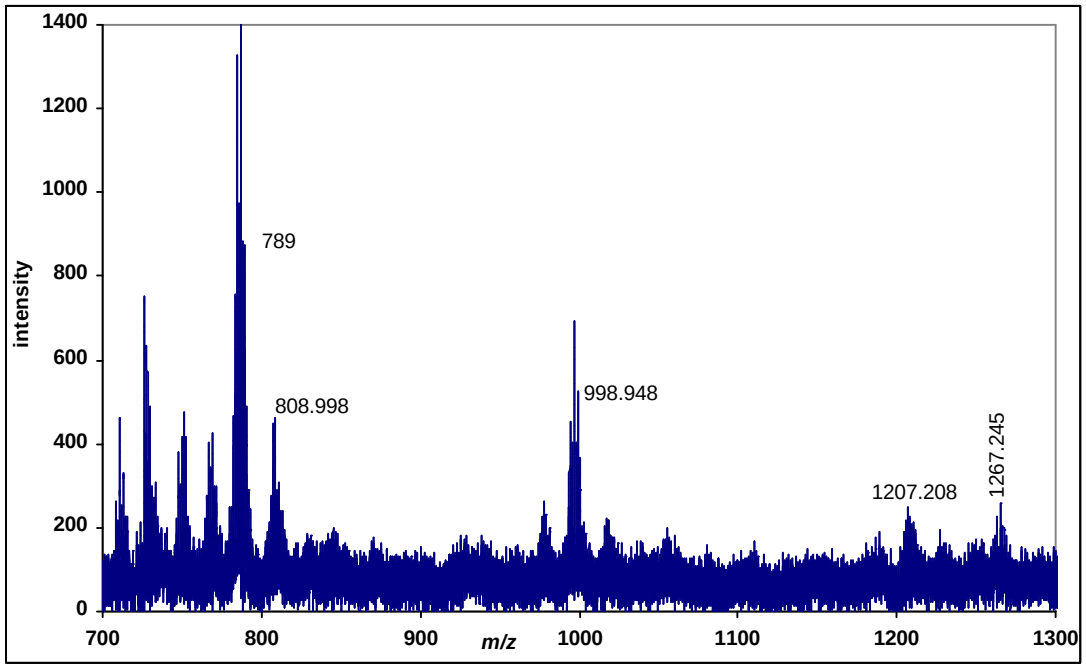

Fig. 11. Mass spectrum of sample 5h.

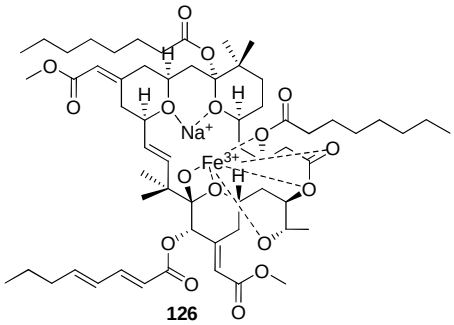

126

$(M+Fe+Na)^+$

($C_{63}H_{98}O_{17}FeNa$, 1205.6045 g/mol)

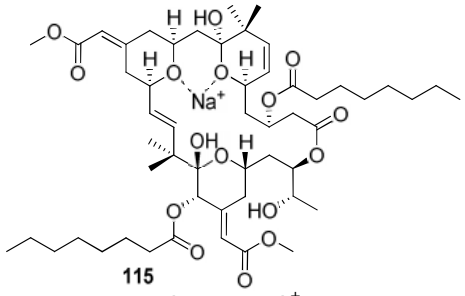

115

$(M+Na+H)^+$

($C_{53}H_{83}O_{16}Na$, 998.5573 g/mol)

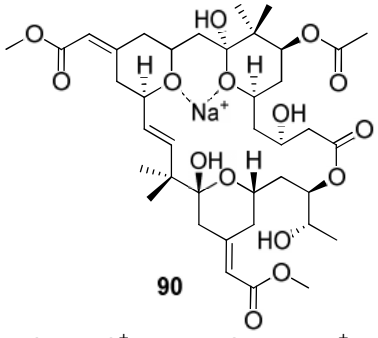

90

$(M+Na)^+$ Bryostatin 11+Na^+

($C_{39}H_{58}O_{15}Na$, 789.3668 g/mol)

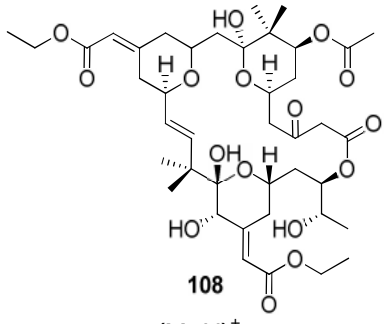

108

$(M+H)^+$

($C_{41}H_{61}O_{16}$, 809.3954 g/mol)

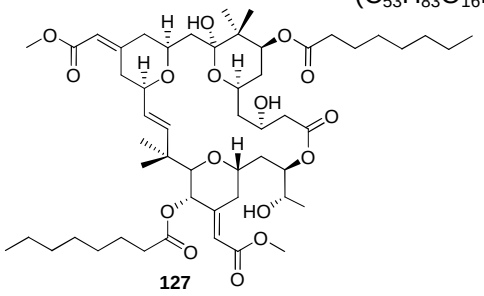

127

$(M+2H)^+$

($C_{53}H_{86}O_{16}$ 978.5910 g/mol)

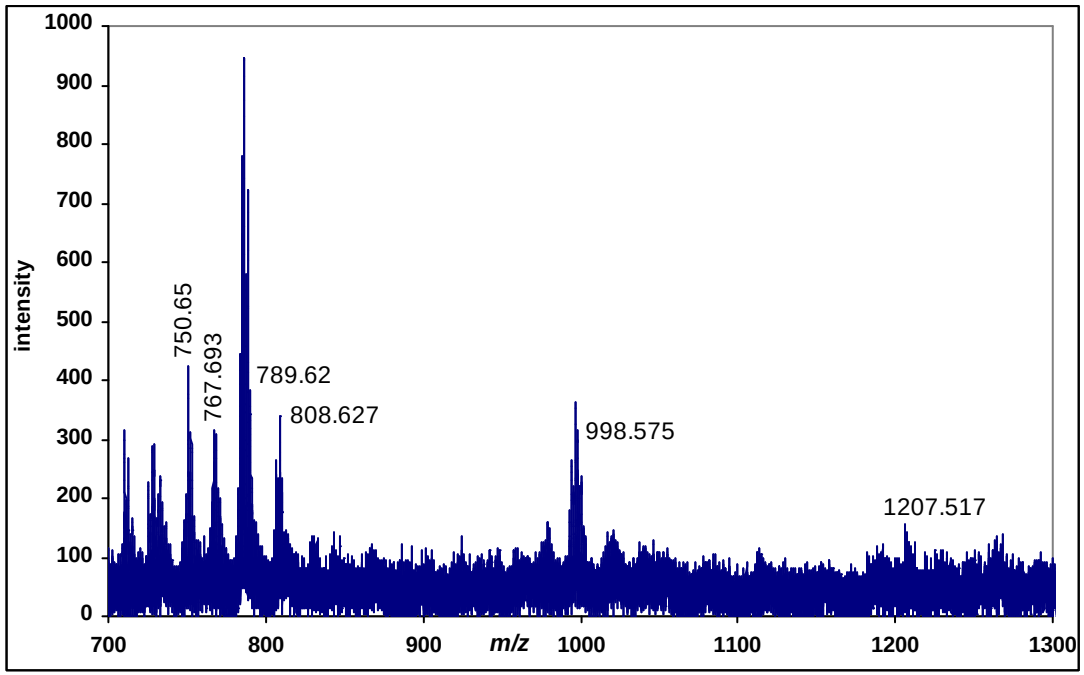

Fig. 12. Mass spectra of sample 6g (Table 3).

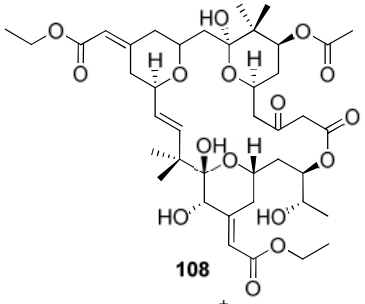

126

$(M+Fe+Na)^+$

($C_{63}H_{98}O_{17}FeNa$ 1205.6045 g/mol)

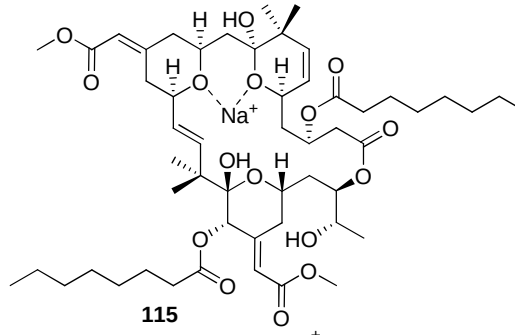

115

$(M+Na+H)^+$

($C_{53}H_{83}O_{16}Na$, 998.5573 g/mol)

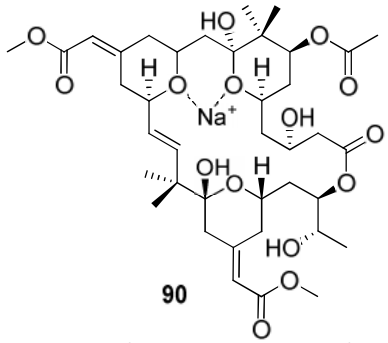

108

$(M+H)^+$

($C_{41}H_{61}O_{16}$, 809.3954 g/mol)

90

$(M+Na)^+$ Bryostatin 11+Na^+

($C_{39}H_{58}O_{15}Na$, 789.3668 g/mol)

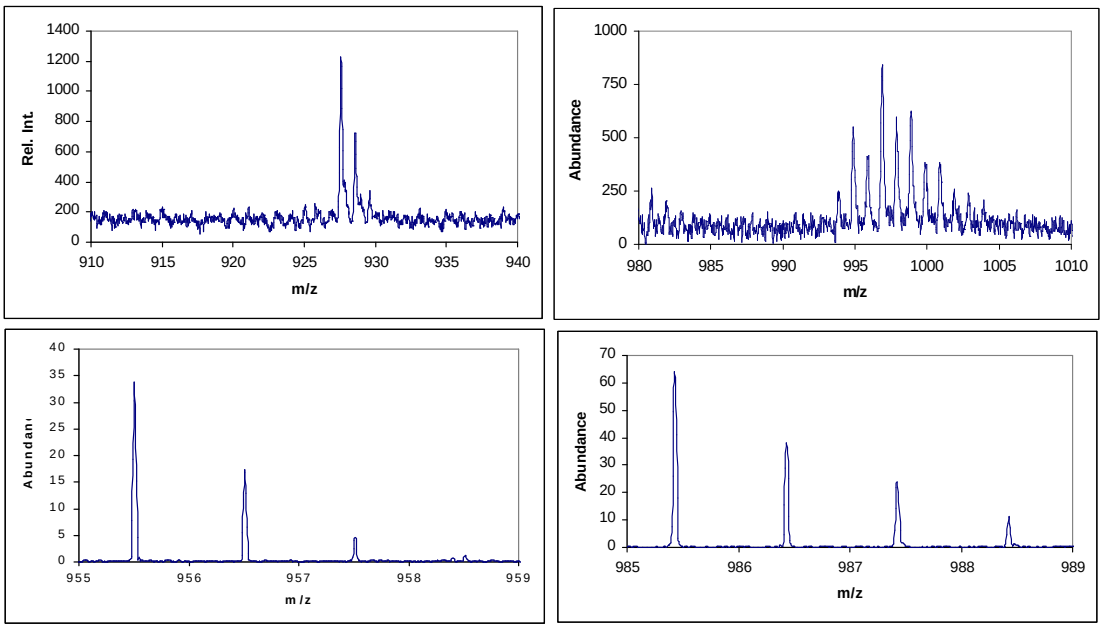

Fig. 13. Top left mass spectra shows bryostatin 1 at an *m/z* of 927. Top right mass spectra shows bryostatin 1-FeOH+Na^+ at a *m/z* 997. Bottom left shows the mass spectra of bryostatin 1+Fe^{3+} at an *m/z* of 955. Bottom right shows the mass spectra of bryostatin 1+Na^++Fe^{3+} at an *m/z* 985.

Previous work has shown that when Fe^{3+} was reacted with bryostatin 1, a [Bryostatin 1+Fe^{3+}+Na^+-2H]$^+$ complex formed (Fig. 13).[18] While bryostatin 1 has performed well in cell line tests, it has faltered as a sole agent in some human trials.[8] Understanding its medicinal activity *in vivo* is currently ongoing. Based on this study, several suggestions can be made with regards to its reported poor efficacy in some clinical trials. Firstly, bryostatin 1 has a low solubility in the body because it readily diffuses into tissues, cells, *etc*., before reaching the target site. Secondly, its ester bonds are reactive resulting in degradation of the compound once it has entered the patient. Binding bryostatin 1 to Fe^{3+} may solve these problems. This is based on the notion that binding to a Fe^{3+} ion will produce a charged complex which should increase its water solubility. The bryostatin-Fe complex should be more rigid and subsequently more stable than the uncomplexed bryostatin, making it a more effective medicinal agent.[18,19] This proposition was subsequently explored and is further discussed in chapters 7 and 8.

Although there is no conclusive evidence to support this idea, or others mentioned, it is feasible to propose that the formation of C8 esters at the various hydroxylated sites is possible. Results from each of the conditions investigated were compared to bryostatin 1 standard to determine the possibility of esterification reactions forming. Comparing both data, it is clearly seen that many of the peaks, shown in the samples, are not present in the bryostatin standard. This suggests, 1) that the proposed reactions can occur where hydroxyl groups are located, forming species with $m/z > 927$ 2) the molecule can also undergo degradation, forming species with $m/z < 927$ and 3) the production of different bryostatin compounds is not only a result of bacterial genetics or production of gene fragments, but can be a mixture of both due to the effects of the environmental conditions where *Bugula neritina* is located.[10]

The microbial symbiont bacterium, *Candidatus Endobugula sertula*, is believed to produce these compounds by gene fragments that combine together to give the complete structure of these bryostatin compounds.[4-7] Based on the expression of this symbiont bacterium, it is suggested that the production of bryostatin compounds through the biosynthesis of these gene fragments show some consistency between *Bugula* collected off the coast of California with *Bugula* collected from North Carolina. However, there is no conclusive evidence supporting the proposition of gene fragments being responsible for the production of these compounds. Results from this study clearly demonstrate the ability for these compounds can be formed under different environmental conditions as well.[20] The stability assessment of bryostatin under various conditions was also reported by Zhao *et al*..[21]

6.4 References

[1] T. J. Manning, M. Land, E. Rhodes, L. Chamberlin, J. Rudloe, D. Phillips, T. T. Lam, J. Purcell, H. J. Cooper, M. R. Emmett, and A. G. Marshall. *Nat. Prod. Res*., 2005, **19(5)**, 467-91.

[2] G. R. Pettit, Y. Kamano, C. L. Herald, and M. Tozawa. *J. Am. Chem. Soc*., 1984, **106(22)**, 6768-71.

[3] G. R. Pettit, J. E. Leet, C. L. Herald, Y. Kamano, F. E Boettner, L. Baczynskyj, and R. A. Neiman. *J. Org. Chem*., 1987, **52(13)**, 2854-60.

[4] M. G. Haygood, and S. K. Davidson. *Appl. Environ. Microbiol*., 1997, **63(11),** 4612-16.

[5] S. Sudek, N. Lopanik, L. E. Waggoner, M. Hilderbrand, H. B. Liu, A. Patel, C. Anderson, D. H. Sherman, and M. G. Haygood. *J. Nat. Prod.,* 2007, **70(1)**, 67-74.

[6] S. K. Davidson, and M. G. Haygood. *Bio. Bull.,* 1999, **196(3)**, 273-80.

[7] S. K. Davidson, S. W. Allen, G. E. Lim, C. M. Anderson, and M. G. Haygood. *Appl. Environ. Microbiol.*, 2001, **67(10)**, 4531-37.

[8] http://www.clinicaltrials.gov/ (January 21st 2009).

[9] T. J. Manning, E. Rhodes, R. Loftis, D. Phillips, D. Demaria, D. Newman, and J. Rudloe. *Nat. Prod. Res*., 2006, **20(5)**, 461-73.

[10] G. Abadi, T. J. Manning, D. Phillips, P. Groundwater, and L. Noble. *Nat. Prod*. *Res*., 2008, **22(10),** 865-78.

[11] X. Zhang, R. Zhang, H. Zhao, H. Cai, K. A. Gush, R. G. Kerr, G. R. Pettit, and A. S. Kraft. *Cancer Res.*, 1996, **56(4)**, 802-08.

[12] B. K. Carte. *Biosci.,* 1996. **46(4)**, 271-86.

[13] T. Rispens, M. F. Lensink, H. J. C. Berendsen, and J. B. F. N. Engberts. *J. Phys. Chem*. *B*, 2004, **108(17)**, 5483-88.

[14] Hillenkamp, F., and J. Peter-Katalinić. MALDI MS: A practical guide to instrumentation, methods and applications. Wiley-VCH, 2007.

[15] J. D. Martin, Y. Ito, W. Homann, M. G. Haygood, and A. Butler. *J. Biol. Inorg. Chem*., 2006, **11(5)**, 633-41.

[16] J. S. Martinez, J. N. Carter-Franklin, E. L. Mann, J. D. Martin, M. G. Haygood, and A. Butler. *Proc. Natl. Acad. Sci*. *USA*, 2003, **100(7)**, 3754-59.

[17] S. K. Davidson, S. W. Allen, G. E. Lim, C. M. Anderson, and M. G. Haygood. *Appl. Environ. Microbiol.*, 2001, **67(10)**, 4531-37.

[18] T. J. Manning, J. Thomas, G. Abadi, D. Phillips, S. Osiro, L. Noble, and D. Phillips. *Nat. Prod. Res.* 2008, **22(5),** 399-413.

[19] T. Manning, L. Noble, G. Abadi, and J. Smith. *Fl. Sci*., 2008, **71(4)**, 341-59.

[20] N. B. Lopanik, N. M. Targett, and N. Lindquist. *Appl. Environ. Microbiol*., 2006, **72(12)**, 7941-44.

[21] M. Zhao, M. A. Rudek, P. He, B. D. Smith, and S. D. Baker. *Anal. Biochem*., 2005, **337(1)**, 143-48.

CHAPTER 7

Computational studies of the bryostatins and MNPs as potential siderophores

7.1 Introduction

Siderophores are iron chelating compounds, secreted by microorganisms to bind iron, as many marine organism cannot easily ingest iron.[1,2] In the presence of Fe^{3+}, these compounds form a stable hexavalent structure and, due to their complex binding, increase the aqueous solubility of hydrated iron. In the body/cells, Fe^{3+} is then taken up by an active transport mechanism, as a source of nutrient for the marine organism.[3] Many studies have been conducted to further understand the mechanism of these compounds and to isolate, synthesize and produce artificial siderophores that could be utilised for industrial and medical usage.[4,5,6,7,8] Research has shown that many pathogenic bacteria can produce more than one siderophore compound, as some target iron better than others. The production of different siderophores has shown to be environment specific (pH, temperature and availability of carbon sources where bacteria strains are present).[9] For example, *E. coli* K12 produces enterobactin; however, one particular strain, *E. coli* Nissle 1917, produces four different siderophores.[9] In the 1970s O'Brien *et al*., identified five compounds produced by *E. coli* and *Aerobacter aerogenes* under iron deficiency conditions.[10] In cell culturing studies, Konopka *et al*., showed that serum albumin inhibits the transfer of iron(III) from protein receptors to enterobactin; however, serum albumin had no effect on the iron intake by aerobactin.[11]

It is important to note that many siderophores are not solely iron specific and bind to other metals forming metal-ligand complexes.[12,13] For example, a recent study was carried out to determine the physical role of methanobactin, a novel chromopeptide known to be Cu^{2+} ion binding, produced by *Methylosinus trichosporium* OB3b, when bound to a range of metal ions. Despite methanobactin's capability as a copper-siderophore, in the absence of copper, methanobactin showed binding to other metals, such as Ag^{1+}, Au^{3+}, Co^{2+}, Cd^{2+},

and Fe^{3+} but did not bind Ba^{2+}, Cr^{6+}, La^{3+}, Mg^{2+}, or Sr^{2+}. However, in the presence of copper, only two metals, Ag^{1+} and Au^{3+}, were able to displace copper to bind methanobactin.(12)

Few computational studies have been conducted using siderophores. One example is the computational study using semi-empirical methods to determine the interaction of gallium with different siderophores. Results from the interaction of gallium and enterobactin showed no strain on the conformation of the complex. However, short chain groups attached to the siderophore can lead to deformations when binding the metal.(14)

Based on the importance and new roles of siderophores, a computational investigation of several MNPs, bryostatin analogues, siderophores and the twenty bryostatin compounds, was carried out to determine any similarity in geometric changes when bound to Fe^{3+}.(15) The geometric parameters of all the molecules were calculated using the semi-empirical (PM3) method, to determine the bond distances, bond angles and dipole moments of each molecule as a monocation (1^{+}), dication (2^{+}), and neutral species, which can be found on the attached DVD.

The semi empirical method works by making large assumptions and ignoring non-valence electrons. There are many advantages and disadvantages to the method. The advantages of using this method are, 1) it reduces the time taken for calculations to be determined; 2) it is an excellent method to study organic molecules; 3) it provides relatively good results in the calculation and visualization of molecular orbitals; and, 4) it addresses the issue of limitations on calculations of large molecules. The disadvantages are, 1) it does not allow the effect of some inclusion of electron correlation in the method; 2) it is unable to compute all the molecules of the complex using this method; 3) inaccuracy in the calculations occur for parameterized molecules, such as nitrogen; and, 4) inaccuracies of calculations with hydrogen bonding, transition states, or

molecules with non-parameterized atoms.[16] Consideing the advantages and disadvantages stated for the use of this semi-empirical method, the advantages outweighed the disadvantages. Particularly pertinent for this study is that, the semi-empirical method ignores the nonvalence electrons in molecules, and this may have restricted the data collected, as the non valence electrons on iron(III) are ignored during the calculations process.

The rationale for this study was to determine the probability of MNPs acting as possible siderophores in nature, thereby explaining their presence in marine organisms, aside from any defence mechanistic role that some may have. Many of the compounds used in this study are currently in preclinical or clinical studies for the treatment of various diseases. This computational study could therefore assist in the prospect of using these compounds as medicinal agents, and thereby enhance the efficacy of NPs as sole agents.

Based on results from the first computational investigation, a second computational study was conducted. This focused on the correlation of the seventeen oxygen atoms in bryostatin 1 that could bind Fe^{3+}, forming a fer-mer complex. The formation of these hexavalent complexes did not limit the bonding between the oxygens on bryostatin and Fe^{3+}.[17] The significance of this was to establish the different configurations that this complex could adopt, when using the available oxygens on bryostatin 1 to bind Fe^{3+}. The stability and probability, of the best configurations generated by this study, was determined by using the geometric parameters from the initial computational study. Based on the different configurations that were calculated, the most stable conformations could then be proposed based on the most probable Fe-O bond distances for each structure. This could then establish that the configurations are not specific, despite their stability, and could therefore rearrange in the body to form the most suitable configurations. This information would further support the feasibility of the fer-mer

complex to exist and act as a more effective medicinal agent than bryostatin 1 alone.

7.2 Experimental

The Spartan ’04 cluster version software was used to build the molecules and calculate the geometric parameters (dipole moment, bond angle, bond length, surface area and volume). The calculations were carried out using SUN Micro-system cluster hardware.

In the first computational study, the molecules with a Fe^{3+}-ligand complex (L = bryostatins, bryostatin analogues, marine natural products and siderophores) were evaluated, having a neutral, monocation or dication charge. In order to calculate the geometries for all of the molecules, each molecule was developed using the six shortest Fe-O bonds. Despite the fact that bryostatin 1 only has three main oxygens used for binding (Fig. 1, O^8, O^{12} and O^{15}),[18,19] three other oxygen atoms were selected, based on the shortest Fe-O bond lengths, forming a stable hexavalent complex. The three main oxygen atoms remained constant for all the bryostatin compounds.

This second computational study was conducted to determine the importance of the different possible configurations formed, when binding Fe^{3+} to bryostatin 1 (Fig. 1). Using the seventeen oxygens available, one hundred and seventy three structures were developed using six oxygen atoms per configuration to form the hexavalent structure. Siderophores typically have a Fe-O bond length of approximately 2 Å, which was used as an approximate control for the iron complexes built in both studies. For this reason, twenty-two of the most probable configurations from this batch were selected based on the average bond distances of the Fe-O bonds, ranging between 2.0-2.5 Å.

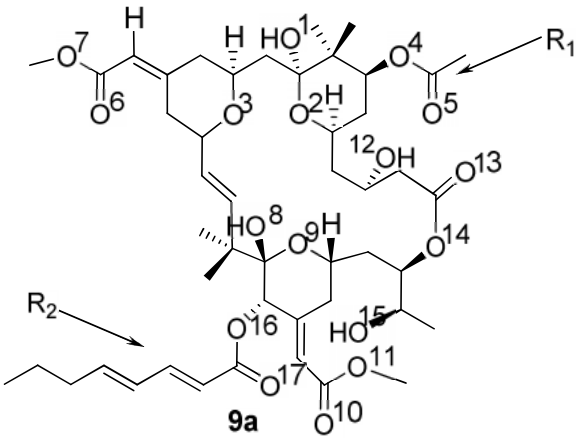

Fig. 1. Bryostatin 1 **9a** with oxygens numbered to correlate to bonds formed with Fe^{3+} as listed in Tables 9-11.

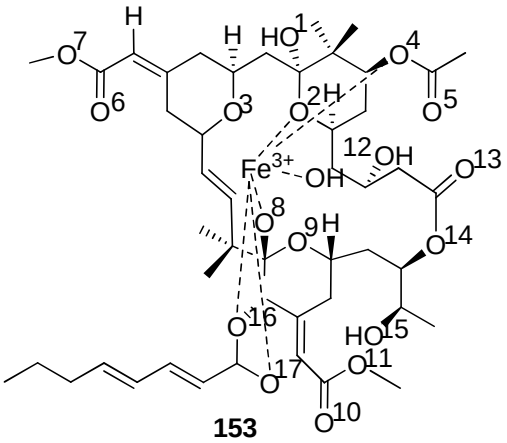

Fig. 2. The high polarity bryostatin 1-Fe^{3+} bonded to 5 bryostatin oxygens and one OH ion.

From this batch, five of the most probable structures were recalculated by replacing one Fe-O bond with an OH ion, then secondly replacing it with a H_2O molecule as shown in Fig. 2. The Spartan '04 cluster version software was used to build the molecules and calculate the geometric parameters (dipole moment, bond angle, bond length, surface area and volume), using the same SUN Micro-system cluster hardware. From the data collected, the D/V (dipole moment versus surface volume) ratio were calculated and compared to the D/V ratios of polar and non-polar solvents, to suggestively show the structures that appear to be polar and beneficial as medicinal agents. The accuracy of both computational studies was verified by comparing the computational values of the terricolin-Fe^{3+}

complex using the geometric parameters in this study calculated by the semi-empirical method to the experimental data of its crystal structure.[20]

7.3 Results and Discussion

7.3.1 First computational study

Only recently has the significance of understanding siderophores (their beneficial role as agents, structural complexity and chemical properties) and their potential to exist, grown in interest. For instance, Aquachelin D **128** and Marinobactin E **129** are two marine siderophores extracted from the marine organisms *Halomonas aquamarina* and *Marinobacter spp*., respectively; both contain non-polar and polar structural components (Figs. 3 and 4).[21,22]

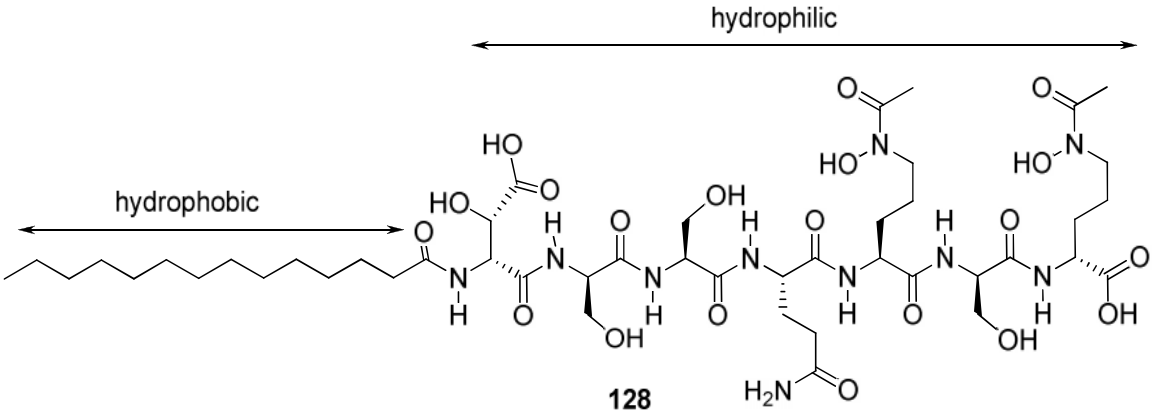

Fig. 3. Aquachelin D ($C_{46}H_{80}N_{10}O_{20}$, 1092.5545 g/mol) extracted from the marine organism *Halomonas aquamarina*.

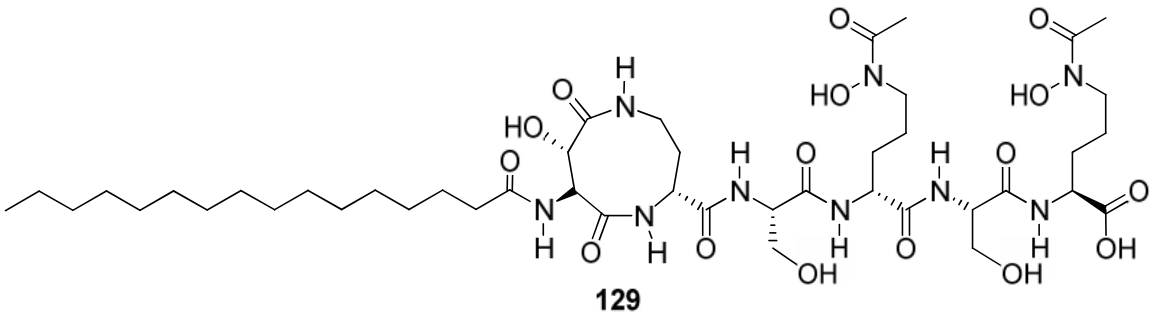

Fig. 4. Marinobactin E ($C_{44}H_{77}N_9O_{16}$, 987.5483 g/mol) extracted from the marine organism *Marinobacter spp.*.

In the absence of iron, these amphiphilic siderophores form micelles, which are clusters of molecules attached together by their fatty-acid tails. In the

presence of Fe^{3+}, these siderophores transform their structures from micelles to vesicles; which are spherical shells, hollow in the middle, with many siderophore molecules bound together (Fig. 5).[22] It is suggested that this formation from micelles to vesicles may be due to specific adaptations of the compounds in aqueous environments. Their dipole activity is responsible for the siderophores forming a micelle structure when placed in water.

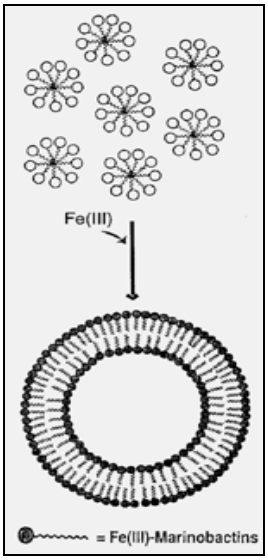

Fig. 5. Illustrates the configuration of siderophores before (micelle) and after binding Fe^{3+} (vesicle). The above illustration applies to marinobactin.[22]

For compounds such as aquachelin and marinobactin, the number of oxygens present is enough to make the structure flexible for the binding of up to two Fe^{3+} ions by Fe-O bonds, as shown in Table 4. All of the molecules surveyed in this study were bound to Fe^{3+} forming an octahedral geometry, with results showing bond distances averaging from 2.05-2.20 angstroms (Å). This suggests a strong correlation between the bond distances to that of known siderophores, based on the complexes that were formulated. Therefore, this strongly supports the claim, as stated, for the bryostatin's, and other natural products', ability to act as possible siderophores.

In a marine environment, bacteria may reside primarily in the sediment, in other materials (minerals, organisms, *etc*.), on surfaces, or within the water

supply.[23] Previous work, however, has shown that bryostatins are present in marine sediment containing large amounts of non-polar molecular species and dipole moments closer to that of desferrioxamine B, which is produced by a terrestrial bacterium.[24] The magnitude of the species dipole moment may provide an insight into its host ecosystem.

The semi-empirical method used in this computational study was also applied to terricolin **130** (Fig. 6), a metal-ligand complex isolated from the mycelium of the fungus, *Tolypocladium terricola*.[20] The computational data obtained for terricolin, see Tables 1 and 2, calculated using the SUN-Micro system hardware was then compared to the crystal structure of the metal-ligand, to determine the correlation of this siderophore to the proposed metal-ligand complexes exhibited by the natural products.

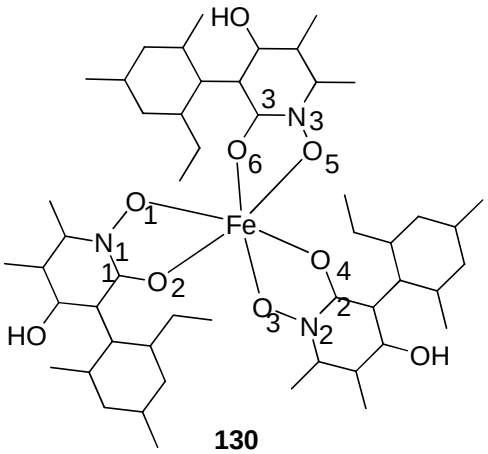

130

Fig. 6. Terricolin ($C_{45}H_{60}N_3O_9Fe$, 842.3673 g/mol), a siderophore isolated from the fungus *Tolypocladium terricola.* The numbers on the oxygens and nitrogens correlate to the bonds in Tables 1 and 2.

Table 1. Comparison of bond angles obtained from the computational study, to the crystal structure of terricolin.[20]

Terricolin-Fe^{3+} complex (FeL_3)			
Bond angles (degrees) of computational data VS crystal structure			
Bonds	Angles (Computed)	Angles (Crystal struc)	Difference
O2-Fe-O1	82.03	78.60	3.43
O3-Fe-O1	92.90	93.10	-0.20
O3-Fe-O2	95.70	103.70	-8.00
O4-Fe-O1	165.66	162.60	3.06
O4-Fe-O2	85.41	89.20	-3.79
O4-Fe-O3	81.46	77.80	3.66
O5-Fe-O1	97.76	84.90	12.86
O5-Fe-O2	170.58	158.10	12.48
O5-Fe-O3	93.72	91.30	2.42
O5-Fe-O4	95.76	109.80	-14.04
O6-Fe-O1	92.67	104.80	-12.13
O6-Fe-O2	88.44	90.70	-2.26
O6-Fe-O3	173.48	159.00	14.48
O6-Fe-O4	93.88	87.40	6.48
O6-Fe-O5	82.16	79.70	2.46
N1-O1-Fe	109.22	112.00	-2.78
C2-N1-O1	113.13	115.70	-2.57
C2-O2-Fe	108.82	116.60	-7.78
O2-C2-N1	109.18	116.90	-7.72
N2-O3-Fe	107.90	112.30	-4.40
C2-N2-O3	112.53	115.90	-3.37
C2-O4-Fe	110.27	118.50	-8.23
O4-C2-N2	110.55	115.10	-4.55
N3-O5-Fe	109.27	110.10	-0.83
C3-N3-O5	112.87	117.10	-4.23
C3-O6-Fe	108.61	117.80	-9.19
O6-C3-N3	109.48	114.80	-5.32

Table 2. Comparison of bond distances of the crystal structure of terricolin,[20] to the data obtained from the computational study.

Terricolin- Fe^{3+} complex (FeL_3)			
Bond distances (Angstroms) of computational data VS crystal structure			
Bonds	Bond length (Computed)	Bond length (crystal struc)	Difference
Fe-O1	2.039	2.012	0.027
Fe-O2	2.068	1.982	0.086
Fe-O3	2.029	2.019	0.010
Fe-O4	2.076	1.974	0.102
Fe-O5	2.030	2.038	-0.008
Fe-O6	2.072	1.977	0.095
N1-O1	1.388	1.371	0.017
N1-C1	1.457	1.361	0.096
C1-O2	1.428	1.268	0.160
N2-O3	1.385	1.380	0.005
N2-C2	1.460	1.361	0.099
C2-O4	1.435	1.276	0.159
N3-O5	1.387	1.382	0.005
N3-C3	1.458	1.400	0.058
C3-O6	1.429	1.277	0.152

The bond distances and angles of terricolin, calculated using the semi-empirical method, were compared to the experimental data of the crystal structure. This comparison served as a reference to test the semi-empirical method used and to correlate the complexes formed to that of known siderophores. Comparing the difference in bond distances and angles collected from the computational method and the experimental data, little significance was evident. The minor differences noted could be attributed to experimental error; nonetheless, the differences are not sufficiently significant to fully negate the semi-empirical method used for this study.

7.3.1.1 Bryostatin analogues

The dipole moments for some of the bryostatin analogues increased (7b **54**, 7c **54**, 8 **55**) while others (7a **54**, 7d **54**) showed a decrease in the dipole moment (Table 3). This is important as it shows the probability of these analogues to act as efficient medicinal agents. The higher the dipole moment the more polar the complex will be, thus increasing the likelihood of them to exist and act as more efficient agents (Table 7 and 8). The analogues used above have been tested to determine their efficacy as medicinal agents alone; from all five analogues, 7b, 7c and 8 showed substantial efficacy, with 7c showing the most potency.[18]

As shown below, the dipole moments for these analogues did increase when bound to Fe^{3+}. The surface volumes for the complexes bound to Fe^{3+} were similar in value to the analogues alone; however 7b did show a slight increase in surface volume, (Table 3). This consistency in surface volume is most likely due to the structure of the compounds, especially with regard to the Fe-O bonds that were used; all consistent for each analogue. Therefore, the consistency in surface volume and change in surface area for the analogues is most likely due to the change in conformation of the complex when bound to Fe^{3+}.

The decrease in surface area for all the analogues respectively, can be correlated to the contraction of the compounds when bound to Fe^{3+}. The increase in dipole moment is also important as the D/V ratio (dipole moment to surface volume) suggestively determines the ability for the analogues to act as polar or non-polar complexes. For example, 7c has a D/V = 0.0578 (Table 7) with references to the D/V ratios of polar and non-polar solvents listed in Table 8.

Table 3. Bryostatin analogues with and without Fe^{3+}. [18]

Bryostatin analogues	Molecular Formula	Molecular weight (amu)	Dipole moment (debye)	Surface Volume (Å^3)	Surface Area (Å^2)	Average Fe–O bond distances (Å)
7a	$C_{33}H_{50}O_{13}$	654.750	22.384	650.271	667.229	
7a w/ Fe^{3+}	$C_{33}H_{48}FeO_{13}$	708.581	21.618	651.103	653.024	2.103 ± 0.150
7b	$C_{39}H_{62}O_{12}$	722.913	37.712	752.619	778.372	
7b w/ Fe^{3+}	$C_{39}H_{62}FeO_{13}$	794.759	42.928	769.307	775.394	2.098 ± 0.129
7c	$C_{39}H_{62}O_{13}$	738.912	40.386	760.137	787.003	
7c w/ Fe^{3+}	$C_{39}H_{60}FeO_{13}$	792.743	43.945	760.913	772.613	2.105 ± 0.151
7d	$C_{41}H_{64}O_{14}$	780.949	45.796	801.845	827.404	
7d w/ Fe^{3+}	$C_{41}H_{64}FeO_{14}$	836.796	33.838	805.185	811.364	2.128 ± 0.164
8	$C_{43}H_{70}O_{13}$	795.020	28.528	833.764	862.859	
8 w/ Fe^{3+}	$C_{43}H_{68}FeO_{13}$	848.851	43.634	832.937	840.560	2.118 ± 0.183

Structures for the bryostatin analogues **54-56** (7a-d and 8) see chapter 1, section 1.2.3.

7.3.1.2 Bryostatin structures

The geometric shift, shown for bryostatin 1 **9a** in Fig. 7(a-c), demonstrates the decrease of surface area from bryostatin 1 alone to bryostatin 1 when bound to two Fe^{3+} ions. The slight increase in distance when bound to one Fe^{3+} ion could be due to the Fe-O bonds used, as well as the configuration that is formed when the Fe-O bonds are made. This geometric shift is similar to that of the amphiphilic siderophore acinetoferrin, which has shown to significantly alter its geometry when bound to Fe^{3+}, resulting in a change in surface area. Changing the Fe-O bonds used to from the hexavalent complex can result in the formation of different configurations; further discussed in section 7.4.2.

The decrease in surface area, however, (Fig. 7c), could facilitate an increase in the ability of the complex to penetrate a cell membrane.[25,26] The computational data also showed that molecules bound to a second Fe^{3+} ion resulted in even shorter, and subsequently stronger, Fe-O bonds than those only bound to one Fe^{3+} ion, (Table 4).

(a)

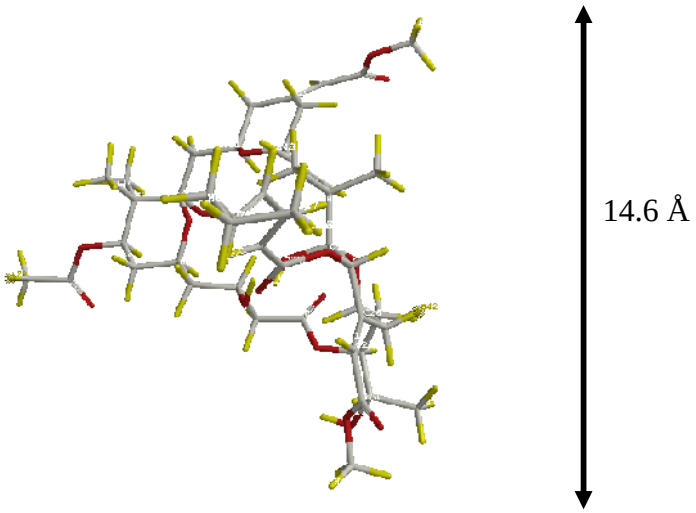

(b)

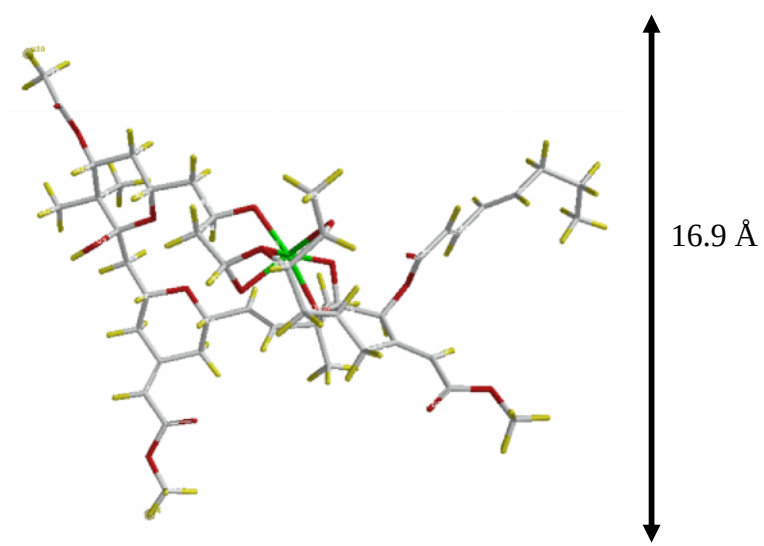

(c)

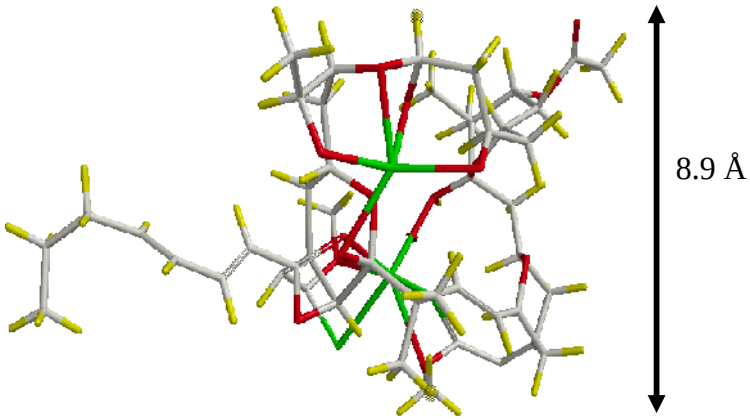

Fig. 7. (a) bryostatin 1 alone (14.6 Å), almost 1.5 nm in diameter; (b) bryostatin 1 bound to one Fe^{3+} results in a complex almost 1.7 nm in diameter; and (c) bryostatin 1 bound to two Fe^{3+} results in a complex that is less than 1 nm in diameter.

The difference in area and length that the binding of iron(III) can have on a compound are shown in Fig. 7. Bryostatin 1 alone has a surface area of 931.642 $Å^2$ and a surface volume of 911.037 $Å^3$. When bound to iron(III) the surface area of the compound decreased to 929.195 $Å^2$ and the surface volume increased to 915.911 $Å^3$.

The dipole moment for all the bryostatin compounds increased when bound to Fe^{3+}. This increase in dipole moment is important as it coincides with the surface volume of the complexes; suggesting a change in chemical properties of the complexes to act as more polar or non-polar agents (Table 7 and 8). The

ratio of the average dipole moment for all twenty bryostatins (DBryo) was less than the average dipole moment for the neutral bryostatins Fe (DFe-Bryo), where the (DFe-Bryo / DBryo) = 1.15 D. This increase in the dipole moment, thus suggests the likelihood of the complex to exist as a polar agent. All the bryostatin compounds showed similar correlations in the geometric parameters; with an equal or slight increase in surface volume and a decrease in surface area (Table 4). The twenty bryostatin compounds have a macrolid structure and each compound differs by the R_1 and R_2 groups (Fig. 1), which can explain the limited change in surface volume for the bryostatins.

For example, bryostatin 1 and bryostatin 2 both have a C8 chain at the R2 position. However, the carboxylic oxygens played no role in the Fe-O bonds used to form the complex, hence, there is no significant difference in the surface volume of either complex. The surface area for bryostatin 2 was much smaller than that of bryostatin 1, most likely due to the replacement of the acetate group of the R_1 side chain of bryostatin 1, by a hydroxyl group to form bryostatin 2. Another example is bryostatin 8, which has the same substituent groups at the R_1 and R_2 position. There was no significant change in the surface volume, however, the surface area decreased significantly when bound to Fe^{3+} (Table 2), which is mostly likely due to the contraction of the molecule.

Most of the other bryostatin compounds all showed a decrease of > 10 $Å^2$ in the surface area when the compounds were bound to Fe^{3+}. This may be due to the difference in the side chains of these bryostatin compounds. The loss of the carboxyl group at the R_2 position for many of the bryostatin compounds results in a decrease in surface area; when bound to Fe^{3+}, the surface area for the complex decreases even more. This is most likely due to the change in geometry and conformation of the complex. However, it is important to note, that this change in

surface area is also dependent on the Fe-O bonds used; since the compound contracts, when bound to Fe^{3+}, with an accompanying decrease in surface area.

The similarity in surface volume of the complexes with and without Fe^{3+} may be due to bryostatins macrolid structure. When the compounds are bound to Fe^{3+}, the iron fills the empty space of the compound contracting the molecule, thereby decreasing the surface area of the complex. Due to the Fe-O bonds that were used, this contraction did not affect the surface volume of the complex; however other configurations may alter these paramters, see section 7.4.2. The Fe-O bonds used were based on the shortest Fe-O bonds formed when the compounds were bound to Fe^{3+}. These results are supported by the concept that shorter bond distances form more compact and stable complexes, and are more likely to exist in nature, as previous studies have reported in relation to other iron chelating compounds.[26]

Table 4. Bryostatin compounds 1-20 with and without Fe^{3+}. Bryostatin 1, like the siderophores in section 7.3.1.3, has a non-polar (C8 group) and a polar (macrolid) structure. The table below shows the geometric parameters calculated for the twenty bryostatin compounds, before and after binding to Fe^{3+}.[15]

Structures	Molecular formula	Molecular Weight (amu)	Dipole moment (debeye)	Surface volume ($Å^3$)	Surface area ($Å^2$)	Average Fe-O bond distance (Å)
bryostatin 1	$C_{47}H_{68}O_{17}$	905.044	48.783	911.037	931.642	
bryostatin 1 w/ Fe^{3+}	$C_{47}H_{66}FeO_{17}$	958.875	33.462	915.911	929.195	2.104 ± 0.126
bryostatin 2	$C_{45}H_{66}O_{16}$	863.007	7.308	872.999	894.609	
bryostatin 2 w/ Fe^{3+}	$C_{45}H_{64}FeO_{15}$	916.838	29.018	874.760	884.751	2.228 ± 0.253
bryostatin 3	$C_{46}H_{64}O_{17}$	889.001	6.695	882.278	896.238	
bryostatin 3 w/ Fe^{3+}	$C_{46}H_{62}FeO_{17}$	942.832	26.223	884.834	886.467	2.103 ± 0.121
bryostatin 4	$C_{46}H_{70}O_{17}$	895.049	6.406	905.960	931.165	
bryostatin 4 w/ Fe^{3+}	$C_{46}H_{68}FeO_{17}$	948.880	28.314	905.268	913.769	2.091 ± 0.116
bryostatin 5	$C_{44}H_{66}O_{17}$	866.995	2.858	868.260	888.089	
bryostatin 5 w/ Fe^{3+}	$C_{44}H_{64}FeO_{17}$	920.826	37.042	870.207	886.959	2.308 ± 0.330
bryostatin 6	$C_{43}H_{64}O_{17}$	852.968	7.376	849.498	864.338	
bryostatin 6 w/ Fe^{3+}	$C_{43}H_{62}O_{17}$	906.799	10.482	848.734	836.732	2.150 ± 0.145
bryostatin 7	$C_{41}H_{60}O_{17}$	824.914	2.940	813.728	831.086	
bryostatin 7 w/ Fe^{3+}	$C_{41}H_{58}FeO_{17}$	878.745	16.529	815.666	829.861	2.308 ± 0.329
bryostatin 8	$C_{45}H_{68}O_{17}$	881.022	5.833	888.581	918.609	
bryostatin 8 w/ Fe^{3+}	$C_{45}H_{66}FeO_{17}$	934.853	19.234	887.740	895.777	2.112 ± 0.140
bryostatin 9	$C_{43}H_{64}O_{17}$	852.968	5.779	851.952	878.810	
bryostatin 9 w/ Fe^{3+}	$C_{43}H_{62}FeO_{17}$	906.799	14.423	851.380	863.050	2.122 ± 0.120
bryostatin 10	$C_{42}H_{64}O_{15}$	808.959	6.199	818.793	839.137	
bryostatin 10 w/ Fe^{3+}	$C_{42}H_{62}FeO_{15}$	862.790	19.541	820.713	827.993	2.242 ± 0.254

bryostatin 11	$C_{39}H_{58}O_{15}$	766.878	3.983	763.779	776.237	
bryostatin 11 w/ Fe^{3+}	$C_{39}H_{56}FeO_{15}$	820.709	9.228	764.304	764.038	2.098 ± 0.144
bryostatin 12	$C_{49}H_{72}O_{17}$	933.098	9.272	950.561	971.828	
bryostatin 12 w/ Fe^{3+}	$C_{49}H_{70}FeO_{17}$	986.929	17.735	948.788	950.136	2.165 ± 0.146
bryostatin 13	$C_{41}H_{62}O_{15}$	794.932	6.795	800.947	820.674	
bryostatin 13 w/ Fe^{3+}	$C_{41}H_{60}FeO_{15}$	848.763	20.835	801.459	805.079	2.103 ± 0.152
bryostatin 14	$C_{42}H_{64}O_{16}$	824.958	4.692	828.135	849.643	
bryostatin 14 w/ Fe^{3+}	$C_{42}H_{62}FeO_{16}$	878.789	35.495	828.174	833.572	2.108 ± 0.120
bryostatin 15	$C_{47}H_{68}O_{18}$	921.043	8.989	921.670	947.743	
bryostatin 15 w/ Fe^{3+}	$C_{46}H_{66}FeO_{18}$	974.874	20.382	921.703	932.350	2.139 ± 0.156
bryostatin 16	$C_{42}H_{62}O_{14}$	790.944	2.488	808.941	834.381	
bryostatin 16 w/ Fe^{3+}	$C_{42}H_{62}FeO_{14}$	846.791	14.318	813.351	811.701	2.231 ± 0.207
bryostatin 17	$C_{42}H_{62}O_{14}$	790.944	2.488	808.941	834.381	
bryostatin 17 w/ Fe^{3+}	$C_{42}H_{62}FeO_{14}$	846.791	14.318	813.352	811.707	2.231 ± 0.207
bryostatin 18	$C_{42}H_{64}O_{15}$	808.959	8.490	820.235	841.554	
bryostatin 18 w/ Fe^{3+}	$C_{42}H_{62}FeO_{15}$	862.790	31.415	820.137	826.972	2.139 ± 0.148
bryostatin 19	$C_{45}H_{66}O_{17}$	879.006	5.757	873.359	887.340	
bryostatin 19 w/ Fe^{3+}	$C_{45}H_{64}FeO_{17}$	932.837	30.848	874.076	871.615	2.103 ± 0.121
bryostatin 20	$C_{41}H_{60}O_{15}$	792.916	4.179	788.651	802.506	
bryostatin 20 w/ Fe^{3+}	$C_{41}H_{58}FeO_{15}$	846.747	30.653	790.164	787.589	2.122 ± 0.128

The three main oxygens (Fig. 1, O^{8}, O^{12} and O^{15})[18] used to form the Fe-O bonds, have been identified as the three oxygens on bryostatin 1, which are used for pkc binding. In this study, these three main oxygens were used to propose that if bryostatin binds Fe^{3+} using these oxygens it can; 1) protect the bonds from hydrolysis or degradation, see Fig. 8, and 2) aid in the delivery of the complex at the active site in the body more efficiently.

The contraction of the complex is important, as it protects many of the groups that are susceptible to hydrolysis (Fig. 8). Fig. 8a shows some of the oxygens that appear to be less hindered, therefore more susceptible to hydrolysis in comparison to the bryostatin-Fe^{3+} complex (Fig. 8b), which has protected the bonds. The binding of bryostatin complex to two Fe^{3+} ions showed a significant decrease in the overall diameter of the complex. This clearly shows the change in geometric shift and contraction of the molecule when bound to iron to form a more rigid complex.

(a) (b)

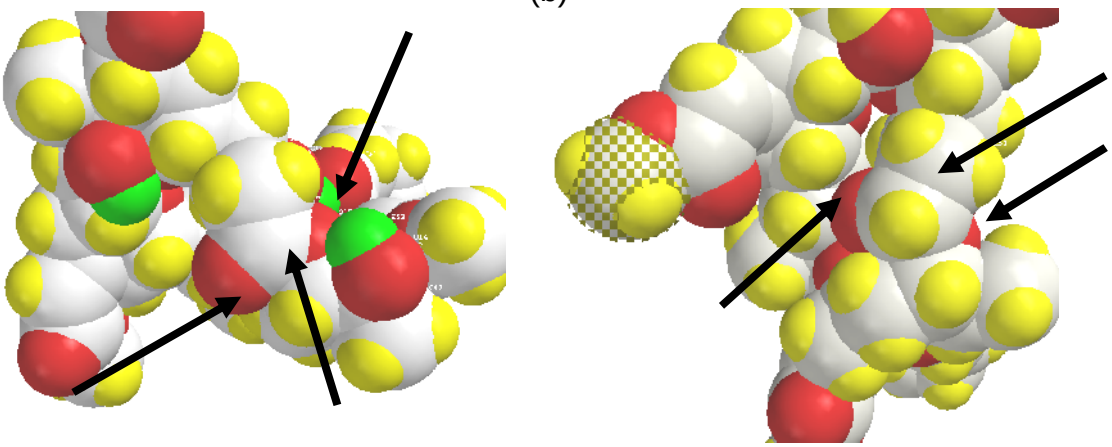

Fig. 8. (a) The space filling model of bryostatin 1 alone; (b) The space filling model of bryostatin 1 bound to Fe^{3+}. In both illustrations arrows point to the carbon (white), two oxygens (red) and the hydrogen (yellow/green) can also be identified in the calculated structure.

The primary interest here was to analyze the Fe-O bond distances; however, Fe-N bonds in siderophores containing nitrogen atoms were also examined. This information was then compared to the Fe-O bond distances of the same compound. The results below show that Fe-O and Fe-N bonds can also

be used to form the hexavalent complex. Data showed that the average bond distances and angles from the combined structure were consistent with the Fe-O bond distances of bryostatin bound to Fe^{3+}. The six shortest respective Fe-O/Fe-N (2.067 Å, 2.170 Å, 2.154 Å, 2.050 Å, 2.037 Å, 1.886 Å) bond distances for aerobactin, ($C_{22}H_{36}N_4O_{13}$, 564.2273 g/mol) remained the same when compared to the Fe-O bond distances and angles of bryostatin, other siderophores, and MNPs (Fig. 9).[15]

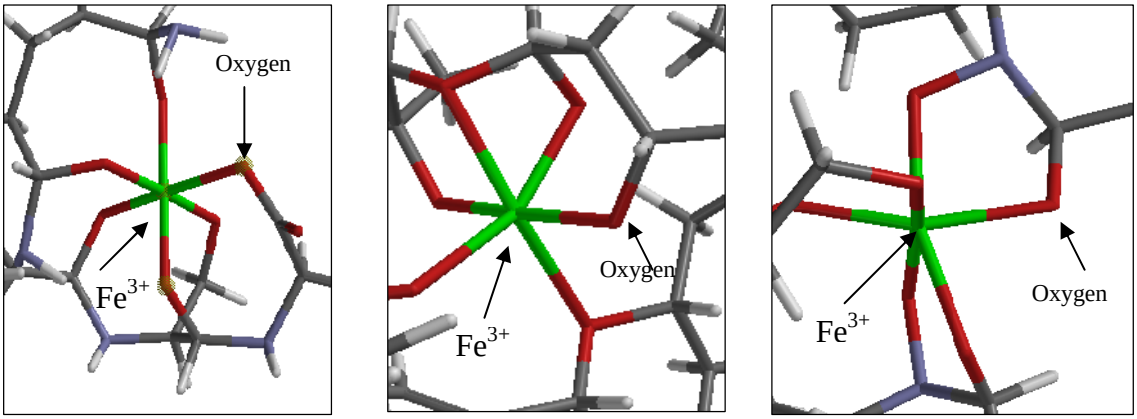

Fig. 9(a-c). a) the aquachelin a-Fe^{3+} complex, b) the marinobactin B-Fe^{3+} complex, and c) the bryostatin19-Fe^{3+} complex.[15]

The C-O and C=O bond distances on the bryophan ring were calculated for bryostatins 1-20 and were compared to the same C-O bonds when Fe^{3+} was complexed. The C-O distances showed an increase from 1.357 Å and 1.223 Å to 1.383 Å and 1.479 Å respectively, indicating a reduction in C-O bond strength. Binding Fe^{3+} to the C=O bond shifted the bond, forming a Fe-O-H bond. A strong correlation can be shown by comparing the calculated charges for bryostatin 1 (-0.32), aquachelin (-0.38), desferrioxamine (-0.56), bryostatin analogue (-0.30) and dolostatin 10 (-0.36). Despite the fact that the charge for desferrioxamine is significantly larger in comparison to the other compounds, a close correlation can be made using aquachelin as a strong reference.

It was also evident that the ester bonds were susceptible to hydrolysis in an acidic, neutral or basic medium, which is important in the formation or

rearrangement of the bryostatin 1 bonds in the body. Additionally the charge impact that binding Fe^{3+} has on water solubility of the complex is an important parameter.

7.3.1.3 Siderophores

The dipole moments for the different siderophores (Table 5) show either a decrease or an increase in dipole moment, when bound to Fe^{3+}. Table 5 also shows that siderophores bound to two Fe^{3+} ions had a higher dipole moment than the same siderophore bound to only one Fe^{3+} ion. Aside from a change in dipole moment, many of the complexes also show a change in surface volume. Many siderophore compounds such as the marinobactins and the aquachelins are separated into two sections; 1) a hydrophilic region and 2) a hydrophobic region (Fig. 3). Siderophores bind Fe^{3+} at the hydrophilic region, transforming the conformation of the complex to act as phospholipds in order to penetrate the cell membrane. This new conformation could explain the change in surface area and volume as indicated inTable 5. Other siderophores form vesicles when bound to Fe^{3+}, resulting in a change in the surface area and volume of the complex (Fig. 5). It is important to note, however, that this change in surface area of the compounds is also dependent on the Fe-O or Fe-N bonds that are used in the hydrophilic region, to form the hexavalent complex.

This increase in surface volume is suggestively based on the configuration of the bonds used to form the hexavalent complex. The bonds used in this study show an increase in surface volume and a decrease in surface area for most of the complexes. It is proposed that there is a correlation between those two properties, whereby as the surface area decreases the volume increases due to the contraction of the molecule when the Fe-O bonds form. It is suggested that this results from an increase in the overlapping of molecules of the complex, and

hence an increase in surface volume. The change in dipole moment is important as it coincides with the surface volume of the complexes; suggesting a change in chemical properties of the complexes to act as more polar or non-polar agents (Table 7 and 8).

As put forward by other studies, the change in surface area is probably due to the change in conformation of the compound when bound to Fe^{3+}. Previous work comparing the surface area of marinobactin and acinetoferrin bound with and without Fe^{3+} showed that the surface area of marinobactin increased when bound to Fe^{3+}, whereas in contrast the surface area of acinetoferrin decreased when bound to Fe^{3+}.[27,28] This change in surface area was suggestively correlated to the conformation that the complex forms when bound to Fe^{3+}. As described earlier, the specific Fe-O bonds that were used to form the siderophore complexes, in this study, were based on the shortest Fe-O bond lengths, with most of the siderophores showing an increase in surface area and decrease in surface volume. However it is important to be aware that varying the Fe-O bonds could alter these parameters.

Table 5. Computational data for the siderophores studied, with and without Fe^{3+}.[15] Known siderophores, some currently in clinical trials, acting as different medicinal agents were subjected to the same calculations.

Species	Molecular formula	Molecular weight (amu)	Dipole moment (debeye)	Surface volume ($Å^3$)	Surface area ($Å^2$)	Average Fe-O bond distances (Å)
aerobactin	$C_{22}H_{36}N_4O_{13}$	564.545	28.647	524.837	556.054	
aerobactin w/ 1 Fe^{3+}	$C_{22}H_{34}FeN_4O_{13}$	618.376	18.809	528.110	547.086	2.077 ± 0.057
alpidine	$C_{57}H_{87}N_7O_{15}$	1112.373	1.3641	1148.747	1157.035	
alpidine w/ 1 Fe^{3+}	$C_{57}H_{93}FeN_7O_{15}$	1172.252	20.691	1165.283	1165.553	2.135 ± 0.143
aquachelin a	$C_{44}H_{74}N_{10}O_{20}$	1063.126	51.717	1024.458	1094.540	
aquachelin a w/ 1 Fe^{3+}	$C_{44}H_{76}FeN_{10}O_{20}$	1120.989	39.793	1034.619	1068.828	1.765 ± 0.798
aquachelin a w/ 2 Fe^{3+}	$C_{44}H_{78}Fe_2N_{10}O_{20}$	1178.852	39.255	1045.879	1056.077	2.001 ± 0.051
aquachelin b	$C_{44}H_{76}N_{10}O_{20}$	1065.142	35.717	1031.363	1098.865	
aquachelin b w/ 1 Fe^{3+}	$C_{44}H_{78}FeN_{10}O_{20}$	1123.005	40.206	1041.949	1079.730	2.087 ± 0.055
aquachelin b w/ 2 Fe^{3+}	$C_{44}H_{80}Fe_2N_{10}O_{20}$	1180.868	45.627	1050.356	1062.959	1.991 ± 0.049
aquachelin c	$C_{46}H_{78}N_{10}O_{20}$	1091.180	37.991	1063.511	1133.680	
aquachelin c w/ 1 Fe^{3+}	$C_{46}H_{80}FeN_{10}O_{20}$	1149.043	37.428	1074.169	1110.287	2.143 ± 0.086
aquachelin c w/ 2 Fe^{3+}	$C_{46}H_{82}Fe_2N_{10}O_{20}$	1206.906	48.975	1085.751	1101.872	2.149 ± 0.096
aquachelin d	$C_{46}H_{80}N_{10}O_{20}$	1093.196	42.594	1067.962	1138.214	
aquachelin d w/ 1 Fe^{3+}	$C_{46}H_{82}FeN_{10}O_{20}$	1151.059	38.408	1078.411	1123.971	2.179 ± 0.152
aquahcelin d w/ 2 Fe^{3+}	$C_{46}H_{84}Fe_2N_{10}O_{20}$	1208.922	48.384	1090.305	1117.350	2.169 ± 0.168
dolastatin 10	$C_{42}H_{68}N_6O_6S$	785.108	18.932	848.573	874.826	
dolastatin 10 w/ 1 Fe^{3+}	$C_{42}H_{72}FeN_6O_6S$	844.987	15.489	860.335	856.057	2.189 ± 0.191
dolastatin 15	$C_{45}H_{68}N_6O_9$	837.072	50.139	888.085	912.794	
dolastatin 15 w/ 1 Fe^{3+}	$C_{45}H_{74}FeN_6O_9$	898.967	32.901	905.904	899.573	2.221 ± 0.151
enterobactin	$C_{30}H_{27}N_3O_{15}$	669.552	13.901	593.574	613.654	
enterobactin w/ 1 Fe^{3+}	$C_{30}H_{29}FeN_3O_{15}$	727.415	14.770	604.596	598.227	2.206 ± 0.189

Et-743	$C_{39}H_{43}N_3O_{11}S$	761.849	15.632	711.825	683.061	
Et-743 w/ 1 Fe^{3+}	$C_{39}H_{42}FeN_3O_{11}S$	816.688	13.837	712.990	653.299	2.238 ± 0.298
marinobactin a	$C_{40}H_{69}N_9O_{16}$	932.039	70.010	915.728	973.253	
marinobactin a w/ 1 Fe^{3+}	$C_{40}H_{69}FeN_9O_{16}$	987.886	50.189	919.446	953.124	2.045 ± 0.048
marinobactin a w/ 2 Fe^{3+}	$C_{42}H_{73}Fe_2N_9O_{16}$	1047.765	60.865	934.739	929.829	2.105 ± 0.097
marinobactin b	$C_{42}H_{71}N_9O_{16}$	958.077	71.999	948.352	1009.735	
marinobactin b w/ 1 Fe^{3+}	$C_{42}H_{71}FeN_9O_{16}$	1013.924	64.766	951.945	983.553	2.046 ± 0.025
marniobactin b w/ 2 Fe^{3+}	$C_{42}H_{75}Fe_2N_9O_{16}$	1073.803	89.768	968.320	972.604	2.059 ± 0.054
marinobactin c	$C_{42}H_{73}N_9O_{16}$	960.093	84.663	952.276	1011.999	
marinobactin c w/ 1 Fe^{3+}	$C_{42}H_{73}FeN_9O_{16}$	1015.940	80.085	955.125	978.997	2.050 ± 0.033
marinobactin c w/ 2 Fe^{3+}	$C_{42}H_{77}Fe_2N_9O_{16}$	1075.819	94.006	970.237	973.300	2.084 ± 0.059
marinobactin d1	$C_{44}H_{75}N_9O_{16}$	986.131	93.838	985.031	1048.212	
marinobactin d1 w/ 1 Fe^{3+}	$C_{44}H_{75}FeN_9O_{16}$	1041.978	81.426	988.433	1027.461	2.045 ± 0.049
marinobactin d1 w/ 2 Fe^{3+}	$C_{44}H_{79}Fe_2N_9O_{16}$	1101.857	86.747	1002.195	1002.303	2.075 ± 0.049
marinobactin d2	$C_{44}H_{75}N_9O_{16}$	986.131	92.791	984.942	1047.869	
marinobactin d2 w/ 1 Fe^{3+}	$C_{44}H_{75}FeN_9O_{16}$	1041.978	87.699	988.464	1020.479	2.039 ± 0.023
marinobactin d2 w/ 2 Fe^{3+}	$C_{44}H_{79}Fe_2N_9O_{16}$	1101.857	50.395	1003.720	1002.450	2.029 ± 0.033
marinobactin e1	$C_{44}H_{77}N_9O_{16}$	988.147	102.015	988.941	1051.520	
marinobactin e1 w/ 1 Fe^{3+}	$C_{44}H_{77}FeN_9O_{16}$	1043.994	97.333	992.427	1024.834	2.039 ± 0.023
marinobactin e1 w/ 2 Fe^{3+}	$C_{44}H_{81}Fe_2N_9O_{16}$	1103.873	106.858	1007.867	1012.481	2.028 ± 0.032
peloruside a	$C_{27}H_{48}O_{11}$	548.670	14.313	560.189	572.823	
peloruside a w/ 1 Fe^{3+}	$C_{27}H_{45}FeO_{11}$	601.493	14.924	563.297	562.969	2.145 ± 0.326
spongastatin	$C_{63}H_{95}ClO_{21}$	1223.885	25.413	1222.082	1244.903	
spongastatin w/ 1 Fe^{3+}	$C_{63}H_{91}ClFeO_{21}$	1275.700	15.895	1219.238	1231.336	2.315 ± 0.163

7.3.1.4 Marine natural products

Many of the MNPs used in this study are families of compounds, with each differing by specific substituent groups on the compound. For example briarellin has four different families (briarellin M, N, O, and P), when bound to Fe^{3+} all briarellin compounds showed similar changes in geometry. The dipole moment, surface area and surface volume for each increased when bound to Fe^{3+}. This is significant as it shows consistency with the binding of Fe^{3+}. The increase in dipole is also crucial for these compounds as it improves the efficacy of the compound as a medicinal agent. The consistent increase of both dipole moment and surface volume is symmetrically important as this determines the ability of the compounds to act as polar or non-polar agents. The higher the dipole moment the more likely the complex is to exist as a polar agent, thereby increasing its permeability across the cell membrane.

The surface area and volume for the MNPs used in this study, increased when an iron complex was formed. The variance in conformations when bound to Fe^{3+} is a plausible argument for the subsequent change in both these parameters. However, it is important to note, that if different Fe-O bonds are utilized, it is likely that these parameters may change also, depending on the new conformation that is formed. The Fe-O bonds used in this study were chosen as the most appropriate, based on the shortest bond lengths that were formed when bound to Fe^{3+}. This is based on the supposition that shorter bond lengths form more stable complexes and the likelihood of the complexes to exist is more probable.

Many MNPs have available substituent groups (N, O) to bind more than one Fe^{3+} ion. Table 6 shows two examples of MNPs (spirastrellolide and phakellistatin) bound to one and two Fe^{3+} ions respectively. This demonstrates 1) that these complexes can bind more than one Fe^{3+} ion; 2) any dipole moment

change in comparison to the compound bound to one Fe^{3+} ion, and 3) the increase in rigidity of the complex when bound to two Fe^{3+} ions. Phakellistatin 12 bound to one Fe^{3+} ion showed an increase in dipole moment from 13.496 to 31.486; when bound to two Fe^{3+} ions, the dipole moment was 20.791 debeye. Even though the dipole moment was lower than the complex bound to one Fe^{3+} ion, it was still higher than the dipole moment of the compound alone. In comparison some of the siderophores', dipole moments increased when bound to two Fe^{3+} ions. There are many factors that could account for such changes, such as 1) the structure of the compound, 2) the conformational change of the complex when bound to two Fe^{3+} ion, and 3) the Fe-O or Fe-N bonds used to form the hexavalent complexes.

Table 6. MNPs with and without Fe^{3+}. The structures for the marine natural products used in this study are as referenced.[29]

Species	Molecular formula	Molecular Wt.(amu)	Dipole moment (debye)	Surface volume (Å^3)	Surface area (Å^2)	Average Fe-O bond distances (Å)
170 - lobophorolide	$C_{42}H_{70}O_{12}$	767.010	24.465	821.262	827.763	
170 - lobophorolide w/ Fe^{3+}	$C_{42}H_{72}FeO_{15}$	872.870	20.356	874.094	888.383	2.171 ± 0.124
277 - myriastramide a	$C_{45}H_{58}N_8O_9$	855.006	33.464	859.918	869.386	
277 - myriastramide a w/ Fe^{3+}	$C_{45}H_{64}FeN_8O_{10}$	932.900	16.240	895.184	893.534	2.229 ± 0.124
278 - myriastramide b	$C_{45}H_{57}ClN_8O_9$	889.451	33.350	874.214	884.921	
278 - myriastramide b w/ Fe^{3+}	$C_{45}H_{63}ClFeN_8O_{10}$	967.345	40.485	906.271	894.824	2.200 ± 0.144
279 - myriastramide c	$C_{42}H_{53}N_9O_7S$	828.008	21.484	817.097	815.829	
279 - myriastramide c w/ Fe^{3+}	$C_{42}H_{59}FeN_9O_8S$	905.902	16.120	851.769	846.524	2.168 ± 0.146
283 - phakellistatin 12	$C_{60}H_{86}N_{10}O_{12}$	1139.406	13.496	1162.423	1148.878	
283 - phakellistatin 12 w/ 1 Fe^{3+}	$C_{60}H_{90}FeN_{10}O_{13}$	1215.284	31.486	1193.910	1179.445	2.106 ± 0.079
283 - phakellistatin 12 w/ 2 Fe^{3+}	$C_{60}H_{96}Fe_2N_{10}O_{14}$	1293.178	20.791	1229.863	1188.992	2.108 ± 0.084
284 - phakellistatin 13	$C_{42}H_{54}N_8O_7$	782.943	20.470	799.640	813.080	
284 - phakellistatin 13 w/ Fe^{3+}	$C_{42}H_{60}FeN_8O_7$	844.838	24.186	819.235	808.058	2.152 ± 0.165
285 - spirastrellolide a	$C_{52}H_{81}ClO_{17}$	1027.252	28.179	1038.984	1058.221	
285 - spirastrellolide a w/ 1 Fe^{3+}	$C_{52}H_{83}FeClO_{20}$	1096.074	22.993	1049.247	1058.917	2.109 ± 0.112
285 - spirastrellolide a w/ 2 Fe^{3+}	$C_{52}H_{81}Fe_2ClO_{21}$	1165.904	22.432	1064.709	1056.299	2.113 ± 0.118
287 - reidispongiolide a	$C_{54}H_{87}NO_{13}$	958.284	22.387	1055.534	1079.636	
287 - reidispongiolide a w/ Fe^{3+}	$C_{54}H_{92}FeNO_{16}$	1067.168	23.258	1111.367	1135.666	2.124 ± 0.064
289 - simplakidine a	$C_{24}H_{37}NO_6$	435.561	20.243	459.882	460.833	
289 - simplakidine a w/ Fe^{3+}	$C_{24}H_{41}FeNO_8$	527.438	18.898	505.459	519.775	2.087 ± 0.076
315 - dicotyodendrins a	$C_{43}H_{33}N_2NaO_{11}S$	808.796	22.488	743.902	751.922	
315 - dicotyodendrins a w/ Fe^{3+}	$C_{43}H_{37}FeN_2NaO_{15}S$	932.671	23.091	811.962	835.947	2.142 ± 0.125
480 - leptocladolides b	$C_{19}H_{24}O_6$	348.395	14.831	345.930	345.943	
480 - leptocladolides b w/ Fe^{3+}	$C_{19}H_{30}FeO_9$	458.287	14.766	407.228	414.032	2.056 ± 0.086
481 - leptocladolides c	$C_{19}H_{24}NO_7$	364.394	5.237	344.905	340.811	

481 - leptocladolides c w/ Fe^{3+}	$C_{19}H_{27}FeNO_9$	455.263	3.966	386.291	375.441	2.206 ± 0.180
490 - diterpine providencin	$C_{23}H_{24}O_{10}$	460.435	8.198	431.225	440.031	
490 - diterpine providencin w/ Fe^{3+}	$C_{23}H_{28}FeO_{13}$	568.311	11.649	481.595	464.461	2.209 ± 0.136
499 - pachyclavulariolides O	$C_{20}H_{30}O_4$	334.456	17.795	362.782	374.889	
499 - pachyclavulariolides O w/ Fe^{3+}	$C_{20}H_{33}FeO_8$	457.323	20.936	429.125	447.993	2.151 ± 0.175
500 - pachyclavulariolides P	$C_{20}H_{28}O_5$	348.439	23.861	363.824	368.024	
500 - pachyclavulariolides P w/ Fe^{3+}	$C_{20}H_{31}FeO_8$	455.307	22.921	417.712	430.093	2.150 ± 0.145
501 - pachyclavulariolides Q	$C_{20}H_{30}O_5$	350.455	19.106	368.305	375.177	
501 - pachyclavulariolides Q w/ Fe^{3+}	$C_{20}H_{33}FeO_8$	457.323	16.571	421.019	433.146	2.163 ± 0.209
512 - briarellin M	$C_{22}H_{34}O_7$	410.507	2.538	409.253	400.052	
512 - briarellin M w/ Fe^{3+}	$C_{22}H_{36}FeO_{11}$	532.366	16.388	475.337	496.179	2.061 ± 0.010
513 - briarellin N	$C_{23}H_{36}O_7$	424.534	1.249	429.518	421.010	
513 - briarellin N w/ Fe^{3+}	$C_{23}H_{39}FeO_{11}$	547.401	11.287	496.390	510.385	2.002 ± 0.072
514 - briarellin O	$C_{24}H_{38}O_7$	438.561	12.003	445.882	439.332	
514 - briarellin O w/ Fe^{3+}	$C_{24}H_{40}FeO_{11}$	560.420	24.975	511.624	532.260	2.060 ± 0.009
515 - briarellin P	$C_{25}H_{40}O_7$	452.588	7.526	466.005	459.895	
515 - briarellin P w/ Fe^{3+}	$C_{25}H_{43}FeO_{11}$	575.455	12.370	532.871	549.244	2.063 ± 0.045
589 - azaspiracid analog	$C_{47}H_{71}NO_{13}$	858.079	33.793	867.838	878.722	
589 - azaspiracid analog w/ Fe^{3+}	$C_{47}H_{75}Fe_2NO_{21}$	1101.797	64.890	995.897	1050.188	2.073 ± 0.025
590 - azaspiracid analog	$C_{47}H_{71}NO_{13}$	858.079	11.398	866.547	871.894	
590 - azaspiracid analog w/ Fe^{3+}	$C_{47}H_{71}FeNO_{16}$	961.923	10.098	915.143	942.871	2.122 ± 0.184
591 - azaspiracid analog	$C_{47}H_{71}NO_{13}$	858.079	19.475	866.879	873.497	
591 - azaspiracid analog w/ Fe^{3+}	$C_{47}H_{74}Fe_2NO_{20}$	1084.79	53.756	981.952	1038.864	2.089 ± 0.121
592 - azaspiracid analog	$C_{47}H_{71}NO_{13}$	858.079	2.917	866.113	870.285	
592 - azaspiracid analog w/ Fe^{3+}	$C_{47}H_{73}FeNO_{17}$	979.938	30.149	933.402	968.081	2.059 ± 0.038
593 - azaspiracid analog	$C_{48}H_{73}NO_{13}$	872.106	28.662	885.390	894.762	
593 - azaspiracid analog w/ Fe^{3+}	$C_{48}H_{77}Fe_2NO_{21}$	1115.824	50.297	1017.023	1082.658	2.057 ± 0.016
594 - azaspiracid analog	$C_{47}H_{71}NO_{12}$	842.080	16.986	859.199	861.406	
594 - azaspiracid analog w/ Fe^{3+}	$C_{47}H_{73}FeNO_{16}$	963.939	28.704	925.202	957.385	2.082 ± 0.054
640 - trunkamide a	$C_{43}H_{63}N_7O_8S$	838.084	21.293	866.264	891.007	

640 - trunkamide a w/ Fe^{3+}	$C_{43}H_{75}Fe_2N_7O_{14}S$	1057.868	33.928	986.172	1024.215	2.003 ± 0.049
660 - shishijimicins b	$C_{45}H_{50}N_4O_{12}S_3$	930.134	32.306	859.915	875.856	
660 - shishijimicins b w/ Fe^{3+}	$C_{45}H_{57}Fe_2N_4O_{19}S_3$	1161.885	13.593	985.899	1015.463	2.064 ± 0.046
664 - diazonamide a	$C_{40}H_{34}Cl_2N_6O_6$	765.654	28.206	698.840	687.669	
664 - diazonamide a w/ Fe^{3+}	$C_{40}H_{40}Cl_2FeN_6O_{10}$	891.545	28.113	774.294	778.160	2.072 ± 0.027
665 - diazonamide analog	$C_{40}H_{33}Cl_2N_5O_7$	766.638	33.514	697.466	686.262	
665 - diazonamide analog w/ Fe^{3+}	$C_{40}H_{39}Cl_2FeN_5O_{11}$	892.529	34.447	771.174	774.637	2.069 ± 0.015

Many of the complexes in this study, that showed a decrease in surface area when bound to Fe^{3+}, may be a result of 1) the contraction of the ligand-Fe^{3+} complex and/or 2) due to the Fe-O bonds used, forming a more stable and compact complex. The overall increase in surface volume could be due to; 1) the Fe-O bonds used and this could impact the overall volume of the complex; and/or 2) the overlapping of the bonds of the molecule, as a result of the contraction of the molecule.[30] However, it is important to note that the major factor in rationalizing the difference in surface area and volume area is most likely related to the oxygen atoms used in the configuration of the complexes.

The D/V ratios, for the ligand-Fe^{3+} complexes in this study are important as they suggest the probability of these molecules to act as polar or non-polar compounds, depending on their D/V value. When comparing the D/V ratios of polar and non-polar solvents (Table 8), it shows the likelihood of the complexes with similar D/V ratios to act accordingly. Therefore, complexes with D/V ratios similar to that of water or methanol are likely to have polar properties, while complexes with D/V ratios similar to hexane or pentanol are likely to have non-polar properties. Bryostatin 1-Fe^{3+} complex has a D/V ratio of 0.0365 and methanol has a D/V ratio of 0.0379. This suggests the ability of the bryostatin 1-Fe^{3+} complex to behave as a polar compound when administered in a polar environment, thus enhancing its benefit as a medicinal agent. Conversely, the bryostatin 11-Fe^{3+} complex has a D/V ratio of 0.0121, in close proximity to that of pentanol with a D/V ratio of 0.0124. This would predict the bryostatin 11-Fe^{3+} complex is likely to have non-polar properties and be ineffective as a medicinal agent.

Table 7. D/V ratios of the different bryostatin analogues bound to Fe^{3+}.

NPs	Dipole moment (D)	Molecular Volume ($Å^3$)	D/V ratio
Bryostatin 1	33.4622	915.9110	0.0365
Bryostatin 2	29.0185	874.7599	0.0332
Bryostatin 11	9.2279	764.3039	0.0121
Et-743	13.8367	712.9895	0.0194
Marinobactin A	60.8652	934.7386	0.0651
Aerobactin	18.8095	528.1101	0.0356
Aquachelin A	39.2551	1045.8799	0.0375
Dolastatin 15	32.9013	905.9043	0.0363
Analogue 7A	21.6177	651.1026	0.0332
Analogue 7b	42.9282	769.3069	0.0558
Analogue 7c	43.9446	760.9129	0.0578
Analogue 8	43.6345	832.9369	0.0524
Phakellistatin 12	31.486	1193.910	0.0264
Briarellin O	24.975	511.624	0.0488
Trunkamide A	33.928	986.172	0.0344
Azaspiracid analog	28.704	925.202	0.0310

Table 8. D/V ratios of common polar and non polar solvents used as a reference to compare against D/V ratios of compounds bound to Fe^{3+}.

solvents	dipole moment (D)	molecular volume ($Å^3$)	D/V ratio
water	1.74	19.24	0.0904
methanol	1.54	40.66	0.0379
ethanol	1.48	59.08	0.0251
propanol	1.59	77.37	0.0206
pentanol	1.41	114.06	0.0124
hexane	0	124.8	0.0000

The importance of charge verses dipole moment on the solubility of these complex compounds can be illustrated by the following example. Hexane has sp^3 hybridized carbons and a small local dipole moment along each C-H bond, but the total molecule has essentially no dipole moment and, subsequently, has little solubility in water. Two anions, ClO_4^- and SO_4^{2-}, are also sp^3 hybridized and have essentially no dipole moment due to their symmetry, but have significant water solubility due to their negative charge.[15] A molecule of low water solubility due to its non-polar nature and neutral charge would either quickly aggregate like a

micelle, or adhere to a low polarity surface. If bryostatin 1 or any of the other marine natural products are in fact siderophores, similarities between the three groups may provide further circumstantial evidence.(15)

7.3.2 Second computational study

In this study, one hundred and seventy-three different configurations of the bryostatin-Fe^{3+} complex were determined, using different oxygens on bryostatin 1. This study was conducted to show the different configurations that the compound can undergo when bound to Fe^{3+} and to also show that the Fe-O bonds formed by the complex are not bond specific, suggesting that the complex can rearrange bonds in order to form stable conformations. Despite the fact, that the structure for the bryostatin-Fe^{3+} complex has not been determined as yet; MALDI-MS data has shown the complex to exist as shown in Fig. 10.

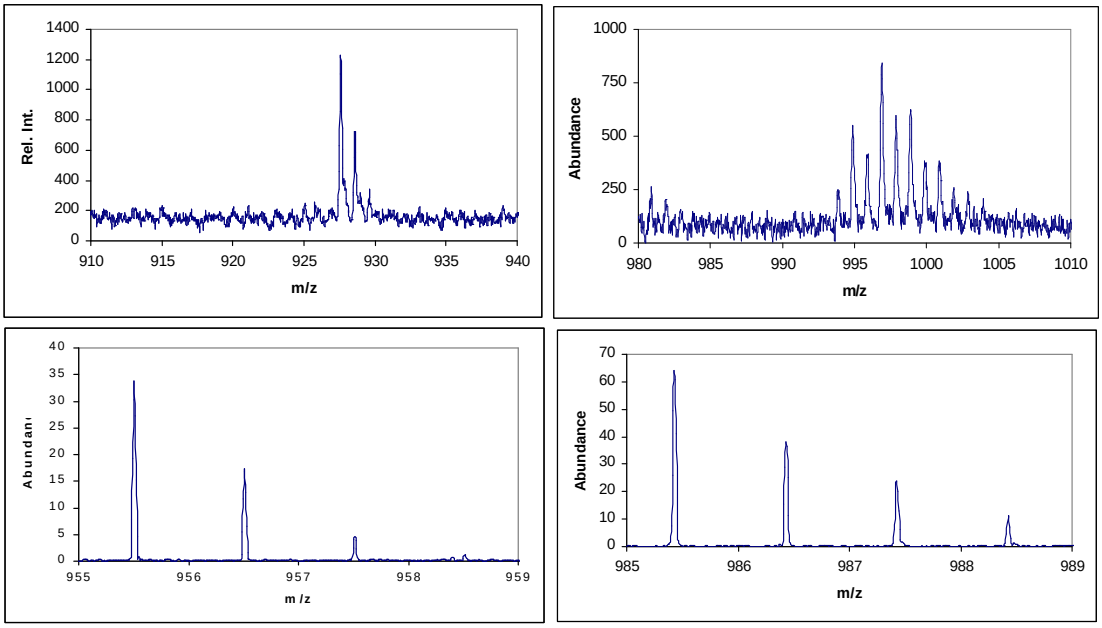

Fig. 10. Top left mass spectrum shows bryostatin 1, *m/z* of 927. Top right mass spectrum shows bryostatin 1+FeOH+Na^{+}, *m/z* of 997. Bottom left shows the mass spectrum of bryostatin 1+Fe^{3+}, *m/z* of 955. Bottom right shows the mass spectrum of bryostatin 1+Na^{+}+Fe^{3+} *m/z* of 985.

Firstly, the data showed that the Fe-O bond distances for the structures given in Tables 10 and 11 were shorter than those in Table 9. The longest, bond

distance found in any of the configurations was 2.7 Å with an average of 2.37 Å, with most of the distances ranging from 1.8-2.5 Å, well within the desired range. The average bond distance obtained for the molecules listed in Table 9 was 2.17 Å, a closer correlation than those obtained from known siderophores.[17] This is important as most siderophores are found in aqueous solution and would indicate the probable existence of such structures.

Secondly, it showed that these compounds could configure their coordinate bonds with iron in water resulting in a more stable conformation, notwithstanding the possible effects of pH, *etc*.. It is important to note that, in some cases, hexadentate compounds can interact one Fe^{3+} coordinating site with water, resulting in the formation of free radicals, causing toxicity, depending on the compound.[26] The need to completely mask the surface of the iron is therefore important in order to minimize this production.

Thirdly, this computational study illustrates numerous configurations available to the fer-mer compound to achieve its most stable conformation. However, the formation of free radicals generally occurs under neutral or alkaline pH values, when the solubility of non-complexed iron is severely limited. Several other factors such as kinetic stability, metal affinity and selectivity, toxicity and bioavailability must be considered to develop effective siderophores as medicinal agents.[26] For example, the binding of Fe^{3+} to six oxygen atoms in bryostatin 1 results in a stable conformation; however, any Fe-O bond has the possibility of breaking at any particular position in the presence of water (in the body) and can bind at another position using a different oxygen atom, resulting in a new configuration. This rearrangement is based on the fact that free solvated ligands and metals bind to form a metal-ligand complex. In doing so the complex is more prone to forming hexavalent geometry, due to its thermodynamically more stable properties.[26]

The difference in molecular masses, shown in the Tables 9-11 is a result of the addition of an hydrogen (H^+) ion when a carbon-oxygen double bond is broken, or when an OH loses its hydrogen ion in order to form a strong Fe-O bond.

7.3.2.1 Most probable conformations

From this batch, a total of twenty-two configurations were selected based on the shortest Fe-O bond distances (Table 9). Structures with bond distances between 1.8-2.5 Å were collected and further analyzed. The complexes in Table 9 were selected based on the theory that shorter bond distances form more stable complexes; hence increasing the likelihood of their existence in nature.

Based on the different configurations shown in Table 9, it is evident that the change in Fe-O bonds to form the hexavalent complex alters the overall D/V ratio of the complex. This is most likely due to the different conformations that arise when the Fe-O bonds form in the different complexes. It is important to note that many of the complexes have short bond distances, however, not all of these complexes have high D/V ratios. This suggests that despite the probability of these complexes to exist based on the stability of their short Fe-O bonds, some might not be effective as medicinal agents, owing to their low D/V values. Ideally the higher the D/V value the more likely it is to act as a polar solvent, implied by comparison to the solvents shown in Table 8. Fig. 11 shows examples of different configurations selected from Table 9, with variable D/V ratios based on the Fe-O bonds and substitution to Fe-OH bonds.

(a)

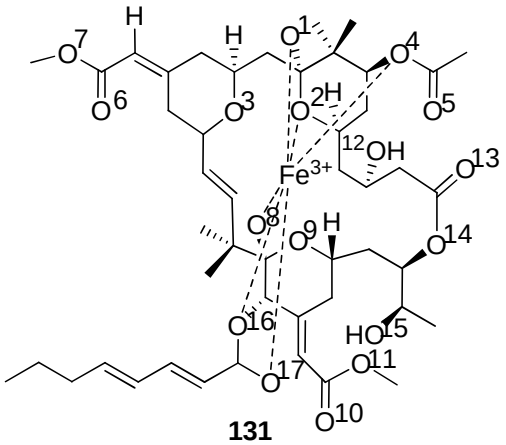

131

(b)

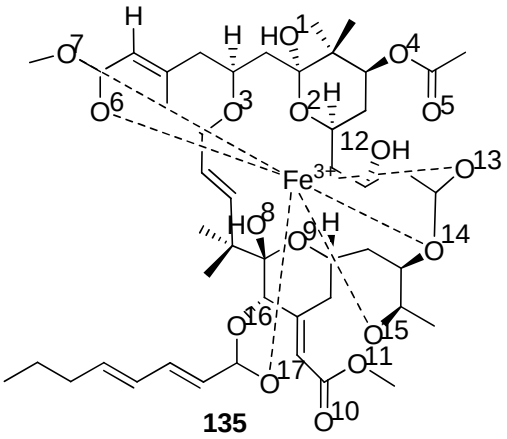

135

(c)

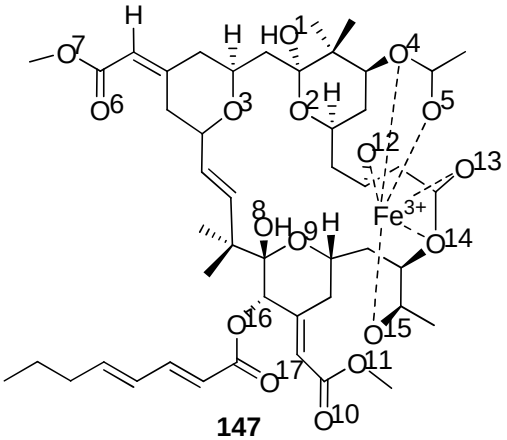

147

(d)

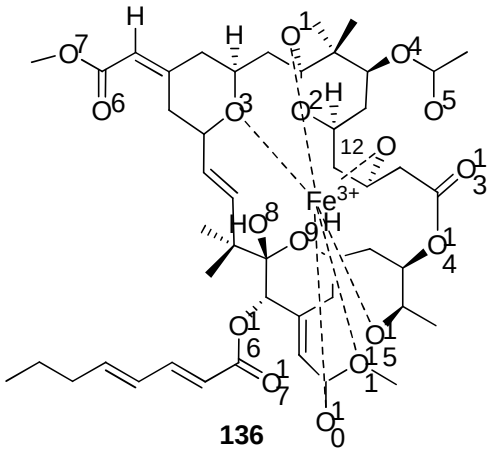

136

Fig. 11. Some configurations with the shortest Fe-O bond distances, with variable D/V ratios for each: a) **131**, D/V = 0.014; b) **135**, D/V = 0.008 and c) **147**, D/V 0.017. d) A configuration of bryostatin 1-Fe^{3+} with an average bond length that is higher than the others shown above, however the D/V ratio is also the highest of all 22 structures shown in Table 9, **136**, D/V = 0.040. The highlighted numbers correlate to those in Table 9.

Table 9. Average bond distances, of the bryostatin-Fe bonds, selected from Appendix VI, showing the most probable bond distances.[17]

Semi empirical PM3 Fe-O Bonds							
code #	Fe-O bonds	Fe-O Bond Distance (Å)	Molecular Wt. (amu)	Surface volume (Å³)	Surface area (Å²)	Dipole moment (Debye)	D/V
131	1,2,4,8,16,17	1.794, 1.894, 2.424, 1.870, 2.212, 1.961	959.883	912.306	879.461	12.562	0.014
132	8,9,12,13,14,15	1.974, 2.533, 2.209, 2.040, 2.018, 2.507	958.875	913.046	907.899	8.945	0.01
133	9,7,12,8,16,13	2.540, 1.875, 2.524, 2.186, 2.091, 2.493	959.883	917.409	914.165	4.224	0.005
134	6,7,8,9,13,17	2.154, 2.185, 2.600, 1.776, 2.327, 2.498	963.915	924.669	897.108	5.534	0.006
135	6,7,13,14,15,17	1.915, 2.371, 1.972, 2.439, 2.005, 2.359	962.907	924.238	922.175	7.129	0.008
136	10,15,12,11,3,1	1.999, 2.534, 1.893, 2.493, 2.153, 2.307	958.875	908.735	874.456	36.768	0.04
137	2,12,6,7,17,1	2.060, 2.466, 2.034, 2.472, 2.227, 2.334	960.891	920.272	905.771	12.045	0.013
138	1,5,8,14,16,17	2.231, 2.152, 1.989, 2.566, 2.480, 2.031	960.891	918.718	903.121	4.480	0.005
139	2,8,9,13,16,17	2.488, 1.885, 2.585, 2.327, 2.448, 2.076	961.899	919.307	903.123	4.891	0.005
140	4,6,10,11,12,13	2.579, 2.467, 2.110, 2.150, 1.874, 2.198	962.907	917.925	878.814	11.592	0.013
141	1,5,8,10,14,15	2.325, 2.036, 2.455, 2.477, 2.442, 2.083	946.864	901.853	889.277	11.914	0.013
142	2,4,6,7,10,15	2.496, 2.567, 1.961, 2.519, 2.290, 2.120	961.899	915.196	843.222	7.117	0.008
143	1,2,10,12,14,15	2.184, 2.407, 2.135, 1.907, 2.572, 2.154	958.875	911.176	892.182	10.924	0.012
144	2,5,12,14,15,17	2.517, 2.230, 1.845, 2.566, 1.996, 2.305	960.891	917.354	900.442	14.974	0.016
145	2,4,5,8,9,12	2.557, 2.452, 2.142, 1.903, 2.495, 2.051	959.883	912.942	893.183	9.271	0.01
146	1,2,4,5,8,10	2.001, 2.445, 2.118, 1.977, 2.427, 2.345	960.891	919.445	912.563	13.158	0.014
147	4,5,12,13,14,15	2.368, 2.001, 2.047, 2.027, 2.275, 2.017	960.891	919.212	923.815	14.922	0.016
148	9,13,14,15,16,17	2.530, 2.075, 2.394, 2.228, 2.524, 2.052	961.899	922.236	924.169	2.567	0.003
149	6,7,13,14,16,17	1.903, 2.495, 1.924, 2.535, 2.556, 2.042	963.915	924.113	913.28	4.683	0.005
150	2,5,6,8,10,15	2.524, 2.313, 2.382, 2.489, 2.440, 1.956	961.899	916.834	865.04	6.000	0.007
151	2,5,6,8,12,16	2.323, 2.461, 2.407, 1.950, 2.008, 2.553	960.891	916.173	880.757	9.501	0.01
152	13,14,15,16,17,1	2.421, 1.924, 2.253, 2.504, 2.505, 1.940	960.891	918.719	897.324	19.417	0.021

7.3.2.2 Configuration with Fe-OH bond

From the most probable configurations listed in Table 9, five were selected based on shortest bond distances. Of these five, six different configurations were developed for each, by replacing a Fe-O bond with a Fe-OH bond. This was investigated as iron and ligands form bonds in aqueous solutions and it may be possible for the bonds to rearrange in water. This would suggest that a Fe-O bond could be replaced with a Fe-OH bond. The bond distances of these complexes were compared to see: 1) which structure is most likely to exist based on the bond distances formed for the complex and 2) which ones have the most suitable D/V ratio to function as possible medicinal agents. The D/V ratio is an important parameter as it suggests the polar properties of the complexes (Table 8). These results also showed that some complexes may have shorter bond distances than others; this in turn alters the D/V ratio.

As shown in Fig. 12 the replacement of a single Fe-O bond with Fe-OH alters the average bond distance, dipole moment and D/V ratio of the complex. For example, Fig. 12a, **153** has an average bond distance of 2.237 and **155** has an average bond distance of 2.086; the dipole moment also increases from 8.145 to 11.333 debeye. This is merely one example of how the substitution of a single bond can alter the parameters of a complex. Based on the bond distances it is probable that these structures would exhibit some stability.

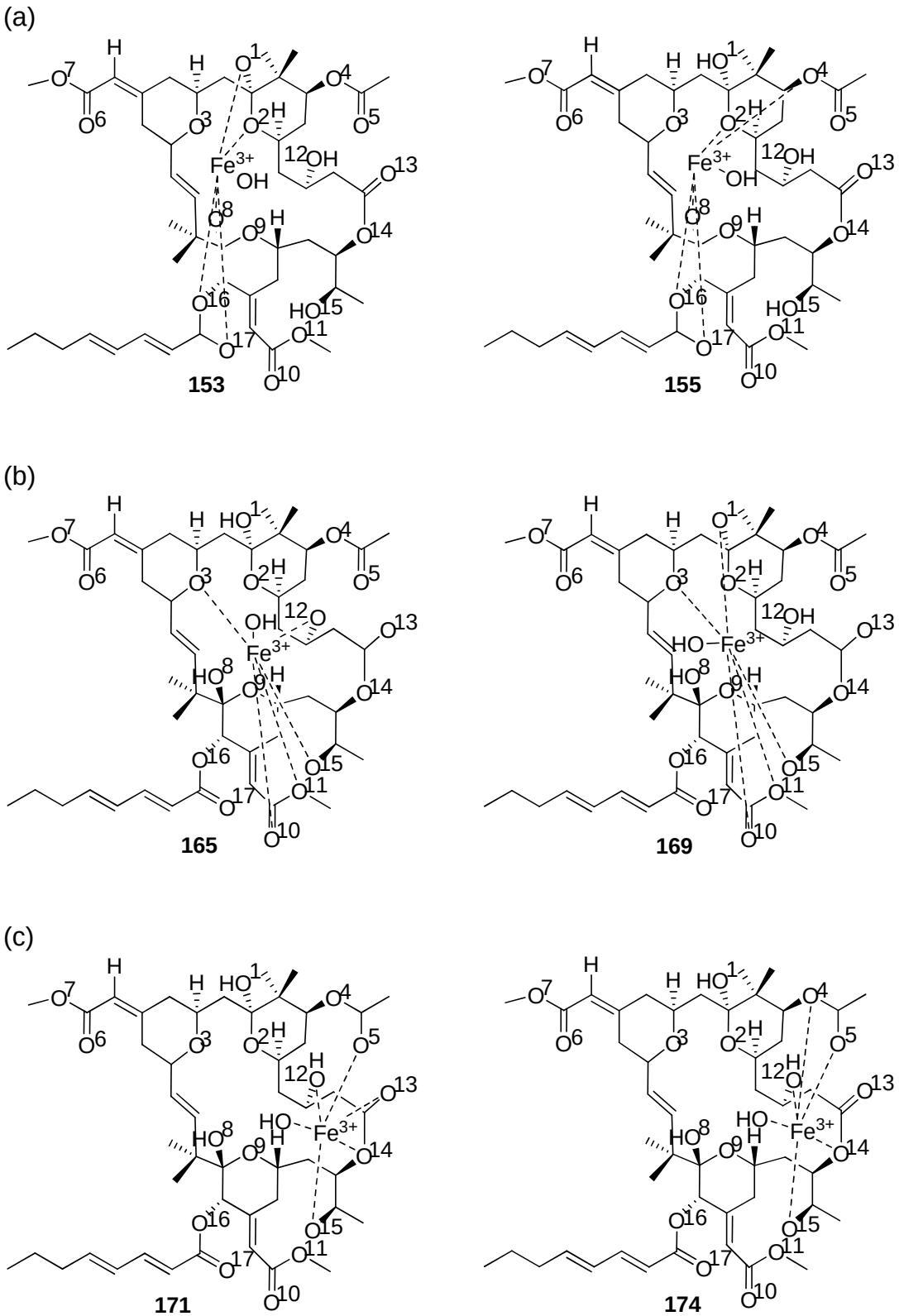

Fig. 12. Shows the change in the D/V ratio by substituting a single Fe-O bond with a Fe-OH bond in each set of samples; a) **153, 155**, D/V = 0.009 and 0.012 respectively; b) **165, 169** D/V = 0.038 and 0.027 respectively; c) **171, 174** D/V = 0.016 and 0.024 respectively.

Table 10. Bond distances and values for the five most probable conformations listed in Table 5. Each conformation has 5 bryostatin oxygens bonded to Fe plus an OH^- ion.[17] The highlighted numbers correlate with the structures in Fig. 12.

Semi empirical PM3, 5 Fe-O BONDS + OH							
code #	Fe-O bonds	Fe-O Bond Distance (Å)	Molecular Wt. (amu)	Surface volume (Å^3)	Surface area (Å^2)	Dipole moment (D)	D/V
153	OH,2,4,8,16,17	1.972, 2.510, 2.612, 1.889, 2.447, 1.997	977.898	932.697	907.235	8.145	0.009
154	1,OH,4,8,16,17	1.913, 2.361, 2.555, 1.901, 2.378, 2.164	976.89	930.873	911.454	14.456	0.016
155	1,2,OH,8,16,17	1.964, 2.198, 2.071, 1.971, 2.330, 1.980	976.89	932.776	927.174	11.333	0.012
156	1,2,4,OH,16,17	1.825, 2.358, 2.577, 2.283, 2.500, 2.017	977.898	932.596	910.289	11.407	0.012
157	1,2,4,8,OH,17	1.902, 2.282, 2.497, 1.934, 2.182, 2.456	976.89	931.156	921.299	9.941	0.011
158	1,2,4,8,16,OH	1.847, 2.208, 2.570, 1.874, 2.511, 2.108	975.882	926.552	898.327	10.69	0.012
159	OH,7,13,14,15,17	1.974, 2.528, 1.978, 2.415, 2.018, 2.361	978.906	935.245	927.698	5.939	0.006
160	6,OH,13,14,15,17	2.084, 2.135, 2.032, 2.345, 2.076, 2.325	979.914	939.313	939.751	10.369	0.011
161	6,7,OH,14,15,17	1.928, 2.407, 2.217, 2.519, 2.022, 2.307	978.906	936.837	931.823	8.806	0.009
162	6,7,13,OH,15,17	1.994, 2.145, 2.325, 1.940, 2.116, 2.327	979.914	937.83	923.925	7.863	0.008
163	6,7,13,14,OH,17	1.912, 2.406, 1.983, 2.422, 2.003, 2.360	980.922	940.032	934.563	7.677	0.008
164	6,7,13,14,15,OH	1.957, 2.339, 1.990, 2.468, 2.017, 2.152	978.906	936.858	938.797	12.35	0.013
165	OH,3,10,11,12,15	2.047, 2.559, 1.872, 2.506, 2.341, 2.334	976.89	924.125	895.112	35.543	0.038
166	1,OH,10,11,12,15	2.299, 2.038, 1.963, 2.406, 2.147, 2.332	975.882	924.884	888.31	10.715	0.012
167	1,3,OH,11,12,15	2.072, 2.547, 2.024, 2.563, 2.188, 2.110	974.874	917.134	875.794	9.545	0.01
168	1,3,10,OH,12,15	1.981, 2.513, 2.273, 2.212, 2.130, 2.289	975.882	923.472	893.026	12.87	0.014
169	1,3,10,11,OH,15	1.998, 2.544, 1.895, 2.410, 1.970, 2.340	976.89	926.19	888.578	24.915	0.027
170	1,3,10,11,12,OH	2.049, 2.514, 1.990, 2.432, 2.039, 2.264	976.89	929.383	905.184	13.905	0.015
171	OH,5,12,13,14,15	2.117, 2.193, 2.112, 2.030, 2.008, 2.019	977.898	933.886	937.849	14.689	0.016
172	4,OH,12,13,14,15	2.508, 2.021, 2.049, 2.036, 2.380, 1.978	976.89	931.157	936.011	11.678	0.013
173	4,5,OH,13,14,15	2.419, 2.000, 2.077, 1.942, 2.269, 2.014	978.906	936.82	942.04	12.624	0.013

174	4,5,12,OH,14,15	2.500, 1.997, 2.081, 2.100, 2.409, 2.054	976.89	932.636	939.553	22.449	0.024
175	4,5,12,13,OH,15	1.970, 1.991, 2.064, 2.166, 2.114, 2.161	977.898	933.553	928.863	18.538	0.02
176	4,5,12,13,14,OH	2.124, 1.990, 2.008, 2.065, 2.294, 2.110	978.906	936.536	942.146	18.241	0.019
177	OH,2,8,13,16,17	2.135, 2.544, 1.935, 2.285, 2.017, 2.372	978.906	935.494	928.377	4.378	0.005
178	1,2,8,13,16,17	2.259, 2.148, 2.013, 2.158, 2.089, 2.075	977.898	933.778	924.853	3.061	0.003
179	1,2,OH,13,16,17	1.912, 2.395, 2.006, 2.253, 2.016, 2.368	978.906	934.874	923.49	7.83	0.008
180	1,2,8,OH,16,17	1.916, 2.458, 1.974, 2.095, 2.031, 2.297	976.89	930.591	930.706	6.688	0.007
181	1,2,8,13,OH,17	1.916, 2.438, 1.977, 2.206, 2.092, 2.438	976.89	932.566	939.206	7.715	0.008
182	1,2,8,13,16,OH	2.076, 2.028, 2.081, 2.310, 2.286, 2.169	977.898	935.485	939.005	6.834	0.007

7.3.2.3 Conguration with Fe-H_2O bond

Bryostatin 1 was bound to Fe^{3+}, by replacing one of the Fe-O bonds with an H_2O ion. It is not known whether iron binds water molecules as an OH ion or an hydroxonium ion. This shows; 1) the probability of the complex to exist if one of the Fe-O bonds is broken and replaced with an hydroxonium ion, and 2) the likelihood of the complexes to exist based on the probable conformation of the Fe-O bond distances.

Aside from the Fe-O bond distances, the surface area and dipole moment of the complexes were analyzed to establish D/V ratios. This would determine the probability of these complexes to act as polar or non-polar agents in comparison to solvents used as references (Table 8). From the structures in Fig. 13 and the data in Table 11, it is clearly seen that the change in Fe-O, Fe-H_2O bonds directly affect the dipole moment, surface area, and surface volumes of the structures. For example, **183** has a D/V ratio of 0.006 and **187** has a D/V ratio of 0.011. The difference between these two structures is the substitution of the Fe-H_2O bond with the Fe-O^{16} bond. This substitution also decreased the average bond distance of the complex from 2.377 to 2.265 Å. The five most probable structures from Table 9 show bond distances of less than 2.5 Å, well within the range of known siderophores.

(a)

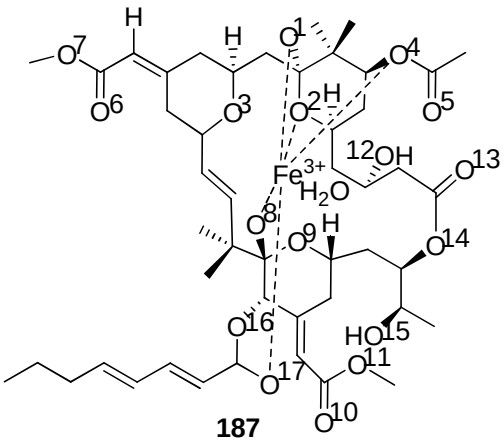

187

(b)

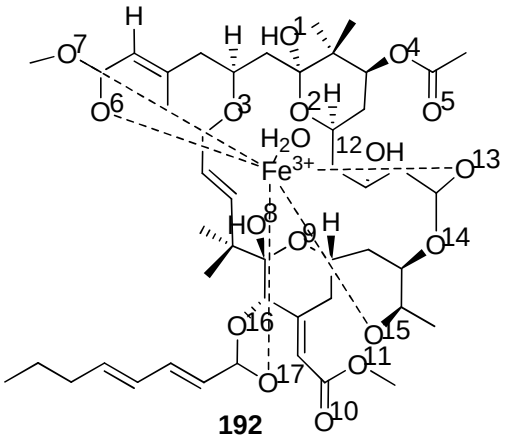

192

(c)

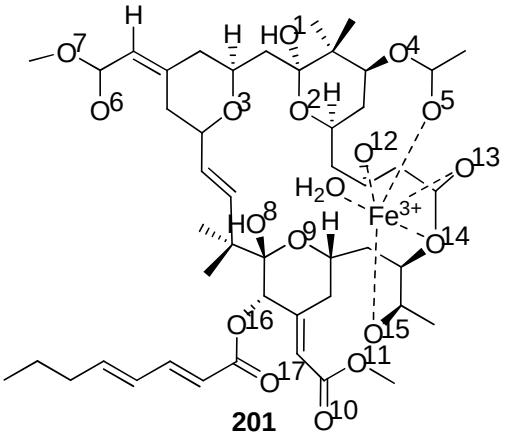

201

(d)

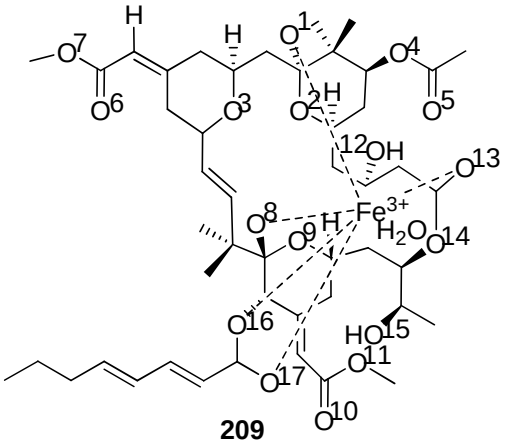

209

Fig. 13. Some configurations with the most probable bond distances and D/V ratios; a) **187**. D/V = 0.011 b) **192**, D/V = 0.024 c) **201**, D/V = 0.016 and d) **209**, D/V = 0.017.

Table 11. Bond distances and values for the five most probable conformations, based on the Fe-O bond distances, listed in Table 10. Each conformation has 5 bryostatin oxygens bound to Fe + H_2O.[17] The highlighted numbers correlate with the structures in Fig. 13.

Semi empirical PM3, 5 Fe-O BONDS + H_2O							
code #	Oxygen-Fe bonds	Fe-O Bond Distance (Å)	Molecular Wt. (amu)	Surface volume (Å^3)	Surface area (Å^2)	Dipole moment (Debye)	D/V
183	H_2O,2,4,8,16,17	2.585, 2.530, 2.627, 1.903, 2.532, 2.087	978.906	935.808	927.630	5.903	0.006
184	1, H_2O,4,8,16,17	1.907, 2.564, 2.567, 1.908, 2.402, 2.111	977.898	935.090	919.351	7.234	0.008
185	1,2, H_2O,8,16,17	1.964, 2.262, 2.529, 1.959, 2.348, 1.983	977.898	936.871	938.595	5.269	0.006
186	1,2,4, H_2O,16,17	1.824, 2.368, 2.581, 2.575, 2.532, 2.038	978.906	937.010	919.977	10.503	0.011
187	1,2,4,8, H_2O,17	1.888, 2.289, 2.494, 1.924, 2.548, 2.447	977.898	936.093	930.372	10.379	0.011
188	1,2,4,8,16, H_2O	1.837, 2.222, 2.579, 1.877, 2.500, 2.501	976.890	931.274	908.722	8.612	0.009
189	H_2O,7,13,14,15,17	2.018, 2.517, 1.981, 2.432, 2.031, 2.351	979.914	939.462	935.553	5.613	0.006
190	6,H_2O,13,14,15,17	2.072, 2.554, 2.020, 2.347, 2.052, 2.328	980.922	944.316	952.120	8.314	0.009
191	6,7, H_2O,14,15,17	1.934, 2.401, 2.549, 2.522, 2.009, 2.290	979.914	941.677	944.211	9.02	0.01
192	6,7,13, H_2O,15,17	2.002, 2.158, 2.304, 1.908, 2.114, 2.340	980.922	942.045	925.459	22.732	0.024
193	6,7,13,14, H_2O,17	1.913, 2.413, 1.984, 2.435, 2.519, 2.347	981.930	944.907	948.922	9.211	0.01
194	6,7,13,14,15, H_2O	1.945, 2.350, 1.978, 2.448, 2.002, 2.526	979.914	940.897	948.171	10.52	0.011
195	H_2O,3,10,11,12,15	2.535, 2.568, 1.854, 2.524, 2.210, 2.394	977.898	930.300	911.272	11.043	0.012
196	1,H_2O,10,11,12,15	2.311, 1.994, 1.939, 2.404, 2.190, 2.353	976.890	929.553	895.581	10.266	0.011
197	1,3, H_2O,11,12,15	2.178, 2.508, 2.476, 2.560, 2.116, 2.096	975.882	922.996	885.715	9.022	0.01
198	1,3,10, H_2O,12,15	1.976, 2.504, 2.215, 2.561, 2.177, 2.294	976.890	927.917	900.545	13.323	0.014
199	1,3,10,11, H_2O,15	2.044, 2.538, 1.899, 2.419, 1.941, 2.374	977.898	930.817	893.905	10.465	0.011
200	1,3,10,11,12, H_2O	2.048, 2.487, 2.135, 2.332, 2.031, 2.547	977.898	934.385	930.635	11.588	0.012
201	H_2O,5,12,13,14,15	2.531, 2.197, 2.191, 2.020, 2.003, 2.021	978.906	938.999	952.927	14.687	0.016
202	4,H_2O,12,13,14,15	2.513, 2.519, 2.034, 2.049, 2.377, 1.969	977.898	934.696	946.255	13.48	0.014
203	4,5, H_2O,13,14,15	2.415, 2.005, 2.521, 1.929, 2.261, 2.009	979.914	940.647	953.641	12.697	0.013
204	4,5,12, H_2O,14,15	2.505, 1.995, 2.038, 2.528, 2.430, 2.042	977.898	936.516	951.681	15.885	0.017
205	4,5,12,13, H_2O,15	2.063, 1.968, 2.086, 2.235, 2.538, 2.060	978.906	938.167	943.537	16.88	0.018
206	4,5,12,13,14, H_2O	2.128, 1.984, 2.021, 2.040, 2.344, 2.465	979.914	940.819	955.172	16.904	0.018
207	1,2, H_2O,13,16,17	2.534, 1.936, 2.405, 2.259, 2.060, 2.387	979.914	940.609	938.443	6.123	0.007

208	H_2O,2,8,13,16,17	2.541, 2.551, 1.963, 2.290, 1.983, 2.251	979.914	940.184	938.185	7.011	0.007
209	1, H_2O,8,13,16,17	1.980, 2.290, 2.572, 2.184, 2.129, 2.104	978.906	940.389	946.352	15.707	0.017
210	1,2,8, H_2O,16,17	1.959, 2.363, 1.983, 2.524, 1.989, 2.335	977.898	936.104	949.580	5.869	0.006
211	1,2,8,13, H_2O,17	1.984, 1.918, 2.445, 2.159, 2.525, 2.432	977.898	936.285	948.262	6.628	0.007
212	1,2,8,13,16, H_2O	2.039, 2.102, 2.219, 2.071, 2.306, 2.557	978.906	945.636	960.896	14.252	0.015

From the data in Tables 9-11, it can be noted that the bryostatin 1-Fe^{3+} complex has many likely stable conformations. It also suggests that the arrangements of the different complexes are not bond specific to any fixed configuration. Data in Tables 1 and 2 was also valuable to show the accuracy of our method, based on the close proximity of the bond distances and angles of the crystal structure of terricolin to the semi-empirical method used in this study.

The D/V ratios (Table 7 and 8) indicate the physical property (polar or non polar) of the complex in different solvents. A D/V = 0 strongly indicates a non-polar complex, which suggests that the complex would favor the non-polar environment found in a cell wall. Complexes with a D/V = 0.04 have a polarity similar to methanol, indicating their potential to attach to polar surfaces and move freely in a polar environment, such as the blood stream.[17] Several of the compounds listed, in both computational studies, have D/V ratios with similar proximity to the polar and non-polar solvents shown in Table 8. Complexes with a D/V ratio close to 0.04 suggest their potential suitability for medicinal use.

It is not known if the fer-mer compound exists as a neutral, 1^+, 2^+ or 3^+ species, but it is critical for understanding its solubility and an important consideration for its viability as a medicinal agent. Studies have shown that uncharged molecules are able to penetrate the cell membrane more rapidly as opposed to charged molecules.[26] It has also been reported that the permeability of these chelating compounds through the cell barrier in the body can be affected by the ionic state of the complex, as well as the pH value, as some chelators are pH dependent.[26] Other factors that determine the success of chelators in the body include the ability to form hydrogen bonds, partition coefficient value, lipophilicity, ionisation, molecular weight and the number of substituent groups on the compound (OH, NH). Some of these parameters, however, do not fully apply to all hexadentate chelators as they do to bi/tridentate chelators.[26,31]

Showing that the fer-mer complex has the potential to break and form bonds, with different oxygens clearly shows the dynamic nature of Fe-O bonds in the aqueous phase. The molecule can shift polarity and adapt to suit its environment, hence the name “smart molecule”.[17] Both computational studies have added greatly to a more detailed understanding of bryostatin’s role as a viable siderophore and allowed a broadening of the work to determine the feasibility of a bryostatin-Fe^{3+} complex as a medicinal agent.

7.4 Conclusion

Results from both computational studies illustrated two factors. 1) the calculated bond distances and angles were almost identical to those of the crystal structure of terricolin, showing accuracy and precision in the semi-empirical parameters used; 2) the data in Tables 9-11, when compared to Tables 3-6, also showed a consistency in the computational measurements compared to the crystal structure of terricolin (Tables 1 and 2).

These findings validate the proposal that natural products have the ability to bind to Fe^{3+} forming a metal-ligand complex, and evidence the possibility of the different configurations of the bryostatin-Fe complex existing in nature.

7.5 References

[1] J. D. Martin, Y. Ito, W. Homann, M. G. Haygood, and A. Butler. *J. Biol. Inorg. Chem*., 2006, **11(5)**, 633-41.

[2] J. S. Martinez, J. N. Carter-Franklin, E. L. Mann, J. D. Martin, M. G. Haygood, and A. Butler. *Proc. Natl. Acad. Sci*. *USA*, 2003, **100(7)**, 3754-59.

[3] I. J. Schalk. *J. Inorg. Biochem.,* 2008, **102(5-6)**, 1159-69.

[4] R. G. Soengas, C. Anta, A. Espada, R. M. Nieto, M. Larrosa, J. Rodrıguez, and C. Jimenez. *Tetrahedron Lett.*, 2007, **48(17)**, 3021-24.

[5] P. Ding, C. E. Schous, and M. J. Miller. *Tetrahedron Lett.,* 2008, **49(14),** 2306-10.

[6] A. Braud, K. Jezequel, and T. Lebeau. *J. Hazard. Mater.*, 2007, **144(1-2)**, 229-39.

[7] K. A. Mies, P. Gebhardt, U. Mollamann, and A. L. Crumbliss. *J. Inorg. Biochem*., 2008, **102(4)**, 850-61.

[8] D. Wolff-Boenisch, and S. J. Traina. *Chem. Geol.*, 2007, **243(3-4)**, 357-68.

[9] M. Valdebenito, A. L. Crumbliss, G. Winkelmann, and K. Hantke. *Int. J. Med. Microbiol.*, 2006, **296(8)**, 513-20.

[10] I. G. O'Brien, and F. Gibson. *Biochim. Biophys. Acta,* 1970, **215(2)**, 393-402.

[11] K. Konopka, and J. B. Neilands. *Biochem*., 1984, **23(10)**, 2122-27.

[12] D. W. Choi, Y. S. Do, C. J. Zea, M. T. McEllistrem, S. W. Lee, J. D. Semrau, N. L. Pohl, C. J. Kisting, L. L. Scardino, S. C. Hartsel, E. S. Boyd, G. G. Geesey, T. P. Riedel, P. H. Shafe, K. A. Kranski, J. R. Tritsch, W. E. Antholine, and A. A. DiSpirito. *J. Inorg. Biochem.*, 2006, **100(12)**, 2150-61.

[13] W. J. Barreto, R. A. Ando, P. S. Santos, and W. P. Silva. *J. Inorg. Biochem*., 2008, **102(2)**, 359-63.

[14] M. Meyer, and W. Trowitzsch-Kienast. *J. Mol. Struct.*, 1997, **418(1)**, 93-98.

[15] T. J. Manning, J. Thomas, G. Abadi, D. Phillips, S. Osiro, L. Noble, and D. Phillips. *Nat. Prod. Res.*, 2008, **22(5),** 399-413.

[16] http://chemistry.ncssm.edu/book/Chap8SemiEmp.pdf (May 21st 2009).

[17] T. Manning, L. Noble, G. Abadi, and J. Smith. *Fl. Sci*., 2008, **71(4)**, 341-59.

[18] P. A. Wender, J. DeBrabander, P. G. Harran, J. M. Jimenez, M. F. T. Koehler, B. Lippa, C. M. Park, C. Siedenbiedel, and G. R. Pettit. *Proc. Natl. Acad. Sci. USA,* 1998, **95(12)**, 6624-29.

[19] P. A. Wender, J. L. Baryza, S. E. Brenner, M. O. Clarke, M. L. Craske, J. C. Horan, and T. Meyer. *Curr. Drug Discov. Technol.*, 2004, **1(1)**, 1-11.

[20] A. Jegorov, V. Matha, M. Husak, B. Kratochvil, J. Stuchlik, P. Sedmera, and V. Havlicek. *J. Chem. Soc. Dalton Trans*., 1993, **8**, 1287-93.

[21] J. S. Martinez, and A. Butler. *J. Inorg. Biochem*., 2007, **101(11-12)**, 1692-98.

[22] J. S. Martinez, G. P. Zhang, P. D. Holt, H. T. Jung, C. J. Carrano, M. G. Haygood, and A. Butler. *Sci*., 2000, **287(5456)**, 1245-47.

[23] H. M. Macrellis, C. G. Trick, E. L. Rue, G. Smith, and K. W. Bruland. *Mar. Chem*., 2001, **76(3)**, 175-87.

[24] J. S. Martinez, M. G. Haygood, and A. Butler. *Limnol. Oceangr*., 2001, **46(2)**, 420-24.

[25] E. A. Fadeev, M. K. Luo, and J. T. Groves. *J. Amer. Chem. Soc*., 2004, **126(38)**, 12065-75.

[26] Z. D. Liu, and R. C. Hider. *Coord. Chem. Rev.,* 2002, **232(1-2)**, 151-71.

[27] M. Luo, E. A. Fadeev, and J. T. Groves. *J. Amer. Chem. Soc***.,** 2005, **127(6)**, 1726-36.

[28] G. Xu, J. S. Martinez, J. T. Groves, and A. Butler. *J. Amer. Chem. Soc*., 2002, **124(45)**, 13408-15.

[29] J. W. Blunt, B. R. Copp, M. H. G. Munro, P. T. Northcote, and M. R. Prinsep. *Nat. Prod. Rep.*, 2005, **22(1)**, 15-61.

[30] C. L. Bajaj , V. Pascucci , A. Shamir, R. J. Holt, and A. N. Netravali. *Discrete Appl*. *Math*.*,* 2003, **127(1)**, 23-51.

[31] D. Y. Liu, Z. D. Liu, and R. C. Hider. *Best Pract. Res. Clin. Haematol.*, 2002, **15(2)**, 369-84.

CHAPTER 8

Cell line testing of a bryostatin-Fe^{3+} complex versus bryostatin 1

8.1 Introduction

The discovery of antibiotics in the early 1900s was a new development that revolutionized medicinal treatment worldwide. However, this quickly resulted in the development of many resistant bacteria after the administration of antibiotics such as penicillin, tetracycline, erythromycin and others, to treat patients. Much research has since focused on modifying and preventing the possibility of resistant antibiotic bacteria. The potential of using siderophores is currently being explored. Some encouraging properties, such as inhibitory conjugates for microbial growth (leading to iron starvation and microbe death), or functioning as active transport drug delivery agents, have been identified. Numerous other studies are also being conducted to determine more applicative properties of siderophores as medicinal agents.[1] In the past fifteen years, the role of siderophores has been diverted away from industrial usage and more towards different medicinal applications. Many preclinical studies have trialed the administration of siderophores with medicinal agents, to form metal-ligand complexes. This approach has been shown to be effective against various diseases unresponsive to other initial treatments.[2]

Administering siderophore carriers linked to antibiotics has also been tested with results showing much success in efficiently overcoming the resistance of antibiotics.[3,4,5] Resistant bacteria produce an impermeable barrier that protects the membrane from antibiotics entering the cell. A recent study involved administering a siderophore complex with the antibiotic albomycin, to overcome the barrier that is formed after a bacterium becomes resistant to treatment. By binding albomycin to Fe^{3+}, the drug complex is able to enter the cell via an active transport mechanism of the siderophore, its recognition by iron dependent receptors such as FhuA and TonB, promoting translocation of siderophores bound to iron across the plasma membrane into cells. Penetration of the outer

membrane increases the drug concentration in cells, resulting in a more effective medication for patients.[6] With much success in using this method, treatments can be greatly improved by synthetically developing siderophores to fit the drug, alleviating the need to develop new antibiotic compounds. Based on the molecular composition of albomycin, highly efficient antibiotics can be easily designed to transport active drugs into resistant bacteria.[6]

Data from other initial studies have shown that this new method of utilizing siderophores has also been successful in conjugation with other medicinal agents. There is no current vaccine against serogroup B meningococci, the virus responsible for meningitis, even though there have been many attempts to develop an effective agent against the virus. Preliminary studies showed that meningococcus virus scavenges iron from its host organism. Consequently, an iron loaded protein (FrpB-, Ferric-repressed protein B) was proposed as a possible vaccine for patients. By administering the siderophore-protein complex, high levels of antibodies were produced, providing sufficient protection against a large range of hyper-invasive meningococcal strains.[7,8]

Since then, the use of siderophores has been applied to all aspects of medicinal applications, from drug treatment to drug detection. New work is developing a siderophore conjugate for the diagnosis of prostate cancer by MRI (magnetic resonance imaging) scans. A siderophore is bound to an inhibitor which then binds to the prostate cancer receptor. Results from this work showed that the linker between the inhibitor and siderophore was not necessary to promote the binding of iron by the trihydroxamate siderophore component. However, the detection of these cells was successful using the inhibitor bound to a siderophore using either iron or gadolinium.[9]

Administering siderophores with drugs to modify their function has become a novel and increasingly beneficial application. Cell line tests using various

siderophores (anguibactin, vibrobactin and desferrioxamine B) have shown viability as medicinal agents.[10] Bryostatin 1 has been tested in over thirty phase I/II clinical trials and has shown much success against various cancers; however, it has often shown to be a better agent *in vitro* than *in vivo*. On this basis, a bryostatin-Fe^{3+} (fer-mer compound) complex was formulated to determine its effectiveness in comparison to bryostatin 1 alone. The complex was formulated based on the results collected from the computational studies as described in Chapter 7.

In vitro cell line testing of the bryostatin-Fe^{3+} complex against chronic myeloid leukaemia was undertaken, followed by cell testing against human lung carcinoma (A549) cells. The effectiveness of bryostatin 1 was compared to that of the complex, to determine their respective viability and efficacy. Preliminary results were encouraging, showing the essential viability of such iron complexes as a proposition for further clinical studies. The correlation of the preclinical data, in combination with both computational studies, further supports the premise of the fer-mer complex being a better medicinal agent than bryostatin 1 alone. Results from both compounds against A549 cells clearly showed the increased efficacy of the fer-mer complex as opposed to just bryostatin 1. The potential siderophore applications, for the discovery and distribution of drugs, have generated an innovative and interesting field, as it presents another available therapy regime for patients.

8.2 Experimental section

Bryostatin 1 standard (stored at 4°C) was donated by the US National Cancer Institute. A 6.741 x 10^{-5} M solution of bryostatin 1 was made up using 0.4875 mg bryostatin 1 in 8 mL of anhydrous methanol (Fisher Scientific). This solution was placed into four separate vials each containing 2 mL (equivalent to

$1.3482x10^{-7}$ mol of bryostatin 1) per vial. A $5x10^{-4}$ M solution of $FeCl_3.6H_2O$ (Sigma Aldrich) in methanol was prepared of which 540 µL was added into two vials respectively. The other two vials remained as controls (bryostatin 1 only). The vials were placed under vacuum to dryness and then stored at 4°C. A vial of each compound was sent to the Medical College of Georgia (MCG) for *in vitro* cell testing against chronic myeloid leukaemia; the other 2 vials were tested against human lung carcinoma. It should be noted, that an $FeCl_3.6H_2O$ control was not included in this study.

8.2.1 Chronic myeloid leukaemia cells

Western blot analysis for PKC alpha (α) and PKC delta (δ) levels in (CML) chronic myeloid leukaemia (K562) cells were studied using both compounds. Both compounds were re-suspended in DMSO (dimethyl sulphoxide) and used for cell line tests at a range of concentrations (5, 10 and 50 nM) to determine a suitable dosage of each. The CML cells were cultured in the presence of increasing concentrations of bryostatin 1 (5 nM, 10 nM, and 50 nM) and the bryostatin-Fe^{3+} complex, respectively, for 24 hr. Cells were then harvested for cell cycle analysis and Western blot analysis, carried out to determine the PKC α and PKC δ levels. For Western blot analysis, cells were lysed in a lysis buffer containing 1% Triton X-100. Protein concentrations were determined by BCA (bicinchoninic acid) protein assay. One hundred micrograms of total cell lysate were separated by SDS-PAGE (sodium dodecyl sulfate polyacrylamide gel electrophoresis) and transferred to a PVDF membrane. For cell cycle analysis, harvested cells were fixed in 70% ethanol for 2 hr, stained with propidium iodide and then analyzed via flow cytometry.

8.2.2 Human lung carcinoma cells

8.2.2.1 Chemicals

Human lung carcinoma (A549) cells were originally purchased from the American type culture collection. RPMI-1640 medium (Sigma) was used as growth medium for the cells. Transfer flasks (T-75) were purchased from Iwaki, isopropanol was purchased from VWR, trypsin was purchased from Difco and EDTA was purchased from Sigma. MTT [3(4, 5-dimethylthiazolyl-2)2, 5-diphenyltetrazolum bromide)] stock solution (Sigma) and DMSO and PBS (phosphate buffered saline), both purchased from BDH, were used in this study. Solutions and instruments were sterilized before use. Bryostatin 1 and the bryostatin-Fe^{3+} complex are as described in Section 8.2.

8.2.2.2 Cell culturing

Human lung carcinoma cells were cultured by passaging a confluent flask. This was done by first removing the medium then rinsing cells with PBS buffer. A mixture of 0.25% (w/v) trypsin/0.03% (w/v) EDTA solution (3 mL) was added to the flask which was then incubated for approximately 3 min for cells to detach. Medium was subsequently added to the flask to subculture equally into flasks, in a ratio of 1:4, and then incubated for 72 hr for cells to reach confluency. After confluency, cells were detached as described, then counted using a haemocytometer to adjust the density of cells to $5x10^4$ in a medium suspension, before seeding the micro-plates.

8.2.2.3 Drug administration

Plates (96 well micro-plates) were seeded with 200 µL of cell suspension, and then incubated at 37°C for 24 hr. The medium was then removed and replaced with 100 µL of fresh medium containing 1% DMSO; which was added to

all the wells, excluding column 2 on each initial plate, where the initial concentration (1.3484×10^{-5} M) of the drug was added for each compound, respectively. Drug concentration was diluted across two plates, for each compound, with a final concentration of 2.0578×10^{-10} M. Samples were then incubated at 37°C for 72 hr. This was repeated twice to show the efficiency of both compounds. All plates contained a negative control consisting of medium only (medium + 0.1% DMSO) and one control for each compound consisting of cells and medium only.

8.2.2.4 MTT test

The medium was removed from wells of each plate, and then the cells were rinsed with 200 µL of PBS. A 1:10 dilution of MTT stock into PBS buffer was prepared, of which 200 µL was added to each well. Plates were incubated at 37°C for 2 hr, and then the MTT solution removed. Wells were washed with PBS (200 µL per well), then the cells treated with 200 µL of 10% DMSO and 90% isopropanol, collectively. Plates were left at RT for 10 min, and wrapped in aluminum foil, before analysis using a 96 well plate reader.

8.3 Results and Discussion

Siderophores are iron chelating compounds secreted by marine bacteria to bind iron as many organisms cannot ingest iron.[11,12] Siderophores can function differently as medicinal agents, for example: 1) transporting drugs across a cell membrane, 2) removing excess iron in the body and 3) sequestering iron from cancerous cells, resulting in cell apoptosis. Siderophores, for instance, have recently been used for the treatment of iron overload in humans. This is important as excess iron in the body can lead to hepatocellular carcinoma.[13] Other studies using siderophores have shown success in promoting cell apoptosis by

sequestering the iron from cells, resulting in the anti-proliferation of HL60 cells and murine lymphoma 38C13 cells.[14] Clinical trials using siderophores have shown promising results in the treatment of various cancers and many preclinical studies are beginning to further determine the efficacy of such compounds.

8.3.1 Chronic myeloid leukaemia cells

Preliminary results from the Western blot analysis of both compounds showed similar reduction levels of PKC α and PKC δ. However, the fer-mer compound showed a more significant decrease in PKC α level than bryostatin 1 at a low concentration dosage of 5 nM. This decline, however, was most evident at a 50 nM dosage of the complex. Both compounds instigated the leukaemia cells to accumulate in the G_1 phase of the cell cycle, with no real difference between both compounds evident.

Results from the CML cell line tests showed that both bryostatin 1 and the fer-mer complex induced equal amounts of G_0/G_1 accumulation (cell cycle arrest) of chronic myeloid leukaemia cells at a 5 nM dose levels. Higher concentrations of both compounds (10 and 50 nM) did not induce a greater accumulation in G_0/G_1 of the cell cycle. Western blot analysis showed that both compounds depleted the levels of PKC α and PKC δ in CML. However, the bryostatin-Fe^{3+} complex showed a greater depletion of PKC α levels at the 5 nM dosage than bryostatin 1, with the most significant depletion seen at the 50 nM concentration of the complex. Overall, the effects of bryostatin 1 and bryostatin-Fe^{3+} complex against CML cells displayed a similar reduction in PKC δ levels.

8.3.2 Human lung carcinoma cells

Results from the anti-proliferation effects of bryostatin 1 and bryostatin-Fe^{3+} complex against A549 cells are shown (Figs. 1 and 2). Tables 1 and 2 show the nonlinear regression data sets for both tests illustrating the efficacy of the bryostatin-Fe^{3+} complex in comparison to bryostatin 1. The average EC_{50} value for bryostatin 1 (446.15 nM ± 200) in comparison to that of the bryostatin-Fe complex (89.6 nM ± 21) distinctly shows that the bryostatin-Fe^{3+} complex was more effective than bryostatin 1. Overall results showed that the cell growth inhibition of the fer-mer compound was greater than that of bryostatin 1 against A549 cells.

Table 1. Nonlinear regression data sets for bryostatin 1.

Sigmoidal dose-response		
Best-fit values	Bryostatin 1	Bryostatin 1
Bottom	0.384	-21.11
Top	101.6	93.05
Log EC_{50}	-6.689	-6.163
EC_{50}	204.8 nM	687.5 nM
Std error Bottom	6.773	8.388
Std error Top	4.518	3.574
Log EC_{50}	0.1505	0.1319
95% CI - Bottom	-13.07 to 13.84	-37.78 to -4.447
95% CI - Top	92.64 to 110.6	85.95 to 100.2
Log EC_{50}	-6.988 to -6.390	-6.425 to -5.901
EC_{50} range	102.9 to 407.6 nM	376.0 nM to 1257 nM
Degrees of Freedom	99	99
R^2	0.6631	0.7189
Absolute Sum of Squares	81281	63331
Sy.x	28.65	25.29
# of pts analyzed	102	102

EC_{50} – effective concentration of a compound where 50% of its maximal effect is observed
CI – confidence interval
Std – standard

Table 2. Nonlinear regression data sets for bryostatin 1-Fe complex.

Sigmoidal dose-response		
Best-fit values	Bryostatin 1-Fe	Bryostatin 1-Fe
Bottom	-1.407	5.199
Top	89.88	190.9
Log EC_{50}	-6.955	-7.166
EC_{50}	111 nM	68.25 nM
Std. error - Bottom	8.762	11.6
Std error - Top	7.058	10.77
Log EC_{50}	0.2377	0.1661
95% CI - Bottom	-18.82 to 16.00	-17.85 to 28.24
95% CI - Top	75.85 to 103.9	169.5 to 212.3
Log EC_{50}	-7.427 to -6.482	-7.496 to -6.836
EC_{50} range	37.42 nM to 329.3 nM	31.91 nM to 145.9 nM
Degrees of Freedom	99	99
R^2	0.4424	0.6194
Absolute Sum of Squares	173314	356847
Sy.x	41.84	60.04
# of pts analyzed	102	102

EC_{50} – effective concentration of a compound where 50% of its maximal effect is observed
CI – confidence interval
Std – standard

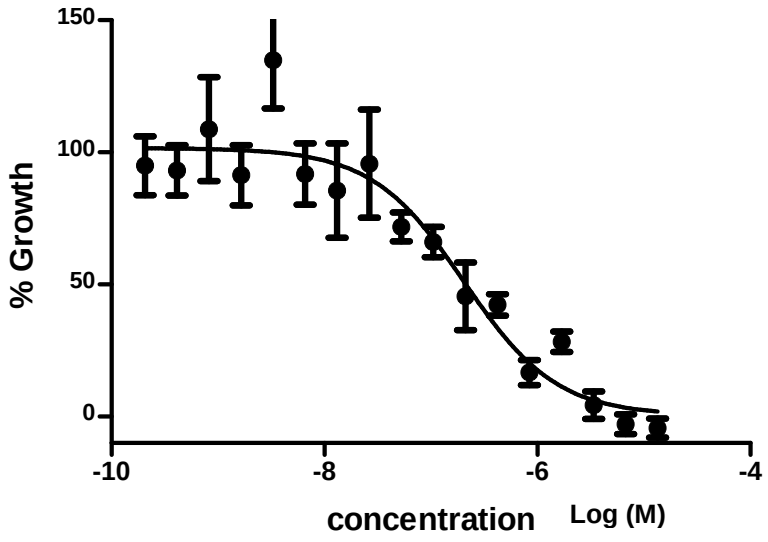

Fig. 1. Bryostatin 1 standard against A549 cells. The average EC_{50} value of bryostatin 1 was 446 nM.

The above figure shows the efficacy of bryostatin 1 against the A549 cells. The graph shows that at high concentrations of bryostatin 1 the anti-proliferative properties of the drug are very effective. However, as the concentration of the drug decreases, there is a gradual decrease in the efficacy of the drug. This

gradual decrease, suggests that the drug is not as effective as the concentration falls, resulting in the increase or presence of cell growth. At low concentrations of bryostatin 1, results showed no efficacy of the drug on the cells, as growth inhibition is prohibited. The presence of cell growth, however, is shown to be relatively constant, which suggests that the drug at low concentration has negligible effect on cell growth.

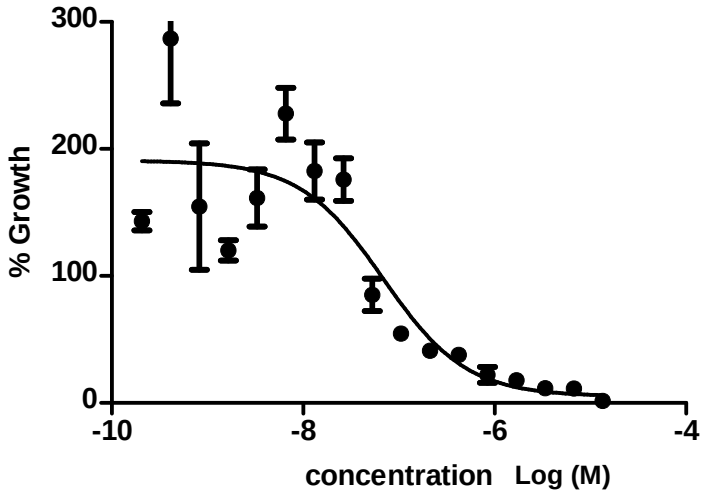

Fig 2. Bryostatin 1-Fe complex against A549 cells. The average EC_{50} value of the bryostatin-Fe complex was 89.6 nM.

In comparison to bryostatin 1 alone, the Fig. 2 graph shows the bryostatin-Fe^{3+} complex to be a more effective agent, whereby the anti-proliferative effect of the complex, exceeded to a lower concentration value than bryostatin 1 alone. Compared to bryostatin 1 alone, there is no gradual increase in cell growth as the concentration of the bryostatin 1-Fe^{3+} complex decreases. Fig. 2 shows two bands, one showing the constant anti-proliferative effect of the drug complex and the second showing cell growth over 100%.

In this study, Fe^{3+} was administered to the cells with bryostatin 1 to aid in the transportation of the drug into the cells. Based on the data shown in both graphs, it is clear that the bryostatin-Fe^{3+} complex has a higher anti-proliferative effect on cell growth than bryostatin 1 alone, suggesting the efficacy of Fe^{3+}. This

efficacy may be due to increased penetration of the complex (and hence increased concentration of the drug itself) into the cells than the drug alone, due to its binding to Fe^{3+}. The presence of Fe^{3+}, at low concentrations of bryostatin 1, suggests the over production of cell growth, see Fig. 2. The bryostatin-Fe^{3+} complex was prepared with Fe^{3+} in excess, therefore at low concentrations of the drug the concentration of iron(III) is still high; showing the increase in cell growth as mentioned. This effect is supported by studies conducted by other groups, showing the increase of iron(III) above what is normally administered, resulted in an increase in tumor growth and inhibition of cells apoptosis.[15,16] Other groups have suppressed iron(III) in cells showing subsequent suppression of tumor growth of breast cancer cells.[17] Despite the fact that an $FeCl_3 6H_2O$ control was not included, in our method, indications from the graph suggests that the iron(III) itself may not be responsible for the apoptosis of the A549 cells.

Results from both compounds showed that the bryostatin-Fe^{3+} complex (average EC_{50} of 89.6 nM) was a better agent than bryostatin 1 (average EC_{50} value of 446 nM). Even though the PKC interaction of both drugs was not analyzed in this study, previous studies from other groups have shown that PKC α is the only PKC isozyme present in A549 cells.[18] This data can be correlated to that in section 8.2.1, which show the effects of both compounds on the down-regulation of PKC (δ and α) and the effectiveness of both compounds against both isozymes in CML cells. This is important, as it links the efficacy of both compounds to A549 cells. Aside from the down-regulation of PKC, bryostatin 1 also inhibits DNA replication in cell growth and delays cell growth at concentrations of 100 nM.[18]

Bryostatin 1 binds to PKC resulting in the down-regulation of the enzyme, thus inhibiting cell growth at the site of action.[19] This down-regulation results from the activation and self-phosphorylation of PKC, leading to the passage of

the enzyme through the cell membrane. Protein kinase C (PKC) is responsible for cell signaling, proliferation and differentiation through phosphorylation. There are twelve isozymes of PKC, each interacting with bryostatin 1 differently, with some being inhibited by the drug more than others. One study has shown that bryostatin 1 has no effect on atypical PKC isozymes, but down-regulates classic PKC and novel PKC.[20]

Bryostatin 1 has shown significant success in the treatment of various cancers *in vitro*; however, its efficacy has not been matched *in vivo*. Reasons for this can be related to its low solubility, degradation or distribution of the drug into tissues/organs in the body, resulting in low concentrations of the drug reaching the site of action. Therefore, it can be suggested, that one reason for the ineffectiveness of bryostatin 1, can be attributed to the dispersal of the drug in the body. Data reported on the dispersal of bryostatin 1 into tissues, such as kidney, liver, gastrointestinal tract, spleen, and fatty tissues, *etc*., are useful in showing the effectiveness of the compound for the treatment of cancer in these organs. However, this dispersal is disadvantageous: 1) when the drug is administered for a specific treatment, lower concentrations of the drug reach the active site than originally administered; 2) when higher concentrations of bryostatin 1 were found in other tissues than in the plasma alone, after 4 hr of administering the drug, with an absorption half-life of 48.6 min in the plasma; and 3) when the method of administration can influence the concentration of the drug in different tissues in the body.[21]

Based on this supposition, two computational studies were conducted to determine the possible viability of bryostatin 1 and other natural products to act as siderophores, which led to the formulation of a bryostatin-Fe^{3+} complex. This complex tested on the cell lines described earlier, showed promising value as a medicinal agent and was slightly more efficient than bryostatin 1 alone. This fer-

mer complex is an important step towards an enhanced delivery of bryostatin 1 *in vivo*, potentially leading to an improved treatment outcome for patients.

These results illustrate the viability of bryostatin 1 to act as a better medicinal agent when bound to Fe^{3+} and its likely potential against other cell lines. Theoretically, by forming a fer-mer complex, the properties of the compound are altered and the rigidity increased by Fe^{3+} binding, resulting in a higher solubility in the blood. The increase of drug permeability into cells results in improved concentration of the drug at the active site than is achievable without iron. The polarity of molecules having an anionic charge changed after forming the fer-mer complex, increasing the solubility and allowing it to be more miscible in polar solvents such as methanol or water.

On the other hand, hydrophobic molecules form a lipid bi-layer in a cell membrane, which can then be penetrated by a non-polar molecule. This change in polarity is important, as it allows the molecule to move freely in a polar environment such as the blood stream, allowing it to reach its site of action. By shifting the Fe-O bonds, the dynamic nature of these bonds in the aqueous phase can alter the molecule's polarity and allow adaptation to its environment.[22] Therefore, mixed ligand siderophores (containing more than one type of iron binding moiety) can suggestively gain access to the cell, resulting in efficient drug delivery agents.

A recent study utilizing a siderophore to transport drugs, to their active site, used a linker to bind the siderophore and drug together to form a conjugate. This is a key step as the linker dictates when the drug is released, thereby controlling how it is dissipated within the cell. Using this method the conjugate is able to penetrate the membrane to reach the site of action. Other benefits of using the siderophore-drug complex, aside from release at the site of action and acting as an anti-bacterial agent to overcome resistance, is that it blocks any

further assimilation of iron in cells.[23] This idea is similar to the proposed method of binding bryostatin 1 to iron as a method of improving the efficacy of the drug regime.

The fer-mer complex has supported the theoretical propositions regarding its enhancing properties as a medicinal agent. Data from the graph in Fig. 2 suggest that higher concentrations of the compound were penetrating into cells resulting in cell apoptosis. For this reason it is suggested that the complex may be a better agent, with potential properties of increased aqueous solubility and better dissolution of the drug into the blood stream. This is further facilitated by the penetration of the cell membrane by the siderophore-drug conjugate, effectively eliminating a barrier to the drug. The active transport of the complex thus increases the rate of entry into the cell beyond the passive diffusion rate.[24]

In the continuous effort to develop new iron chelators for clinical use, such compounds must first possess the necessary properties to be effective in the body. These include the ability to be lipophilic, which is dependent on the partition coefficient of the complex (log P < 5), low molecular weight (< 500), less than five hydrogen donors and less than ten hydrogen acceptors (*e.g.* OH, NH) *etc*..[25,26] For example, in a recent study, the anti-proliferative effects of a lipophilic compound versus a hydrophilic compound on rat hepatoma cells were assessed. The hydrophilic compound (CP20) generally used to treat iron(III) overload in humans had no effect on the cell apoptosis, whereas the lipophilic compound (CP411) entered the rat hepatoma cells 13 times more than CP20. It is suggested that this increase in efficacy is due to the partition coefficient of CP411, which is 8 fold more efficient than CP20, resulting in a more efficient agent against hepatoma cells.[13]

The three crucial properties that determine the simple diffusion of molecules across the cell membrane are molecular weight, lipophilicity and net

charge. The molecular weight of a compound is a key factor in determining its permeability across the cell membrane. Ideally, smaller compounds are able to penetrate better than large molecular weight compounds, due to their ability to diffuse faster. It is important to note that this rule does not apply to all siderophores as some, having a molecular weight greater than 500 Daltons, are still as effective. There are many examples of successful drugs in clinical trials with a molecular weight > 500.

The partition coefficient is dependent on the lipophilicity of the compound which is determined by the distribution of the compound between octanol and water. This is significant as a compound needs to have both lipophilic and hydrophilic properties to be able to penetrate through the cellular membrane in order to get into the blood stream. The presence of hydrogen bonding groups allow for hydrogen bonding of the compound with water, thereby enhancing the solubility of the compound in water. The more hydrogen bonds present, the more hydrophilic the drug is, resulting in minimal penetration across the cell wall.

Since iron(III) is known for its permeability across cell membranes, this is a key factor in utilizing iron as a transport system for lipophilic compounds. Therefore, by binding bryostatin to iron(III), iron serves to enhance drug transport across the membrane into cells. This effect is demonstrated by comparing the efficacy of the bryostatin-Fe^{3+} complex versus bryostatin 1 against A549 cells, as shown in Figs. 1 and 2. The use of such a complex to assist drug release triggered by the reductive removal of the metal inside the cell, has further boosted the prospect of a more robust drug delivery regime for the treatment of cancer patients.

8.4 References

[1] A. Ghosh, M. Ghosh, C. Niu, F. Malouin, U. Moellmann, and M. J. Miller. *Chem. Biol.,* 1996, **3(12)**, 1011-19.

[2] P. Ding, C. E. Schous, and M. J. Miller. *Tetrahedron Lett.,* 2008, **49(14),** 2306-10.

[3] Y. Tatsumi, T. Mejima, and S. Mitsuhashi. *Antimicrob. Agents Chemother*., 1995, **39(3),** 613-19.

[4] P. Silley, J. W. Griffith, D. Monsey, and A. M. Harris. *Antimicrob. Agents Chemother*., 1990, **34(9),** 1806-08.

[5] B. A. Weissberger, G. K. Abruzzo, R. A. Fromtling, C. Gill, S. Ponticas, M. E. Valiant, D. L. Shungu, and H. H. Gadebusch. *J. Antibiot.*, 1989, **42(5),** 795-06.

[6] V. Braun. *Drug Resist. Updat.,* 1999, **2(6)**, 363-69.

[7] R. Urwin, J. E. Russell, E. A. L. Thompson, E. C. Holmes, I. M. Feavers, and M. C. J. Maiden. *Infect. Immun*., 2004, **72(10),** 5955-62.

[8] J. Kortekaas, S. A. Muller, P. Ringler, M. Gregorini, V. E. Weynants, L. Rutten, M. P. Bos, and J. Tommassen. *Microbes Infect.*, 2006, **8(8),** 2145-53.

[9] P. Ding, P. Helquist, and M. J. Miller. *Bioorg. Med. Chem*., 2008, **16(4)**, 1648-57.

[10] H. M. Macrellis, C. G. Trick, E. L. Rue, G. Smith, and K. W. Bruland. *Mar. Chem*., 2001, **76(3)**, 175-87.

[11] J. D. Martin, Y. Ito, W. Homann, M. G. Haygood, and A. Butler. *J. Biol. Inorg. Chem*., 2006, **11(5)**, 633-41.

[12] J. S. Martinez, J. N. Carter-Franklin, E. L. Mann, J. D. Martin, M. G. Haygood, and A. Butler. *Proc. Natl. Acad. Sci. USA*, 2003, **100(7)**, 3754-59.

[13] F. Gaboriau, K. Chantrel-Groussard, N. Rakba, P. Loyer, N. Pasdeloup, R. C. Hider, P. Brissot and G. Lescoat. *Biochem. Pharmacol.*, 2004, **67(8)**, 1479-87.

[14] D. Hileti, P. Panayiotidis, and A. V. Hoffbrand. *Br. J. Haematol*., 1995, **89(1)**, 181-87.

[15] H. W. L. Hann, M. W. Stahlhut, and B. S. Blumberg. *Cancer Res.,* 1988, **48(15)**, 4168-70.

[16] N. Rakba, P. Loyer, D. Gilot, J. G. Delcros, D. Glaise, P. Baret, J. L. Pierre, P. Brissot, and G. Lescoat. *Carcinogenesis*, 2000, **21(5)**, 943-51.

[17] H. J. Thompson, K. Kennedy, M. Witt, and J. Juzefyk. *Carcinogenesis*, 1991, **12(1)**, 111-14.

[18] C. Stanwell, A. Gescher, T. D. Bradshaw, and G. R. Pettit. *Int. J. Cancer.*, 1994, **56(4)**, 585-92.

[19] Z. Szallasi, L. Du, R. Levine, N. E. Lewin, P. N. Nguyen, M. D. Williams, G. R. Pettit, and P. M. Blumberg. *Cancer Res*., 1996, **56(9)**, 2105-11.

[20] M. K. Sun, and D. L. Alkon. *CNS Drug Reviews*, 2006, **12(1),** 1-8.

[21] B. K. Carte. *Biosci.,* 1996. **46(4)**, 271-86.

[22] T. Manning, L. Noble, G. Abadi, and J. Smith. *Fl. Sci*., 2008, **71(4)**, 341-59.

[23] J. M. Roosenberg, Y. M. Lin, Y. Lu, and M. J. Miller. *Curr. Med. Chem*., 2000, **7(2)**, 159-97.

[24] V. Braun, and M. Braun. *Curr. Opin. Microbiol*. 2002, **5(2)**, 194-201.

[25] Z. D. Liu, and R. C. Hider. *Coord. Chem. Rev.,* 2002, **232(1-2)**, 151-71.

[26] D. Y. Liu, Z. D. Liu, and R. C. Hider. *Best Pract. Res. Clin. Haematol.,* 2002, **15(2)**, 369-84.

CHAPTER 9

Future work

FUTURE WORK

With the foundation made on using artificial methods as a means for the production of the bryostatins and Et-743, these methods are currently being implemented for the production of Taxol. This is important to shows that this innovative method can be used for the production of other natural products as well. The method of isolating the bacteria responsible for the production of these natural products will hopefully open the market for the economical availability of such drugs. Results obtained thus far for the production of Taxol has shown some success with the identification of a peak correlating to the taxane ring. From this, it is suggested that the results show that the chemical compilation used is most likely successful in isolating the fungi located near the roots of the yew tree.

Further studies are therefore being conducted to modify the chemicals used for this artificial production method as well as the parameters for the broths in the lab. With further work in developing these modifications, it won't be long before an exceptional method is developed for the production of these natural products and others. With successful results obtained from the cell line testing of the fermer compound against A549 cells; more studies will need to be conducted to determine the efficacy of the compound against other cancer cell lines to fully understand its overall effectiveness in comparison to bryostatin 1 alone.

APPENDIX